INSTITUT FÜR NUTZPFLANZENWISSENSCHAFTEN UND RESSOURCENSCHUTZ LEHRSTUHL FÜR PFLANZENBAU

UAV-Based Methods for Biomass and Biodiversity Monitoring in Grasslands

Dissertation

zur

Erlangung des Grades

Doktorin der Agrarwissenschaften

(Dr. Agr.)

der

der Agrar-, Ernährungs- und Ingenieurwissenschaftlichen Fakultät

der

Rheinischen Friedrich-Wilhelm-Universität Bonn

von

Clara Oliva Gonçalves Bazzo

aus

Pará – Brazil

Bonn, 2025

Referent: Dr. Thomas Gaiser

Korreferent: Prof. Dr. Thomas Döring

Tag der mündlichen Prüfung: 10.04.2025

Angefertigt mit Genehmigung der Agrar-, Ernährungs- und Ingenieurwissenschaftlichen Fakultät der Universität Bonn

To the women who came before me,

whose strength, sacrifice, and resilience made my steps possible.

I walk as the continuation of their dream.

Bloom—is Result—to meet a Flower
And casually glance
Would scarcely cause one to suspect
The minor Circumstance

Assisting in the Bright Affair
So intricately done
Then offered as a Butterfly
To the Meridian—

To pack the Bud—oppose the Worm—
Obtain its right of Dew—
Adjust the Heat—elude the Wind—
Escape the prowling Bee

Great Nature not to disappoint
Awaiting Her that Day—
To be a Flower, is profound
Responsibility—

Emily Dickinson

Acknowledgments

The journey of a PhD is both challenging and transformative. While it is often seen as a solitary endeavor, I was fortunate to have the support and companionship of extraordinary individuals who made this path brighter and taught me invaluable lessons along the way.

First and foremost, my deepest gratitude goes to my supervisor, Thomas Gaiser. Your consistent academic support, encouragement, and kindness have been invaluable throughout this journey. It has been an immense privilege to have a mentor who not only inspires me professionally but also as a person. Your guidance has left a lasting impact on my work and the principles I strive to uphold, and for that, I am deeply grateful.

I would also like to extend my gratitude to Bahareh Kamali, who played a key role in guiding me through my research. Thank you for your valuable contributions and for the time and effort you invested in my academic development.

A deeply personal thank you to Murilo Vianna, whose friendship and constant support were essential during this period. Your patience in teaching me, your brilliance as a collaborator, and your generosity in sharing your knowledge have not only advanced my work but also inspired me to become a professional who leads with both expertise and heart. Your ability to make a difference through your kindness and talent is a rare gift, and I feel truly fortunate to have learned from you.

To my colleagues at the Institute of Crop Science and Resource Conservation, University of Bonn, thank you for the camaraderie, support, and shared moments that enriched my PhD experience. Special thanks to Gina Lopez, Anna Engels, Dereje Tamiru, Andrea Enders, Sabine Seidel, Ixchel Hernandez, Thuy Nguyen, Aram Gorooei, Farshid Jahanbakhshi, Silvia Otternberg, Amit Srivastava, Petra Weber and Frank Ewert for making the department a vibrant and supportive place.

In particular, I am deeply grateful to Hubert Hüging, Ahsan Raza and Jasper Mohr for their companionship and assistance during countless field trips to Brandenburg, and to Gunther Krauss, whose invaluable support in data analysis and insightful discussions—paired with the best jokes—made a challenging process more enjoyable.

A special acknowledgment to my office mate and now dear friend, Dominik Behrend, whose presence made workdays lighter and whose support, both in the field and in scientific discussions, was indispensable. Your friendship and encouragement have been deeply meaningful, and I am forever thankful.

I am profoundly grateful for the financial support provided by the DAKIS project, funded by the German Federal Ministry of Education and Research (BMBF). My work was made possible through this funding and benefited greatly from the collaboration with project partners Inga Schleip, Paul Mosebach, and Almut Haub from the Eberswalde University for Sustainable Development, as well as the coordination and field technicians at the Leibniz Centre for Agricultural Landscape Research (ZALF) in Paulinenaue. Your contributions to fieldwork and scientific discussions enriched this research in countless ways.

On a personal note, my deepest thanks go to my family. To my parents, Rosangela and Francisco, for their imperfections and strengths that laid the foundation of who I am today. To my sister

Katiane, and my beloved nephew Miguel and niece Sophia, for their constant love and support. And a special acknowledgment to my sister Manoella, whose enduring belief in me has always been my greatest source of inspiration and strength.

To my friends, thank you for being the pillars I could lean on when the weight of this journey felt too heavy. While it would be impossible to name everyone here, I want to express my gratitude to those whose presence was most impactful during my PhD: Raissa Radaeli, Murilo Sandroni, Matheus Cardim, Gemma Garcia, Laia Romero, Francesca Laurini, Maryel Ayala, Ida Dareskog, Gosia Stramowska, Júlia Mesquita, Max Czekalla, Anna Nyffenegger, Markus Paffhausen and Sara Schjølberg. Your kindness and encouragement have been a source of endless motivation.

Finally, I want to thank myself. For showing resilience on the hardest days, for embracing growth through challenges, and for finding the strength to keep going even in the toughest moments.

Abstract

Grasslands are critical ecosystems that provide essential ecological services, including biodiversity conservation, carbon sequestration, water regulation, soil stabilization, and habitat provision for wildlife. However, these ecosystems are increasingly threatened by land-use intensification, climate change, and biodiversity loss. This thesis investigates the application of Unmanned Aerial Vehicles (UAVs) and advanced data integration techniques to improve the monitoring and management of grasslands, with a focus on biomass estimation and biodiversity assessment under varying management practices.

The systematic review presented in this thesis consolidates current methodologies for UAV-based biomass estimation, identifying key strengths, limitations, and emerging trends. It emphasizes the growing potential of integrating structural, spectral, and textural image data to address the challenges posed by grassland heterogeneity and complex vegetation dynamics. This review provides a comprehensive framework for designing UAV-based monitoring systems and serves as a foundation for the experimental studies conducted in subsequent chapters.

Experimental field studies were conducted over three years in a managed wet grassland to monitor key ecosystem services, specifically biomass production and biodiversity, under different cutting management regimes. The research demonstrated that disturbances such as molehills and lodging can impact the relationship between canopy height and biomass, leading to potential inaccuracies in UAV-derived models. Following this, the study explored the integration of UAV-derived features—structural (e.g., canopy height), spectral (e.g., vegetation indices), and textural metrics—to improve biomass estimation accuracy. By combining these features, the research achieved improved predictive accuracy, highlighting the utility of UAV-derived multi-dimensional data in capturing the complexity of grassland ecosystems.

Biodiversity assessment was another key focus of this thesis. The study investigated the estimation of plant species richness in managed grasslands using UAV-derived data, focusing on the influence of cutting regimes and spatial heterogeneity on prediction accuracy. The results demonstrated that integrating structural, spectral, and texture features of the grassland extracted from a UAV-based multi-spectral sensor improved the ability to estimate species richness, particularly in systems with high cutting frequencies. Texture features of the grassland, in particular, provided valuable insights into the spatial variability of vegetation structure, enabling more accurate predictions in areas with more intensive management.

While the findings demonstrate the potential of UAV technologies for ecological monitoring, several challenges remain. These include the complexity of data processing workflows, the need for precise calibration and validation, and logistical constraints associated with field operations. Overcoming these challenges will require the advancements in sensor technologies, more accessible machine learning tools, and scalable frameworks to broaden the application of UAV-based monitoring across diverse grassland ecosystems.

This thesis provides a comprehensive framework for integrating UAV-derived data into grassland monitoring and management, offering valuable insights for both scientific research and practical applications. By addressing the challenges identified, future research can refine these

approaches, supporting the conservation and sustainable management of grasslands under changing environmental conditions.

Zusammenfassung

Grünlandsysteme sind entscheidende Ökosysteme, die wesentliche ökologische Dienstleistungen bereitstellen, darunter die Erhaltung der Biodiversität, die Kohlenstoffspeicherung, die Wasserregulierung, die Bodenstabilisierung und die Bereitstellung von Lebensräumen für Wildtiere. Diese Ökosysteme sind jedoch zunehmend durch die Intensivierung der Landnutzung, den Klimawandel und den Verlust der biologischen Vielfalt bedroht. Diese Dissertation untersucht die Anwendung von unbemannten Luftfahrzeugen (UAVs) und fortschrittlichen Datenintegrationstechniken zur Verbesserung der Überwachung und des Managements von Grünlandsysteme, mit besonderem Schwerpunkt auf der Biomasseschätzung und der Bewertung der Biodiversität unter verschiedenen Bewirtschaftungsregimen.

Die in dieser Arbeit präsentierte systematische Übersicht fasst aktuelle Methoden zur UAV-gestützten Biomasseschätzung zusammen und identifiziert wesentliche Stärken, Schwächen und aufkommende Trends. Sie betont das wachsende Potenzial der Integration von strukturellen, spektralen und texturalen Daten, um die Herausforderungen der Heterogenität von Grünlandsysteme und der komplexen Vegetationsdynamik zu bewältigen. Diese Übersicht bietet einen umfassenden Rahmen für die Entwicklung von UAV-gestützten Überwachungssystemen und bildet die Grundlage für die experimentellen Studien in den folgenden Kapiteln.

Experimentelle Feldstudien wurden über drei Jahre in einer bewirtschafteten Feuchtwiese durchgeführt, um zentrale Ökosystemleistungen, insbesondere die Biomasseproduktion und Biodiversität, unter verschiedenen Schnittregimen zu überwachen. Die Ergebnisse zeigten, dass Störungen wie Maulwurfshügel und Lagerung die Beziehung zwischen Kronenhöhe und Biomasse beeinflussen und zu potenziellen Ungenauigkeiten in UAV-Modellen führen können. Anschließend wurde die Integration von UAV-abgeleiteten Merkmalen – strukturelle (z. B. Kronenhöhe), spektrale (z. B. Vegetationsindizes) und texturale Metriken – untersucht, um die Genauigkeit der Biomasseschätzung zu verbessern. Durch die Kombination dieser Merkmale konnte die Vorhersagegenauigkeit gesteigert werden, was den Nutzen multidimensionaler UAV-Daten zur Erfassung der Komplexität von Grünlandsysteme unterstreicht.

Ein weiterer Schwerpunkt dieser Dissertation lag auf der Bewertung der Biodiversität. Die Studie untersuchte die Schätzung des pflanzlichen Artenreichtums in bewirtschafteten Grünlandsysteme mithilfe von UAV-Daten und analysierte dabei den Einfluss von Schnittregimen und räumlicher Heterogenität auf die Vorhersagegenauigkeit. Die Ergebnisse zeigten, dass die Integration von strukturellen, spektralen und texturalen Merkmalen ebenfalls die Fähigkeit zur Schätzung des Artenreichtums verbesserte, insbesondere in Systemen mit hohen Schnittfrequenzen. Insbesondere texturale Merkmale lieferten wertvolle Einblicke in die räumliche Variabilität der Vegetationsstruktur und ermöglichten genauere Vorhersagen in intensiver bewirtschafteten Bereichen.

Obwohl die Ergebnisse das große Potenzial von UAV-Technologien für die ökologische Überwachung verdeutlichen, bestehen weiterhin Herausforderungen. Dazu gehören die Komplexität der Datenverarbeitung, die Notwendigkeit präziser Kalibrierung und Validierung sowie logistische Einschränkungen bei Feldoperationen. Die Bewältigung dieser

Herausforderungen erfordert Fortschritte in der Sensortechnologie, benutzerfreundlichere Werkzeuge für maschinelles Lernen und skalierbare Rahmenbedingungen, um die Anwendung UAV-gestützter Überwachung auf unterschiedliche Graslandsysteme auszudehnen.

Diese Dissertation liefert einen umfassenden Rahmen für die Integration UAV-abgeleiteter Daten in die Überwachung und das Management von Grünlandsysteme. Sie bietet wertvolle Erkenntnisse sowohl für die wissenschaftliche Forschung als auch für praktische Anwendungen. Durch die Bewältigung der identifizierten Herausforderungen kann die zukünftige Forschung diese Ansätze weiter verfeinern und so den Erhalt und die nachhaltige Bewirtschaftung von Grünlandsysteme unter sich verändernden Umweltbedingungen unterstützen.

TABLE OF CONTENTS

LIST OF FIGURES

LIST OF TABLES

LIST OF ACRONYMS

3D .....Three-Dimensional

AGB .....Above-Ground Biomass

ANN .....Artificial Neural Networks

ANOVA .....Analysis of Variance

BNDVI .....Blue Normalized Difference Vegetation Index

CCCI .....Canopy Chlorophyll Concentration Index

CH .....Canopy Height

CHM .....Canopy Height Model

CV .....Cross-Validation

CVI .....Chlorophyll Vegetation Index

DBM .....Dry Biomass

DEM .....Digital Elevation Model

DNN .....Deep Neural Network

DSM .....Digital Surface Model

DTM .....Digital Terrain Model

EVI .....Enhanced Vegetation Index

ExG .....Excess Green

FBM .....Fresh Biomass

GCI .....Green Chlorophyll Index

GCP .....Ground Control Point

GIS .....Geographic Information Systems

GLCM .....Grey Level Co-occurrence Matrix

GNDVI .....Green Normalized Difference Vegetation Index

GNSS .....Global Navigation Satellite System

GPS .....Global Positioning System

GSD .....Ground Sample Distance

HS ..... Hyperspectral

HVH ..... Height Variation Hypothesis

LAI ..... Leaf Area Index

LiDAR ..... Light Detection and Ranging

LR ..... Linear Regression

MCARI ..... Modified Chlorophyll Absorption in Reflectance Index

ML ..... Machine learning

MLR ..... Multiple Linear Regression

MS ..... Multispectral

MSAVI ..... Modified Soil-Adjusted Vegetation Index

NDRE ..... Normalized Difference Red Edge

NDVI ..... Normalized Difference Vegetation Index

NGI ..... Normalized Green Intensity

NGRDI ..... Normalized Green Red Difference Index

NIR ..... Near-infrared

OSAVI ..... Optimization Soil-Adjusted Vegetation Index

PLSR ..... Partial Least Squares Regression

PR ..... Polynomial Regression

RDVI ..... Renormalized Difference Vegetation Index

RF ..... Random Forest

RGB ..... Red-Green-Blue

RMSE ..... Root Mean Square Error

RPM ..... Rise Plate Meter

rRMSE ..... Relative Root Mean Square Error

RS..... Remote Sensing

SAVI ..... Soil-Adjusted Vegetation Index

SfM ..... Structure from Motion

SH ..... Sward Height

SR ..... Simple Ratio

SVH ..... Spectral Variation Hypothesis

SVM ..... Support Vector Machines

SWL .....Stepwise Linear Regression

UAV .....Unmanned Aerial Vehicles

VI .....Vegetation Indices

CHAPTER I

GENERAL INTRODUCTION

1 General introduction

Grasslands are defined as ecosystems predominantly covered by grasses, forbs, and other herbaceous plants, with minimal tree coverage (White, Murray and Rohweder, 2000). They are one of the most extensive terrestrial biomes, occurring in every continent except Antarctica, and include various types such as prairies, steppes, pampas, savannas, and velds (Allen *et al.*, 2011). Each type is defined by specific climatic conditions, soil types, and fire regimes, which in turn influence their ecological characteristics (Gibson and Newman, 2019).

The classification of grasslands within agricultural systems can be categorized into three primary types: natural, semi-natural, and improved, each defined by the degree of human intervention and the ecological processes that dominate their formation and maintenance (Lemaire, Hodgson and Chabbi, 2011). Natural grasslands are primarily formed by natural processes such as climate, fire, and wildlife grazing, though they are also utilized for livestock grazing. These areas are typical of what one might envision as traditional grassland biomes (Parr et al. 2014).

Semi-natural grasslands are developed by human activity but still depend on natural processes for their maintenance (Allen *et al.*, 2011). These grasslands require regular human intervention such as livestock grazing or hay cutting to prevent encroachment by shrubs and trees. Without such management, semi-natural grasslands would gradually transition to other forms of vegetation, thus losing their grassland characteristics (Bonari *et al.*, 2017).

Compared to other two types, improved grasslands are the most intensively managed. They are created by the deliberate modification of the natural landscape, including plowing, sowing of high-yield agricultural grass varieties or non-native species and regular application of artificial fertilizers (Bengtsson *et al.*, 2019). These practices are aimed at maximizing productivity for agricultural purposes, often at the cost of ecological diversity. Such grasslands are maintained through intensive management practices that support high agricultural output but may also lead to ecological imbalances if not carefully managed (Pilgrim *et al.*, 2010).

Covering about 40% of the Earth's land surface, grasslands are essential to global biodiversity and are among the most important carbon sinks, influencing the global carbon cycle (White, Murray and Rohweder, 2000; Andrade *et al.*, 2015). They play a critical role in water regulation and are essential for the hydrological stability of many regions, supporting both human and wildlife requirements (Bengtsson *et al.*, 2019). Grasslands also provide important ecosystem services such as erosion control, flood protection, and the support of diverse wildlife habitats, contributing significantly to biodiversity conservation (Lemaire, Hodgson and Chabbi, 2011). Economically, they are fundamental to the agricultural sector, occupying 70% of agricultural land globally and offering a primary source of low-cost feed for the livestock industry, which is important for food security and the livelihoods of millions (FAOStat, 2016; Van Den Pol *et al.*, 2018). Culturally, they offer recreational opportunities and contribute to the cultural tradition of communities (Hussain *et al.*, 2019). Despite their extensive utility, grasslands face significant threats from overgrazing, urbanization, and climate change, which necessitate robust management and conservation

strategies to maintain their ecological and economic functions (Le Clec'h *et al.*, 2019; Huber *et al.*, 2022).

1.1 Wet grasslands: characteristics and ecological importance

Wet grasslands are dynamic and biologically diverse ecosystems within agricultural landscapes, characterized by their semi-natural formation through processes such as drainage of other wetlands or clearing of forests on floodplains (Dixon *et al.*, 2014; Chris B. Joyce, Simpson and Casanova, 2016). These ecosystems are maintained by traditional management practices such as mowing for hay and extensive grazing, which are essential for conserving their ecological integrity (Joyce and Wade, 1998). Characterized by a variety of grasses and sedges, these lands experience periodic flooding and maintain a high water table for much of the year, factors that significantly influence their vegetation and associated biodiversity (Čop, Vidrih and Hacin, 2009).

The ecological importance of wet grasslands extends beyond biodiversity; they provide a multitude of ecosystem services including flood attenuation, groundwater recharge, sediment storage, nutrient removal, and erosion protection (Joyce and Wade, 1998). These services are particularly valuable in regions susceptible to flooding or in need of water quality maintenance, often characterized by their historical use in agriculture which has shaped regional identities and conserved traditional land-use practices (Joyce, 2014).

Despite their ecological importance, wet grasslands across Europe have suffered from intensive land use practices, including fertilization, artificial drainage, and fragmentation, leading to significant ecological degradation (Rosenthal, 2006). Restoration efforts have focused on reducing fertilizer input, increasing the water table, and extending land use, but recovering biodiversity in these areas has proven challenging and slow (Joyce, 2014). Often, lands previously subjected to intensive use remain deficient in species diversity for extended periods, despite management adjustments aimed at increasing botanical diversity and structural complexity (Rosenthal, 2010).

Research indicates that modifying management strategies, such as implementing less frequent and later cutting regimes, along with reducing inorganic fertilizer application, can significantly bolster the diversity of plant species in semi-natural wet grasslands (Tallowin, 1996). However, the success of such strategies can be reduced by environmental stress factors that inherently limit species richness (Čop, Vidrih and Hacin, 2009). The current challenge for conservationists and land managers is to effectively balance traditional practices with innovative management strategies to enhance biodiversity and sustain ecosystem services within changing environmental conditions and historical impacts.

1.2 Grassland monitoring

1.2.1 Techniques and importance

The continuous monitoring of grasslands is fundamental to understand their ecological dynamics and effectively respond to environmental pressures (Alves Oliveira *et al.*, 2022). Ecological surveys, typically limited in spatial and temporal scope, struggle to comprehensively monitor biodiversity and ecosystem changes across grassland areas (Fauvel *et al.*, 2020). These limitations highlight the need for advanced monitoring techniques that can extend beyond local assessments and capture the broader environmental impacts affecting these ecosystems.

Monitoring grasslands facilitates sustainable management and conservation by providing crucial data on biomass yield, quality, and floristic composition (Schucknecht *et al.*, 2022). This information is vital for managing the intensity of grassland use, ranging from extensive management on marginal lands to intensive management practices that involve high fertilizer inputs and frequent harvesting (Wengert *et al.*, 2022). For example, extensive grasslands, which are often harvested fewer times per year with a focus on conservation, contrast sharply with intensively managed grasslands that prioritize yield and are harvested more frequently (Weiss *et al.*, 2001). This contrast in management strategies underscores the importance of regular and detailed monitoring to maintain ecological balance and prevent overuse.

The degradation of grasslands —manifested as desertification, biodiversity loss, and a decline in productivity—poses serious threats to both ecological security and socioeconomic development (Zhao, Liu and Wu, 2020). Monitoring helps mitigate these threats by providing essential information needed for strategic vegetation growth analysis and management planning (Jin *et al.*, 2019). Moreover, the preservation of grassland ecosystems requires a thorough mapping and assessment of key traits such as above-ground biomass and biodiversity, which are crucial for sustaining their ecological functions (Wachendorf, Fricke and Möckel, 2018; Schucknecht *et al.*, 2020)

However, achieving detailed and accurate grassland monitoring at different scales remains a challenge due to the lack of spatially explicit data (Schucknecht *et al.*, 2022). Innovative approaches such as remote sensing offer promising solutions by enabling cost-effective, rapid, quantitative, and repeatable assessments across diverse and extensive landscapes (Wachendorf, Fricke and Möckel, 2018).

1.2.2 Challenges to estimate above-ground biomass

Biomass, specifically above-ground biomass (AGB), is a crucial indicator of grassland health, productivity, and carbon cycling (Wang *et al.*, 2014; Zhang *et al.*, 2018; Shi *et al.*, 2022). It serves as a key metric for assessing the sustainability and ecological balance of grassland ecosystems, making accurate estimation models essential for effective grassland management, livestock

balancing, and eco-environmental protection (F. Zhao *et al.*, 2014; Liang *et al.*, 2016; Fan *et al.*, 2018; Shi *et al.*, 2021). Furthermore, AGB plays a significant role in the carbon cycle by reflecting the net primary productivity of grasslands, which is essential for understanding carbon sequestration and how it affects climate regulation (Zhang *et al.*, 2022).

Despite its importance, accurate quantification of AGB presents several technical and methodological challenges. Traditional field-based methods of biomass sampling are highly labor-intensive and time-consuming, especially when applied to large areas (Morais *et al.*, 2021; Adar *et al.*, 2022; Alves Oliveira *et al.*, 2022). These methods often involve destructive sampling, which can affect the grassland itself and is not feasible for frequent monitoring (Gnyp *et al.*, 2014). Additionally, the prediction accuracy of biomass using traditional field methods can be low, particularly over large, heterogeneous areas where environmental variables such as soil, climate, and topography vary widely (Ghajar and Tracy, 2021; Wang *et al.*, 2021)

The variability of biomass production within and across years adds another layer of complexity. This variability arises from factors such as climate change, grazing pressure, and other anthropogenic activities, which can influence the spatial and temporal distribution of biomass and make consistent monitoring challenging (Taylor and Browning, 2021; Franceschini *et al.*, 2022; Zhang *et al.*, 2022). Moreover, remote locations pose additional difficulties in terms of accessibility and the ability to conduct regular surveys, further complicating the comprehensive monitoring of grassland conditions (Schulze-Brüninghoff, Wachendorf and Astor, 2021).

1.2.3 Plant species biodiversity: key to ecosystem health

Grasslands are a significant source of biodiversity, providing a range of ecosystem services essential for the survival of plant and animal species and human life (Lamarque *et al.*, 2011; Dinnage *et al.*, 2012). Biodiversity in grasslands contributes to the stability of plant productivity over time, carbon storage, and pollinator abundance, making its preservation vital (Lemaire, Hodgson and Chabbi, 2011; Bonari *et al.*, 2017). Plant species diversity is a key component in providing these ecosystem services, with species richness serving as a strong indicator of plant diversity (Oldeland *et al.*, 2010; van Oijen, Bellocchi and Höglind, 2018). Additionally, the variety of plant species present in grasslands is strongly influenced by long-term management practices, with livestock grazing being a major driving force affecting vegetation dynamics, species distribution, and landscape-scale biodiversity (Marriott *et al.*, 2004; van Oijen, Bellocchi and Höglind, 2018).

Despite the critical role of biodiversity, traditional methods of its measurement are labor-intensive, time-consuming, and costly, requiring extensive field sampling by experienced biologists (Palmer *et al.*, 2002; Wang and Gamon, 2019). These methods are also limited by inconsistent data sets and the lack of standardized procedures, which makes it difficult to acquire sufficient information on changing species distributions over time (Conti *et al.*, 2021; Thornley *et al.*, 2023). Furthermore, grassland biodiversity faces numerous threats from urban development,

agricultural practices, eutrophication, overgrazing, and climate change, all of which exacerbate the challenge of effective monitoring (Hautier *et al.*, 2014; Harrison, Gornish and Copeland, 2015). To address these challenges, comprehensive and consistent monitoring is necessary to ensure the conservation and sustainable management of grasslands (Rapinel *et al.*, 2019).

1.3 Remote sensing and UAV: technological advances in ecological monitoring

Remote sensing is an important technology in ecology and conservation, enabling the observation and monitoring of ecosystems from a distance (Atzberger, 2013; Ali *et al.*, 2016; Tang *et al.*, 2021). Utilizing sensors mounted on various platforms, this technology captures data about the Earth's surface, providing essential insights into environmental conditions without the need for direct contact (Mulla, 2013). In grassland ecology, remote sensing plays a crucial role by facilitating the continuous monitoring of vegetation dynamics, enabling assessments of ecosystem services, and helping to define conservation strategies (Wachendorf, Fricke and Möckel, 2018; Fauvel *et al.*, 2020). Traditional remote sensing platforms include satellites and aircraft, which offer the advantage of wide-area coverage and rapid data collection (Zhang *et al.*, 2018; Chao *et al.*, 2019). However, these methods often struggle with issues such as low spectral resolution and long intervals between data captures, which can limit their effectiveness in capturing the detailed and frequent data required for precise ecological management (Atzberger, 2013; Dusseux *et al.*, 2015; Zhang *et al.*, 2018).

Unmanned Aerial Vehicles (UAVs), commonly referred to as drones, have significantly enhanced the capabilities of remote sensing, especially in the context of ecological and conservation research (Von Bueren *et al.*, 2015; Eskandari *et al.*, 2020; Tmušić *et al.*, 2020). UAVs are particularly beneficial for their ability to provide high spatial and temporal resolution data, which is critical for accurately capturing the fine-scale structural and temporal variations within ecosystems (Shahbazi, Théau and Ménard, 2014; Possoch *et al.*, 2016). These high-resolution datasets are invaluable for detailed vegetation mapping, species identification, and monitoring the rapid ecological changes that may occur due to environmental pressures or seasonal transitions (Manfreda *et al.*, 2018; Insua, Utsumi and Basso, 2019; Jenal *et al.*, 2020; da Costa *et al.*, 2021; Plaza *et al.*, 2021; Villoslada Peciña *et al.*, 2021).

Operating at lower altitudes than traditional remote sensing platforms, UAVs can gather superior spectral data with minimal signal degradation, capturing hundreds of narrow-band spectral channels that are essential for detailed phenotypic and physiological assessments (Atzberger, 2013; Tian and Fu, 2022). The flexibility and cost-effectiveness of UAVs also allow for more frequent and targeted data collection, enabling researchers to conduct time-series analyses that are crucial for understanding long-term ecological trends and responses to environmental management actions (Eskandari *et al.*, 2020; Li *et al.*, 2020; Wang *et al.*, 2021).

Moreover, the adaptability of UAV platforms facilitates the integration of diverse sensing technologies, from traditional photographic cameras to advanced multispectral and hyperspectral

sensors, and even thermal and LiDAR sensors (Poley and McDermid, 2020; Tmušić *et al.*, 2020; Wang *et al.*, 2021). This versatility allows for comprehensive ecological assessments across multiple spectral domains, providing a deeper understanding of ecosystem health, plant phenology, and species distribution (Michez *et al.*, 2020; Villoslada *et al.*, 2020; Villoslada Peciña *et al.*, 2021). Such detailed and multi-dimensional data are pivotal for developing robust models of biomass, and biodiversity, which are key metrics for assessing the sustainability and resilience of grassland ecosystems.

1.3.1 Challenges in using proximal and remote sensing for grassland monitoring

One of the primary challenges in using proximal and remote sensing for grassland monitoring is accurately estimating aboveground biomass through canopy height (CH) (Bareth *et al.*, 2015; Borra-Serrano *et al.*, 2019; Lussem *et al.*, 2019). Traditional techniques for measuring grassland height, such as using a rising plate meter or a ruler stick, can be labor-intensive and time-consuming (Bareth *et al.*, 2015; Michez *et al.*, 2020; Togeiro de Alckmin *et al.*, 2021). Recent advancements have allowed vegetation height to be derived efficiently from remote sensing sensors, particularly through the use of three-dimensional (3D) data (Bendig *et al.*, 2014; Näsi *et al.*, 2018; Wachendorf, Fricke and Möckel, 2018; Rueda-Ayala *et al.*, 2019; Wijesingha *et al.*, 2019). However, their application in grasslands remains limited due to the challenges in accurately distinguishing vegetation from the ground in shorter plants (Bareth *et al.*, 2015; Bareth and Schellberg, 2018; Lussem *et al.*, 2019) and the need for high-quality point cloud data to ensure accurate height information (Bendig *et al.*, 2015; Wijesingha *et al.*, 2019).

Additionally, spectral data derived from remote sensing data, including vegetation indices (VIs) such as the normalized difference vegetation index (NDVI), are crucial for assessing plant and vegetation characteristics (Tucker, 1979; Carlson and Ripley, 1997). VIs highlight specific properties of vegetation, aiding in mapping density and monitoring ecological changes (Sha *et al.*, 2018). Despite their usefulness, VIs can suffer from saturation problems in areas with high vegetation cover, which can limit their accuracy in vegetation characteristics estimation (Zhang *et al.*, 2021). Other indices like the soil-adjusted vegetation index (SAVI) and the enhanced vegetation index (EVI) have been developed to address specific issues such as soil background effects and NDVI saturation, further refining biomass and plant biodiversity estimation models (Rondeaux, Steven and Baret, 1996; Huete *et al.*, 2002). Nevertheless, VIs remain a critical tool for understanding vegetation dynamics and are often used in combination with other data types to improve monitoring precision (Huete *et al.*, 2002).

In addition to spectral data, image texture derived from high-resolution optical imagery provides valuable information on vegetation structure. Image texture measures the variation in pixel intensity within an image, which can serve as a proxy for vegetation heterogeneity and structure (Culbert *et al.*, 2009; Wood *et al.*, 2012). Texture analysis techniques, such as the Grey Level Co-occurrence Matrix (GLCM), incorporate both spectral and spatial information, enabling finer distinctions of structural detail within grasslands (Barrett *et al.*, 2014; Dos Reis *et al.*, 2020;

Grüner, Wachendorf and Astor, 2020). However, these methods are computationally intensive and require substantial processing power to achieve accurate results (Grüner, Wachendorf and Astor, 2020).

Integrating structural, spectral, and textural features from RS data can significantly enhance the accuracy of biomass and biodiversity estimates. Combining canopy height models (CHM) with vegetation indices (VIs) improves the precision of biomass estimation by providing a comprehensive assessment of vegetation characteristics (Viljanen *et al.*, 2018; Pranga *et al.*, 2021). This multi-faceted approach leverages the strengths of each data type, providing a more robust and detailed understanding of ecological dynamics (Karunaratne *et al.*, 2020). However, the complexity and computational demands of integrating multiple data sources pose additional challenges.

1.4 Machine learning: advanced methods for ecological prediction

Machine learning (ML) has emerged as a powerful empirical method in the estimation of AGB and plant biodiversity, significantly advancing the field over the past two decades (Zeng *et al.*, 2021). Various ML models, including random forest (RF), artificial neural networks (ANN), and support vector machines (SVM), have been widely applied due to their ability to handle complex and nonlinear relationships between predictive and objective variables (Morais *et al.*, 2021). These models offer greater accuracy and flexibility compared to traditional regression models, making them particularly advantageous in ecosystem research (Wang *et al.*, 2017; Eskandari *et al.*, 2020).

This flexibility has led to the widespread adoption of ML techniques in grassland biomass estimation and plant species biodiversity (Viljanen *et al.*, 2018; Fauvel *et al.*, 2020; De Rosa *et al.*, 2021; Pranga *et al.*, 2021; Alves Oliveira *et al.*, 2022; Muro *et al.*, 2022). For instance, partial least squares regression (PLSR) effectively explains relationships between hyperspectral data and grassland traits, reducing the dimensionality of input datasets while maintaining predictive power (Darvishzadeh *et al.*, 2008; Capolupo *et al.*, 2015). The RF model has also demonstrated high performance in grassland AGB simulations, explaining 86% of observed data variation on the Tibetan Plateau (Zeng *et al.*, 2019). Muro *et al.* (2022) compared the performance of a deep neural network (DNN) with a RF for spatial predictions of biomass production and plant biodiversity in grasslands, demonstrating the potential of advanced ML models to enhance the accuracy and efficiency of ecological predictions

Processing large quantities of data collected by UAV-based sensors necessitates robust analytical frameworks, and ML algorithms are well-suited to this task. (Lussem *et al.*, 2022). They can manage multicollinearity and high-dimensional datasets, making them ideal for processing complex remote sensing data (Wachendorf, Fricke and Möckel, 2018). The evolution of ML techniques has unlocked the potential to handle highly autocorrelated features from remote sensing data, optimizing predictions of heterogeneous grassland biomass (Grüner, Wachendorf and Astor, 2020; Morais *et al.*, 2021). Diverse ML methods, such as RF and SVM, have been particularly effective in analyzing spectral data, offering enhanced capabilities for handling large, complex

datasets (Eskandari *et al.*, 2020; Morais *et al.*, 2021). These methods have evolved from basic indices and linear estimations to sophisticated ML-based approaches that optimize models by extracting structural and spectral features from remote sensing datasets (Karunaratne *et al.*, 2020; Villoslada *et al.*, 2020; K. Y. Li *et al.*, 2021).

1.5 General Objective and research questions

The overarching objective of this thesis is to develop and validate innovative methodologies for accurate estimation of aboveground biomass and biodiversity assessment in grassland ecosystems using UAVs combined with advanced analytical techniques. This research aims to use UAV-derived data to enhance ecological monitoring, improve management practices, and support conservation efforts in grasslands. This thesis aims to answer the following four questions:

- **Question 1 (Q1):** What are the most effective UAV-based methods for estimating aboveground biomass in grasslands, and what are their limitations and potential?
- **Question 2 (Q2):** How do field disturbances, such as lodging and molehills, impact the accuracy of biomass estimation using UAV-derived canopy height models in grasslands?
- **Question 3 (Q3):** Can the integration of structural, spectral, and textural features from UAV imagery improve the accuracy of biomass estimation models in heterogeneous grasslands?
- **Question 4 (Q4):** How can UAV-derived data be utilized to accurately assess species richness and diversity in wet grassland ecosystems, and what are the implications for conservation and management?

1.6 Structure of the thesis

This work is cumulative doctoral thesis and based on four peer-reviewed papers. The content is structured as follow:

Chapter I provides the general introduction, setting the context for the research by emphasizing the significance of accurate aboveground biomass estimation and biodiversity assessment in grassland ecosystems, and highlighting the potential of UAVs to meet these needs. It outlines the general objective and specific research questions, and gives an overview of the thesis structure, explaining how each chapter contributes to the overall research objective.

Chapter II is dedicated to a comprehensive review of existing methods for estimating AGB in grasslands using UAVs. This review evaluates the strengths, limitations, and potential progresses of UAV-based techniques in comparison to traditional ground-based methods. By synthesizing current knowledge and identifying gaps in the literature, this chapter sets a solid foundation for the experimental studies that follow.

In **Chapter III**, the focus shifts to the impact of field disturbances such as lodging and

molehills on the accuracy of UAV-derived biomass estimates. This study investigates how these disturbances affect canopy height models and consequently biomass estimation. Through field data collection and analysis, the chapter quantifies the impact of these disturbances in AGB estimation.

Chapter IV explores the integration of structural, spectral, and textural features derived from UAV imagery to enhance AGB estimation accuracy. Advanced machine learning algorithms are applied to combine these features into robust biomass estimation models. The chapter discusses the methodology used, presents the results, and highlights the implications of integrating multiple UAV-derived data types for biomass estimation accuracy.

Chapter V extends the application of UAV technology to biodiversity assessment in wet grasslands. It utilizes UAV-derived structural, spectral, and textural data to assess species richness and diversity. By employing machine learning techniques to integrate these features, the chapter provides biodiversity assessments. The effectiveness of these methods is evaluated, and their implications for conservation and management practices are discussed.

Chapter VI synthesizes the findings from the experimental studies, providing a cohesive narrative that integrates the results and discusses their interactions and broader implications. The practical implications of the research are explored, addressing how the findings contribute to the field of ecological monitoring and suggesting directions for future research. The chapter also critically examines the limitations of the studies, providing a balanced view of the research results.

CHAPTER II

A REVIEW OF ESTIMATION METHODS FOR ABOVEGROUND BIOMASS IN GRASSLANDS USING UAV

This chapter has been published as:

Bazzo, Clara Oliva Gonçalves, Bahareh Kamali, Christoph Hütt, Georg Bareth, and Thomas Gaiser. 2023. "A Review of Estimation Methods for Aboveground Biomass in Grasslands Using UAV." *Remote Sensing* 15 (3): 1–50. https://doi.org/10.3390/rs15030639.

Abstract

Grasslands are one of the world's largest ecosystems, accounting for 30% of total terrestrial biomass. Considering that aboveground biomass (AGB) is one of the most essential ecosystem services in grasslands, an accurate and faster method for estimating AGB is critical for managing, protecting, and promoting ecosystem sustainability. Unmanned aerial vehicles (UAVs) have emerged as a useful and practical tool for achieving this goal. Here, we review recent research studies that employ UAVs to estimate AGB in grassland ecosystems. We summarize different methods to establish a comprehensive workflow, from data collection in the field to data processing. For this purpose, 64 research articles were reviewed, focusing on several features including study site, grassland species composition, UAV platforms, flight parameters, sensors, field measurement, biomass indices, data processing, and analysis methods. The results demonstrate that there has been an increase in scientific research evaluating the use of UAVs in AGB estimation in grasslands during the period 2018–2022. Most of the studies were carried out in three countries (Germany, China, and USA), which indicates an urgent need for research in other locations where grassland ecosystems are abundant. We found RGB imaging was the most commonly used and is the most suitable for estimating AGB in grasslands at the moment, in terms of cost–benefit and data processing simplicity. In 50% of the studies, at least one vegetation index was used to estimate AGB; the Normalized Difference Vegetation Index (NDVI) was the most common. The most popular methods for data analysis were linear regression, partial least squares regression (PLSR), and random forest. Studies that used spectral and structural data showed that models incorporating both data types outperformed models utilizing only one. We also observed that research in this field has been limited both spatially and temporally. For example, only a small number of papers conducted studies over a number of years and in multiple places, suggesting that the protocols are not transferable to other locations and time points. Despite these limitations, and in the light of the rapid advances, we anticipate that UAV methods for AGB estimation in grasslands will continue improving and may become commercialized for farming applications in the near future.

Keywords: photogrammetry; grassland monitoring; precision agriculture; biomass estimation; vegetation indices; effective workflow.

2.1 Introduction

Grasslands are among the largest ecosystems on the planet, playing an important ecological and economic role and contributing to the food security of millions of people (Hopkins and Wilkins, 2006). According to FAO (FAOStat, 2016), grasslands cover 25% of the terrestrial surface, equivalent to around 68% of the world's agricultural areas. This makes grasslands an important provider of ecosystem services in different parts of the world (Wang, Li and Bian, 2016; Bengtsson *et al.*, 2019). When properly managed, grasslands can effectively contribute to carbon sequestration and improve air and water quality, nutrient cycling, and biodiversity, as well as food production (Sala and Paruelo, 1997; Egoh *et al.*, 2016; Bengtsson *et al.*, 2019).

Grasslands store 30% of the world's terrestrial biomass (Bar-On, Phillips and Milo, 2018). Moreover, the provision of aboveground biomass (AGB) is one of the most important ecosystem services in grasslands and constitutes the basis for increasing fodder productivity (Zhang *et al.*, 2018). Thus, a precise and rapid method for the estimation of AGB is critical for the management and protection of grasslands (Psomas *et al.*, 2011; F. Zhao *et al.*, 2014; Jin *et al.*, 2014) and for enhancing the sustainability of these ecosystems (Yang *et al.*, 2012).

Current approaches to estimating AGB can be classified as either ground-based or remote sensing (RS) methods. Ground-based methods can be either destructive or non-destructive. Destructive methods traditionally involve cutting the grass in the field, followed by drying and weighing it in the laboratory (Yang, 2013). Although these measurements generate the most accurate estimates of grassland biomass, they are time-consuming and labor-intensive (Nordberg and Evertson, 2003).

Ground-based methods for non-destructive measurement of grassland AGB have been studied for decades (Santillan, Ocumpaugh and Mott, 1979; Lussem, Schellberg and Bareth, 2020). These approaches estimate AGB using equations relating biomass to measurable biophysical factors such as plant height and plant density ('t Mannetje and Jones, 2000). Handheld devices are the most straightforward instruments for measuring these biophysical factors (Lussem *et al.*, 2019). The most widely used and well-documented ground-based method for the non-destructive measurement of AGB in grasslands is the rising plate meter (RPM) (Sanderson *et al.*, 2001). These instruments measure compressed sward height by integrating sward height and density over a specific area (Wachendorf, Fricke and Möckel, 2018). The ability of RPM-based compressed sward height to estimate AGB grass using regression models is now well established (O'Sullivan, O'Keeffe and Flynn, 1987; O'Donovan *et al.*, 2002; López Díaz, Roca-Fernández and González-Rodríguez, 2011). In view of this, farmers use RPM devices to create electromechanical models, which produce accurate and reliable estimates (Bareth and Schellberg, 2018).

Despite the benefits of fast and regular assessments, the RPM method also has drawbacks, including operator variability and paddock slope. Through uneven and undulating terrain, the RPM method's ability to measure grass height effectively can be impacted, frequently leading to inaccurate measurements due to the RPM base not effectively touching the true ground surface

(Barnetson, Phinn and Scarth, 2020). The RPM also presents limitations when the sward is high and lacks a flat top structure, or when the grass sward is sparse and grows poorly and unevenly (Viljanen *et al.*, 2018). It is also not suitable for grasses with tender erect stems, including some tropical grasses (Edvan *et al.*, 2015). Additionally, RPM measurements are also point measurements, and therefore, the within-paddock spatial variability of grassland biomass production is not taken into account because only an average paddock estimate is observed (Alvarez-Hess *et al.*, 2021).

In recent years, RPM devices have become more sophisticated as technology has advanced. Ultrasonic distance sensors are used in devices such as the GrassHopper (TrueNorth Technologies, Shannon, Ireland) and the GrassOmeter (Monford AG Systems Ltd., Dublin, Ireland) (Lussem *et al.*, 2019). In addition to handheld devices, vehicle-mounted devices have also been developed. Examples are the Pasture Meter (C-Dax Agricultural Solutions, Palmerston North, New Zealand) and the Pasture Reader (Naroaka Enterprises, Narracan, Australia). These sensors can monitor grass height while driving the vehicle through the center of a towing tunnel, where optical sensors detect grass height, which is then calibrated to estimate AGB (Bareth and Schellberg, 2018).

Despite the benefits of fast and regular assessments provided by these sensing systems, there are still several drawbacks. In particular, the precise estimation of AGB in large-scale grassland ecosystems is difficult due to (1) limited spatial coverage, especially for handheld equipment, hence limiting the within-field description of the variability of the sward, (2) the requirement for heavy technical equipment, (3) limited access to the field due to grazing animals, (4) potential disturbances at a greater frequency for repeated measurements for vehicle-mounted sensors, and (5) applicability restrictions based on field conditions (e.g., soil moisture) (Bareth and Schellberg, 2018; Lussem *et al.*, 2019).

RS-based methods offer potential for rapid and automated measurements to quantify both structural and biochemical properties of the vegetation at high spatial and temporal resolution at a range of spatial scales (Lussem *et al.*, 2019). These methods include digital imaging (hyperspectral, multispectral, optical (red–green–blue, RGB), radar), photogrammetry, laser scanning, and combinations of various sensors on different platforms (Atzberger, 2013). Numerous studies have evaluated the feasibility of using satellite RS to estimate plant parameters. Although satellite platforms offer an effective way to collect data over large areas (Nordberg and Evertson, 2003), using satellite imaging for calibrating and validating an AGB estimation model in grasslands may be inefficient due to low spatial resolution (Zhang *et al.*, 2018). Most satellite systems with high spatial resolution (<5 m) are commercially operated, and therefore, image acquisition costs for short revisit times can become a limiting factor (Manfreda *et al.*, 2018). In a fragmented agricultural landscape, as seem in some grassland fields, where the average field size is low, high-spatial-resolution images are required (Dusseux *et al.*, 2015). Additionally, the applicability of satellite imagery can be significantly hampered and negatively impacted by weather conditions (cloud cover obstructing free sight) (Whitcraft *et al.*, 2015).

In recent years, unmanned aerial vehicles (UAVs), also known as remotely piloted aircraft

systems, unmanned aircraft systems, or drones, have proven to be an important and viable tool for measuring and estimating biophysical parameters at a scale appropriate to grassland distribution (Dusseux *et al.*, 2015). With flexibility, UAVs can be operated quickly, simply, and economically. Most importantly, they can collect imagery data at high spatial, spectral, and temporal resolutions at exactly the point in time when the information is needed. In fact, when surveying objects at small (5 ha) to medium (5–50 ha) spatial scales, UAV-based photography outperforms alternative imaging acquisition technologies, such as satellites and manned aerial systems. Specifically, in this context, UAVs show higher temporal and spatial resolution as well as exhibit greater versatility at a lower cost (Matese *et al.*, 2015).

In the past ten years, the number of research articles describing UAV applications has increased dramatically, with these studies encompassing a diversity of UAV types and applications (Librán-Embid *et al.*, 2020). More recently, there has been increased interest in applying UAV remote sensing to the estimation of AGB in grasslands. In this context, structural features of grasslands have been used for the estimation of grassland height and AGB (Bareth and Schellberg, 2018; Zhang *et al.*, 2018; Lussem *et al.*, 2019). Nevertheless, image-based approaches using UAV to estimate forage biomass are still in their infancy (Possoch *et al.*, 2016; Forsmoo *et al.*, 2018; Rueda-Ayala *et al.*, 2019). In view of this, there is no standard process for planning, collecting, and analyzing these data in order to extract AGB information. Considering the grassland's inherent properties, several aspects linked to data collection and analysis methodologies, as well as the study species and study site, can affect the accuracy and prediction of the resulting models. The methods often used to estimate AGB in grasslands by UAV imagery are similar to those used to monitor arable crops (Schellberg *et al.*, 2008). However, arable crops generally show lower heterogeneity than grasslands. Grasslands often exhibit substantial spatio-temporal heterogeneity due to highly diverse floristic compositions and co-occurrence of different phenological stages (Lussem *et al.*, 2019). This heterogeneity affects the assessment of AGB in grasslands using UAVs (Moeckel *et al.*, 2017). AGB estimation in grasslands may be inaccurate or imprecise if these aspects are not taken into account.

A comprehensive review of the different methods and factors influencing the AGB estimation in grasslands is therefore essential to understand how each stage of the process affects outcomes so that subsequent data collection and analysis can produce accurate and reliable data. Although the utility of UAVs is well known in biomass estimation in agriculture, recently developed applications of UAVs to AGB estimation in grassland ecosystems have not yet been evaluated or systematically reviewed. To date, the majority of review studies of UAV for biomass estimation in agriculture have been broad, involving numerous fields and different remote sensing systems, and the description of biomass estimation with little emphasis on grassland-specific properties. To address this gap, we systematically review the use of UAVs in the estimation of AGB in grassland ecosystems. We perform a comprehensive literature review of the topic to (1) give an overview on common practices of the use of sensors, scale of work, ground truth methods, data processing, and analysis methods and (2) to identify which spectral and structural data are most accurate with respect to AGB estimation. We conclude by discussing the challenges and future prospects of UAV

remote sensing in AGB estimation in grassland ecosystems.

2.2 Materials and methods

Using the PRISMA protocol (Moher *et al.*, 2009), we conducted a systematic review and meta-analysis of studies that use Unmanned Aerial Vehicles (UAVs) to estimate biomass in grassland systems. Figure 2.1 presents a flow diagram of the study selection process. In the identification step, relevant literature was retrieved from Google Scholar and Web of Science using search terms comprising keywords related to UAVs ("UAS", "UAV", "unmanned aerial system", "unmanned aerial vehicle") and to aboveground grassland biomass ("grass", "grassland", "pasture", "forage", "biomass", "aboveground biomass", "above ground biomass"). The search was limited to English-language research articles published from January 2011 to August 2022. We considered all types of grassland systems. This review did not consider studies classified as review papers, book chapters, reports, or Ph.D. theses.

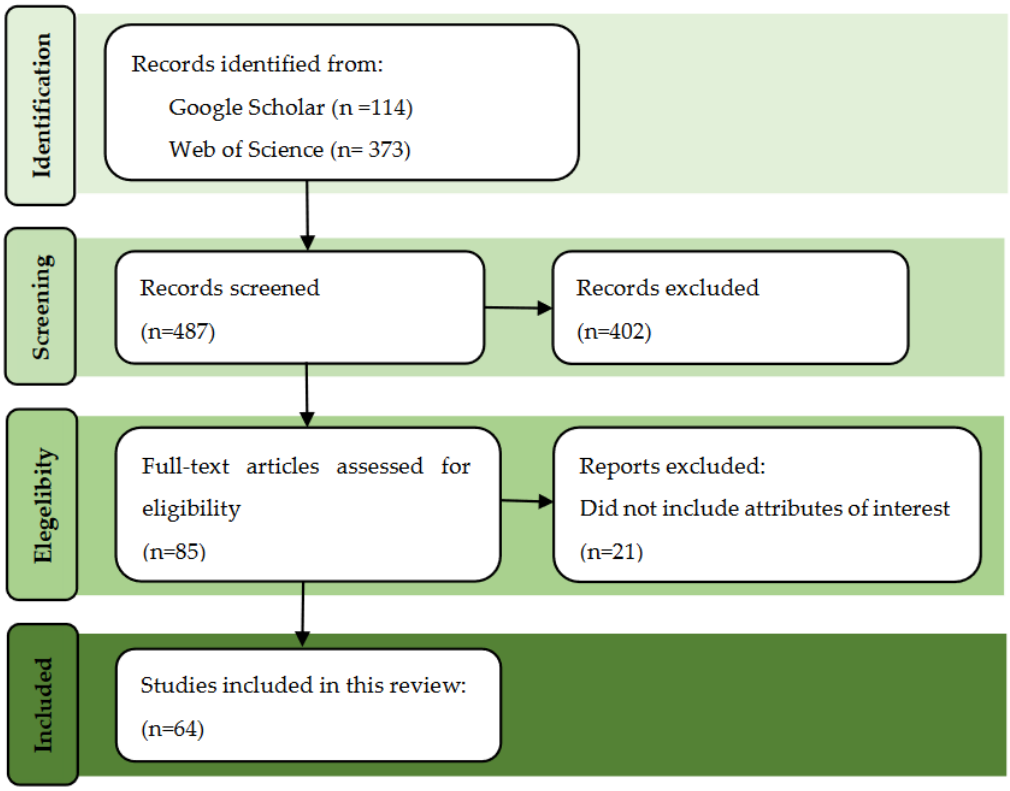

Figure 2.1. PRISMA flow diagram for study selection.

A total of 487 articles were obtained as a result of the Google Scholar and Web of Sciences searches. To be included in the review, a study was required to fulfill the following three criteria: (1) the study uses UAV and no other system type; (2) it focuses on grassland ecosystem; (3) it presents AGB estimation from UAV imagery. The articles identified in the first step were screened,

and we consulted the title and abstract. After the screening phase, 85 research articles remained. We confirmed each study's eligibility by reading the full text, after which 21 studies were discarded because they did not contain extractable data for the following four features of interest: site attributes, biomass measures, UAV platform, and sensors. In total, 64 studies were retained, which had extractable data for all four features. For each article, we extracted metadata (Appendix A), including information related to the characteristics of the study site, grassland species composition, UAV platforms, flight parameters, sensors, field measurement, biomass indices, data processing, and analysis method.

2.3 Results and discussion

An automated search of Google Scholar and Web of Sciences resulted in a final set of 64 papers that used UAV imagery to estimate AGB of grassland areas (Table A1, supplementary material). The following sections provide a detailed description of meta-analysis findings, including general features of the articles and biomass estimation data analysis.

2.3.1 General characteristics of studies

Figure 2.2a presents the locations of the 64 studies considered in this review. In total, grasslands located in 15 countries were studied. Germany accounted for the largest number of studies (N = 14), followed by China (N = 10), the United States of America (USA) (N = 7), Australia (N = 5), Belgium (N = 4), Finland (N = 5), Brazil (N = 4), Estonia (N = 3), and Norway (N = 3). Studies in Canada, Ecuador, Ireland, Israel, Japan, Spain, South Korea, and Switzerland were represented by one publication each.

Figure 2.2b presents the number of articles published annually from 2012 to 2022. The first article, published in 2014 in the USA (Y. Zhao *et al.*, 2014), used high-resolution imagery from a UAV to estimate biomass in a natural grassland site in the USA. From 2014 to 2017, only six papers were published, and subsequently, the number of publications increased steadily. Figure 2.2c shows only journals that published more than two papers. The most represented journals include Remote Sensing (16 papers), Sensors (4 papers), and Ecological Indicator (4 papers).

Considering the representation by continents, thirty-two of the sixty-four studies were conducted in European countries, twelve in Asia, eight in North America, seven in Oceania, and only five in South America, and no studies were conducted in the African continent. Although there are many significant areas of grassland in Europe and North America, which are often part of mixed farmland systems, much of the world's grassland area is located in the extensive natural grasslands of Central Asia, Sub-Saharan and Southern Africa, North and South America, and Australia/New Zealand. Considering the scenario above, the productivity of journal articles about UAV applications for AGB biomass estimation in grassland regions with the largest representation of this vegetation worldwide is generally low. Studies should preferably be carried out in grassland biomes across several areas and continents (Van Der Merwe, Baldwin and Boyer, 2020). More

numerous and diverse grassland systems should be studied in order to improve UAV applications for AGB biomass estimation in grassland, particularly grasslands in regions that will be specifically impacted by climate change (e.g., tropical regions) (Ali *et al.*, 2016), which are currently significantly under-represented in the available research survey.

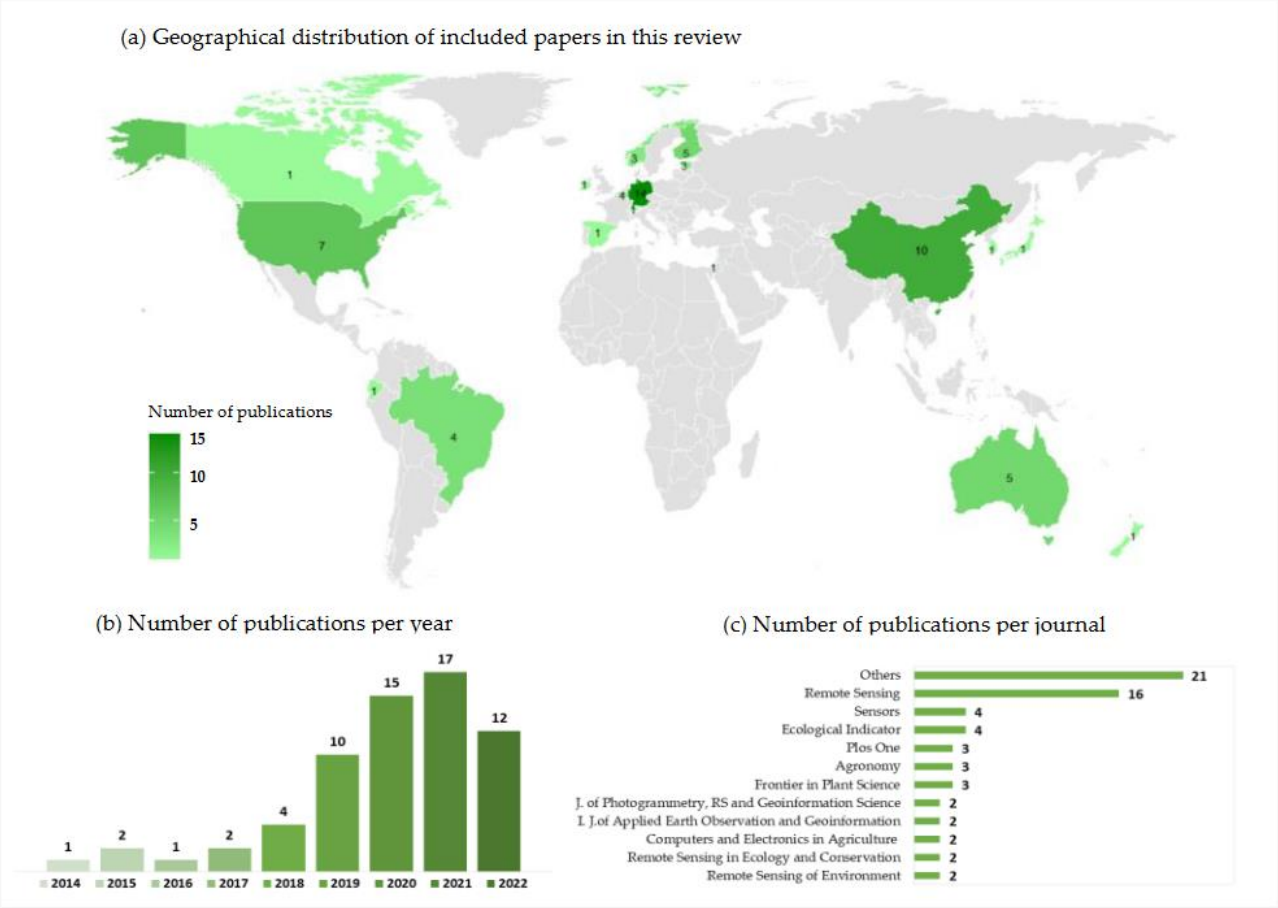

Figure 2.2. (a) Geographical distribution of included papers in this review. (b) Number of publications per year. (c) Number of publications per journal.

2.3.2 Characteristics of the study sites

Regarding the characteristics of the study sites, 64 articles reported the type of grassland. Of these, 34 studies investigated fields as experimental sites, 18 investigated naturalized grasslands, and 12 investigated grassland farms. In addition, 62 publications reported whether the site included mono or multi-species grasslands. Of these, 46 publications studied multi-species grasslands, 15 studied mono-species systems, and 1 studied both systems (mono and mixed grasses). Fertilization conditions were described in 27 publications, of which only 3 studied organically fertilized grasslands. Animal presence in the grasslands was reported in 14 studies, of which 9 analyzed the effect of grazing activities on the biomass estimation.

The heterogeneity of the experimental site is an important feature since many studies suggest that increasing the species richness of grassland can reduce AGB estimation models' performance. According to Wijesingha *et al.* (2019), biomass prediction for species-poor and homogenous grasslands had higher accuracy than biomass prediction for species-rich, diverse grasslands. Michez *et al.*'s (2020) results also suggest that the low species diversity in their experimental site (timothy-dominated pastures) probably improved the biomass modeling process. Grüner *et al.* (2021) reported that the high variability of the canopy surface in legume–grass mixtures results in lower prediction accuracy compared with more homogeneous arable crops. They achieved r2 values of 0.46 and up to 0.87 depending on the sward composition for mixed legume–grass swards and pure legumes and grass stands. Villoslada *et al.* (2020) indicated similar trends in modeling accuracies, where sites characterized by the presence of more productive communities or a higher herbage yield show lower prediction accuracies than short-sward sites.

The distinct plant architectures in heterogeneous grasslands may have an impact on image acquisition due to poor modeling of plant extremities, resulting in a larger variability than monocultures and reflecting in lower r^2 values (DiMaggio *et al.*, 2020). It has also previously been demonstrated that the complexity of sward structures, vegetation height, and plant species richness all influence the spectral properties of training samples (Villoslada *et al.*, 2020). The high heterogeneity in some grassland fields can also intensify the mixed pixel effect, an important remote sensing issue that affects the ability to monitor phenology (Adar *et al.*, 2022). This, in turn, influences the overall prediction accuracy. In addition, the potential for generalization of some studies is limited because they are based on approaches using site-specific data, which makes the relationships obtained difficult to transfer to other areas. Thus, study site selection should take into account local and regional variations, with the goal of incorporating a fair representation range of vegetation into the data collection process.

2.3.3 UAV data collection, UAV data processing, and analysis methods

In general, studies used a similar workflow to estimate AGB in grasslands using UAV data, as shown in Figure 2.3. Even though not all studies followed all of the steps, the standard process was adopted by many of the publications considered in this review. Typically, workflows included the following steps: (1) UAV imagery recording concurrent with ground control points (GCP) and ground-based field data collection; (2) UAV data processing, including pre-processing, creation of photogrammetric 3D point clouds and/or orthomosaics, georeferencing of point clouds and orthomosaics, creation of canopy height models (CHM) using digital terrain models (DTM) and digital surface models (DSM) derivate from a digital elevation model (DEM), derivation of structural, textural, and/or multispectral, hyperspectral, or RGB spectral index; (3) generation of predictive AGB models using UAV-derived variables as predictors and ground-based AGB and/or CHM, and/or vegetation index. The overall goal of the next sections is to provide a comprehensive workflow description for AGB estimation in grasslands using UAV, with a specific focus on the main elements of the three steps: (1) field data collection, (2) image pre-processing, and (3) data

analyses.

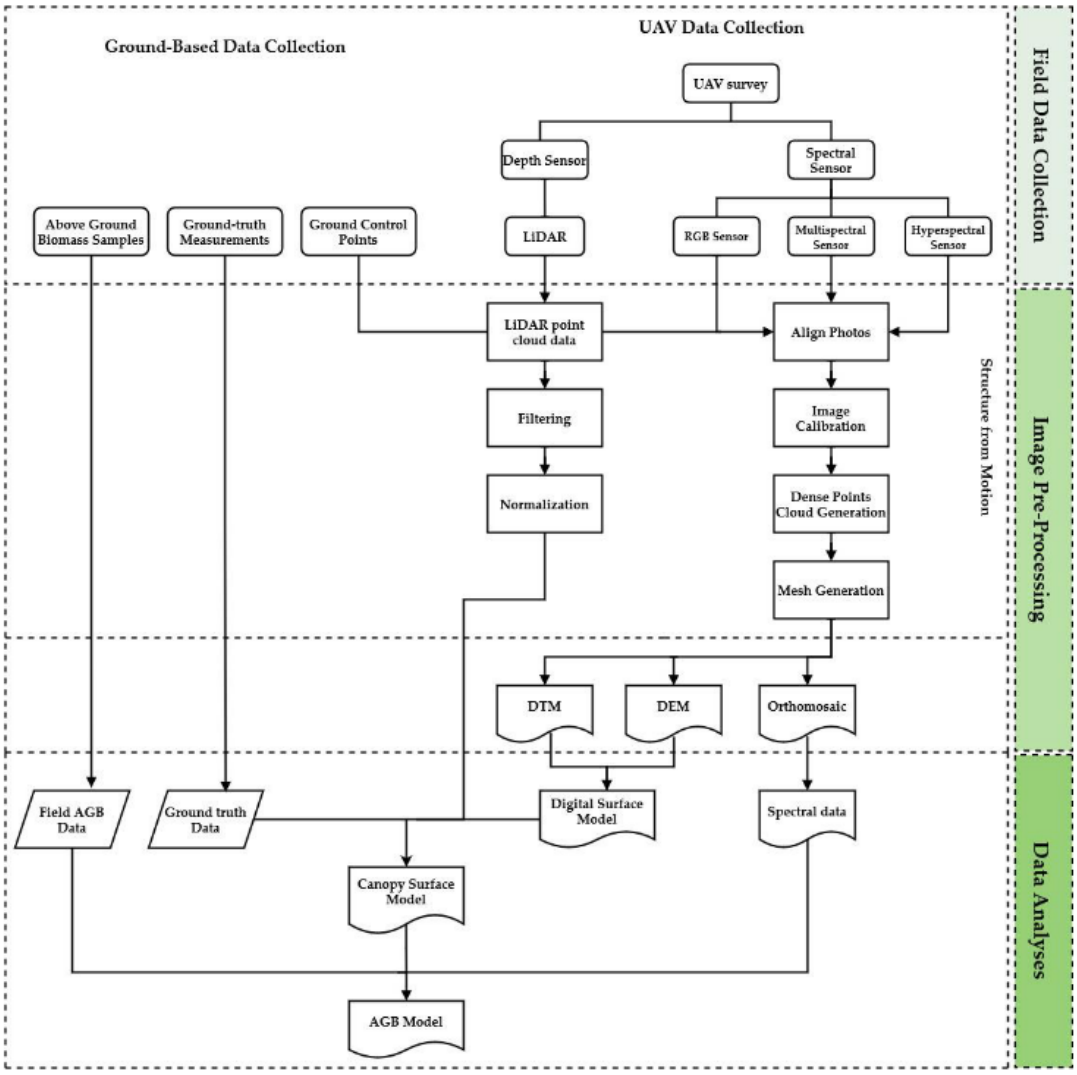

Figure 2.3. The data processing workflow by which grassland AGB model estimations are generated using Structure from Motion photogrammetry and LiDAR.

2.3.3.1 Field data collection

Data sampling as ground-based data collection and UAV flight is a critical step in AGB estimation. Some elements must be taken into consideration for an accurate data collection to ensure a reliable result. Table A2 (supplementary material) presents a summary of field data information collected from the papers reviewed. Items recorded include location, type of field, type of grassland, number of sites, UAV platform, sensors, flight altitude, image front and side overlap, number of GCPs, ground sample distance (GSD), frequency of data collection, biomass ground truth, total number of biomass samples, biomass sample size, and canopy height measurement.

Ground-based data collection

Field measurements, such as biomass sampling and plant height measurements, are established methods for biomass estimation in grassland monitoring (Bareth *et al.*, 2015). The quantitative collection of data in the field is essential to establish, train, and evaluate biomass estimation models derived from UAV images. Additionally, in grassland ecosystems, the accuracy of canopy height and AGB estimation can be improved by using ground-measured data for calibration (Zhang *et al.*, 2021). Grasslands typically have heterogeneous vegetation, and species contribution and yield vary in the field throughout the growing season, being influenced by different factors such as cutting intensity, soil management, and fertilization (DiMaggio *et al.*, 2020). For reliable and precise biomass estimations in areas with such complex vegetation variety and high dynamics, sampling should be performed on a frequent temporal basis and with a large number of samples (Franceschini *et al.*, 2022). Morais *et al.* (2021) reviewed the use of machine learning to estimate AGB in grasslands and concluded that the size of the field sampling is the most important factor to improve estimation accuracy, and increasing the size of the datasets should be one of the main priorities to improve the estimation models.

Regarding the frequency of the sampling, most parts of the studies performed only one field sampling (n = 25). The study of Borra-Serrano *et al.* (2019) had the highest sampling frequency, with 22 collections in one year. The average number of field samples was 90, and the range was between 13 and 1403. According to Geipel *et al.* (2021) the capacity of a model to perform well when applied to new scenarios improves with the size and variation of the calibration dataset, and many researchers have too small datasets to produce generalizable models. Qin *et al.* (2021) concluded that, despite taking into account the spatial heterogeneity of AGB in vegetation patches, they are unable to validate the applicability of inversion results for each grassland type due to the small sample size. Capolupo *et al.* (2015) also suggest that a larger and more representative training model sample size would improve model accuracy in their study. The intrinsic complexity and repeatability of field trial design, as well as the small sample size, were also constraints in the study of Lin *et al.* (2021).

Compared to crops, the heterogeneous sward structure with high spatiotemporal variability in grasslands has the potential to alter the spatial distribution of biomass depending on the growth stage. As the results indicate, most studies use data from a minimal time span (e.g., a fraction of the growing season), limiting the ability to predict biomass in these complex and dynamic environments. When biomass prediction models are calibrated to the site, year, and even phenological stage of dominant plants, they become more robust (Cunliffe, Brazier and Anderson, 2016). In addition, the frequent collection of data over the course of the growing season could ensure that the dataset is diverse and that the models can be applied to various locations (Van Der Merwe, Baldwin and Boyer, 2020). In this sense, Lussem, Schellberg and Bareth (2020) recommended evaluating different swards under varying conditions and sites over multiple years. Pranga *et al.* (2021) evaluated several growth periods, but the observation period was only one year with three cutting treatments. They also suggested that future research should incorporate data from

other seasons/years, as well as different locations/conditions.

Regarding the AGB data collection method, samples were collected manually in 22 studies, mechanically in 20, and both methods in two studies. In seven studies, the method to collect samples was not specified, and in two studies, biomass samples were not directly collected but estimated by RPM calibration. There were two main procedures to sample AGB on the ground, collecting from quadrants or harvesting the entire plot. The sizes of the quadrants used for sampling varied between papers from 0.01 to 1 m^2. The most frequently used sizes were 0.25 m^2 (16 papers) and 1 m^2 (13 papers). The mechanical collection was the method used for all studies that sampling the entire plot and the size of the sampling ranged from 1 to 19.5 m^2.

Morais *et al.*'s (2021) review concluded that the data collection procedure had a minimal impact on AGB estimation in grassland using machine learning methods. In their study, the average r^2 was lowest for the papers that used manual cutting (0.65) compared to mechanical harvesting (0.75). However, these findings are not statistically significant and are primarily a result of the different number of observations. We found comparable results, with an average r^2 for manual cutting of 0.68, which was lower than the r^2 observed for mechanical harvesting (0.82). These results can also indicate that the number of observations can have a greater impact on the accuracy of AGB estimation than the collection procedure. In fact, similar to Morais *et al.*'s (2021) results, we found that studies that employed manual cutting had both the lowest and greatest r^2 values (0.25 and 0.98). It should be noted, however, that the study with the lowest r^2 used 96 samples (Zhao *et al.*, 2022), whereas the study with the highest r^2 used 520 samples (Villoslada Peciña *et al.*, 2021).

The plant cutting height is possibly a significant factor to take into account when collecting AGB samples in the field since it is challenging to cut vegetation right at ground level. Grassland biomass is distributed vertically in a pyramidal pattern, with increased biomass density closer to the ground (Tackenberg, 2007). In an Irish meadow, 40–60% of total biomass was distributed 0–10 cm aboveground, 30% was 20–30 cm aboveground, and less than 20% was more than 30 cm aboveground (Beltman *et al.*, 2003). Only 17 of the studies included in this review reported the cutting height, which ranged from 2 to 10 cm above the ground. However, just two studies mentioned a height correction in the terrain model to compensate for the cutting height. In order to reduce the impacts of any residual stubble, Borra-Serrano *et al.* (2019) used a correction factor of 5 cm to their baseline DTM. Karunaratne *et al.* (2020) applied a constant offset of 7 cm to baseline DSM to compensate for the mowing height and pasture accumulation prior to the first measurement period. In this way, considering the distribution pattern of biomass in grasslands, we recommend that future models account for this factor to try to reduce discrepancies in reported results.

As for canopy height measurements, 29 studies did not mention the use of these data for biomass estimation. At least three studies mentioned the use of canopy height data in the field for biomass estimation but did not specify the data collection method. Of the 22 studies that used canopy height for biomass estimation, 11 used a ruler, tape, or height stick. In eight studies, the RPM was used to measure compressed canopy height. In three studies, field equipment such as a ground-based platform (PhenoRover) (Gebremedhin *et al.*, 2020), Lidar Laser Scan (Michez *et al.*,

2019), and the Rapid Pasture Meter (machine) (Insua, Utsumi and Basso, 2019) was used.

Most studies using SfM (Structure from Motion) to derive canopy height models for grassland have obtained reference measurements in the field with a height stick or a ruler and RPM since this equipment is more accessible and easier to use than mechanical equipment. However, because grassland plants differ significantly in canopy height, single or multiple tiller height measurements using manual methods would inevitably result in uncertainty about canopy height (Li *et al.*, 2020). Batistoti *et al.* (2019) reported a high correlation between height measured with a ruler and a UAV with a multispectral sensor ($r^2 = 0.89$).The canopy heights estimated from UAV imagery and those measured using the ruler varied by about 8 cm. When comparing canopy surface models from UAV with manual reference measurements from height sticks, Grüner, Astor and Wachendorf (2019) achieved r^2 values of 0.56 to 0.70 depending on the sward structure, species composition, and growing stage, while Viljanen *et al.* (2018) report r^2 values of 0.61 to 0.93. Zhang *et al.* (2021) also found that even though LiDAR-derived canopy height was lower than the ground-measured data, it showed a strong correlation with the height measured with a ruler ($r^2 = 0.92$). Wang *et al.* (2017) reported that when compared to ground data measured with a ruler, LiDAR consistently overestimated the canopy height.

Because it effectively analyzes both canopy height and density, RPM is one of the most frequently used techniques for physical measurements of grassland sward height and the assessment of standing biomass (Vogel *et al.*, 2019). Bareth *et al.* (2015) report r^2 of 0.89 between RPM measurements and UAV-derived sward height. According to Lussem *et al.* (2019), the performance of low-cost UAV-derived DSMs for estimating forage mass varies ($r^2 = 0.57–0.73$) depending on the harvest cut, but RPM measurements outperform the UAV model. However, canopy density, architecture, and plant developmental stage limit the accuracy of linear connections between RPM-based measurements and biomass. The results of some studies suggest that the agreement between the RPM and the UAV-borne equipment for measuring canopy height varied depending on canopy height and that the agreement was negatively impacted by low and high canopy heights in general (Bendig *et al.*, 2015; Viljanen *et al.*, 2018; Borra-Serrano *et al.*, 2019). RPM measurements demonstrated lower accuracy in sparse swards or tall, non-uniform canopies but better accuracy in dense swards and when the canopy has reached a height of 20–30 cm (Viljanen *et al.*, 2018). This inconsistency could be caused by the compression of the pasture induced by the RPM and canopy closure at high canopy heights. In the case of low canopy heights, this inconsistency may be caused by the ground being visible in the images, which reduces the digital surface model as a result of the photogrammetry software's point cloud interpolation. Considering this, RPM seems more suitable for measuring low grasses in their early phases of development.

Despite the significance of ground truth data for AGB model estimations, it is critical to remember that the available methodologies for measuring AGB and canopy height ground-based can also be subjective (Poley and McDermid, 2020). In addition, usually, ground truth data are either measured at a few locations in the field or at a single point on a plot and therefore do not

necessarily provide a complete representation of the region of interest. In this way, in order to improve the validity of the ground-measured biomass data, it is important to take into account the limitations of the method and the biases of over- or under-estimate canopy height and AGB.

UAV platforms

Multirotor platforms were the most commonly used UAV systems in the reviewed studies (87.66%), among which the quadcopter was the most widely deployed (58.46%) (Figure 2.4). In a review of studies on the use of UAVs and machine learning for agro-environment monitoring, Eskandari *et al.* (2020) reported that fixed-wing models were the most used between 2015 and 2018. However, from 2018 to 2019, there was an increase in the use of quadcopter and hexacopter models, and these became the most used. Multirotor UAVs have increased in popularity since they are extremely versatile, with the ability to hover, rotate, and take images from nearly any angle. However, multirotor UAVs also present some disadvantages. Due to their vertical takeoff and landing and ability to hover, multirotor platforms demand more energy to fly, resulting in reduced sustainability and shorter flight periods (Poley and McDermid, 2020). If the survey height is low, backwash from the rotors may affect the vegetation being monitored by producing plant movements (Willkomm, Bolten and Bareth, 2016). Multirotors are sometimes associated with inadequate Global Positioning System (GPS) receivers, which can lead to decreased position accuracy, particularly in hilly places where GPS coverage is limited (Eskandari *et al.*, 2020). When compared with fixed-wings, the most significant disadvantage of rotor UAVs is their short range and flight time (Wang *et al.*, 2021). Fixed-wing aircraft tend to have a faster top speed, a longer flying time, and a greater range than rotorcraft. Fixed-wing systems are useful for collecting data across broad areas for these reasons. Nonetheless, fixed-wing aircraft have less mobility and require more landing space.

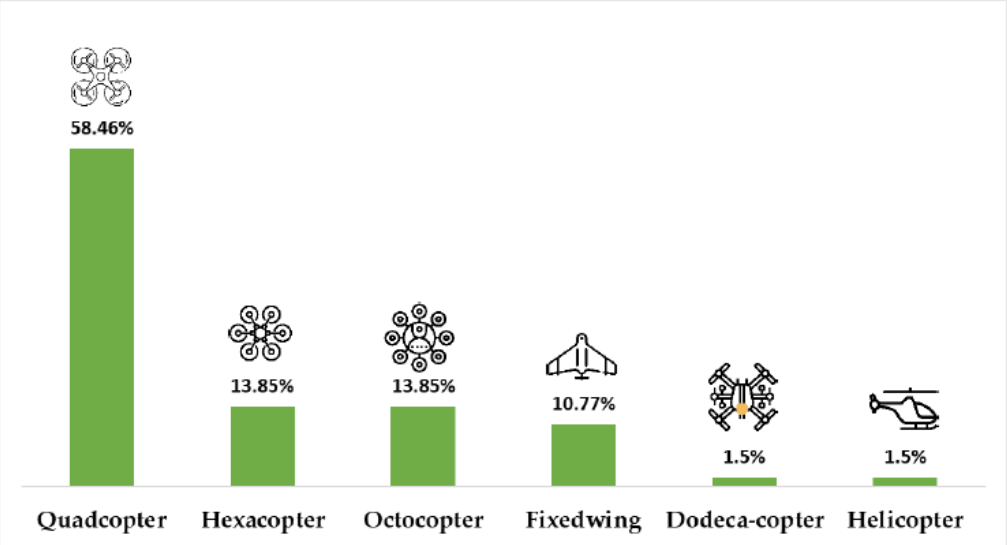

Figure 2.4. UAV platform types utilized per article.

According the review study of Poley and McDermid (2020), there is no consistent difference

in the accuracy of the biomass estimate model between studies using fixed-wing and multirotor platforms, and the selection of UAV platform depends on the research objective. A fixed-wing could be suitable if the study area is extensive, as in natural grasslands or larger grassland fields. A multirotor would be preferable for smaller and more challenging places, such as small grasslands and heterogeneous fields, where detailed vegetation imagery from a more stable platform is required.

Flight parameters

Multiple interconnected elements during the UAV flight influence the quality of UAV-based outputs and, consequently, the AGB estimation. Because the precision of the output terrain data is determined by the accuracy of estimating tie points—and as a result, the reconstructed surface geometry—flight altitude is an important parameter. Reduced flight height results in smaller coverage areas, an increase in the number of flight missions required for a specific study site, and potentially increased variability in environmental conditions (e.g., cloudiness, sun angle), which complicates radiometric adjustment and decreases spectral accuracy. On the other hand, increasing altitude shortens flight time and allows one to cover larger areas, which can be important for maintaining relatively constant environmental conditions during the flight mission (Tmušić *et al.*, 2020). Higher altitude flights produce sparser point spacing, resulting in a less detailed DSM. For low-altitude flights, the result is a more irregularly shaped DSM, and these effects must be considered (Colomina and Molina, 2014).

The 64 studies reviewed here deployed UAV flights at altitudes ranging from 2 to 120 m. The two flights with the lowest altitudes of 2 m were carried out in two studies by Zhang *et al.* (2018, 2022) that evaluated the use of high-resolution images in generating quadratic models. The highest altitude flight (120 m) was carried out by Wang *et al.* (2017) in a study testing if the relationship between tallgrass AGB measurements and spectral data is constant at different image spatial resolutions associated with different flight altitudes. The modal value for UAV altitude was 50 m (23% of studies), followed by 30 m (16%), 20 m (14%), 120 m (10%), 40 m (8%), less than 10 m (8%), 100 m (6%), 25 m (3%), 70 m (3%), 35 m (2%), 80 m (2%), 140 m (2%), 75 m (1%), 110 m (1%), 115 m (1%), and 120 m (1%).

Considering that plants and particularly grass leaves can be as thin as 2 cm, a higher spatial resolution may improve texture resolution and, as a result, biomass prediction accuracy. In the studies addressed in this review, most of the flights were performed at altitudes considered low (less than 100 m), with the most commonly used altitude being 50 m. Wang *et al.* (2014) reported that surveying at 5 m above the canopy was more accurate than surveying at 20 or 50 m above the canopy in a tallgrass prairie ecosystem Grüner, Wachendorf and Astor's (2020) study with different flight heights of 50 and 20 m resulted in an image resolution of 2–4 cm, which then had to be resampled to 4.5 cm. These authors recommend that different ground resolutions should be avoided in future studies to keep unified conditions for data analysis. Viljanen *et al.* (2018) employed 30 and 50 m flight heights to estimate AGB in a mixed grassland field. The results for the 30 m flights produced lower reprojection errors (0.53–0.58) than the 50 m flights (0.783–1.25). The flights from

a 30 m flying height also provided slightly better 3D RMSE (2.7–2.9 cm) than the 50 m flying height (2.8–5.0 cm). Näsi *et al.* (2018) estimated grassland AGB using two flying heights of 50 and 140 m. Their study suggested that although employing datasets from 140 m produced promising results, adopting lower-height data can enhance AGB estimations.

The results obtained by DiMaggio *et al.* (2020) indicate that flying at 50 m height can increase the area that is covered without considerably losing AGB estimation accuracy. The authors also recommended testing different altitudes to understand the relationship between pixel resolution and field data for AGB estimation. Karunaratne *et al.* (2020) also evaluated the influence of different flight heights in their grassland AGB estimation models. The results indicate that the model generated at 25 m outperformed the other flying altitude models. However, the authors pointed out that, practically speaking, acquiring UAV data at a 100 m altitude provides a lot of benefits for farm-scale applications: (a) more coverage of the land extent, (b) faster UAV data acquisition, and (c) smaller file sizes that allow for faster pre- and post-processing of collected datasets.

In this way, to establish best practice guidelines for using UAVs for on-farm applications and to adapt to changing technological advancements, it is also necessary to better understand the impacts of flying at various altitudes on the prediction quality of grassland AGB models. We also recommend that considering the specifications of the employed sensor, researchers should establish what GSD is necessary for identifying features of interest to AGB estimation. Then, in order to balance the necessary spatial resolution, tolerable error, and point cloud density with the most effective coverage of the study region, fly at the highest altitude where this GSD is possible (Poley and McDermid, 2020).

The sequence in which the UAV flies also has an impact on data quality. The determination of forward and side image overlap is an important part of mission planning, especially for SfM photogrammetric reconstructions, which require features observed in multiple photos for building digital models, orthomosaics, and 3D models. The percentage of image overlap can affect the quality of the final SfM product, with more overlap leading to more precise final models. High overlap, on the other hand, necessitates the acquisition of more photos, increasing data volumes and computing time (Tmušić *et al.*, 2020). There are optimal overlap thresholds for specific vegetation types based on the surveyed area's specific characteristics and type of study. Agriculture fields and grasslands, which have low feature diversity and a relatively flat topography, demand a higher percentage of overlaps in order to extract tie points for the SfM algorithm (Eskandari *et al.*, 2020). Many studies examined in this review have employed considerable front and side overlap (median of about 80–70%). In the majority of the studies, a forward overlap of 80% and a side overlap of 60–75% resulted in high-quality orthoimages. The data are in agreement with the study by Eskandari *et al.* (2020), which points out that the median for forward and side overlap is 80% and 70%, respectively, for UAV flights carried out in grasslands. Viljanen *et al.*'s (2018) results also confirmed the main conception that the large image forward and side overlaps of approximately 80%, combined with self-calibration during photogrammetric processing, can

provide a non-deformed photogrammetric block.

Sensor technology

UAVs' ability to fly considerably closer to the ground than satellites or full-scale manned aircraft expands the range of sensors available and the spectral imaging. The spectral data obtained by an UAV can be simple RGB (red–green–blue) from an off-the-shelf camera or more specialized when employing multispectral, thermal, or even hyperspectral cameras. Among the studies reviewed here, visible sensors (RGB) are the most commonly employed sensor technology (48% of studies), followed by multispectral (29%), hyperspectral (16%), and LiDAR (Light Detection and Ranging) (7%) (Figure 2.5a). In terms of resolution, the sensors used in sensing can be classified as high resolution (between 0 and 10 cm), medium resolution (10 to 20 cm), and low resolution (more than 20 cm) (Eskandari *et al.*, 2020). The most commonly used data sources across the research are of high spatial resolution ranging from 0 to 10 cm (Figure 2.5b). Most studies (>80%) used data at high spatial resolution (0 to 10 cm), with visible and multispectral images being the preferred image types. Very few (<4%) studies used image data at low spatial resolution (>20 cm).

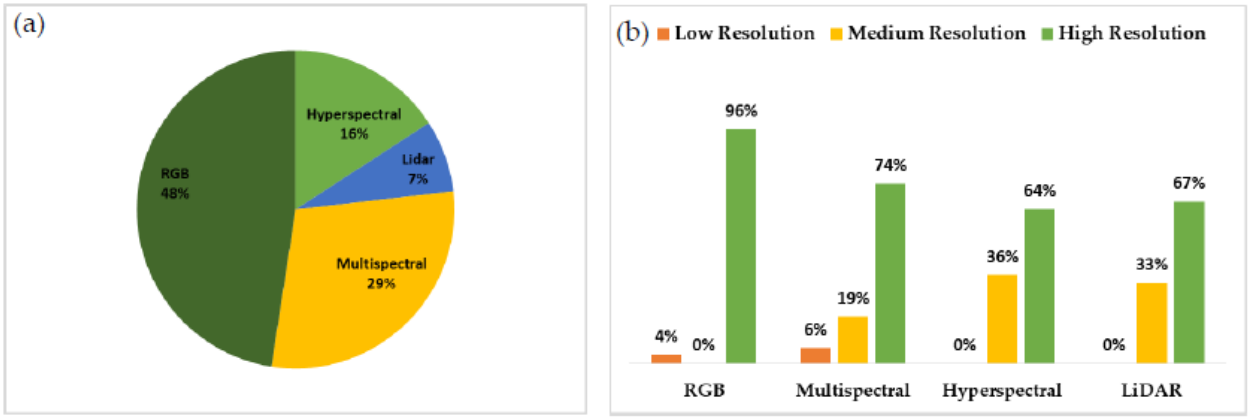

Figure 2.5. (a) Number of studies per sensor technology. (b) Image spatial resolution vs. sensor type.

The increasing number of UAVs equipped with RGB commercial cameras has facilitated research using these low-cost sensors for grassland monitoring (Bareth and Schellberg, 2018; Lussem, Schellberg and Bareth, 2020). Compared to multispectral, hyperspectral, or thermal sensors, RGB sensors have a lower spectral resolution but a higher spatial resolution, and it is possible to calculate vegetation indices and estimate plant height from the same set of photographs. RGB sensors are also a more economical option, which is a significant benefit, especially for farm-scale applications.

Near-infrared (NIR) multi- and hyperspectral sensors have become more commonly accessible for UAVs over the past decade (Manfreda *et al.*, 2018). Initially, researchers used modified off-the-shelf RGB and near-infrared (NIR) cameras, as in the studies of F. Zhao *et al.* (2014), Lee *et al.* (2015), and Fan *et al.* (2018). These modified off-the-shelf RGB cameras were then replaced by specialized multispectral or hyperspectral cameras, which have decreased in cost and weight.

Multispectral cameras, along with RGB cameras, are among the most commonly used sensors in the studies examined (30%). Multispectral sensors (e.g., MicaSense RedEdge 3 camera, Micasense, WA, USA) provide more spectral bands (e.g., red edge: 760 nm; near-infrared (NIR): 810 nm). The advantages of obtaining more spectral information for vegetation applications at an extremely high resolution collaborated for the increase in the use of multispectral sensors. The availability of a downwelling light sensor and radiometric calibration target are also key advantages of multispectral images. This allows the images to be radiometrically calibrated for repeatable and exact measurements less affected by environmental factors (Pranga *et al.*, 2021). Hyperspectral sensors also measure reflectance in a wide range of spectral wavelengths. Such data are frequently processed into 3D point clouds utilizing Structure from Motion (SfM) procedures to offer information about the structure, texture, and variability of grassland areas (Poley and McDermid, 2020). This integration offers a lot of potential for accurate AGB estimation in grasslands. Especially when specific or many wavelengths are desired, multispectral and hyperspectral sensors can be used to obtain precise estimates of AGB. However, hyperspectral and multispectral sensors are still significantly more expensive than digital RGB cameras, which may be a drawback in farm-scale applications.

Even with the limitation on the spectral resolution range, the indices generated by RGB sensors can be cost-effective and have been applied in grassland for biomass estimation with acceptable or high levels of accuracy (Näsi *et al.*, 2018; Lussem *et al.*, 2019; Lussem, Schellberg and Bareth, 2020). When evaluating several sensor types for detecting biophysical properties of vegetation, multiple studies discovered that RGB data from low-cost digital cameras produced AGB estimations comparable to or better than data from more expensive multispectral or hyperspectral sensors (Näsi *et al.*, 2018; Grüner, Astor and Wachendorf, 2019, 2021; Lussem *et al.*, 2019). Few studies compared results from different sensors among the articles investigated for this review. However, in the studies that compared sensors, in most cases, there was no significant difference in accuracy in AGB estimation between RGB and other sensors. Lussem *et al.* (2019) confirmed the potential of RGB techniques in AGB grassland modeling, achieving equivalent performance (r2 = 0.7) using RGB or multispectral VIs. Näsi *et al.* (2018) also stated that RGB can produce good results for AGB grassland modeling, even though it is inferior to the results of hyperspectral sensors. Compared with multispectral or hyperspectral imaging, the higher spatial resolution of RGB imagery could probably influence its ability to predict vegetation biomass more accurately (Grüner, Astor and Wachendorf, 2019, 2021).

The spectral resolution of UAV visible sensors is anticipated to continue to increase. Given the affordable prices, this platform will continue to be heavily utilized in AGB estimates in grasslands. However, because the passive optical sensors mostly collect data from the top of the vegetation, there is little information available regarding the vertical structure of the vegetation, which limits the biomass estimate's accuracy. Another issue with optical imagery techniques is the possibility of natural light saturation when detecting high-density biomass plants.

Compared to optical sensors, LiDAR is an active remote sensing technology that can capture

the vertical structure and height of vegetation as well as the three-dimensional coordinates of the target (Figure 2.6) (Wang *et al.*, 2021). LiDAR sensor is also unaffected by lighting conditions. In grassland ecosystems, UAV LiDAR has recently been employed to estimate canopy height and AGB. The study of Wang *et al.* (2017) demonstrated that the LiDAR sensor has high potential for providing highly accurate grassland vegetation measurements, such as canopy height and fractional cover, which can then be used to estimate AGB on a large scale. The authors, however, pointed out that LiDAR alone would underestimate grassland canopy height and that field data calibration is required to achieve centimeter-level accuracy. Li *et al.* (2020) concluded that incorporating LiDAR data considerably improved the performance of the spectral index in modeling and estimating AGB in grasslands in a non-destructive manner. Zhang *et al.*'s (2021) results demonstrate that grassland AGB can be estimated using UAV LiDAR data under various grazing intensities.

The study by Zhao *et al.* (2022) indicates that, despite the tremendous potential for grassland AGB estimation, UAV LiDAR's sensor has a propensity to miss canopy data at canopy tops in grassland ecosystems. The canopy information loss can occur because UAV LiDAR collects data using a top-to-bottom view, and laser pulses may not completely penetrate the vegetation canopy. The challenge for UAV laser pulses to penetrate the canopy is further increased by the density of grassland vegetation, which may be, in some cases, much higher than in a forest (Xu *et al.*, 2020). According to Zhang *et al.* (2021), the propensity of LiDAR sensors to not completely penetrate the high-density grassland canopy and the difficulty in receiving returns from the ground led to an underestimation of most canopy heights and the majority of fractional covers in the LiDAR data. As these attributes are used for AGB estimation, an underestimation in the data can lead to limitations in AGB estimation from LiDAR data.

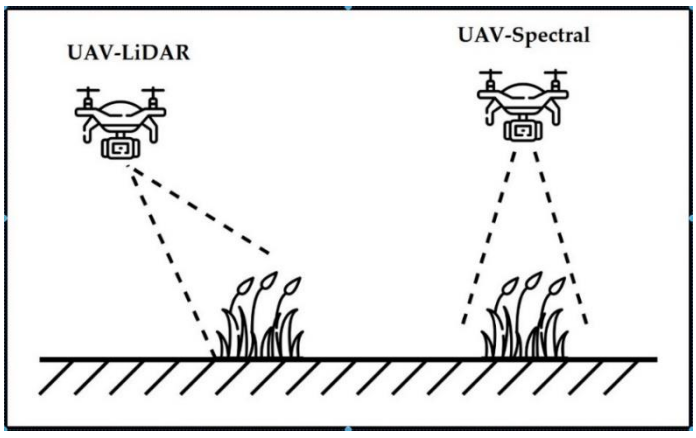

Figure 2.6. A schematic illustration of the difference between LiDAR and spectral data capture (adapted from Wang *et al.*, 2021).

Despite these limitations, LiDAR has been shown to outperform image-based techniques in terms of ground point capture and physical biomass parameter estimation (Madec *et al.*, 2017), making it a promising technology for AGB estimation in grasslands. Nevertheless, in practice, the fact that commercial LiDAR sensors adapted for UAVs are still substantially more expensive than

spectral sensors emphasizes the need to carefully evaluate the most cost-effective sensor for each specific aim.

2.3.3.2 Image pre-processing

The data collected by the UAV cannot be utilized directly to estimate biomass. In this way, a preprocessing step is usually included to guarantee that the data are suitable for further processing. Images taken from a UAV flight can be converted into 3D data using SfM-based software. Then, several objects can be classified from 3D data. Different companies have offered software solutions for processing photographs captured by UAVs, including functionalities for generating 3D spatial data for use in GIS (Geographic Information Systems) platforms, digital terrain and elevation models, generation of georeferenced orthophotos, and area and volume measurements. The different SfM software packages use different algorithms and processing options, which can affect the final outputs (Smith, Carrivick and Quincey, 2015). Of the 51 papers that mentioned the use of processing software, 52% (28 papers) used Agisoft Metashape (Agisoft LLC, St. Petersburg, Russia) to process UAV imagery data, followed by Pix4Dmapper (Pix4D, S.A., Lausanne, Switzerland) with 32% (17 papers). Furthermore, five papers employed other software, such as QGIS, ArcMap, and TerraScan.

None of the papers assessed in this review compared image preprocessing software, but previous studies have used Agisoft Metashape and Pix4Dmapper programs and evaluated the performance of both types of software. Kitagawa *et al.* (2018) captured characteristics from two experiments and compared them. Agisoft Metashape exhibited a clearer image but poor displacement extraction, whereas Pix4Dmapper had a z-value fluctuation but excellent displacement extraction. Isacsson (2018) also examined the orthomosaic accuracies created from the same survey using Pix4Dmapper and Agisoft Metashape and also found that using Agisoft Metashape results in larger x and y position errors, whereas using Pix4Dmapper results in higher z error. Fraser and Congalton (2018) compared the Agisoft Metashape and Pix4Dmapper software packages over a forested area of 235.2 ha. They concluded that Agisoft Metashape produced more detailed UAS-SfM outputs.

GCPs are high-visibility materials that are georeferenced using the Global Positioning System (GPS) after they are placed in a visible site to provide a point of reference for determining the position of the UAV in the area being photographed. By identifying GCPs with known coordinates visible in the imagery, a transformation that describes the relationship between the point cloud coordinate system and a real-world coordinate system can be used to georeference the point cloud that results from the reconstruction of SfM data (Dandois and Ellis, 2013). Among the papers evaluated in this review, at least 62% (N = 33) mentioned the use of GCPs for the geometric correction of UAV images.

Reliable ground reference data are necessary for successful georeferencing (Eskandari *et al.*, 2020). Hence, the quantity and location of GCPs at the study site are crucial (Poley and McDermid,

2020). The geometric accuracy of surface and terrain models created from UAV imagery is likely to improve with more GCPs (Borra-Serrano *et al.*, 2019; Wijesingha *et al.*, 2019). In the study of Wijesingha *et al.* (2019), the small number of GCP was pointed out as a possible reason for the limitations of the DSM generated from the UAV data. The authors used only four GCP, which is the minimum for proper geo-referencing. They concluded that increasing the number of GCPs could increase the precision of SfM data and improve the model performance. It is also critical to place GCPs correctly (Poley and McDermid, 2020). The use of ground control points only around the edges of the study area rather than within plots can reduce the accuracy of surface and terrain models, so more GCPs should be placed throughout the entire area of interest (Roth and Streit, 2018). Borra-Serrano *et al.* (2019) reported that as grasses grew taller, GCP targets became more challenging to detect in imagery due to elongated plants. They recommended opening the area around the targets to guarantee they can be seen in all images throughout the growing season.

After the geometric correction step, the georeferenced sparse cloud is converted into a dense point cloud. The software computed the depth information by the image alignment for all points of the images. In the last step of pre-processing, the dense point cloud can be exported in the form of a DEM. DEMs are used to build a CHM of the grassland field (Figure 2.7). For this purpose, two types of DEMs are usually built: (1) DTM, corresponding to the ground, and (2) DSM derived from the imagery collected with the presence of canopy on the terrain.

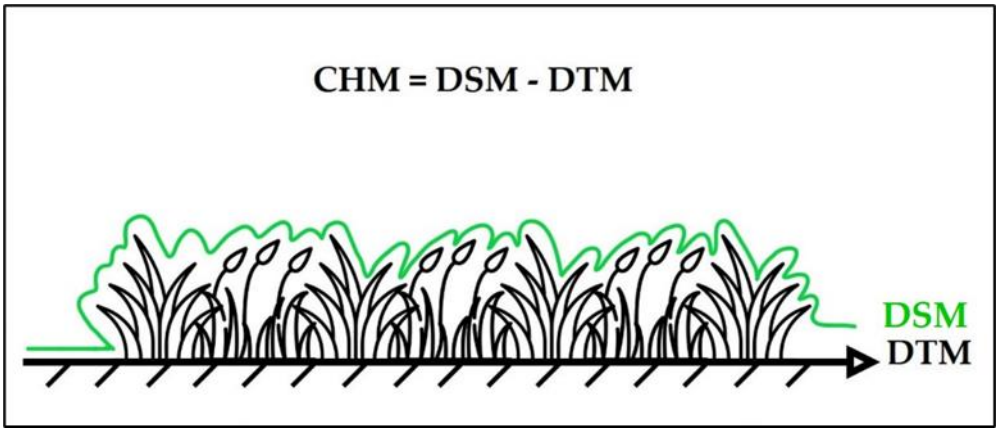

Figure 2.7. Graphical illustration of relation between digital surface model (DSM), digital terrain model (DTM), and canopy height model (CHM).

There are two main methods for extracting CHM information from UAV data. One method is to generate both DSM and DTM in raster format. This method considers the difference between DSM and DTM as the CHM Viljanen *et al.* (2018). This method is relatively simple, and since the analysis is carried out using raster analysis, the calculation is quick. However, applying interpolated DSMs and DTMs may lead to unwanted data smoothing. In the context of heterogeneous pasture growth, the use of such datasets could lead to the loss of information regarding the variability of CHM (Karunaratne *et al.*, 2020). The second method uses the raw SfM point cloud dataset instead of an interpolated DSM raster. To determine CHM for every single point in the point cloud, the

difference between the interpolated DTM raster of the study region is used (Wijesingha *et al.*, 2019). Viljanen *et al.* (2018) evaluated both methods and concluded that both provided similar DTMs and correlations to the AGB in grasslands.

A high-quality DTM with precise and accurate terrain representation is critical for extracting reliable estimates of vegetation structure from UAV imagery and therefore produce a reliable AGB estimation (Poley and McDermid, 2020). In areas with a dense vegetation canopy, such as some grassland fields, producing high-quality DTMs can be challenging (Schucknecht *et al.*, 2022). Zhang *et al.* (2018) pointed out that the density of grassland influenced the quality of DTM generated by an RGB sensor. An accurate DTM could not be produced because there were not enough ground points if the vegetation density was too high, but it was simple to extract ground points if it was moderate. In an ideal scenario, a reference DTM would be created beforehand when there is no vegetation, but this is not feasible, for example, in natural grasslands (Théau *et al.*, 2021). When a DTM is unavailable to represent the bare ground, point cloud classification is a frequently used technique to discriminate ground points (DTMs) and canopy height points (CHMs) from the same set of images (Näsi *et al.*, 2018). Batistoti *et al.* (2019) also found a solution by manually collecting GPS points to create the DTM, but this method is too time-consuming for large grassland fields. Alternatively, hybrid approaches combining SfM-derived DSMs with DTMs derived from LiDAR sensors have been explored (Michez *et al.*, 2020). Even so, special attention should be paid to potential errors in the LiDAR DTM, which is primarily based on ground point density and terrain variability. It is also important to notice that although producing input data such as DTM is a relatively simple task with LiDAR, the costs to obtain such products are high compared to RGB-only imagery (Castro *et al.*, 2020).

2.3.3.3 Data analyses

The ability of UAV image-derived models to accurately predict AGB is influenced by a variety of parameters connected to analysis methodologies. Table A3 (supplementary material) summarizes the data analysis methods and essential results of the 64 papers considered in this review.

Most studies used statistical regression methods such as linear regression (LR), polynomial regression (PR), stepwise linear regression (SWL), multiple linear regression (MLR), and partial least squares regression (PLSR). LR was the most commonly used method (n = 25). PLSR was used in 13 studies and MLR in 9 studies. Viljanen *et al.* (2018) obtained the highest r^2 value (r^2 = 0.98) with MLR in a mixed grass experimental site using an RGB and HS sensor. The lowest r^2 value (r^2 = 0.25) was obtained by Zhao et al. (Zhao *et al.*, 2022) with SWL to estimate AGB in a mixed natural grassland field using a LiDAR sensor. Among the machine learning methods, random forest (RF) was the most popular and was employed by 16 studies. The highest median r^2 among all the papers assessed was obtained by Villoslada Peciña *et al.* (2021) with RF and MLR (0.981), followed by Oliveira *et al.* (2020) also using RF and MLR (0.97). RF has demonstrated competitive accuracy in biomass estimation when compared to other estimation methods used in agricultural applications (Näsi *et al.*, 2018). Morais *et al.* (2021) reviewed the use of machine

learning to estimate biomass in grasslands. RF was also the method with the most applications, followed by PLSR.

The results of the different studies are highly variable and difficult to compare since they substantially depend on the type of grassland being monitored, the sensor (RGB, multispectral, hyperspectral, LiDAR), the usage of ground data, and 3D data. In the case of Zhao *et al.* (2022) for instance, the lower result can be explained by the loss of canopy information in UAV LiDAR, which is an important factor influencing the estimation accuracy of AGB. Wang *et al.* (2017) found comparable results ($r^2 = 0.34$) using a linear regression model and UAV LiDAR to estimate AGB in an experimental grassland site. On the other hand, da Costa *et al.* (2021) estimated AGB in a natural grassland using UAV LiDAR and simple linear regression but obtained a higher r^2 value ($r^2 = 0.78$).

Evaluating the result from different papers that use machine learning to estimate AGB in grasslands, Morais *et al.* (2021) inferred that MLR has the greatest median r^2 (0.76), followed by PLSR (0.75) and RF (0.69). We found similar results evaluating the papers that informed the r^2 value for AGB estimation. Among the methods with more applications used in the papers evaluated in this review, RF has the greatest median r^2 (0.798). However, it differed slightly from the other methods, being followed by MLR (0.785), LR (0.78), and PLSR (0.776). Considering the small difference among the statistical methods, we agree with Morais *et al.* (2021) that the accuracy of the analyses depends more on the quantity and quality of the data from field samples than on the type of statistical regression.

Among the papers assessed, at least 11 evaluated different regression methods for AGB prediction models using the same dataset. LR, MLR, and PLSR were commonly evaluated with other methods, probably because they are common regression techniques for predicting plant traits. Askari *et al.* (2019) evaluated two regression techniques, PLSR and MLR, to estimate AGB using a multispectral sensor in a mixed grassland. The authors concluded that both PLSR and MLR techniques produced accurate models for AGB using only spectral data ($r^2 = 0.77$ and 0.76, respectively). The results from both techniques were considered robust enough to be employed, although the PLSR produced better model outputs. Comparing statistical methods for analyzing hyperspectral data from a grassland trial, Capolupo *et al.* (2015) also found that PLSR was more effective at predicting AGB using specific vegetation indices. Lussem *et al.* (2022) evaluated PLSR with other analysis methods, RF and support vector machine regression (SVR), with and without a combination of both structural (sward height; SH) and spectral (vegetation indices and single bands) features. In their study, however, the PLSR models were outperformed by the RF and SVR models. PLSR also was outperformed by other analysis methods (SVR, RF, and cubist regression (CBR)) in the study of Wengert *et al.* (2022) using spectral data from a hyperspectral sensor.

Borra-Serrano *et al.* (2019) also evaluated PLSR with different regression models and one machine learning method (MLR, PCR, and RF) to estimate AGB using an RGB sensor in a monoculture grassland trial. Using spectral and structural data, MLR outperformed both the machine learning approach and other regression techniques in terms of AGB estimation. Geipel *et*

al. (2021) evaluated two regression methods, powered partial least squares regression (PPLSR) and LR, to estimate AGB using a hyperspectral sensor in a mixed grassland in an experimental site. Their results showed that PPLSR modeling approach fitted with reflectance data produced models with high AGB prediction accuracy ($r^2 = 0.91$). On the other hand, LR models using spectral indices and canopy height as predictor variables did not achieve satisfactory prediction accuracies.

Inputs

The selection of parameter(s) acquired from UAV data is probably the main element impacting the accuracy and prediction of AGB estimation in grasslands (Poley and McDermid, 2020). Spectral and structural (e.g., height) characteristics of grasslands are the most frequent inputs for predicting AGB using UAV data. Among the papers reviewed, 18 informed the use of only structural data as input, and 18 used only spectral data. Other 15 papers used both, while 11 papers used spectral and structural data combined with another data type. The study of Cunliffe, Brazier and Anderson, (2016) using canopy height and canopy volume as inputs had the highest r^2 (0.95) value among those that employed only structural data to estimate AGB. Among the studies that only used spectral data, Villoslada Peciña *et al.* (2021) had the highest value for r^2 (0.98). For those studies that used both structural and spectral inputs, Oliveira *et al.* (2020) obtained the best results (r^2 = 0.97) by evaluating different spectral indices and bands from a multispectral sensor, as well as eight canopy metrics from an RGB sensor. The mean r^2 value was 0.74 for studies that used only structural data, 0.77 for papers that only used spectral data, and 0.81 for papers that combined both structural and spectral data.

All studies that only employed structural measures used RGB and LiDAR data to generate metrics that represented the structure of the vegetation, and the most commonly used structural variable was canopy height. Some studies also used data such as vegetation volume, vegetation cover, and density volume factor. For vegetation with sparser or more varied canopies, such as grasslands, variables that reflect this heterogeneity, such as coefficient of variation, standard deviation, or percentiles of height, can be significant (Poley and McDermid, 2020). Zhang *et al.* (2018) observed a significant correlation between AGB in a natural grassland and logarithmic regression using mean height derived from a UAV-RGB sensor ($r^2 = 0.80$). Wijesingha *et al.* (2019) evaluated different canopy height metrics derived from a UAV-RGB sensor to estimate AGB in a mixed grassland farm. The results showed that among the canopy height metrics, the 75th percentile achieved the strongest explanatory power ($r^2 = 0.63$). da Costa *et al.* (2021) assessed different structural metrics derived from LiDAR data to estimate AGB from a natural grassland in the Brazilian savanna. The most accurate method employed metrics that represent canopy height (H98TH = height 98th percentile) and coverage (COV = cover percentage of first return above 1.30 m). For the estimation of AGB in a mixed natural grassland, Barnetson, Phinn and Scarth (2020) selected the maximum canopy height derived from a UAV-RGB sensor to closely approximate the settling height of the RPM measure.

The majority of studies that employed only spectral data used multispectral sensors (n = 9), followed by hyperspectral sensors (n = 3), RGB sensors (n = 3), and a fusion of different sensors

(n = 3). These spectral datasets can be used as narrow bands or processed to derive a vegetation index (VI). VIs (ratios or linear combinations of bands) have been widely used in remote sensing research for vegetation identification, as they emphasize the differences in reflectance of the vegetation. The use of vegetation indices to characterize and quantify biophysical parameters of agricultural crops has two major advantages: (a) reducing the dimension of multispectral information through a simple number while minimizing the impact of lighting and target conditions, and (b) providing a number highly correlated to agronomic parameters. Several studies have found strong relationships between biomass measurements and RS-derived VIs (Capolupo *et al.*, 2015; Askari *et al.*, 2019; Jenal *et al.*, 2020; Villoslada Peciña *et al.*, 2021). Based on this relationship, a simple statistical methodology can be constructed to estimate plant biomass with the most suitable VI and optimal regression results.

Table A4 (supplementary material) shows all 78 vegetation index formulations cited in at least one study for AGB estimation in grassland. Among the articles examined in this review, at least 38 used vegetation indices for biomass estimation analysis. Of the top five, the Normalized Difference Vegetation Index (NDVI) was the index used in most studies (N = 27), followed by Normalized Difference Red Edge (NDRE) (N = 16), the Green Normalized Difference Vegetation Index (GNDVI) (N = 14), the Green Chlorophyll Index (GCI) (N = 10), and the Modified Chlorophyll Absorption in Reflectance Index (MCARI) (N = 9).

The results show a wide variety of indices, some of which might be more specific to certain indicators (e.g., Grassland Index, Plant Senescence Reflectance Index). However, most indices were used only once, and a few studies have compared the efficiency of multiple indices. The overall prevalence of NDVI was expected since this index is widely employed in various study scales to represent green vegetation abundance and net primary productivity in grasslands. Although it was the most used index and showed a good correlation for biomass estimation in a few studies (Insua, Utsumi and Basso, 2019; Gebremedhin *et al.*, 2020), NDVI also has some limitations. NDVI presents sensitivity to the effects of soil brightness, soil color, atmosphere, and leaf canopy shadow and shows saturation in high-density vegetation. In fact, in some studies, NDVI did not perform better than preceding modeling strategies (K. Y. Li *et al.*, 2021; Pranga *et al.*, 2021; Théau *et al.*, 2021). The study of Geipel and Korsaeth (2017) showed that NDVI-based models appeared to be saturated at the first harvest dates and did not achieve an acceptable prediction level. This conclusion is similar to that of Karunaratne *et al.* (2020) and Togeiro de Alckmin *et al.* (2021), who suggested that predicting dry biomass only based on NDVI (as in previous studies) is ineffective. This is probably related to the saturation effect that occurs when the plant achieves higher levels of leaf area index. Indeed, Pranga *et al.* (2021) reported that with leaf area index (LAI) values larger than 3, NDVI exhibited a lower biomass estimation capability. EVI and GNDVI, on the other hand, saturate less at increasing LAI values and have been identified as significant predictive variables. In at least two studies comparing different vegetation indices to estimate biomass in grasslands, GNDVI performed better than NDVI (K. Y. Li *et al.*, 2021; Théau *et al.*, 2021).

Furthermore, it is important to consider a diverse set of vegetation indices in order to avoid the issues that come with less sensitive indices such as NDVI. When assessing various vegetation indexes, it is also critical to consider saturation, sensitivity, plant growth phases, canopy structure, and environmental impact (Jenal *et al.*, 2020).

Recently, several methods investigated the integration of different data by combining spectral and non-spectral data, and they found an improvement in the assessment of AGB in grasslands. According to the study of Lussem *et al.* (2022), the combination of structural and spectral features can improve the estimation accuracy for AGB in grasslands. Viljanen *et al.* (2018) reported that using MLR and RF to combine structural and spectral information resulted in a small improvement in AGB estimation. For the AGB estimation of perennial ryegrass in the study by Pranga *et al.* (2021), the combination of spectral and structural characteristics from a multispectral camera utilizing random forest produced the best results. When combining vegetative indices and 3D features at various flight altitudes, Karunaratne *et al.* (2020) observed a consistent improvement of AGB estimation.

The structural features, such as canopy height, were more significant for the AGB prediction models than the spectral features when both were combined (Lussem *et al.*, 2022). Michez *et al.* (2019) obtained an RMSE of 0.09 kg m^2 by combining VIs and canopy height and concluded that the canopy height had the highest significance in the multilinear regression model. Grüner, Wachendorf and Astor (2020) developed AGB estimation by comparing RF and PLS models of spectral features with and without texture. They concluded that adding texture features improved the estimation models significantly. When predicting AGB using a fused dataset (from the RGB camera and the MS camera), Pranga *et al.* (2021) likewise discovered that the canopy height characteristics were of the utmost significance; nevertheless, estimating the AGB with only the CH features produced rRMSE of 30–35%. Comparatively, the rRMSE of the AGB estimation was generally 10% lower.

It is important to note, however, that although these methods show promising results, combining spectral and non-spectral data in an applied setting can be more challenging because it requires employing several sensors or constructing complex data processing chains (Théau *et al.*, 2021).

2.4 Challenges and future prospects

UAV remote sensing for AGB estimation in grasslands is still challenging, mainly due to the intrinsic characteristics of this ecosystem. The vegetation communities in grasslands are mainly composed of a variety of site-specific plant species that can contrast in size and phenology stage. Additionally, because grasslands are perennial, monitoring systems must be able to adapt to a wider variety of measuring conditions (Franceschini *et al.*, 2022). Future research should consider the inherent characteristics of these ecosystems, seasons, management practices, data collection parameters, and automation techniques in order to establish robust methods that can be transferred

into management tools for grassland professionals (DiMaggio *et al.*, 2020). We also strongly recommend that future studies provide more information on the agronomic aspect of the research area. A detailed overview of soil characteristics, spatial heterogeneity of species distribution, climate, grassland classification, and management practices used enables independent analyses and cross-study comparisons.

A significant constraint of UAV studies for AGB model estimation in grasslands is the low number of sampling intervals or limited representativeness due to the small number of sites and management intensities that can be assessed (Wengert *et al.*, 2022). Furthermore, additional points must be explored. For example, because most studies only consider one growing season, future research could include more observations throughout different growing seasons. In this way, researchers will produce more high-quality datasets describing the temporal dynamics of vegetation in grassland ecosystems, which is recommended for improving AGB estimation models. Models created using a dataset based on numerous years, different management practices, and preferably multiple sites are more generalizable. As a result, they may better represent conditions at other sites and over different years (Sinde-González *et al.*, 2021). Additionally, models should also be validated on a range of grassland fields from diverse locations and years to improve their practical applicability (Wengert *et al.*, 2022).

Apart from data collection, data processing and analysis are major factors in using UAVs for AGB estimation in grasslands. The processing of UAV data differs significantly from the processing of satellite data, creating a new demand for data processing software and suitable workflows. Additionally, image processing takes more time as spatial and spectral resolutions rise; therefore, more effective methods must be designed. Future directions for AGB grassland estimate may be accomplished by the ongoing reduction and cost-effectiveness of sensors, platforms, and computer hardware, as well as strong algorithms.

2.5 Conclusions

The present manuscript provides a comprehensive review of the most recent results in the field of UAV for AGB estimation in grasslands. Several factors can have a significant impact on the performance and generalizability of vegetation AGB estimation in grasslands throughout the data collection to data processing and analysis. Our findings are summarized as follows:

- The frequency of publications on grassland AGB estimation with UAV has increased over time and continues to rise, indicating the scientific community's interest;
- The frequency of studies is poorly distributed around the world, with South American and African grasslands appearing to be underrepresented. As a result, additional research should be conducted on some important grassland areas;
- The type of grassland, the heterogeneity, and the growth stage can strongly influence the AGB estimation model;

- Collecting ground-based data is a crucial step in estimating AGB in grasslands. The biomass sampling method seems to have a small influence on the accuracy of the AGB model estimation, whereas the number of samples is one of the main factors to improve the estimation accuracy;
- The measurement of canopy height is an important variable, especially for models that use structural data as input. However, the methods for collecting canopy height at the field level present limitations. RPM measurements demonstrated lower accuracy in sparse swards or tall, non-uniform canopies, and a measuring tape is based on an "average height", but determined visually and rather subjective. The biases of each method must be taken into account to reduce inconsistencies in the results;
- Quadcopters were the most widely used platform, accounting for almost 60% of all platforms. Nevertheless, the type of platform has a low impact in AGB grassland estimation, and the selection of the platform depends more on the research objective;
- The modal value for UAV flight altitude among the studies was 50 m. Adopting lower altitude flights seems to enhance AGB estimations as this increase the spatial resolution. For farm-scale applications, however, collecting UAV data at higher altitude offers more advantages. We suggest flying at the highest altitude where the desirable GSD is possible;
- Large image forward and side overlaps of approximately 80%, combined with self-calibration during photogrammetric processing, can provide better data quality;
- In terms of sensor type, RGB was the most commonly employed (48%). Despite MS and HS sensor has the advantage to provide more spectral bands RGB data seems capable to produce models with comparable accuracy. In terms of cost–benefit and data processing simplicity, RGB sensors appear to be the most suitable for estimating AGB in grassland at the moment. The emergence of reliable and cost-effective LiDAR and hyperspectral sensors will have a significant impact on future research;
- For the reliable estimation of vegetation structure in grasslands from UAV imagery, a high-quality DTM with a precise and accurate representation of the terrain is necessary. However, UAV-derived DTMs may underestimate or overestimate field terrain differences depending on the canopy's density and the spatial resolution of the image;
- The accuracy of georeferencing models increases when a larger number of ground control points are equally distributed throughout the study area;
- Linear regression was the most commonly used regression model (n = 25). Random forest was the most popular machine learning method (n = 16). The findings suggest that the accuracy of the analysis methods is more dependent on the quantity and quality of data from field samples rather than the method itself;
- The most common inputs for AGB prediction in grasslands using UAV are spectral and structural data. Canopy height metrics were the most used structural data. At least 68% of

the articles used vegetation indices for biomass estimation, with NDVI being the most commonly used. The results indicate that models that employed both data types (structural and spectral) outperformed models that only used one.

CHAPTER III

ASSESSING THE EFFECT OF FIELD DISTURBANCES ON BIOMASS ESTIMATION IN GRASSLANDS USING UAV-DERIVED CANOPY HEIGHT MODELS

This chapter has been published as:

Bazzo, Clara Oliva Gonçalves, Bahareh Kamali, Dominik Behrend, Hubert Hueging, Inga Schleip, Paul Mosebach, Axel Behrendt, and Thomas Gaiser. "Assessing the Effect of Field Disturbances on Biomass Estimation in Grasslands Using UAV-Derived Canopy Height Models". *PFG – Journal of Photogrammetry Remote Sensing and Geoinformation Science* (2024). https://doi.org/10.1007/s41064-024-00322-x

Abstract

Accurate estimation of biomass in grasslands is essential for understanding ecosystem health and productivity. Unmanned Aerial Vehicles (UAVs) have emerged as valuable tools for biomass estimation using canopy height models derived from high-resolution imagery. However, the impact of field disturbances, such as lodging and molehills, on the accuracy of biomass estimation using UAV-derived canopy height models remains underexplored. This study aimed to assess the relationship between UAV-derived canopy height and both reference canopy height measurements and dry biomass, accounting for different management systems and disturbance scenarios. UAV data were collected using a multispectral camera, and ground-based measurements were obtained for validation. The results revealed that UAV-derived canopy height models remained accurate in estimating vegetation height, even in the presence of disturbances. However, the relationship between UAV-derived canopy height and dry biomass was affected by disturbances, leading to overestimation or underestimation of biomass depending on disturbance type and severity. The impact of disturbances on biomass estimation varied across cutting systems. These findings highlight the potential of UAV-derived canopy height models for estimating vegetation structure, but also underscore the need for caution in relying solely on these models for accurate biomass estimation in heterogeneous grasslands. Future research should explore strategies to enhance biomass estimation accuracy by integrating additional data sources and accounting for field disturbances.

Keywords: vegetation structure, monitoring, ecosystem services, remote sensing.

3.1 Introduction

Grasslands are a crucial component of the earth's ecosystems, providing a wide range of ecosystem services, including biomass production (Bengtsson *et al.*, 2019). Biomass is a key indicator of the productivity of grasslands and can be used for a variety of purposes, such as fodder production, energetic use, and fiber production (Sala and Paruelo, 1997). The management system of grasslands can significantly affect biomass production. Understanding this impact can aid in developing sustainable land management practices that maximize the provision of ecosystem services (Zhao, Liu and Wu, 2020). Accurate biomass estimation is essential for assessing the economic value of grassland ecosystem services at regional and farm scales (Huber *et al.*, 2022) as well as for understanding the effects of land use change and intensification on grassland multifunctionality (Schils *et al.*, 2022). Moreover, assessing the spatial variability of multiple ecosystem services in grasslands of different intensities can provide valuable insights for conservation and management (Le Clec'h *et al.*, 2019).

Different methods have been developed for measuring grassland biomass, each with its own advantages and limitations (Harmoney *et al.*, 1997; 't Mannetje and Jones, 2000). Direct measurements such as destructive sampling provide highly accurate results but are time-consuming and costly, especially when applied to large areas (Bareth and Schellberg, 2018; Lussem *et al.*, 2019). Another approach is the use of allometric equations, which relate biomass to easily measurable variables such as sward or canopy height, which, in ground-level assessments, can be obtained using tools such as rulers or rising plate meters (O'Donovan *et al.*, 2002). These allometric equations have been widely used and have proven to be reliable in many cases (O'Sullivan, O'Keeffe and Flynn, 1987; Piggot, 1989; Hakl *et al.*, 2012). However, the selection of the appropriate method depends on the specific characteristics of the grassland and the research question, as the reliability of the methods may be affected by surface heterogeneity and applied management practices (Bazzo *et al.*, 2023).

Another powerful tool for estimating biomass in grasslands can be remote sensing. Remote sensing allows for collecting information on vegetation structure and biomass at a large scale without the need for ground-based measurements (Dusseux *et al.*, 2015). Unmanned Aerial Vehicles (UAVs) have become increasingly popular for this purpose due to their ability to collect high-resolution image data in a relatively short period of time. The data collected by UAVs can provide detailed information on vegetation structure, including canopy height, canopy cover, and leaf area index, which can be used to estimate biomass (Bazzo *et al.*, 2023). The use of UAVs for biomass estimation has been demonstrated in several studies (Lussem *et al.*, 2019; Wijesingha *et al.*, 2019; Alvarez-Hess *et al.*, 2021), and they have been shown to be a cost-effective and efficient method for monitoring grassland ecosystems. Recent studies have shown that using canopy height models derived from UAVs is a reliable method for estimating grassland biomass. For example, Lussem, Schellberg and Bareth (2020) and Bareth and Schellberg (2018) have demonstrated that UAV canopy height data can be used to monitor biomass in grassland experiments effectively.

Similarly, DiMaggio *et al.* (2020) and Borra-Serrano *et al.* (2019) have shown that UAV imagery can be used for non-destructive biomass estimation of specific grass species such as *Lolium perenne*. Cunliffe, Brazier and Anderson (2016) have also highlighted the potential of using drone-acquired Structure-from-Motion (SfM) Photogrammetry for ultra-fine grain landscape-scale quantification of dryland vegetation structure. Studies such as Batistoti *et al.* (2019) and Wijesingha *et al.* (2019) have also investigated the use of UAVs for estimating biomass and canopy height in grassland environments. Overall, these studies provide strong evidence for the effectiveness of UAV-derived canopy height models in estimating biomass in grasslands.

Despite the usefulness, field disturbances such as lodging and molehills can impact the accuracy of biomass estimation using UAV-derived canopy height data. While previous studies have demonstrated the utility of UAVs for biomass estimation, detailed investigations into how these specific field conditions affect the performance of UAV-derived models are still limited. This study focuses on analyzing the influence of disturbances on both canopy height and biomass estimation across different management systems, providing insights that can enhance the accuracy of UAV-based biomass models in disturbed and heterogeneous grassland environments.

To address these concerns, the objectives of this study are to: 1) assess the effect of field disturbances on UAV-derived canopy height models and 2) investigate the impact of these disturbances on aboveground biomass estimation using UAV-derived canopy height data for three different management systems.

3.2 Material and methods

3.2.1 Study site and experimental design

The research site, "Koppel 17," is located 48 km northwest of Berlin near the village of Paulinenaue (52°41'28" N, 12°44'16" E), in the federal state of Brandenburg (Fig. 3.1a). It encompasses an area of 1.3 ha and is situated within the "Havelländisches Luch", a shallow, drained peatland complex (Fig. 3.1b). The site features degraded peat soils with peat thickness ranging from 0.5 to 2.0 m, where the topsoil has degraded, and the subsoil consists of alluvial sand layers up to 12 m in depth. The area is characterized by a continental climate with an average temperature of 9.2 °C and an average precipitation of 530 mm (Pohl *et al.*, 2015).

In 2013, a seed mixture dominated by *Festuca arundinacea* was sown on the site. Furthermore, on the 14th of August 2018, a reseeding was carried out in which *Lolium perenne* seed was sown at a rate of around 20 kilograms per hectare. Fertilization practices were carefully managed to address the nutrient requirements of the site. PK fertilization, including triple superphosphate and potassium-magnesium sulfate, was applied each year in April to compensate for nutrient depletion from plant uptake and soil processes. Additionally, N fertilization using ammonium sulfate was implemented based on the specific nutrient requirements associated with the fen's ecological characteristics and the observed nutrient removal rates from previous harvests.

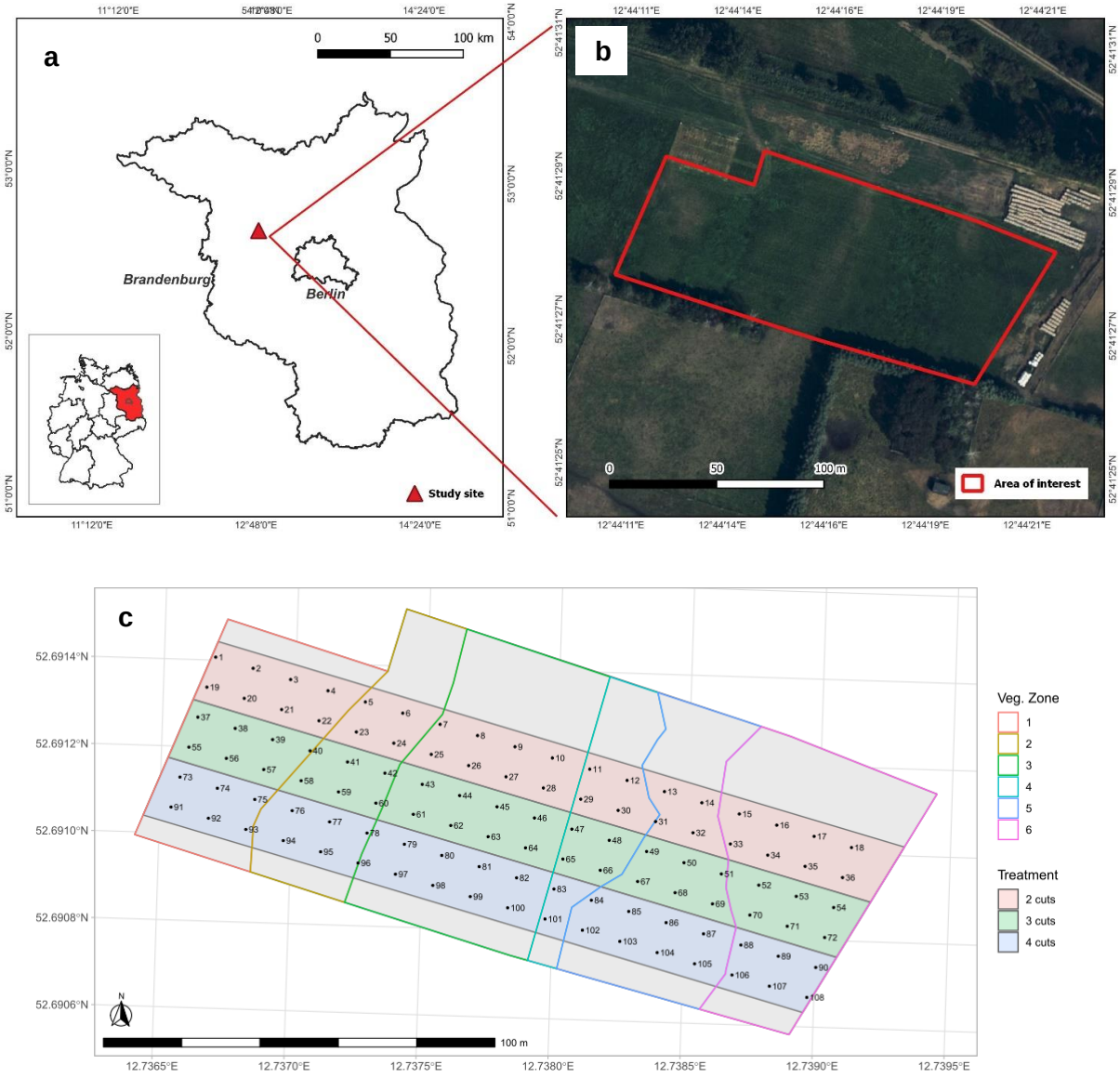

Figure 3.1. Study area located in Brandenburg, Germany (a), study site "Koppel 17" (b), design of the field experiment divided into six vegetation zones and three cutting treatments and the 108 sampling points (c). This figure was originally published in Bazzo et al. (2024).

To assess the impact of sward height and maturity stage on biomass production, the site was divided into three strips with an east-west orientation, each 16 m wide (Fig. 3.1c). To this end, the strips were subjected to different utilization (cutting frequency) regimes to generate varying growth heights and maturity stages of the grassland vegetation. In north-south orientation, the site is additionally divided into six vegetation zones according to the existing species composition.

3.2.2 Data acquisition

The data collection of the experimental field consists of two approaches: the canopy height estimated through UAV data and field measurements on the ground. The methodology of both methods is presented in the subsequent sections. Table 1 summarizes the date of AGB biomass sampling in each field campaign with the number of sampling points in each cutting system.

Table 3.1. Days on which field measurements were conducted, along with the corresponding number of samples and plots.

Year of collection	Cutting date	Cutting systems frequency			Number of samples per date (n)
		Two-cut	Three-cut	Four-cut	
2022	18 May			X	36
	17 Jun	X	X	X	108
	03 Aug		X	X	72
	14 Sep	X	X	X	108
Total number of samples per treatment		**72**	**108**	**144**	**n_{total}= 324**

UAV data collection

The UAV used for data collection in this study was the DJI P4 Multispectral drone. It has a multispectral camera that records data in five narrow spectral bands (Red, Green, Blue, NIR and RedEdge) and an RGB camera for capturing conventional visible imagery. Although the UAV is equipped with a multispectral sensor, only the RGB data were utilized for this study, given that our primary objective was to evaluate the use of a Canopy Height Model rather than to analyze spectral data. The higher resolution of the RGB images makes them more suitable for generating detailed Digital Elevation Models (DEMs) that provide a more accurate representation of the canopy structure. In this study, the drone was flown at a height of 37 m aboveground level, leading to a ground sample distance of two cm/pixel for the RGB images. The image overlap was approximately 80 % forward and 60 % sideward. Camera settings were adjusted to one frame per two seconds (0.5 Hz), with fixed aperture and exposure according to the lighting conditions. As a result, the aperture and exposure settings varied between the acquisition dates. Four flights were conducted with compatible dates with the reference sample field data collection (Table 1) to obtain data for the plant height derived from the Canopy Surface Model. Another four additional flights were conducted after harvest to capture the exact dimension and position of the cutting area in the plots, since the mechanical harvest usually leads to slightly differences in the plot harvest area

length (Table 3.2).

Table 3.2. Acquisition dates of UAV-derived data and ground control point errors (XYZ direction) in cm.

Date	X error (cm)*	Y error (cm)*	Z error (cm)*	XY error (cm)**	Total error (cm)***	RMSE reprojection error (pix)
2022-05-16	1.648	2.437	0.668	2.943	3.018	0.708
2022-05-19	1.100	1.237	0.519	1.655	1.735	0.660
2022-06-14	0.643	0.660	0.364	0.922	0.991	0.785
2022-06-16	0.693	0.773	0.350	1.038	1.096	0.729
2022-08-02	0.960	0.484	1.089	1.075	1.530	0.655
2022-08-04	0.866	0.928	1.391	1.269	1.883	0.567
2022-09-14	0.970	0.586	1.156	1.133	1.619	0.722
2022-09-14	0.966	0.677	1.214	1.180	1.693	0.714
2022-09-29	0.969	0.928	0.302	1.342	1.376	0.736

*X, Y, Z error (cm) - difference in the corresponding direction between source (measured) value and estimated by Agisoft for marker. **XY error (cm) - planar error for marker. ***Total error (cm) - the distance between source and estimated location for marker.

Additionally, a bare-ground model was obtained from a flight on September 30, 2022. For accurate geo-referencing, eleven ground control points were evenly distributed across the experimental site with fixed positions throughout all growth seasons. The coordinates of the GCPs' centers were obtained with a global navigation satellite system (GNSS) receiver (Viva GNSS GS 10, Leica Geosystems AG, Switzerland) an accuracy of approximately one centimeter in position and one and a half centimeters in height.

Reference ground data collection

Compressed canopy height (RPM-CH) was measured with a self-constructed rising plate meter (RPM). Disc diameter was 30 cm and disc weight was 238 g, resulting in a 3.4 kg/m2 pressure. The plots (1.5 m x 1.5 m) were manually measured with the RPM at five different points. From the five replicates per plot, an average RPM-CH value was calculated.

Fresh biomass samples were collected by harvesting the entire plot area mechanically by a forage harvester model HEGE 212. The fresh biomass (FBM) weight for each harvested plot was determined by weighing the clipped biomass per plot. Subsamples of each plot were taken, dried in a forced air drier at 65°C to a constant weight, and reweighed to determine dry biomass (DBM)

yield per unit ground area. Biomass values were upscaled to grams per m^2. Owing to slightly differing plot sizes, the area of each plot was double-checked on-site with a tape measure to determine the correct upscaling factor per hectare and re-calculated based on a high-resolution UAV-derived orthomosaic from all sampling dates.

The collected data from this experiment were affected by two types of disturbance: 1) lodging; (Fig. 3.2a) and 2) mole hills (Fig. 3.2b). Each plot was assessed individually on all field campaign dates to analyze field disturbances related to lodging. The assessment involved manually classifying each plot based on the spatial extent of lodging. The lodging classification was then used to group the plots into three categories: (1) no lodging, for plots that showed no signs of lodging; (2) partial lodging, for plots with less than 50% of their grass area affected by lodging; and (3) severe lodging, for plots with more than 50% of their grass area affected by lodging.

(a) (b)

Figure 3.2. Occurrence of lodging in the field (a), presence of mole hills in the field (b).

As in most cases, the grass covered the presence of molehills; we analyzed the images captured by the UAV after cutting to assess this disturbance (Fig. 2b). The plots were divided into two categories: those with mole hills and those without. Using this methodology, we could accurately identify the presence of molehills, even when they were not initially visible in the field.

3.2.3 Image data processing

The acquired images were processed in the SfM software Agisoft PhotoScan v.1.3 (Agisoft Ltd., St. Petersburg, Russia). After an initial image alignment, the GCPs were placed in the images for accurate data georeferencing. Subsequently, the image alignment was run using ‘high’ quality setting, and the dense point cloud was built using ‘high’ quality settings and ‘mild’ depth filtering to preserve finer details of the sward (Viljanen *et al.*, 2018). Based on the eleven validation GCPs (vGCPs), error and RMSE were estimated for X, Y and Z coordinates for all the dates (Table 3.2). A DSM (Digital Surface Model) was generated and exported from the point cloud as a TIFF file.

The DSMs had a spatial resolution of two cm/pixel horizontally. The base model DSM (T0) from each sampling date was subtracted from the Digital Terrain Model (DTM) obtained through aerial imaging of the bare ground after harvest to derive canopy height metrics. Canopy height metrics were calculated in QGIS, using zonal statistics with a polygonal shape file that represented the plots outline.

3.2.4 Statistical analyses

Statistical analysis was performed using R programming environment version 4.2.2 (R Core Team, 2022). To compare the performance of the mean UAV-derived canopy height model with the field measurements of canopy height and dry biomass, linear regression analyses were performed. Six scenarios, including the disentangled and joint effects of different disturbances, were investigated: a) no lodging plus molehills, b) partial lodging plus molehills, c) severe lodging plus molehills, d) no disturbances, e) partial lodging without molehills, and 6) severe lodging without molehills (Table 3.3).

For the linear regression analyses, the R function "lm()" from the R package "stats" was applied. For error estimation of the model, the coefficient of determination (R^2), the relative root mean square error (rRMSE), and the Pearson correlation coefficient (r) were computed.

3.3 Results

3.3.1 Orthomosaics and canopy surface models

The orthomosaics and Canopy Height Models (CHMs) for the four sampling events in 2022 are presented in Figure 3.3. The sampling collection was conducted aligned with the cutting events, with the number of samples varying according to the treatment and date as presented in Table 3.1.

On May 18 (Fig. 3.3ab), observation was limited to four-cut system plots, revealing relatively low canopy heights indicative of early-season growth. On June 17 (Fig. 3cd) samples from all treatments were gathered and the differentiation in canopy heights becomes evident. The four-cut system areas, having undergone an earlier cut, presented a markedly reduced canopy height compared to the two and three-cut systems which experienced their first cut of the year, resulting in taller standing biomass.

In August (Fig. 3.3ef), the sampling included plots from the three- and four-cut systems, all of which were in a regrowth phase. Despite this, the four-cut system plots exhibit taller canopies, which may suggest a rapid recovery or a denser regrowth pattern.

By September 14 (Fig. 3.3gh), with samples taken from all cutting treatments, we observed a more uniform canopy height across the plots. This final observation suggests an equilibration in growth patterns, possibly due to the plants reaching a growth ceiling or similar recovery responses

post the last cutting events, resulting in a more homogenized canopy structure across the treatments.

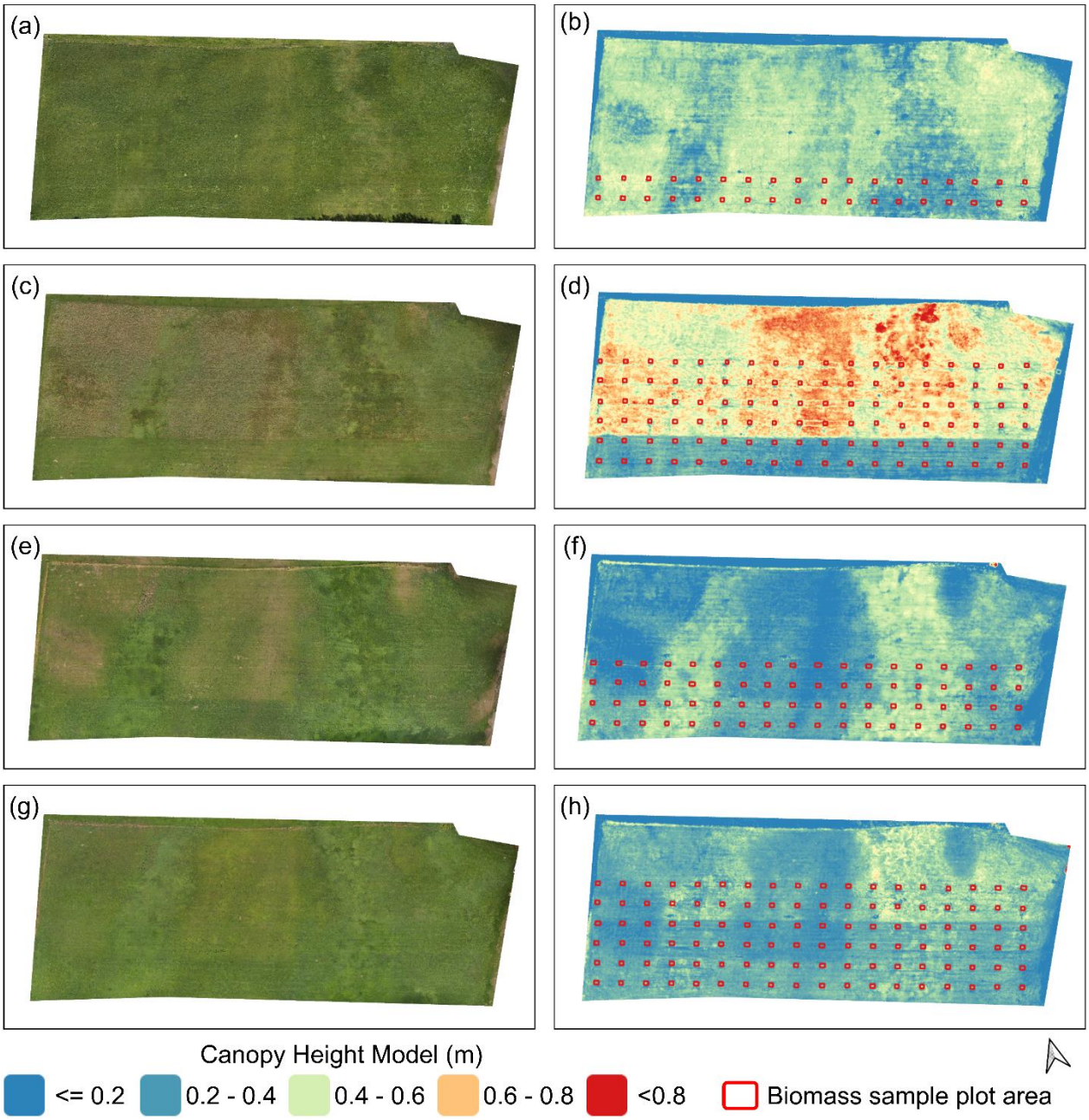

Figure 3.3. Orthomosaics (left panels) and corresponding Canopy Height Models (CHMs) (right panels) for survey dates in 2022: (a) and (b) May 18, (c) and (d) June 17 (e) and (f) August 03, (g) and (h) September 14.

3.3.2 Effect of field disturbances on UAV-derived canopy height models

A linear model was applied to assess the relationship between the UAV canopy height model and the reference canopy height obtained from field measurements using an RPM device to assess the effect of field disturbances on height estimation accuracy in grasslands. The results, displayed in the graphs in Figure 3, revealed a high R^2 (0.93) between the two models for the plots which were not influenced by disturbances in the field (Fig. 3.4a). The positive slope of the regression line with values smaller than one suggests that the UAV canopy height model tended to underestimate the RPM canopy height slightly. When observations with disturbances such as lodging or molehills were added (Fig. 3.4b), the R^2 slightly decreased to 0.92, and a lower rRMSE of 31.28% was observed, suggesting that while disturbances introduce some variability, the UAV model maintains a strong predictive relationship with the RPM measurements. The regression equation demonstrated a similar trend to the graph in Figure 3.4a (i.e., no disturbance), with a slight underestimation of the RPM canopy height by the UAV canopy height model. These findings imply that disturbances in the field, while affecting the estimation error to some extent, did not notably diminish the overall performance of the UAV-derived canopy height models.

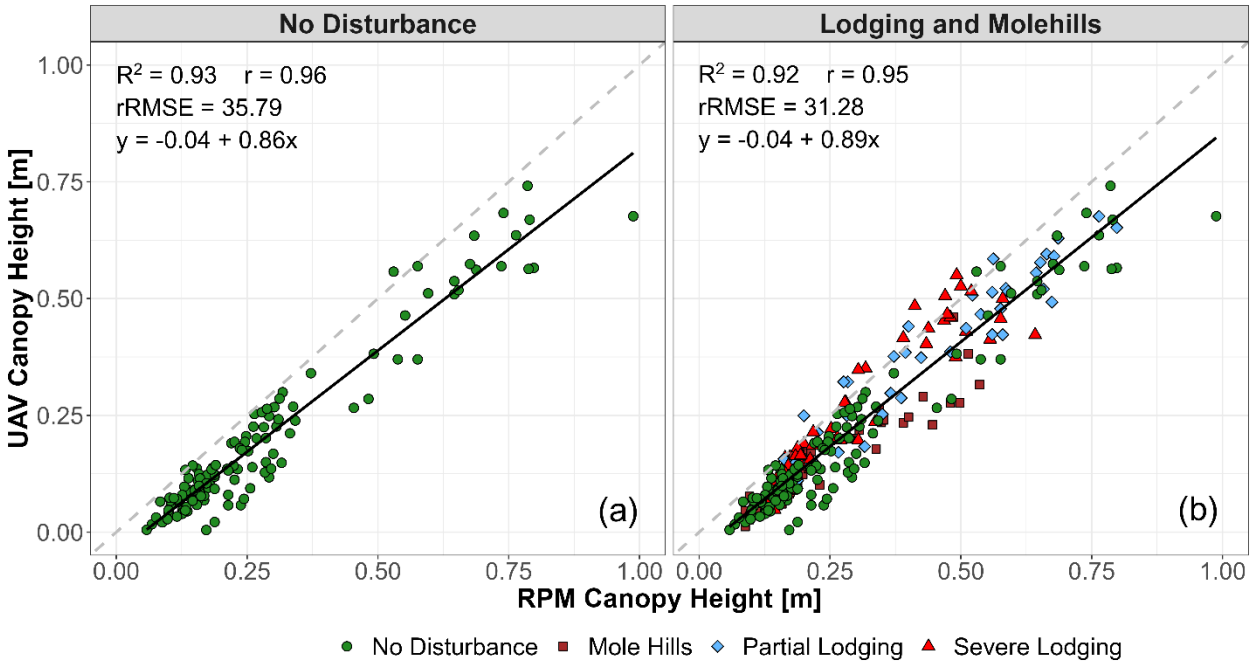

Figure 3.4. Relationship between UAV-derived Canopy Height Model and RPM Canopy Height Model in the absence (a) and plus the presence of field disturbances (b).

Further analyses examined the relationship and regression lines between the canopy height model and RPM canopy height under specific disturbance conditions (Table 3.3). The analyses revealed consistently high R^2 between the two models across different disturbance scenarios.

The results indicated that even when the disturbances were included in all six scenarios, they

had a minimal effect on the correlation and regression lines. In all scenarios, the R^2 values between RPM canopy height and UAV canopy height remained robustly above 0.91, as presented in Table 3.3. The relative RMSE values ranged from 32.5% to 38.1% for different disturbance scenarios, indicating a strong predictive relationship regardless of the presence of disturbances.

Table 3.3. Comparison of relative RMSE, determination, and correlation coefficients between UAV-derived Canopy Height Model and RPM Canopy Height Model under different lodging and molehill disturbance scenarios.

Molehills	Lodging	rRMSE (%)	R^2	r
Molehills	No Lodging	38.1	0.92	0.96
Molehills	Partial Lodging	32.7	0.93	0.96
Molehills	Severe Lodging	33.9	0.92	0.96
No Molehills	No Lodging	35.8	0.93	0.96
No Molehills	Partial Lodging	32.5	0.93	0.96
No Molehills	Severe Lodging	33.4	0.91	0.95

The regression lines also showed only minor variations, with the slope and intercept values changing slightly (Figs. 3.5a-f). More specifically, the presence of severe lodging plus molehills (Fig. 3.5c) or partial lodging and molehills (Fig. 3.5b) had limited impact on the correlation and regression lines. The R^2 values remained above 0.91, and the regression lines demonstrated similar trends to the undisturbed scenario (Fig. 3.5d). Similarly, when disturbances were limited to severe or partial lodging without molehills, the R^2 and regression lines remained consistent with the undisturbed scenario (Figs. 3.5 d-f).

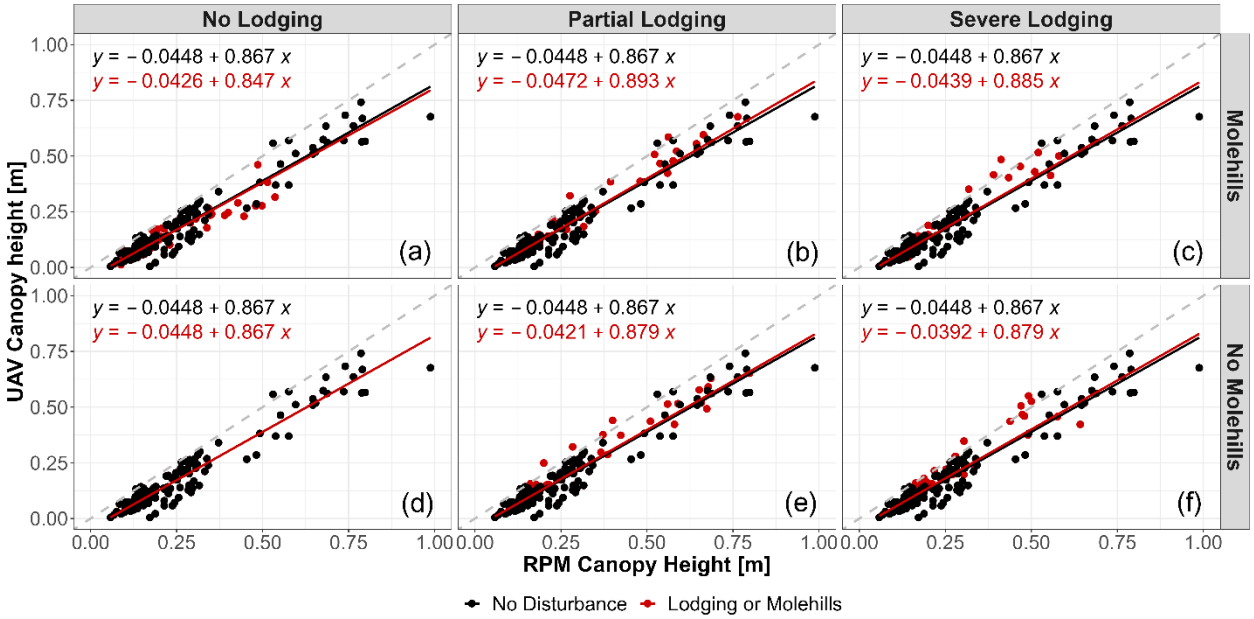

Figure 3.5. Relationship analyses of UAV-derived Canopy Height Model and RPM Canopy Height Model under different field disturbance conditions. Regression lines depict observations without any disturbance (black) and observations without disturbance plus observations without disturbance plus observations with disturbance (red).

3.3.3 Effect of field disturbances on the correlation between UAV-derived canopy height models and dry biomass

The impact of field disturbances on the relationship between dry biomass and UAV-derived canopy height models was explored under the two conditions of no disturbances and with disturbances (e.g., lodging and molehills). Contrary to the relationship between RPM canopy height and UAV-derived height, the results indicated that the estimation of the UAV-derived dry biomass using UAV-derived canopy height is more affected by field disturbances (Figs. 3.6 a, b). When there were no disturbances in the field, there was a strong relationship between UAV canopy height and observed dry biomass, with an R^2 value of 0.89 (Fig. 3.6a). However, when disturbances such as lodging and molehills were present, the R^2 value dropped to 0.75 (Fig. 3.6b). Besides, the intercept and slope values differ noticeably between the two cases, indicating that such levels of disturbance will lead to a substantial overestimation of the grassland dry biomass. The slope of the linear regression line increases in the presence of disturbance. This indicates that for one m unit of UAV canopy height, the presence of disturbance resulted in overestimation by up to 500 g m-2 (difference between the slopes 1830 and 1324).

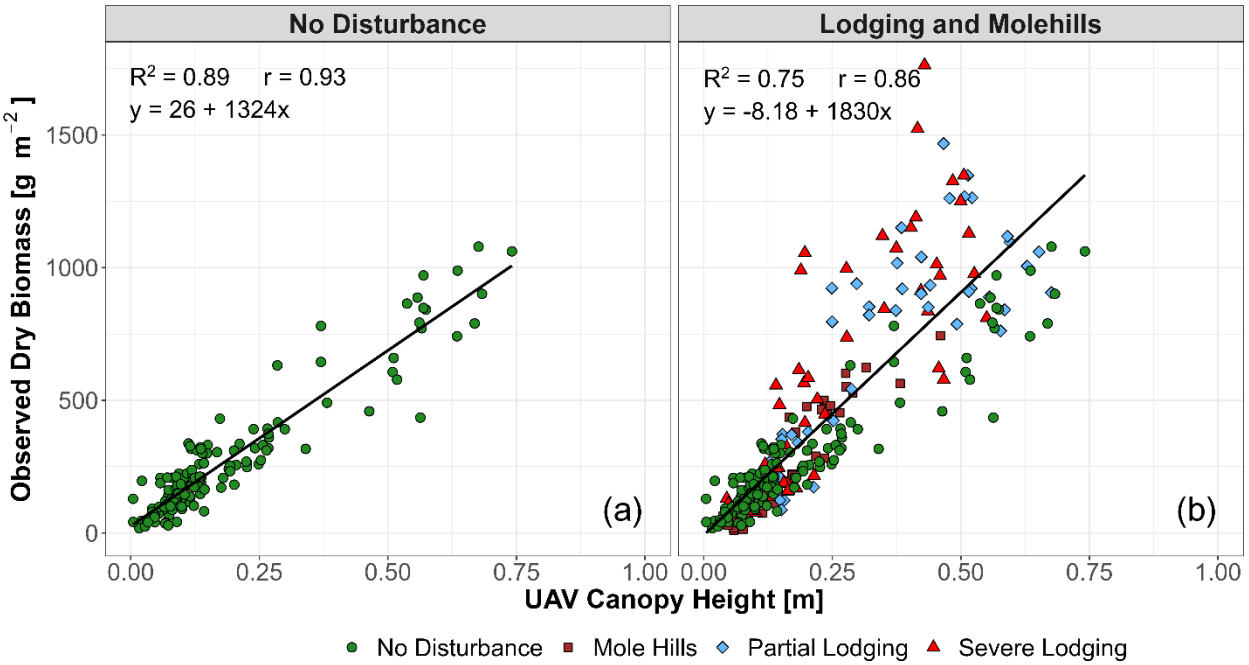

Figure 3.6. Effect of no disturbances (a) and field disturbances (b) on correlation between UAV Canopy Height Model and Dry Biomass.

Further, we explored the relationship between observed dry biomass and the UAV canopy height under different disturbance conditions, i.e., six previously mentioned scenarios (Figs. 3.5 a-f). The results showed that the accuracy of UAV-derived dry biomass estimates is highly dependent on the type and severity of field disturbances, as demonstrated in Table 3.4.

Table 3.4. Comparison of determination, and correlation coefficients between observed dry matter and UAV-derived Canopy Height Model under different lodging and molehill disturbance scenarios.

Molehills	Lodging	R^2	r
Molehills	No Lodging	0.87	0.93
Molehills	Partial Lodging	0.80	0.89
Molehills	Severe Lodging	0.70	0.83
No Molehills	No Lodging	0.89	0.94
No Molehills	Partial Lodging	0.82	0.90
No Molehills	Severe Lodging	0.76	0.87

The presence of molehills with different lodging scenarios (Figs. 3.7b, c) affects the relationship between biomass and the UAV-derived canopy height model. In the presence of

molehills and no lodging (Fig. 3.7a), the R^2 value decreases slightly from 0.89 to 0.87, and a minor shift in the regression line. This suggests a small impact of molehills on biomass estimation.

In the scenarios of partial lodging and severe lodging with the presence of molehills (Figs. 3.7b, c), there is a decrease in R^2 and a noticeable shift in the regression line. In the case of severe lodging and molehills, there is a more pronounced decrease and a shift in the regression line. This highlights a substantial impact of both factors on biomass estimation, likely resulting from significant changes in vegetation structure and ground surface characteristics. When examining scenarios of partial and severe lodging without molehills, the results indicate a decrease in the correlation between biomass and UAV-derived canopy height models compared to the undisturbed scenario (Figs. 3.7e, f).

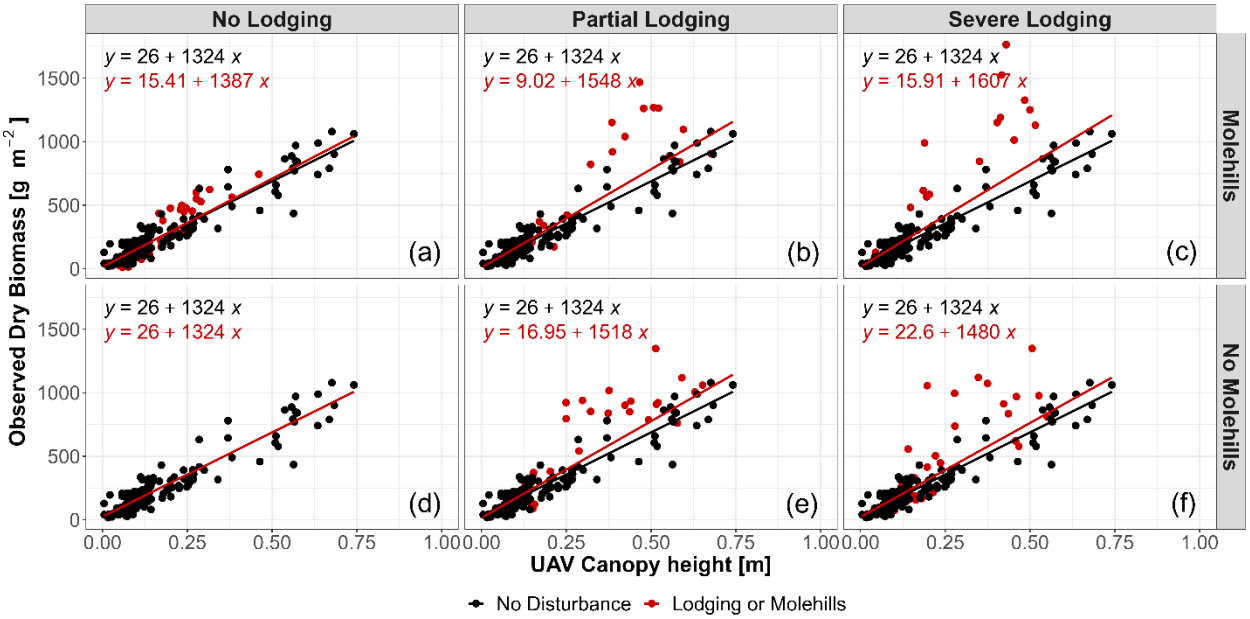

Figure 3.7. Relationship between observed dry matter and UAV-derived canopy height model under different field disturbance conditions. Regression lines depict observations without any disturbance (black) and observations without disturbance plus observations with disturbance (red).

3.3.4 Effect of cutting system and field disturbances on the relationship between UAV-derived canopy height models and dry biomass.

Our results indicate that the presence of two disturbances, i.e., lodging and molehills, affect the relationship between UAV canopy height and dry biomass differently depending on the cut system (Figs. 3.8 a-f).

The results show that the intercepts and slopes of the regression lines vary among different cutting systems and under different disturbance scenarios. In all cutting systems, the slope of the linear regression line increases with the presence of disturbance. In the four cut system (Figs. 3.8 a, b), disturbances had a minimal effect, with the relationship showing only slight changes in slope.

The three cut system experiences a decrease in biomass with disturbances, accompanied by a steeper slope (Figs. 3.8 c, d). The two cut system shows an upward shift in biomass values and a steeper slope when disturbances are present but with a decrease in R^2 value (Figs. 3.8 e, f). This result suggest that disturbances can influence the intercept and slope, altering the biomass estimation and potentially introducing biases.

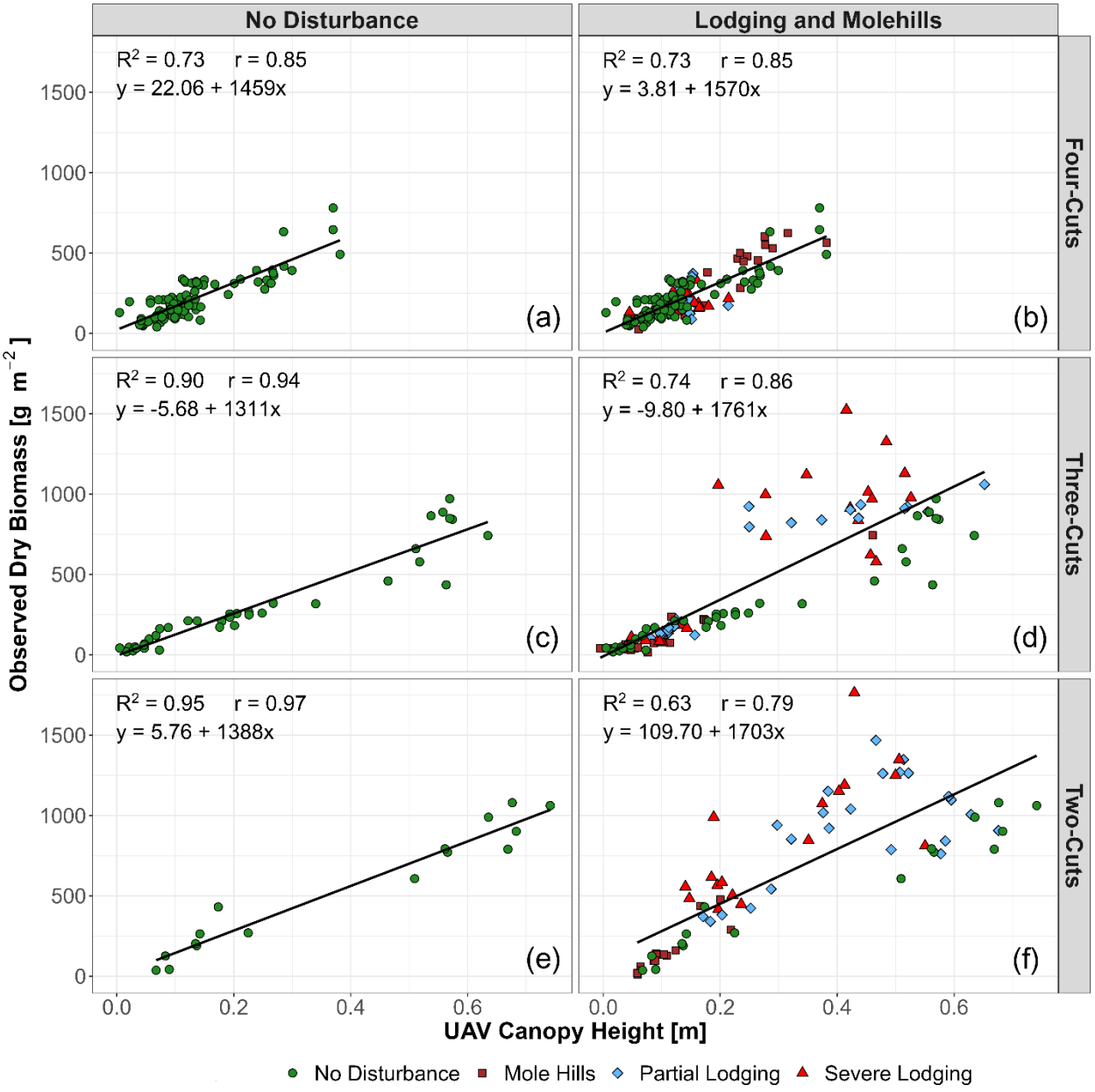

Figure 3.8. Effect of no disturbances (figs. a, c, e) and field disturbances (figs. b, d, f) on relationship between UAV-derived canopy height models and observed dry biomass under different cutting systems in a heterogeneous grassland.

The comparison of the number of samples and the frequency of disturbances across treatments, as presented in Table 3.5, provides additional insights. The variations in the number of samples across the cutting treatments can be attributed to the different cutting frequencies. The four cut system, with more frequent harvests, provided more sampling opportunities, resulting in a more significant number of samples. Conversely, the two cut system, with fewer harvests, had a smaller sample size.

Table 3.5. Total number of samples and frequency of different disturbances for each treatment.

Treatment	Total Number of samples	Partial Lodging Frequency	Full Lodging Frequency	Molehills Frequency
2 cuts	72	33%	24%	52%
3 cuts	108	18%	22%	36%
4 cuts	144	8%	13%	20%

3.4 Discussion

The primary objective of this study was to assess the applicability of UAV canopy height models as indicators of biomass in grassland environments, while also considering the potential influence of disturbances. Although we fitted linear models to examine the relationship between canopy height and biomass, the focus was not on developing a direct biomass estimation model but rather on evaluating how disturbances, such as lodging and molehills, affect the predictive ability of these models under varying conditions.

Several studies have evaluated the correlation between UAV-derived canopy height models and ground-measured height across various vegetation types and environmental conditions (Batistoti *et al.*, 2019; Borra-Serrano *et al.*, 2019; Grüner, Astor and Wachendorf, 2019; Lussem *et al.*, 2019). The relationship between the two measures has been found to be strong even with the presence of disturbances, indicating that UAV-derived canopy height models can accurately estimate vegetation height. For example, Lussem, Schellberg and Bareth (2020) found that lodging in mature swards led to an underestimation of canopy height, despite a strong R^2 value (0.75 - 0.96) between UAV-derived and ground-based measurements. Similarly, Kümmerer and Noack (2023) found as well a strong R^2 value (0.95) between UAV-derived canopy height measurements and ground-based measurements. Yet, the accuracy of the measurements was affected by variations in crop height and structure, as well as the presence of crop lodging.

Similarly, our results indicate that the UAV-derived canopy height model shows robustness in estimating canopy height even in the presence of disturbances. Nonetheless, it is crucial to consider a potential limitation. The estimated vegetation height by UAV-derived, in this case, is a result of interpolation from a point cloud, indicating that it is more appropriate to consider it as an indicator of the general shape of the vegetation canopy rather than an exact measurement of its height (Van

Der Merwe, Baldwin and Boyer, 2020).

When disturbances such as lodging and molehills are present in the field, an impact on the canopy structure is expected (Wilke *et al.*, 2019). Lodging, for instance, can cause the canopy to become more compact and horizontal, leading to an underestimation of the canopy height. In contrast, molehills can cause localized variations in the canopy height, resulting in measurement errors. Thus, despite the precision of UAVs in measuring the distance between the top of the canopy and the ground, these measurements may not reflect the actual canopy height under certain conditions where plants may be bent or compressed. Therefore, the interpretation of UAV-derived canopy height measurements should always consider the specific ecological conditions of the field in question.

In this case, the fundamental question is whether this vegetation height estimation method can provide a consistent parameter for precise biomass estimation in grasslands, especially in highly heterogeneous fields. Our findings suggest that while the relationship between the UAV-derived canopy height model and the reference canopy height from field measurements may not be severely impacted by these disturbances, the link between the UAV-derived canopy height model and biomass can be adversely affected.

In recent years, several studies have been conducted to investigate the relationship between UAV-derived canopy height and biomass in grasslands. Overall, there was a range of R^2 values, reflecting associations between canopy height and biomass that varied from moderate ($R^2 = 0.41–0.59$) to high ($R^2 = 0.76–0.88$). Nonetheless, only a few authors highlight field disturbances as a factor contributing to the decrease in biomass estimation accuracy. For example, Van Der Merwe, Baldwin and Boyer (2020) noted that the accuracy of biomass estimation using UAV-derived canopy height was reduced in areas with high levels of lodging. Lussem *et al.* (2019) suggest that the high rodent activity in a few plots per growth led to higher uncertainties in canopy height calculation, which, in some cases, resulted in negative sward height values and unreasonable biomass values. Their decision to exclude these plots improved the biomass estimation, although these disturbances are likely to occur in the field. Roth and Streit (2018) examined different cover crops, including two clover species, and achieved an R^2 of 0.58. When plants, which were growing close to the ground or even lodging, were excluded from the regression model, R^2 increased to 0.74. They concluded that all examined remotely-sensed characteristics lose their suitability as biomass predictors if lodging occurs.

The reason for this is that the UAV-derived canopy height model uses the height of the plants as a proxy for biomass, assuming that taller plants have more biomass. However, different disturbances in the field can cause a reduction or increase in plant height without necessarily affecting the amount of biomass. This means that UAV-derived canopy height models should be interpreted with caution when disturbances such as lodging are present, as they can affect the relationship between height and biomass. Despite this, our results for biomass estimation using UAV-derived canopy height models ($R^2 = 0.75$) indicate that the estimates remain reasonably accurate even in the presence of disturbances. UAV-based models can capture better the full spatial

variability of biomass across the entire field, offering a more comprehensive view compared to sample-based methods. Therefore, while careful interpretation is needed in disturbed areas, UAV-derived canopy height models continue to be a valuable tool for biomass estimation in heterogeneous grasslands.

We also observed that the cutting system may influence the relationship between dry biomass and UAV-derived canopy height, likely due to variations in grass height and density across treatments. Additionally, lodging could be a contributing factor to the variation in the association between dry biomass and UAV-derived canopy height across different cutting systems. Specifically, when grasslands are managed with cutting systems that lead to taller grasses, such as the two and three cut systems, lodging is more likely to occur, where grass stems bend or break due to their weight. Then, it is possible that irregular growth patterns caused by lodging and molehills can lead to inaccurate representations of the actual canopy height, resulting in over- or under-estimations of aboveground biomass.

The results are consistent with those of Borra-Serrano *et al.* (2019), indicating that the cutting system and harvest day influence the correlation between UAV-derived canopy height and biomass. Similarly, Lussem *et al.* (2019) found that biomass estimation accuracy was influenced by the growth stage of the grassland, with higher accuracy achieved at early growth stages. Grüner, Astor and Wachendorf (2019) investigated the use of an SFM approach based on UAV imaging to predict the biomass of heterogeneous temperate grasslands. They found that biomass estimation accuracy was influenced by the grassland heterogeneity, with higher accuracy achieved in less heterogeneous areas. Additionally, the study found that cutting frequency had an impact on the accuracy of biomass estimation.

An additional consideration is the study design's impact on the results. This is because in order to be able to simulate and evaluate different frequencies of cutting systems, the frequency of data collection varies among the treatments. In this way, the number of samples and disturbance frequency have been shown to influence sensitivity. A more significant number of samples allows for a more representative analysis and increased statistical robustness. Higher frequencies of disturbances can introduce variability and potentially affect the relationship between canopy height and dry biomass. Consequently, the relationship and regression results may be more sensitive to disturbances in treatments with less sample, such as the two cut system.

The number of points influenced by lodging can also impact the results and should be considered when interpreting the findings. In the case of the two cut and three cut systems, which have more sample points affected by lodging, lodging is expected to exert a more significant influence on the overall results compared to the four cut system. The increased number of sample points affected by lodging in the two and three cut system may introduce more variability into the dataset. Ultimately, the balance between sample size, disturbance frequency, and lodging influence can contribute to the sensitivity of the relationship.

Overall, the results highlight the need for innovative techniques to enhance biomass estimation accuracy using UAV-derived canopy height models. To address this issue, we propose that new

techniques should be tested to improve biomass estimation accuracy using UAV-derived canopy height models. One approach is to incorporate other data sources, notably spectral reflectance data. Such data can provide additional information about the health and vigor of the plants in conjunction with ground-based measurements and broader agronomic considerations that can yield a more comprehensive ecological perspective. Another approach is to develop more sophisticated models that consider the effects of lodging on vegetation height and biomass. Advanced machine learning algorithms could be employed to develop these models that can better account for the complex impact of disturbances while also assimilating supplemental data sources, leading to more accurate biomass estimation.

However, it is important to note that lodging quantification in mixed grasslands is challenging, especially in contrast to graminoid monoculture crops like wheat or barley (Lussem, Schellberg and Bareth, 2020). This is due to the diverse emergence of various species throughout the growing season in grasslands, a diversity that varies both spatially and temporally. In this way, future research should address these complexities to advance the accuracy of biomass estimation in real-world grassland ecosystems.

3.5 Conclusion

Our results suggest that UAV-derived canopy height models can be useful for estimating biomass in heterogeneous grasslands, but their accuracy can be affected by disturbances such as lodging and molehills, which alter the height distribution of the canopy. The analysis revealed that while these models are robust in estimating vegetation height, the correlation between canopy height and dry biomass is more sensitive to disturbances, which can lead to over- or underestimation of biomass. Furthermore, the impact of disturbances varied among different cutting systems, highlighting the influence of management practices. However, despite these limitations, the UAV-derived canopy height model still produced reasonably accurate biomass estimations ($R^2 = 0.75$) and offers a significant advantage over sample-based methods by capturing the full spatial variability of biomass across the entire field.

Nonetheless, these findings emphasize the need for caution when interpreting UAV-derived canopy height data as direct biomass indicators, particularly in disturbed fields. Although UAV-derived canopy height models have proven to be valuable tools for biomass estimation, particularly in controlled environments, relying exclusively on these models in heterogeneous and disturbed grasslands can introduce significant uncertainties. While previous studies have shown that multispectral data can enhance biomass estimation by capturing additional vegetation characteristics, the focus of this study was to evaluate the robustness of canopy height models using only RGB data. However, the multispectral data collected will be explored in future work as part of our broader objective to improve biomass estimation accuracy. By combining height-based and spectral data, we aim to develop a more comprehensive and reliable framework for biomass estimation in complex grassland ecosystem.

CHAPTER IV

GRASSLAND ECOSYSTEM ASSESSMENTS: INTEGRATING UAV-DERIVED FEATURES FOR ABOVEGROUND BIOMASS ESTIMATION

This chapter has been submitted to the journal "*Information Processing in Agriculture*" and is under review as: Bazzo, Clara Oliva Gonçalves, Bahareh Kamali, Murilo dos Santos Vianna, Dominik Behrend, Hubert Hueging, Farshid Jahanbakhshi, Inga Schleip, Paul Mosebach, Almut Haub, Axel Behrendt, and Thomas Gaiser. **"**Grassland Ecosystem Assessments: Integrating UAV-Derived Features for Aboveground Biomass Estimation".

Abstract

Monitoring grasslands presents significant challenges due to temporal and spatial dynamics in their vegetation. This is particularly pronounced in wet grasslands, where moisture dynamics also impact vegetation patterns. Recent advancements in data acquisition and analysis via Unmanned Aerial Vehicles (UAVs) have shown potential for a more comprehensive understanding of vegetation dynamics. However, current UAV-based methods focus predominantly on structural and spectral data analysis. This often overlooks the horizontal heterogeneity within vegetation. This study addresses this gap by integrating texture analysis, alongside structural and spectral data, to enhance aboveground biomass (AGB) estimation. The research was conducted in a heterogeneous wet grassland in eastern Germany under three different cutting frequencies. Regular UAV flights were carried out to obtain RGB (Red, Green, and Blue) and multispectral images, analyzed alongside ground-reference data from 108 plots, to evaluate canopy height and biomass. We tested the performance of Random Forest and Partial Least Squares Regression models for AGB estimation considering different combinations of features including canopy height model vegetation indices and texture analysis. The results demonstrate that texture analysis when combined with traditional spectral and structural data, enhances predictive accuracy, yielding the best R^2 values of up to 0.84 for AGB and reducing the relative root mean square errors to 26.6 %. The results underline the potential of combining UAV-based features in AGB estimation of heterogeneous grassland ecosystems offering a path forward for more effective ecological monitoring and sustainable grassland management.

Keywords: remote sensing, vegetation, ecological monitoring, canopy height, texture, agriculture digitalization

4.1 Introduction

Grasslands are the world's most extensive terrestrial ecosystem. They are pivotal in providing ecological and economic services, including wildlife habitat, erosion control, carbon sequestration, and sources for biofuels (Egoh *et al.*, 2016; Bengtsson *et al.*, 2019). Wet grasslands, a crucial subset of these ecosystems, are especially vital for biodiversity conservation and water regulation (Chris B. Joyce, Simpson and Casanova, 2016). Therefore, monitoring the status of wet grasslands is important for understanding their ecological health, managing their biodiversity, and maintaining hydrological balance (Čop, Vidrih and Hacin, 2009). Nevertheless, the complexity of these environments introduces significant challenges for ecological assessment and monitoring, demanding detailed and continuous approaches to ensure effective conservation and management (Barrett *et al.*, 2014).

Accurately estimating aboveground biomass (AGB) is essential for managing these ecosystems, and facilitating informed land management decisions and ecological monitoring practices (Jones and Donnelly, 2004; Le Clec'h *et al.*, 2019). For example, knowing the biomass levels can help farmers determine the optimal times for grazing or mowing, improving both yield and pasture health (Psomas *et al.*, 2011). Ecologically, monitoring AGB is crucial for understanding carbon sequestration dynamics, as grasslands play a significant role in capturing and storing carbon (Bengtsson *et al.*, 2019). Moreover, it supports in maintaining biodiversity by ensuring that different plant species have the opportunity to grow and thrive, thus supporting a diverse ecosystem (Tilman, Wedin and Knops, 1996). Yet, traditional methods for assessing AGB, such as physical measurements and visual evaluations, are labor-intensive and often fail to capture the inherent spatial variability (Borra-Serrano *et al.*, 2019). Furthermore, these methods are limited in assessing intra-plot spatial variability, which is crucial for understanding grassland dynamics (Bareth and Schellberg, 2018).

Satellite remote sensing has become a powerful tool for monitoring agroecosystems, including wetlands (Schmidt and Skidmore, 2003; Klemas, 2011), over the past few decades. It allows for the collection of data over large areas and at frequent intervals, providing valuable insights into vegetation health, biomass estimation, and changes in land cover (Xue and Su, 2017). However, satellite remote sensing has some limitations, such as lower spatial resolution and dependence on clear-sky conditions for accurate image acquisition (Younes, Joyce and Maier, 2021).The advent of UAV-based remote sensing offers a paradigm shift in grassland monitoring. High-resolution UAV image, including digital imaging and photogrammetry, presents an efficient alternative to traditional methods, allowing for the acquisition of detailed data at various spatial and temporal scales (Wachendorf, Fricke and Möckel, 2018; Pranga *et al.*, 2021). UAVs are particularly effective in capturing small-scale heterogeneities that are often overlooked by traditional methods or satellite remote sensing (Michez *et al.*, 2020).

Regarding the image methods, UAVs are commonly used to produce 3-D data using structure from motion photogrammetry and spectral information (Michez *et al.*, 2020). Structure from

motion photogrammetry in particular leverages structural information, with canopy height playing a pivotal role in estimating biomass (Lussem *et al.*, 2019). This process involves computing vegetation height from a UAV photogrammetric Digital Surface Model (DSM) in conjunction with a Digital Terrain Model (DTM) (Possoch *et al.*, 2016). The canopy height data provides valuable spatial insights into grassland vegetation traits such as mean, maximum, and median height (Lussem *et al.*, 2022).

While structural height data obtained from UAVs are crucial for understanding spatial patterns of canopy height within grassland vegetation, this data alone cannot capture the biochemical properties or the spectral diversity of species present which can be important for biomass estimations (Grüner, Astor and Wachendorf, 2021). To address these limitations, spectral sensors come into play. These sensors quantitatively measure multi- and hyperspectral reflectance data and enable the calculation of vegetation indices (VIs) (Moeckel *et al.*, 2017) which could be employed to estimate various grassland attributes, including biomass (Askari *et al.*, 2019). These indices, while informative, must be interpreted with caution as they can be influenced by background color at low biomass levels and saturation at high biomass and LAI levels (Grüner, Astor and Wachendorf, 2021).

Another important feature that can be extracted from remote sensed images is the texture analysis (Yue *et al.*, 2019). Texture analysis refers to the study of spatial patterns and statistical relationships among pixel gray-level values within a defined area of interest in an image (Haralick, Shanmugam and Dinstein, 1973). These texture features provide additional data layers correlating with vegetation's structural and heterogeneity characteristics (Dos Reis *et al.*, 2020). In grassland ecosystems, texture analysis has the potential to play a pivotal role in improving biomass estimation, particularly for species with heterogeneous canopies (Grüner, Wachendorf and Astor, 2020).

With the recent development of artificial intelligence technology, it has become possible to combine multiple systems' features to predict a target property (e.g. biomass). Yet, there's a multitude of methods available and it's still unknown which features and how frequently the corresponding data must be collected for reliable predictions. The latter is particularly important to optimize management costs associated with equipment maintenance and data analysis to effectively support decision making. It was also found that, although the integration of UAV-derived structural and spectral data shows great promise, there is a lack of research conducted at the real field level, incorporating management practices and covering multiple growing seasons (Bazzo *et al.*, 2023). This gap needs to be addressed to evaluate the practical benefits of this integration in terms of improving biomass estimation and grassland management strategies.

Therefore, our study aims to evaluate UAV-feature integration techniques in a real-world grassland field, to identify suitable techniques and remote-sensed features that allow reliable, spatially explicit biomass predictions. By focusing on a heterogeneous grassland, our approach addresses the challenges associated with spatial and temporal variability in vegetation growth and composition. The specific objectives of this study are: (1) to develop aboveground biomass

prediction models for a heterogeneous wet grassland for two growing seasons under three cutting systems; (2) to compare the prediction accuracy of these models with and without the integration of features; (3) to identify key variables of the resulting models.

4.2 Study site and experimental design

The research site is located approximately 48 kilometers northwest of Berlin, near the village of Paulinenaue (52°41'28" N, 12°44'16" E), within the federal state of Brandenburg, Germany (Fig. 4.1a).

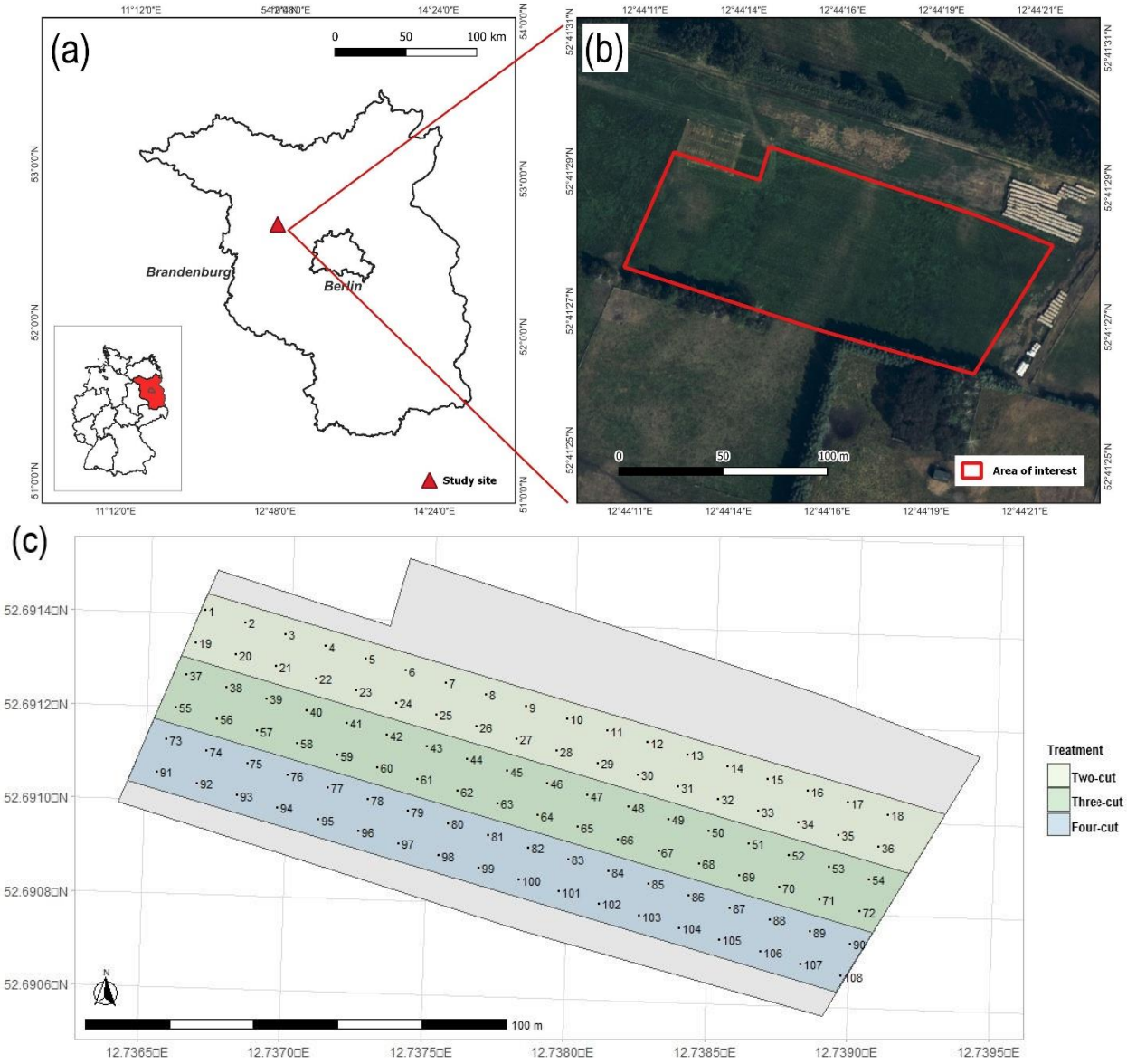

Figure 4.1. (a) Study area located in the federal state Brandenburg, Germany (b) satellite image of the study area from Google Earth Pro, and (c) design of the field experiment divided into three cutting treatments and 108 sampling points.

Encompassing an area of 1.3 hectares of a wet grassland within the "Havelländisches Luch", a shallow, drained fen peatland complex (Fig. 4.1b). The climate is classified as humid continental with warm summer, characterized by an average annual temperature of 9.2 °C and mean annual precipitation of 530 mm (Pohl *et al.*, 2015).

In 2013, the study site was initially seeded with a mixture dominated by *Festuca arundinacea*, followed by a reseeding with *Lolium perenne* in August 2018 at 20 kg/ha. Annual fertilization practices were managed to address the nutrient requirements of the site, with PK fertilization in April and N fertilization as required by the fen's ecological characteristics.

To represent the most typical farmers practice, the site was divided into three east-west-oriented strips, each measuring approximately 16 meters in width and 200 meters in length (Fig. 4.1c). These strips were subjected to different cutting frequencies, to study the effects on grassland vegetation growth and maturity. The treatments ranged from two to four cuts per year, aligned with vegetation phenology and soil moisture conditions, facilitating a comprehensive analysis of grassland dynamics over two years. The study encompassed 108 sampling points, divided into 36 plots per treatment. Throughout the two-year study period, field measurements were synchronized with the cutting events.

4.3 Material and methods

Figure 4.2 depicts the schematic workflow of the methodologies used to fulfill the three objectives of the research. These include four steps: 1) Data collection (section 3.1.); 2) image processing (section 3.2.); 3) feature extraction (section 3.3.); and model development and statistical analysis (section 3.4.).

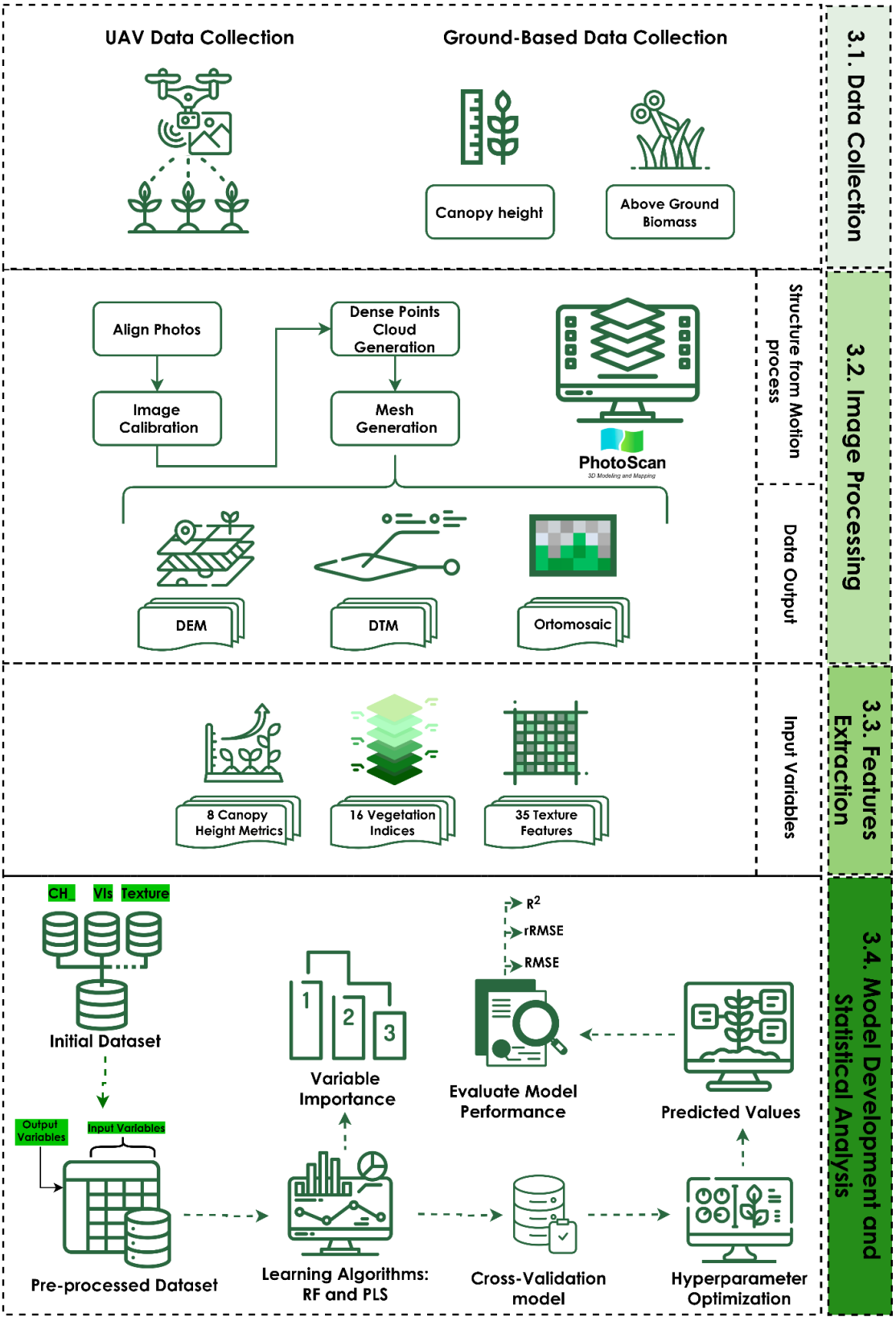

Figure 4.2. Schematic workflow of data acquisition, image processing, feature extraction, model development, and statistical analysis.

4.3.1 Data collection

To obtain essential reference data, we conducted field measurements in 2022 and 2023. The data collection involved two levels: UAV image collection and ground-based field measurements. Table 4.1 summarizes the date of sampling in each field campaign with the number of sampling points in each cutting system.

Table 4.1. Days on which field measurements were conducted, along with the corresponding number of samples and plots.

Year of collection	Harvest date	Cutting systems frequency			Number of samples per date (n)
		Two-cut	Three-cut	Four-cut	
2022	18 May			X	36
	17 Jun	X	X	X	108
	03 Aug		X	X	72
	14 Sep	X	X	X	108
2023	16 May			X	36
	07 Jun	X	X		72
	21 Jun			X	36
	10 Aug		X	X	72
	20 Sep	X	X	X	108
Total number of samples per treatment		**144**	**216**	**288**	**n_{total}= 648**

4.3.1.1 UAV data collection

Data collection was performed with the DJI P4 Multispectral UAV, equipped with a multispectral camera for capturing five spectral bands (Red, Green, Blue, NIR, and RedEdge) and an RGB camera for standard visible image. The UAV was flown at an altitude of 37 meters, achieving a two-centimeter resolution, with 80% forward and 60% sideward image overlap for extensive coverage. Images were captured at two frames per second, with adjustable aperture and exposure settings to match varying lighting conditions. Eleven ground control points (GCPs) were evenly distributed across the experimental site to ensure precise geo-referencing, with their positions fixed throughout all growth seasons. The coordinates of the GCPs' centers were determined using a global navigation satellite system receiver (Viva GNSS GS 10, Leica Geosystems AG, Switzerland), with an accuracy of 0.3 cm horizontally. We conducted nine flights aligning them with compatible dates corresponding to the reference field data collection (Table 1). A bare-ground

model was also generated during a dedicated flight conducted on September 30, 2022. This setup supported the generation of a highly accurate Digital Surface Model (DSM), capturing the nuanced topography of the study area.

4.3.1.2 Reference ground-based data collection

Our reference ground data collection involved the measurement of compressed canopy height, AGB, and vegetation composition survey from the study plots. These methods are described as follows:

Compressed Canopy Height: The variable was determined using a self-constructed rising plate meter (Fig. 4.3a). Measurements were conducted manually within each plot, measuring 1.5 meters by 1.5 meters at five distinct points to capture the structural heterogeneity (Fig. 4.3b). An average of canopy height values was calculated from the five replicates within each plot.

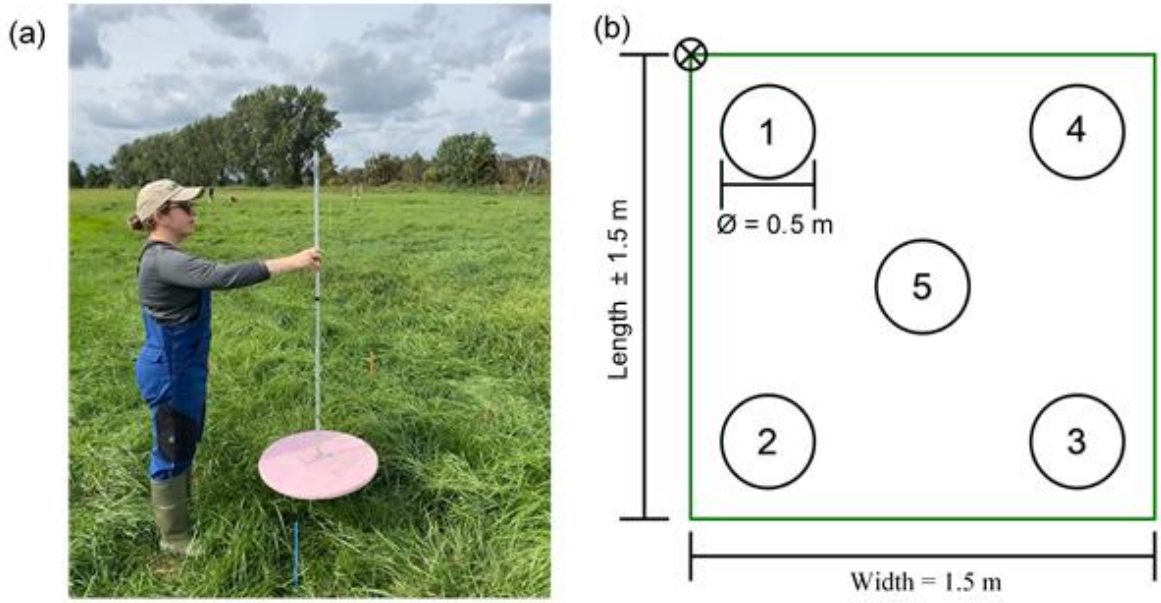

Figure 4.3. (a) In situ grass compressed canopy height measurements by a rising plate meter and (b) schematic overview of point measurements inside the plot.

Aboveground Biomass Sampling: Fresh biomass samples were mechanically collected from each plot using a forage harvester. The fresh biomass weight for each harvested plot was determined by weighing the clipped biomass from each plot. Subsamples from each plot were extracted, dried in a forced air drier maintained at 65 °C until reaching a constant weight, and reweighed to determine dry biomass yield per unit ground area. Biomass values were converted to grams per square meter. To account for slight variations in plot sizes, the area of each plot was validated on-site using a tape measure, ensuring accurate upscaling factors per hectare. These calculations were further refined based on a high-resolution UAV-based orthomosaic generated from data acquired on all sampling dates.

4.3.2 Image processing

The acquired images were processed using Agisoft PhotoScan v.1.3 (Agisoft Ltd. in St. Petersburg, Russia). First, the images were aligned and then adjusted based on the GCPs' spatial information. Next, the optimized cameras command was selected. Subsequently, the image alignment process was executed with a 'high' quality setting to maximize the alignment's precision. The outcome of this step was the generation of a dense point cloud representing the 3-D structure of the vegetation within the study area. In this process, we applied 'high' quality settings and 'mild' depth filtering to preserve fine details of the grassland vegetation, as recommended by Viljanen et al. (2018). The datasets from the multi-spectral camera were then radiometrically calibrated by the calibrate reflectance function using the calibration factors of the irradiance sensor and the gray reference panel. From all flights, a DSM was generated from the dense point cloud and exported as a TIFF file. The model obtained had a spatial resolution of two centimeters per pixel horizontally.

4.3.3 Features extraction from the remote sensing dataset

For each date, a polygonal shape file was created for the biomass sampling area per plot based on an orthomosaic obtained directly after biomass sampling. These shape files were then used to extract representative structural and spectral features from each plot. All the data extraction and processing were done using the statistical computation software R version 4.3.1 and its corresponding packages 'raster' and 'sf'.

4.3.3.1 Canopy height features

For each sampling date, we generated a base Digital Surface Model (DSM) before cutting the grass canopy. The UAV-based canopy height metrics were derived by subtracting the Digital Terrain Model (DTM), obtained from aerial image of the 'bare ground' after harvest, from the DSM (DSM - DTM). In our study 'bare ground' refers to the field condition after harvest, where grass stubbles remain. These remaining stubbles are a common residue in agricultural practices. We extracted the following metrics: mean, minimum, maximum, standard deviation, 90th, 75th, 50th (median), and 25th quartiles (CH_{mean}, CH_{min}, CH_{max}, CH_{sd}, CHq90, CH_{q75}, CH_{q50}, CH_{q25}, respectively). Linear regression models were applied to assess the performance of UAV-based canopy height measurements using the plot-level field measurements as ground-truth reference.

4.3.3.2 Vegetation indices

A total of 16 vegetation indices (VI) were calculated with spectral bands obtained for each flight campaign (Table 4.2). These indices were selected based on their characterization of biochemical and structural traits of vegetation to be comparable to existing studies. The respective shape files from biomass samples were used to extract spectral features from each plot.

Table 4.2. Vegetation indices derived from the visible-to-near-infrared spectral region.

Vegetation Index	Equation
Blue Normalized Difference Vegetation Index (Yang *et al.*, 2004)	$BNDVI = \frac{(NIR - Blue)}{(NIR + Blue)}$
Canopy Chlorophyll Concentration Index (Jago, Cutler and Curran, 1999)	$CCCI = \frac{\left(\frac{(NIR - RedEdge)}{(NIR + RedEdge)}\right)}{NDVI}$
Chlorophyll Vegetation Index (Vincini, Frazzi and D'Alessio, 2008)	$CVI = \frac{NIR}{Green} \times \frac{Red}{Green}$
Enhanced Vegetation Index (Huete *et al.*, 1997)	$EVI = 2.5 \times \frac{NIR - Red}{NIR + 6\,Red - 7.5\,Blue + 1}$
Excess Green (M. Woebbecke *et al.*, 1995)	$ExG = 2\,Green - Red - Blue$
Green Chlorophyll Index (Gitelson, Gritz and Merzlyak, 2003)	$GCI = \left(\frac{NIR}{Green}\right) - 1$
Green Normalized Difference Vegetation Index (Gitelson, Kaufman and Merzlyak, 1996)	$GNDVI = \frac{NIR - Green}{NIR + Green}$
Modified Chlorophyll Absorption in Reflectance Index (Daughtry *et al.*, 2000)	$MCARI = \left[\left((RedEdge - Red) - 0.2\right) \times (RedEdge - Green)\right] \times \left(\frac{RedEdge}{Red}\right)$
Modified Soil-Adjusted Vegetation Index (Qi *et al.*, 1994)	$MSAVI = \frac{2\,NIR + 1 - \sqrt{(2\,NIR + 1)^2 - 8\,\times\,(NIR - Red)}}{2}$
Normalized Difference Red Edge (Barnes *et al.*, 2000)	$NDRE = \frac{(NIR - RedEdge)}{(NIR + RedEdge)}$
Normalized Difference Vegetation Index (Rouse *et al.*, 1973)	$NDVI = \frac{NIR - Red}{NIR + Red}$
Normalized Green Intensity (M. Woebbecke *et al.*, 1995)	$NGI = \frac{Green}{Red + Green + Blue}$
Normalized Green Red Difference Index (Tucker, 1979)	$NGRDI = \frac{(Green - Red)}{(Green + Red)}$
Optimization Soil-Adjusted Vegetation Index (Rondeaux, Steven and Baret, 1996)	$OSAVI = \frac{NIR - Red}{NIR + Red + 0.16}$
Renormalized Difference Vegetation Index (Roujean and Breon, 1995)	$RDVI = \frac{NIR - Red}{\sqrt{NIR + Red}}$
Simple Ratio (Jordan, 1969)	$SR = \frac{NIR}{Red}$

4.3.3.3 Texture features

Texture features were extracted from the generated MS orthomosaic using the R package "glcm" (Gray-Level Co-occurrence Matrix). Seven commonly used texture parameters were calculated to provide insights into the spatial arrangement and variability in the image: contrast, correlation, entropy, homogeneity, dissimilarity, second-moment, variance, and mean ($GLCM_{contrast}$, $GLCM_{entropy}$, $GLCM_{homogeneity}$, $GLCM_{dissimilarity}$, $GLCM_{second\text{-}moment}$, $GLCM_{variance}$, and $GLCM_{mean}$, respectively).

4.3.4 Model development and statistical analysis

To test the predictive power of the extracted features, two machine learning algorithms were employed: Random Forest (RF) and Partial Least Squares regression (PLS). These non-parametric algorithms were selected to address the complexities inherent in our dataset and to align our methods with those validated in similar studies (Oliveira *et al.*, 2020; Pranga *et al.*, 2021; Lussem *et al.*, 2022).

RF, an ensemble learning technique introduced by Breiman (2001), is particularly robust against noise and well-suited for handling remote-sensing data, which are often influenced by atmospheric conditions, clouds, and sensor noise. Its ability to provide accurate predictions for regression tasks and its insensitivity to irrelevant predictors make it an excellent choice for ecological studies, such as mapping plant communities or estimating biomass, where data may include repeated observations and significant variability.

On the other hand, PLS is a multivariate analysis approach that has gained recognition as an alternative to Stepwise Multiple Linear Regression, especially in analyzing of spectral data for vegetation (Gong *et al.*, 2016). The advantage of PLS lies in its capacity to handle multicollinearity and non-linear relationships, which are prevalent in ecological data, allowing for constructing of practical and empirically verified models for spectral analysis (Wang *et al.*, 2019).

UAV-based canopy height (CH), vegetation indices (VIs), texture feature (GLCM), and their combination were employed to predict dry matter yield on a plot basis. As a result, seven feature combinations were tested and compared. First, we built a model using only one class of features: 1.CH, 2.VI and 3.GLCM. In the last stage, we combined structural (canopy height), spectral, and texture information in four new models: 4.CH+VI, 5.CH+GLCM, and 6.VI+GLCM and 7.CH+VI+GLCM.

Table 4.3 presents the feature sets considered in the analysis. Statistical analysis was performed in R. The package "caret" was chosen as a modeling framework, since it provides cross-validation procedures and can be implemented in the machine learning algorithms selected for this study.

Table 4.3. A detailed description of feature sets with the corresponding total number of features for the Canopy Height Model, Vegetation Indices, and GLCM texture parameters.

Name	Description	Features Included	Total Number of Features
CH	Canopy Height Model	CH_{mean}, CH_{min}, CH_{max}, CH_{q90}, CH_{q75}, CH_{q50}, CH_{q25}, CH_{sd}	8
VI	Vegetation indices visible to near-infrared spectrum	See Table 4	16
GLCM	GLCM texture features parameters for each image band	$GLCM_{contrast}$, $GLCM_{entropy}$, $GLCM_{homogeneity}$ $GLCM_{mean}$ $GLCM_{dissimilarity}$ $GLCM_{second\text{-}moment}$	35

4.3.4.1 Cross-validation

In our research, we applied a nested m cross-validation (CV) approach, partitioning the data into three folds for the outer loop and three folds for the inner loop, chosen through a random splitting process and following a similar methodology used by Pranga *et al.*(2021). The inner loop's primary function was to calibrate the hyperparameter values and select the optimal model, while the outer loop was dedicated to assessing the model's predictive capabilities for different dataset folds. We repeated this process five times to mitigate the impact of random variation. The nested CV protocol and parameter tuning were executed in R, employing the 'caret' package.

Model performance was assessed using statistical metrics: Coefficient of Determination (R^2), absolute and relative Root Mean Square Error, RMSE, and rRMSE, respectively. ANOVAs, followed by Tukey's post hoc tests, were performed to identify whether a statistically significant difference exists between the R^2, rRMSE, and RMSE of compared models (datasets). We selected a significance level of $\alpha = 0.05$.

4.3.4.2 Hyper-parameter tuning

Hyper-parameter tuning was performed in both machine learning models (RF and PLS) to achieve optimal performance as recommended in previous literature (Pranga *et al.*, 2021). To this end, we conducted a systematic optimization of the hyper-parameters for employing a grid search approach, a systematic method of working through multiple combinations of hyper-parameter values to find the best solution for our models. This involves creating a 'grid' of all possible value combinations for the hyper-parameters we want to tune and evaluating the model performance for each combination to identify the most effective settings.

For the RF algorithm, we adjusted two key hyper-parameters: 'num.trees', which is the number

of trees in the forest, and 'nodesize', the minimum size of the terminal nodes of the trees. The 'mtry' parameter, which determines the number of variables randomly sampled as candidates at each split, was set to its default value, which is the square root of the number of features in the dataset. The grid search combined 'num.trees' parameter values of 50,100, 250, and 500 and nodesize values of 1 to 5, resulting in 20 combinations.

For the PLS method, we tuned the number of components ('ncomp') used in the model, considering values from 1 to the maximum number of possible features. For example, in our model with 59 features (7. CH + VI + GLCM), the 'ncomp' was tuned from 2 up to 59 to determine the most effective number of components to use.

4.3.4.3 Variable importance

A conditional variable importance technique was implemented to interpret which predictor variables were relevant while generating an RF and PLS model. The higher the importance score, the more influential the predictor variable is. The relative importance of the predictor variables for each treatment and all data sets using RF and PLS models was calculated based on both algorithms' built-in feature importance measures, which are included in the 'caret' package of R, enabling the most important variables in each model run to be interpreted.

For the RF model, the importance of each predictor was determined based on the increase in mean square error when the values of the variable were permuted across the out-of-bag samples. For the PLS model, importance was derived from the weights and coefficients of predictors within PLS components, with higher absolute coefficients indicating greater significance to the model's predictive strength.

4.4 Results

4.4.1 Comparison between the UAV-derived canopy height and the canopy height measured with the rising plate meter

Correlations were established first between the UAV and RPM canopy height measures per treatment for the two growing seasons. Examining the relationship between the pooled data for UAV canopy height against RPM measurements for all sampling campaigns in 2022 and 2023 (Figs. 4.4a-b) revealed a consistent correlation across the three treatments. In 2022, the coefficient of determination (R^2) for two-cut, three-cut, and four-cut systems were 0.93, 0.94, and 0.77, respectively. For 2023, the corresponding R^2 values were 0.89 for the two-cut, 0.90 for the three-cut, and 0.78 for the four-cut system. The regression slopes for the UAV canopy height measurements relative to RPM measurements were close to 1 for most treatments, especially for the three-cut system in both years (0.96 in 2022 and 1.05 in 2023), which implies that the UAV measurements were closely related to the ground-reference data. While the R^2 values exhibit some

consistency from year to year within each treatment, this pattern does not uniformly extend across different cutting systems.

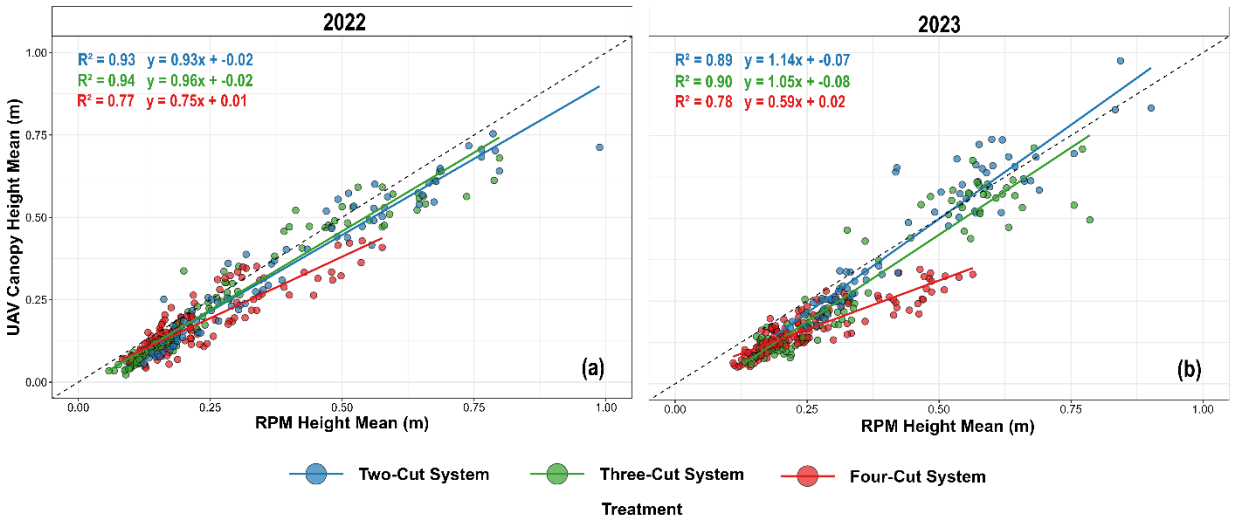

Figure 4.4. Comparison of the mean canopy height using the rising plate meter (RPM) and the mean UAV-derived canopy height for aggregate annual data of 2022 (a) and 20223 (b) in grassland field with treatments (1) two-cut system (2) three-cut system and (3) four-cut system. The dashed line represents a 1:1 ratiot system. The dashed line represents a 1:1 ratio.

4.4.2 Comparative evaluation of feature class performance for AGB prediction across different cutting systems

Figures 4.5 and 4.6 show the performance of PLS and RF models built based on different feature classes - individual classes of CH, VI, GLCM, and their combinations - for the estimation of AGB. As shown, R^2 (Fig. 4.5) and rRMSE (Fig. 4.6) and mean values (Table B1, supplementary material) underscored significant differences among models. The performance of models based on individual feature classes (CH, VI, and GLCM) varied remarkably across the different cutting systems. Among these three models, the one based on CH features was generally a robust predictor regarding both RF and PLS in most cutting systems. Comparing the performance of the other two models (VI and GLCM) showed different performances depending on the cutting system or the algorithm for modeling (PLS or RF). In the two-cut system, the RF model showed CH as a robust predictor with an R^2 of 0.71 and an rRMSE of 29.4 %, indicating a strong correlation with AGB (Figs. 4.5a and 4.6a). The VI feature class, with an R^2 of 0.73 and an rRMSE of 29.19 %, displayed similar predictive strength.

Overall, the models based on a combination of feature classes (CH+VI, CH+GLCM, VI+GLCM, CH+VI+GLCM) showed a higher performance. Comparing these four models showed that those, with the CH feature class included performed better. Across different cutting treatments, feature combinations, particularly CH+VI+GLCM, consistently outperformed the individual-feature models. Combining CH and VI into a single model resulted in a statistically significant

increase in R^2 (0.78) and improved the rRMSE to 25.3 %, suggesting a pronounced enhancement in prediction precision. The CH+VI+GLCM model for RF achieved an R^2 of 0.77 and an rRMSE of 26.6 % and for PLS an R^2 of 0.73 and an rRMSE of 29.1 %, slightly enhancing the model performance.

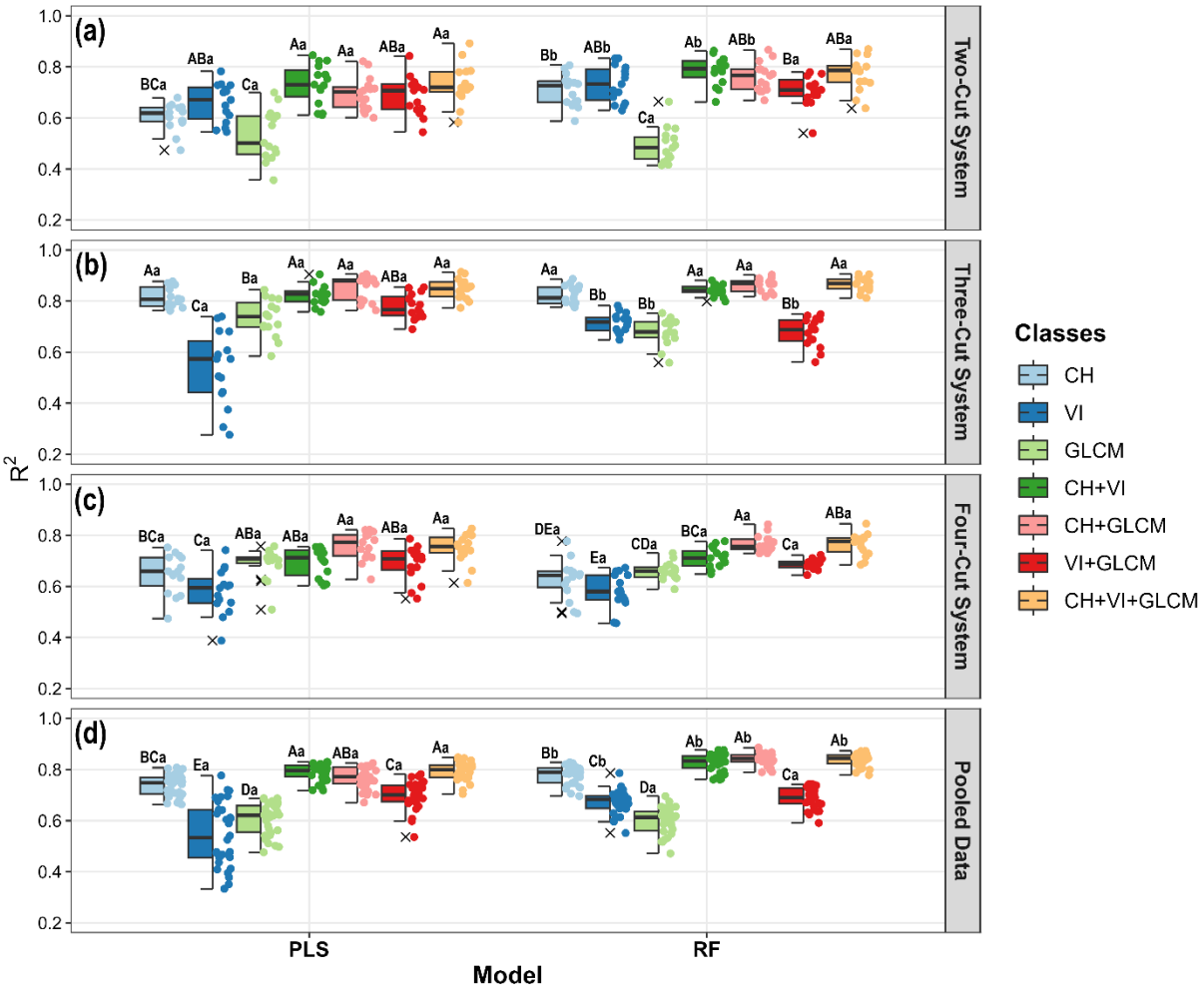

Figure 4.5. Box-dot plots for coefficient of determination (R^2) values for aboveground biomass (AGB) prediction, using two distinct machine learning algorithms: Partial Least Squares Regression (PLS) and Random Forest (RF). The models incorporate various feature classes, including Canopy Height (CH), Vegetation Indices (VI), and texture features (GLCM), applied across different grassland management treatments: two-cut (a), three-cut (b), and four-cut systems (c), as well as a pooled data analysis combining all treatments (d). Uppercase letters compare feature class performance within the same model: identical letters imply no significant differences while differing letters signify significant differences. Lowercase letters evaluate differences between the models for each feature class: identical letters indicate no significant differences, and varying letters denote significant differences.

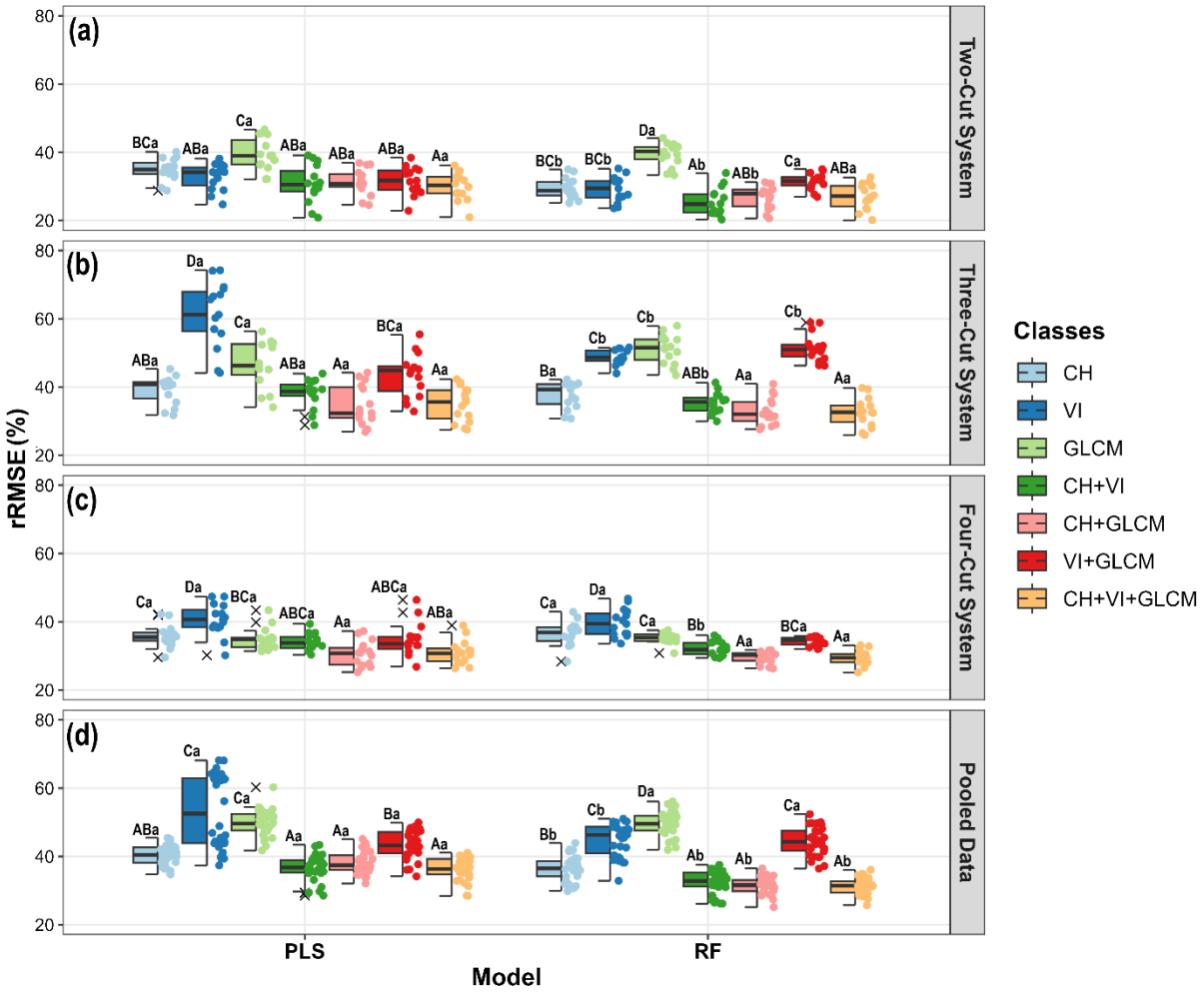

Figure 4.6. Box-dot plots for rRMSE (%) values for aboveground biomass (AGB) prediction, using two distinct machine learning algorithms: Partial Least Squares Regression (PLS) and Random Forest (RF). The models incorporate various feature classes, including Canopy Height (CH), Vegetation Indices (VI), and texture features (GLCM), applied across different grassland management treatments: two-cut (a), three-cut (b), and four-cut systems (c), as well as a pooled data analysis combining all treatments (d). Uppercase letters compare feature class performance within the same model: identical letters imply no significant differences while differing letters signify significant differences. Lowercase letters evaluate differences between the models for each feature class: identical letters indicate no significant differences, and varying letters denote significant differences.

The performance of models varied across cutting systems. The CH+VI+GLCM model in the three-cut system showed superior prediction accuracy, indicated by R^2 values of 0.87 and 0.85 for RF and PLS, respectively (Fig. 4.5b). It is also remarkable that in this treatment, the exclusive use of CH (with mean R^2 value of 0.82 for RF and 0.81 for PLS), showed no significant statistical difference compared to the models based on combined features. However, the CH+VI+GLCM combination resulted in a lower rRMSE (32.6 % for RF and 34.9 % for PLS) (Fig. 4.6b, Table B1, supplementary material). This picture was different in the four-cut system, in which the different

combinations of CH, VI, and GLCM features provided the most accurate predictions with RF and PLS, achieving R^2 values ranging from 0.69 to 0.77 (Fig. 4.5c, Table B1, supplementary material). No statistical differences were observed among the feature combination groups for the PLS model. For the RF model, the CH+GLCM and CH+VI+GLCM combinations were statistically superior. Specifically, CH+VI+GLCM with RF showed significantly lower RMSE and rRMSE values (69.7 g/m² and 29.4 %) (Fig. 4.6c).

When considering the pooled data from all cutting systems, CH+VI+GLCM demonstrated the highest predictive accuracy regarding RF, with an R^2 value of 0.84 (Fig. 4.5d, Table B1, supplementary material). The RMSE and rRMSE values for CH+VI+GLCM in the pooled data were also lower (RMSE = 134.9 g/m², rRMSE = 31.3 %) than for models based on individual feature classes (Fig. 4.6d, Table B1, supplementary material).

4.4.3 Variable importance for AGB estimation

The PLS and RF models highlighted distinct predictor variables with varying degrees of importance across the different cutting systems (Fig. 4.7ab). In the PLS model, CH metrics, such as 'CH_{q50}', 'CH_{q90}', and 'CH_{q75}', obtained high importance scores, particularly in the pooled dataset, indicating their strong influence on biomass estimation under varying cutting frequencies. The texture variable '$GLCM_{homogeneity\_NIR}$' also scored significantly, suggesting the relevance of texture in biomass prediction. Contrastingly, the RF model emphasized a different set of predictors. While CH variables like 'CH_{q90}' and 'CH_{mean}' maintained their influence, vegetation indices such as VI_{NGI} emerged as key predictors across all treatments. Remarkably, texture measures like '$GLCM_{variance\_NIR}$' and '$GLCM_{mean\_NIR}$' were highly ranked in the four-cut system and pooled data, reflecting the importance of NIR texture in these more complex systems.

Comparing treatments, the two-cut system showed a slightly higher importance score for 'VI_{NGRDI}', indicating its particular relevance in less frequently cut grasslands. In contrast, the three and four-cut systems revealed a shift towards '$GLCM_{second\_moment\_NIR}$' and '$GLCM_{entropy\_NIR}$', aligning with the increased complexity of these systems.

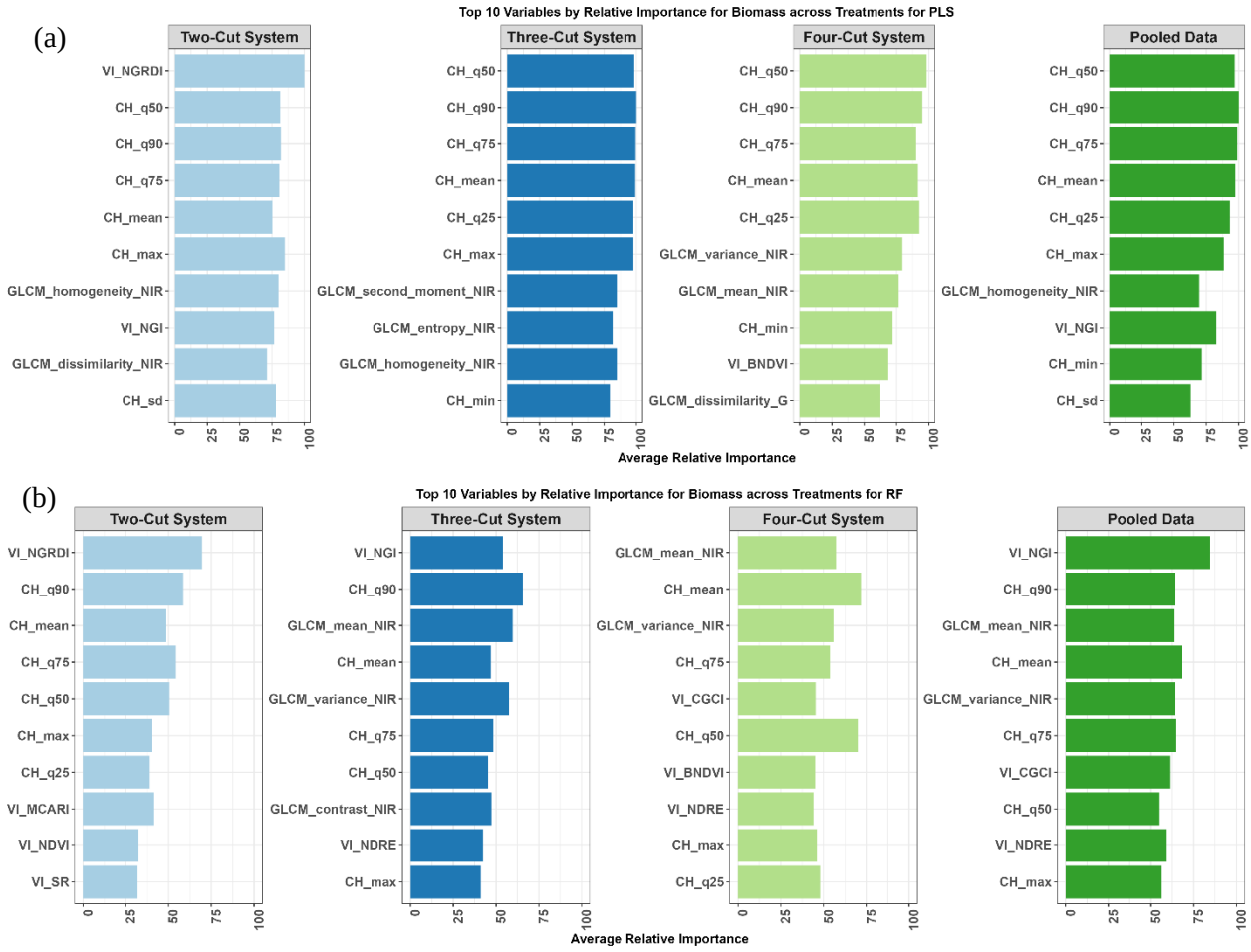

Figure 4.7. The relative importance of the top ten predictor variables as measured by the feature importance metric for Partial Least Square (PLS) (a) and Random Forest (RF) (b) models predicting aboveground biomass (AGB).

4.5 Discussion

In this study, a key objective was to assess the effectiveness of integrating UAV-derived features for estimating AGB in heterogeneous wet grasslands. While the concurrent use of structural and spectral data for AGB estimation in grasslands is increasingly recognized, the incorporation of texture information from UAV imagery remains relatively unexplored. Our research represents a pioneering effort in integrating structural, spectral, and texture features from UAV imagery to estimate AGB in grassland environments.

4.5.1 Analysis of AGB models and their influencing factors

Our findings underscore the effectiveness of combining UAV-derived data types for AGB estimation. Although the differences in accuracy among various feature combinations were small

and often statistically not significant, models utilizing a fusion of features consistently surpassed those relying on a single feature class. Our results align with the existing research trend, where combining UAV-features data tends to enhance the precision of biomass estimation models. For instance, Karunaratne *et al.* (2020) and Lussem *et al.* (2022) found that models incorporating both structural and spectral data significantly improve the AGB prediction accuracy in grassland field studies. Viljanen *et al.* (2018) demonstrated the effectiveness of combining height data with vegetation indices, in a timothy-meadow fescue mixture. Pranga *et al.* (2021) observed similar enhancements when applying this approach to perennial ryegrass. The study of Grüner, Astor and Wachendorf (2021) further emphasized the critical role of texture features, demonstrating that combining structural data, along with multispectral and texture features from UAV high-resolution image, significantly improved the accuracy of estimating aboveground biomass in legume-grass mixtures.

Although our study exhibits a relatively higher rRMSE compared to some of the studies mentioned, direct comparisons are challenging due to the distinct complexities of wet grasslands. These ecosystems often present heterogeneous vegetation, varying micro topography and fluctuating hydrological conditions, which contribute to the spatial and temporal variability of the data. Most recent studies evaluating the combination of UAV-derived data types for AGB estimation were conducted on controlled field trials, which inherently ensure more uniformity in the data. Additionally, they often dealt with more homogeneous grasslands, typically comprising one or a few species, which further contributes to uniformity. Moreover, these studies usually encompass data from a single year, limiting the temporal variability in their data sets.

In contrast, our research was conducted in a permanent wet grassland spanning two years. This setting inherently introduces more variation due to the complex and dynamic nature of wet grasslands, subject to fluctuating environmental conditions and diverse plant communities. The extended time frame of our study captures the inter-annual variability, which is often not addressed in single-year studies. Such variability can significantly affect the results, as factors like weather patterns, water levels, and plant growth cycles can vary substantially between years. Therefore, while our rRMSE might be higher, it reflects the inherent complexity and heterogeneity in a more natural, less controlled grassland ecosystem over an extended period, providing a more comprehensive understanding of biomass estimation in such diverse environments.

Examining the performance of various models and feature classes, it is also crucial to consider the impact of grassland management treatments on our model outcomes. The R^2 and RMSE values variations reflect the complex dynamics introduced by different cutting frequencies. For instance, in the two-cut system, the combination of CH+VI yielded similar results to the combination of CH+VI+GLCM. This suggests that the spectral information provided by vegetation indices becomes particularly valuable in capturing the biomass variation in less frequently cut systems. VIs offers critical information on the plant's health and vigor that canopy height alone does not fully describe. In essence, the VI likely captures the biomass variation due to factors such as plant nutrition and water content, which are not as readily apparent from structural data when cutting

frequency is low.

Although the combination of CH+VI+GLCM leads to the best results in the three-cut system, CH alone also shows good performance compared to the other cutting treatments. This could be because this cutting system strikes a balance between vegetation regrowth and structural uniformity. CH becomes a reliable indicator of biomass, as the plants have sufficient time to regrow between the cuts, but the sward does not become too heterogeneous, which could happen with less frequent cuts. This observation aligns with previous research, which has shown that in grassland environments with moderately uniform canopies - such as those that result from intermediate cutting frequencies - CH alone can provide a sufficient biomass estimation (Borra-Serrano *et al.*, 2019).

The simplicity of using CH alone is advantageous, as it often requires less data processing and can be less labor-intensive compared to models that integrate additional spectral or textural features, making it more practical for on-farm applications. While incorporating a full suite of features, including 'CH+VI+GLCM', has the potential to enhance the model by adding spectral and textural insights, it is essential to weigh the benefits against the increased complexity. If the inclusion of additional data types does not significantly improve the model's performance, the simpler CH alone model should be preferred.

Conversely, the most frequent cutting regime with four cuts produces a more uniform sward, which should simplify the biomass estimation process. However, our findings suggest that adding spectral information from VIs and texture features significantly enhances the model's performance in the four-cut system. This enhanced performance may be because frequent cutting not only standardizes canopy height but also prompts rapid regrowth and recovery of the grassland, which can introduce subtle variations in plant health and density. These nuances are not easily detected by CH measurements alone but can be effectively captured by the combination of CH with spectral reflectance changes that are assessed with VIs.

Furthermore, including texture features becomes particularly important in the four-cut system. Texture captures the spatial arrangement and frequency of patterns within the sward, providing valuable information about the grassland's structural complexity that arises from the frequent disturbances. This information can be crucial for understanding the ecosystem's response to intensive cutting and for accurately estimating the biomass when the visual uniformity masks underlying heterogeneity.

When examining the pooled data, we observe that the 'CH+VI+GLCM' feature combination achieves the lowest relative root mean square error (rRMSE) at 31.3 % and the highest R^2 value of 0.84, suggesting that this combination of features is robust across varying cutting frequencies. The strength of the 'CH+VI+GLCM' model in the pooled data analysis indicates that each feature class brings complementary information that is useful for AGB estimation, regardless of the treatment. CH offers a baseline structural measure, VIs contribute spectral insights related to plant health, and the texture features add a layer of spatial detail that captures the heterogeneity of the grassland. The success of this feature combination in the pooled data underscores the model's adaptability to

highly variable grassland conditions. Although the rRMSE is relatively high, this feature combination could be widely applicable for diverse grassland ecosystems, providing a comprehensive tool for AGB estimation in precision agriculture.

The variable importance analysis across our models reveals that canopy height metrics are vital for AGB across almost all treatments, including the pooled data. This finding is consistent with other studies, reinforcing the notion that CH is a fundamental attribute for biomass estimation models (Michez *et al.*, 2019; Pranga *et al.*, 2021). The persistence of CH metrics as key variables across various treatments underline their universal relevance and stability as biomass indicators, even amidst the structural changes induced by different cutting frequencies.

While variable in their importance, spectral and texture features add depth to the models where CH alone might not be sufficient, particularly in capturing the nuanced biological responses within the grassland ecosystem. For instance, the inclusion of NDVI addresses the vitality of the vegetation, and texture features such as $GLCM_{homogeneity\_NI}$ encapsulate the spatial heterogeneity, which becomes increasingly relevant in less frequently cut systems. Knowing which variables are most critical for each treatment provides a strategic foundation for model refinement, ensuring that future models are scientifically robust and practically applicable for enhancing precision agriculture practices.

4.5.2 Study limitations and opportunities for improvement

Despite the promising potential shown by UAV-based data combined features techniques, several limitations persist. The high dependency on the frequency of data acquisition and the precision of the measurements can introduce variability in the estimation accuracy. The time-sensitive nature of UAV flights, influenced by weather conditions and logistical constraints, also poses challenges in obtaining consistent datasets over extended periods.

The diversity of management strategies and the unique characteristics of wet grasslands also lead to variability in the UAV-derived canopy height measurements. This is consistent with previous studies which showed that different grassland management practices, such as varying cutting frequencies, can significantly alter canopy structure and thus the UAV's ability to capture height accurately (Lussem, Schellberg and Bareth, 2020). Our findings indicate that the lower R^2 values for the UAV-derived canopy height and ground reference data were predominantly observed within the four cut-system treatment, which typically exhibit reduced height due to more frequent harvesting. This observation aligns with prior research indicating that photogrammetric canopy height models provide more accurate height estimates during later growth stages but are less accurate at the beginning of the growth, when the grass is short and the canopy is still sparse (Viljanen *et al.*, 2018; Karila *et al.*, 2022).

Our research was further challenged by the inherent variability of the site's terrain, including fluctuations in ground elevation, the presence of molehills, and uneven groundwater levels. Coupled with the diversity in plant communities and instances of lodging in some treatment areas,

these factors added layers of complexity to our data collection efforts.

In addition, interpreting the UAV-derived data required careful consideration of the complex ecological processes occurring in grasslands. The dynamic nature of these ecosystems, shaped by management practices such as frequency of cutting, demanded sophisticated analysis techniques capable of adapting to these changing conditions.

4.6 Conclusion

Our study has demonstrated the effectiveness of integrating UAV-derived features for estimating aboveground biomass (AGB) in heterogeneous wet grasslands. The developed prediction models accurately estimated biomass in this complex system across two growing seasons, showing differences in performance between the cutting systems. The models performed best in the most intensively managed systems, and provided reliable estimates even in less managed systems. Our results showed that the developed models performed comparably than those reported in studies conducted in more homogeneous and controlled environments, such as field trials.

The integration of structural and spectral data, particularly canopy height, significantly improved the prediction accuracy compared to single-feature models. Both RF (Random Forest) and PLS (Partial Least Squares) algorithms demonstrated enhanced performance with the integration of these features, although RF showed slightly better results in some instances. This integration allowed us to capture the small-scale heterogeneities often missed by traditional methods, providing a more detailed and accurate assessment of biomass.

Key variables identified in our analysis, such as canopy height features, were crucial for accurate biomass estimation. Texture features were especially valuable in models where spatial heterogeneity was a significant factor, such as in the most frequent cutting regimes. These features provided additional layers of data that improved the overall precision of biomass estimates. Therefore, texture analysis is highly recommended for scenarios with high spatial variability within grassland vegetation to enhance model accuracy.

This study represents a significant advancement in grassland ecosystem monitoring, demonstrating the performance of different methods that synergizes diverse UAV-derived features. To advance the potential of UAV-derived data in grassland ecosystem assessments, future research should focus on refining data processing algorithms to enhance the accuracy of feature extraction, such as machine learning techniques for better segmentation and classification of vegetation types, and improved photogrammetric methods for more accurate canopy height models. There is also a need to expand the dataset to include more fields and multi-year data. This expansion would enable testing the model's effectiveness in different grassland environments and refine it for broader applications, ensuring its robustness and reliability across various ecological conditions.

CHAPTER V

INTEGRATION OF UAV-SENSED FEATURES USING MACHINE LEARNING METHODS TO ASSESS SPECIES RICHNESS IN WET GRASSLAND ECOSYSTEMS

This chapter has been published as:

Bazzo, Clara Oliva Gonçalves, Bahareh Kamali, Murilo dos Santos Vianna, Dominik Behrend, Hubert Hueging, Inga Schleip, Paul Mosebach, Almut Haub, Axel Behrendt, and Thomas Gaiser. 2024. "Integration of UAV-Sensed Features Using Machine Learning Methods to Assess Species Richness in Wet Grassland Ecosystems." *Ecological Informatics* 83 (November):102813. https://doi.org/10.1016/J.ECOINF.2024.102813.

Abstract

Wet grasslands are crucial components of terrestrial ecosystems, known for their biodiversity and provision of ecosystem services such as flood attenuation and carbon sequestration. Given their ecological significance, monitoring biodiversity within these landscapes is of utmost importance for effective conservation and management strategies. This study, conducted in a wet grassland of Brandenburg, Germany, utilized unmanned aerial vehicles (UAVs) to facilitate the estimation of species richness by the integration of remotely sensed canopy features such as canopy height (CH), spectral data (Vegetation Indices, VI), and texture features (Gray-Level Co-occurrence Matrix, GLCM) using two machine learning methods (Partial Least Square regression (PLS) and Random Forest (RF)). Data was collected over two growing seasons under three different grass cutting regimes, employing multispectral sensors to capture detailed vegetation characteristics. The analysis revealed that the performance of the machine learning methods varied with the feature combinations. Models combining VI and GLCM features demonstrated the highest predictive accuracy, particularly in frequently cut grasslands, as indicated by higher R^2 values (up to 0.52) and lower root mean square errors (rRMSE as low as 34.9%). RF models generally outperformed PLS models across different feature sets, with the CH+VI+GLCM combination yielding the best results. These findings underscore the potential of spectral and textural data to effectively capture the ecological dynamics of wet grasslands, providing valuable insights into biodiversity patterns.

Keywords: remote sensing, vegetation, ecological monitoring, multispectral, canopy height, texture, agriculture digitalization

5.1 Introduction

Wet grasslands are important yet vulnerable components of terrestrial ecosystems, playing a pivotal role in biodiversity conservation and the provision of essential ecosystem services (Bullock and Acreman, 2003; Bengtsson *et al.*, 2019). Characterized by their rich species diversity, high belowground carbon and hydrological dynamics, these landscapes serve crucial functions such as flood attenuation, groundwater recharge, and carbon sequestration (Joyce and Wade, 1998; Fidelis, Lyra and Pivello, 2013; Khaledi *et al.*, 2024). Historically shaped by centuries of low-intensity agricultural practices such as mowing and grazing, wet grasslands now face severe threats from land-use changes, agricultural intensification, and abandonment (Joyce, 2014; Dengler *et al.*, 2020). The ongoing loss of these ecosystems, underscores an urgent need for effective monitoring tools to preserve their ecological integrity (Čop, Vidrih and Hacin, 2009; Chris B Joyce, Simpson and Casanova, 2016; Fauvel *et al.*, 2020)

The effective conservation of wet grasslands depends on integrating agricultural benefits with ecosystem support and regulatory functions (Tasset *et al.*, 2019). Environmental changes caused by agricultural management practices and alterations in groundwater levels can lead to variations and losses in biodiversity (Schils *et al.*, 2022; Guo *et al.*, 2023). Considering that in wet grasslands, plant communities serve as direct indicators of ecosystem health and services, the maintenance of such communities is particularly critical (Rapinel *et al.*, 2019; Wu *et al.*, 2023). Thus, strategies for effectively monitor species biodiversity are of vital importance in order to preserve the ecological sustainability of these ecosystems (Dumont *et al.*, 2012; Van Vooren *et al.*, 2018; Schils *et al.*, 2022).

Species richness serves as a direct proxy for α-diversity, which refers to the diversity within a particular area or ecosystem and is measured by the number of species in that ecosystem (Rocchini *et al.*, 2021). This measure provides a clear indicator of the ecological condition and conservation value of an ecosystem (Tian and Fu, 2022). It has long been used to inform various ecological objectives, including productivity estimates, reserve network selections, and conservation planning (Tilman, Wedin and Knops, 1996; Fleishman, Noss and Noon, 2006). However, measuring species richness in the field is notoriously difficult, time-consuming, and often troubled by the need to resolve numerous methodological issues such as determining the appropriate number of sampling units, designing sampling strategies, and defining operational species communities (Chiarucci, 2007; Magurran, 2021). Moreover, traditional field-based methods for collecting species information, while accurate, are costly and challenging to upscale to larger spatial extents required for comprehensive monitoring (Lengyel *et al.*, 2008; Fauvel *et al.*, 2020).

Remote sensing technologies have increasingly become vital in biodiversity monitoring and species conservation, primarily due to their ability to provide a continuous, scalable source of data that captures various aspects of biodiversity across different scales (Mairota *et al.*, 2015; Rocchini *et al.*, 2021; Chang, 2023). This is particularly advantageous where field-based data collection is challenged by scale, cost, and accessibility (Palmer *et al.*, 2002; Kamali *et al.*, 2024). Among

remote sensing tools, unmanned aerial vehicles (UAVs) stand out by offering high-resolution data at the leaf and canopy levels, which greatly enhances the potential for accurate mapping of plant diversity in herbaceous communities (Rossi *et al.*, 2022). UAVs also overcome the issue of cloud cover that usually limits satellite monitoring in highly overcast conditions.

Although remote sensing has become an essential tool for biodiversity monitoring, its application in grasslands remains less explored compared to crops and forests (Gholizadeh *et al.*, 2019; Thornley *et al.*, 2023). Wet grasslands, specifically, present unique challenges due to their hydrologic regimes and varied soil compositions, leading to significant variability in plant growth forms (Taddeo, Dronova and Depsky, 2019; Sun *et al.*, 2024). The dense and variable vegetation, along with background factors such as soil, water, shadow, and litter, can interfere with spectral signals, increasing the uncertainty of remote sensed biodiversity assessments (Gholizadeh *et al.*, 2019; Taddeo, Dronova and Harris, 2021). This complexity makes it difficult to accurately reflect local plant diversity, emphasizing the need for advanced remote sensing techniques specific to these ecosystems (Imran *et al.*, 2021; Rossi *et al.*, 2021).

Recent methods to estimating plant biodiversity using remote sensing primarily focus on spectral data (Thornley *et al.*, 2023; Sun *et al.*, 2024). Because of its simple concept, the Spectral Variation Hypothesis (SVH) method has been particularly investigated in recent years across various ecosystems (Chitale, Behera and Roy, 2019; Rocchini *et al.*, 2021). The SVH method presumes that spatial heterogeneity captured in spectral data correlates with variations in environmental and biological diversity (Thornley *et al.*, 2023). This hypothesis suggests that more heterogeneous habitats typically support a greater diversity of species (Rocchini *et al.*, 2021). However, there are significant challenges in applying SVH to estimate species richness. The accuracy of these estimates can be undermined by the complexity of the community, the presence of non-photosynthetic elements, and variations in canopy shadow patterns that may alter the observed spectral diversity (Schweiger *et al.*, 2015; Conti *et al.*, 2021).

To fully exploit the extensive details contained in remote sensing images, novel information retrieval methods need to expand beyond spectral features and incorporate spatial characteristics such as texture (Zhang *et al.*, 2020) and structural diversity (LaRue *et al.*, 2023). Texture metrics, for example, can be used as proxies for habitat heterogeneity (Hall-Beyer, 2017) since it allows for the distinction between more homogeneous landscapes (associated with lower species richness) and spectrally heterogeneous areas (indicating high species richness) (Wood *et al.*, 2012).

In addition to spectral and texture features, structural diversity metrics can be a potential feature for enhancing biodiversity estimates. The Height Variation Hypothesis (HVH) suggest that greater vertical structure complexity increases biodiversity by providing more sub-habitats and niches (Torresani *et al.*, 2020). While extensively explored in forests, this approach remains underutilized in grasslands (Tamburlin *et al.*, 2021; LaRue *et al.*, 2023). In grasslands, canopy height has traditionally been studied for biomass estimation (Batistoti *et al.*, 2019; Bazzo *et al.*, 2023), but it can also indicate species diversity due to significant variability in plant sizes and growth forms, including grasses, herbaceous species, and small shrubs (Petermann and Buzhdygan,

2021). Wet grasslands, specially, with their distinct hydrologic regimes and soil compositions, allow plants to exhibit variability in growth forms and canopy structures (Taddeo, Dronova and Harris, 2021). By capturing the three-dimensional structure of vegetation, remote sensing can provide a more comprehensive understanding of plant diversity in these ecosystems.

Recent studies suggest that the combination of multiple independent variables —such as spectral, texture, and canopy height metrics—can significantly enhance the accuracy of biodiversity estimates compared to models relying on a single type of data (Gholizadeh *et al.*, 2018; Taddeo, Dronova and Harris, 2021; Fu *et al.*, 2024; Sun *et al.*, 2024). This improvement is attributed to the complementary information provided by these variables, which collectively capture nuanced differences in plant biodiversity that may be influenced by factors such as early successional stages or changes in plant composition resulting from various management practice. Despite the potential of combining these metrics, to our knowledge, no previous studies have concurrently utilized spectral, texture, and canopy height data to estimate biodiversity in wet grasslands. Our work addresses this gap by exploring the synergistic effects of these diverse data sources, aiming to develop and validate a robust and estimation model for plant diversity in these complex ecosystems.

To overcome the challenge of integrating multiple variables for biodiversity indicators using remote sensing data, machine learning provides an effective approach (Muro *et al.*, 2022; Chang, 2023). Machine learning algorithms are especially useful for handling large datasets and identifying complex relationships between distinct variables (Holloway and Mengersen, 2018; Morais *et al.*, 2021). This capability is particularly valuable when incorporating diverse data types such as spectral, texture, and canopy height metrics. Two algorithms have been widely used in agroecosystem monitoring: Random Forest (RF) and Partial Least Squares (PLS) regression. RF has been widely used in ecological and remote sensing studies due to its robustness in managing large datasets with numerous predictors and its ability to model complex interactions, providing reliable estimates (Belgiu and Drăguţ, 2016; Viljanen *et al.*, 2018). PLS regression, on the other hand, helps in dimensionality reduction and is effective in dealing with multicollinearity, thereby enhancing the interpretability of the model (Wachendorf, Fricke and Möckel, 2018; Pranga *et al.*, 2021).

This study aims to develop and evaluate different data-driven models for estimating plant biodiversity in a managed wet grassland using diverse data sources (spectral, textural and structural) and two machine learning techniques (RF and PLS). To optimize the species-richness assessment, we compare the prediction accuracy and identify the importance of the different features depending on the cutting system and the ML model. We finally apply the optimized methods to generate species richness maps for wet grasslands, providing insights into the strengths and limitations of our approach in accurately estimating plant biodiversity.

5.2 Material and methods

5.2.1 Study site and experimental design

The study area is situated approximately 48 kilometers northwest of Berlin, close to Paulinenaue village (52°41'28" N, 12°44'16" E), in Brandenburg, Germany (Fig. 5.1a). The research was conducted on a 1.3-hectare area within the "Havelländisches Luch", a peatland complex characterized by shallow drained peat soils (see Fig. 5.1b).

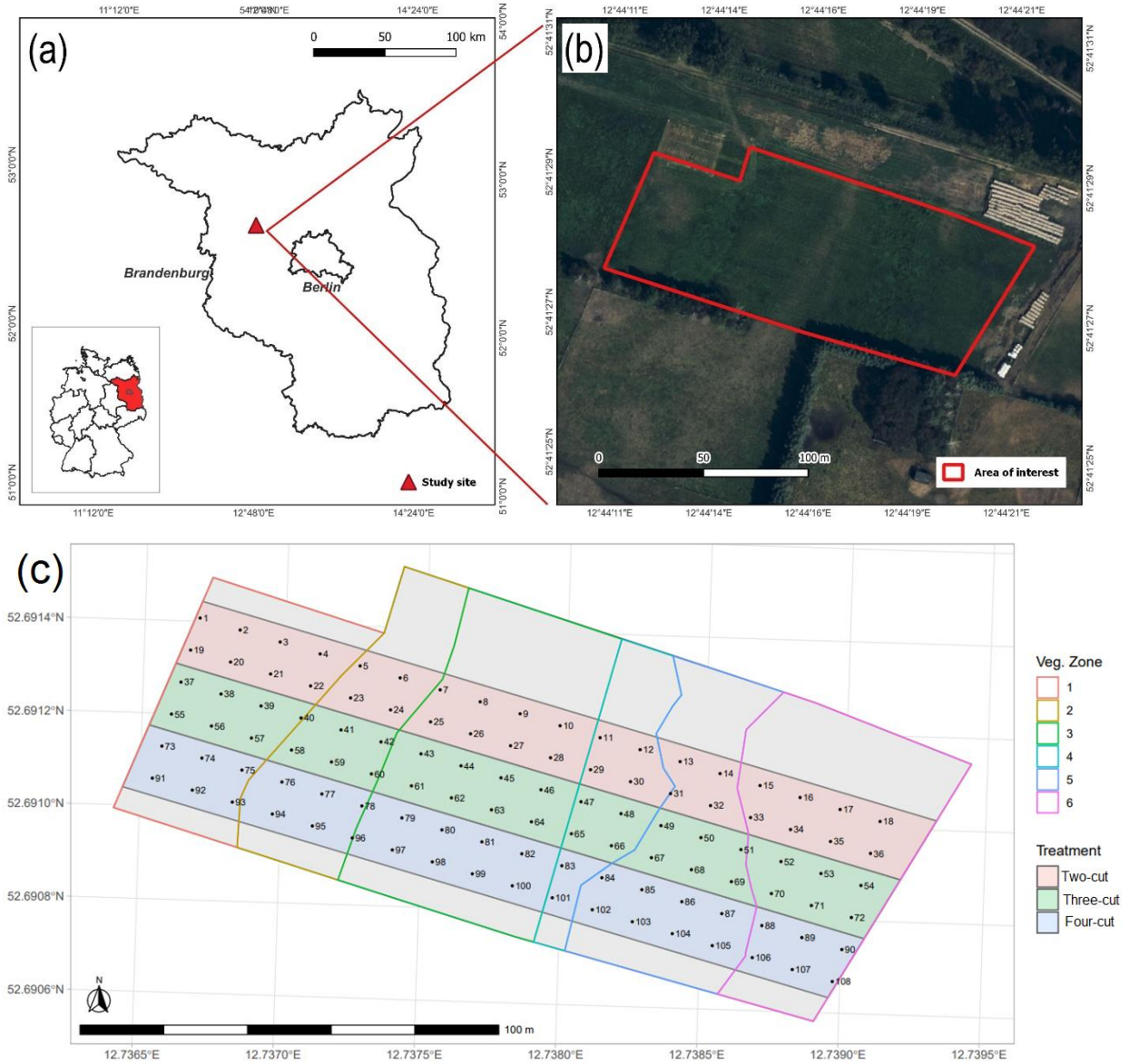

Figure 5.1. (a) Study area located in the federal state Brandenburg, Germany and (b) satellite image of the study area in from Google Earth Pro, and (c) design of the field experiment divided into six vegetation zones, three cutting treatments and 108 sampling points.

The peat soil profiles with varying thickness, ranging from 0.5 to 2.0 meters, with the topsoil experiencing substantial degradation due to long-term drainage. Beneath the topsoil, a significant subsoil layer comprises alluvial sand strata, reaching depths up to 12 meters. The climate in this area is classified as humid continental with warm summer, with an average annual temperature of 9.2°C, and annual precipitation averaging 530 mm (Pohl *et al.*, 2015).

The site was initially sowed in 2013 with a grass mixture dominated by *Festuca arundinacea*. On August 14, 2018, reseeding was performed using *Lolium perenne* seeds at a rate of approximately 20 kilograms per hectare. Fertilization practices were carefully managed to meet the nutrient requirements of the site. PK fertilization, including triple superphosphate and potassium-magnesium sulfate, was applied each year in April to compensate for nutrient depletion from plant uptake and soil processes. Additionally, N fertilization using ammonium sulfate was implemented based on the specific nutrient requirements associated with the fen's ecological characteristics and the observed nutrient removal rates from previous harvests.

The study site was divided into six vegetation zones based on the dominant grass species composition (Figure 5.1c). In May 2020, two vegetation samplings following the Braun-Blanquet method were carried out in each vegetation area (Braun-Blanquet, 1932). According to this, *Festuca arundinacea*, *Holcus lanatus*, *Dactylis glomerata*, *Elymus repens* and *Lolium perenne* dominate the vegetation zone one. In vegetation zone two *Elymus repens* and *Phalaris arundinacea* form the main part of the total vegetation in the southern area. In the northern area *Phleum pratense*, *Holcus lanatus* and *Poa trivialis* occur accompanying a higher species richness. Vegetation zone three is dominated by *Festuca arundinacea*, *Holcus lanatus* and *Elymus repens*. In vegetation zone four *Festuca arundinacea*, *Phleum pratense*, *Poa pratensis* and *Elymus repens* dominate. The vegetation zone five is mainly composed of *Phalaris arundinacea*, *Poa trivialis*, *Elymus repens* and *Alopecurus geniculatus*. In the vegetation zone six *Festuca arundinacea*, *Poa pratensis* and *Elymus repens* dominate. Towards the south the abundance of *Phalaris arundinacea* and *Phleum pratense* increase.

To assess the impact of growth height and maturity stage, the site was further divided into three strips with an east-west orientation, each 16 meters wide and 200 meters long. These strips were subjected to different cutting frequencies to represent the most typical farmers practice and thus enabling diverse growth stages and maturity levels in the grassland vegetation. Treatments are summarized in Tab. 1, where treatment one involved two cuts for strip one, the first at peak maturity in late June/early July and a second in early/mid-September. Treatment two for strip two had three cuts, first in mid-June, second at the end of July/early August, and third in early/mid-September, which coincides with three cuts of strip three. Treatment three's strip had four cuts between mid-May and mid-September at four to six-week intervals, timed according to grass phenology and soil moisture-related trafficability for the harvesting machine.

Overall, the study encompassed 108 sampling points, divided into 36 plots per treatment. Throughout the two-year study period, field measurements were synchronized with the cutting events.

5.2.2 Data collection

In order to obtain essential reference data for our analysis, we conducted comprehensive field measurements in 2022 and 2023. The data collection involved two primary levels: UAV image collection and vegetation composition survey. The specific dates and the number of sampling points for each cutting system are outlined in Table 5.1.

Table 5.1. Days on which field measurements were conducted, along with the corresponding number of samples and plots.

Year of collection	Harvest date	Cutting systems frequency			Number of plots investigated for vegetation survey per date (n)
		Two-cut	Three-cut	Four-cut	
2022	18 May			X	18
	17 Jun	X	X	X	54
	03 Aug		X	X	36
	14 Sep	X	X	X	53
2023	16 May			X	35
	07 Jun	X	X		72
	21 Jun			X	18
	10 Aug		X	X	36
	20 Sep	X	X	X	54
Total number of samples per treatment					**n_{total}= 376**

5.2.2.1 UAV data collection

We utilized the DJI P4 Multispectral drone for data collection. This UAV is equipped with a multispectral camera capable of capturing data in five narrow spectral bands (Red, Green, Blue, NIR, and RedEdge), and an RGB camera for conventional visible imagery. During the course of this research, the drone was flown at an altitude of 37 meters above ground level, resulting in a resolution of two centimeters. The image overlap was approximately 80 % forward and 60 % sideward to ensure comprehensive coverage. Camera settings were adjusted to capture images at a rate of two frames per second, with fixed aperture and exposure settings tailored to the lighting conditions at the time of each flight. Consequently, the aperture and exposure settings varied between different acquisition dates. Eleven ground control points (GCPs) were evenly distributed

across the experimental site to ensure precise geo-referencing, with their positions fixed throughout all growth seasons. The coordinates of the GCPs' centers were determined using a global navigation satellite system receiver (Viva GNSS GS 10, Leica Geosystems AG, Switzerland), with an accuracy of 0.3 cm in the horizontal direction. We conducted nine flights (four in the first year and five in the second year), aligning them with compatible dates corresponding to the reference field data collection (Table 1). A bare-ground model was also generated during a dedicated flight conducted on September 30, 2022.

5.2.2.2 Vegetation composition survey

For each field campaign vegetation surveys of the plots with a size of 1.5 meters by 1.5 meters were carried out. Both the total cover of all plants as a percentage of total ground area and the cover of the individual layers as well as the maximum and average plant heights were recorded. The number of plant species and their cover-abundance were recorded in each layer applying the scale of Luthardt *et al.* (2017), according to Wilmanns (1989) and Londo (1976).

Figure 5.2 presents the timeline and workflow for UAV data collection and vegetation composition surveys conducted across different management systems during the study period.

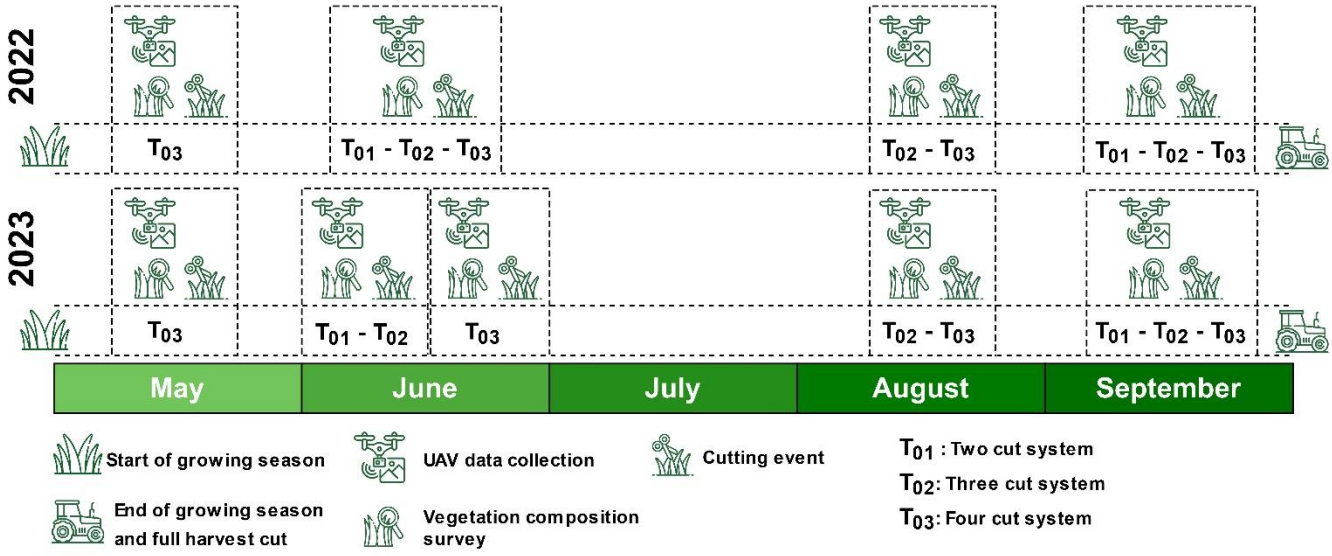

Figure 5.2. Timeline and workflow of UAV data collection, vegetation composition surveys, and cutting events for different management systems (T01: Two-cut system, T02: Three-cut system, T03: Four-cut system) across the study period (2022-2023).

5.2.3 Image processing

The acquired images were processed using Agisoft PhotoScan v.1.3, a Structure-from-Motion (SfM) software developed by Agisoft Ltd. in St. Petersburg, Russia. The first step in image data

processing involves the initial image alignment. During this phase, the acquired images were subjected to a process that established their relative positions and orientations within a three-dimensional space. To ensure the accuracy of the data and its precise alignment with real-world coordinates, ground control points (GCPs) were placed in the images. These GCPs, positioned at known locations within the experimental site, served as reference points for georeferencing. The images were then adjusted based on the GCPs' spatial information. Next, the optimized cameras command was selected. Subsequently, the image alignment process was executed with a 'high' quality setting to maximize the precision of the alignment. The outcome of this step was the generation of a dense point cloud representing the 3-D structure of the vegetation within the study area. In this process, we applied 'high' quality settings and 'mild' depth filtering to preserve fine details of the grassland vegetation, as recommended by Viljanen *et al.* (2018). The datasets from the multi-spectral camera were then radiometrically calibrated by the calibrate reflectance function using the calibration factors of the irradiance sensor and the gray reference panel. A DSM was generated from the dense point cloud and exported as a TIFF file. The model obtained had a spatial resolution of two centimeters per pixel horizontally.

5.2.4 Features extraction from the remote sensing dataset

For each field data collection event, we created a polygonal shape file for the plot sample area. These shape files were then used to extract representative structural and spectral features from each plot. We conducted all data extraction and processing using R statistical software version 4.3.1, utilizing the ‘raster’ and ‘sf’ packages.

5.2.4.1 Canopy height features

For each sampling date, we generated a base Digital Surface Model (DSM). The UAV-based canopy height metrics were derived by subtracting the Digital Terrain Model (DTM), obtained from aerial imagery of the 'bare ground' after harvest, from the DSM (DSM - DTM). It is important to note that in our study 'bare ground' refers to the field condition after harvest, where grass stubbles remain. These remaining stubbles are a common residue in agricultural practices. We extracted the following metrics: mean, minimum, maximum, standard deviation, 90th, 75th, 50th (median), and 25th quartiles (CH_{mean}, CH_{min}, CH_{max}, CH_{sd}, CH_{q90}, CH_{q75}, CH_{q50}, CH_{q25}, respectively).

5.2.4.2 Vegetation indices

We computed a total of 16 vegetation indices (VI) using the spectral bands from the UAV multispectral sensor. These indices were selected based on their characterization of biochemical and structural traits of vegetation in order to be comparable to existing studies. Spectral features for each plot were extracted using the plot shape files. Table 5.2 provides a list of the 16 VIs, based on the visible and near-infrared regions.

Table 5.2. Vegetation indices derived from the visible-to-near-infrared spectral region.

Vegetation Index	Equation
Blue Normalized Difference Vegetation Index (Yang *et al.*, 2004)	$BNDVI = \frac{(NIR - Blue)}{(NIR + Blue)}$
Canopy Chlorophyll Concentration Index (Jago, Cutler and Curran, 1999)	$CCCI = \frac{\left(\frac{(NIR - RedEdge)}{(NIR + RedEdge)}\right)}{NDVI}$
Chlorophyll Vegetation Index (Vincini, Frazzi and D'Alessio, 2008)	$CVI = \frac{NIR}{Green} \times \frac{Red}{Green}$
Enhanced Vegetation Index (Huete *et al.*, 1997)	$EVI = 2.5 \times \frac{NIR - Red}{NIR + 6\,Red - 7.5\,Blue + 1}$
Excess Green (M. Woebbecke *et al.*, 1995)	$ExG = 2\,Green - Red - Blue$
Green Chlorophyll Index (Gitelson, Gritz and Merzlyak, 2003)	$GCI = \left(\frac{NIR}{Green}\right) - 1$
Green Normalized Difference Vegetation Index (Gitelson, Kaufman and Merzlyak, 1996)	$GNDVI = \frac{NIR - Green}{NIR + Green}$
Modified Chlorophyll Absorption in Reflectance Index (Daughtry *et al.*, 2000)	$MCARI = \left[\left((RedEdge - Red) - 0.2\right) \times (RedEdge - Green)\right] \times \left(\frac{RedEdge}{Red}\right)$
Modified Soil-Adjusted Vegetation Index (Qi *et al.*, 1994)	$MSAVI = \frac{2\,NIR + 1 - \sqrt{(2\,NIR + 1)^2 - 8 \times (NIR - Red)}}{2}$
Normalized Difference Red Edge (Barnes *et al.*, 2000)	$NDRE = \frac{(NIR - RedEdge)}{(NIR + RedEdge)}$
Normalized Difference Vegetation Index (Rouse *et al.*, 1973)	$NDVI = \frac{NIR - Red}{NIR + Red}$
Normalized Green Intensity (M. Woebbecke *et al.*, 1995)	$NGI = \frac{Green}{Red + Green + Blue}$
Normalized Green Red Difference Index (Tucker, 1979)	$NGRDI = \frac{(Green - Red)}{(Green + Red)}$
Optimization Soil-Adjusted Vegetation Index (Rondeaux, Steven and Baret, 1996)	$OSAVI = \frac{NIR - Red}{NIR + Red + 0.16}$
Renormalized Difference Vegetation Index (Roujean and Breon, 1995)	$RDVI = \frac{NIR - Red}{\sqrt{NIR + Red}}$
Simple Ratio (Jordan, 1969)	$SR = \frac{NIR}{Red}$

5.2.4.3 Texture features

Texture features were extracted from multispectral (MS) orthomosaic using the R package "glcm" (Gray-Level Co-occurrence Matrix). We calculated seven widely recognized texture parameters that assess the spatial patterns and variability within the image: contrast, correlation, entropy, homogeneity, dissimilarity, second-moment, variance, and mean ($GLCM_{contrast}$, $GLCM_{entropy}$, $GLCM_{homogeneity}$, $GLCM_{dissimilarity}$, $GLCM_{second\text{-}moment}$, $GLCM_{variance}$, and $GLCM_{mean}$, respectively).

5.2.5 Model development and statistical analysis

In this study, we used UAV-derived canopy height (CH), spectral data (VIs), and texture features (GLCM), along with their combinations, to predict species count on a plot-by-plot basis. We explored seven different combinations of these features. Initially, models were developed using single feature classes: 1. CH, 2. VI, 3. GLCM. Subsequently, combinations of structural (canopy height), spectral, and texture data were integrated into four additional models: 4. CH+VI, 5. CH+GLCM, 6. VI+GLCM, and 7. CH+VI+GLCM. Table 5.3 lists the feature sets used in the analysis. Statistical analyses were conducted using the R software, with the "caret" package selected for its robust modeling capabilities, including cross-validation procedures and suitability for the machine learning algorithms employed in this research.

Table 5.3. Detailed description of feature sets with corresponding total number of features for Canopy Height Model, Vegetation Indices, and GLCM texture parameters.

Name	Description	Features Included	Total Number of Features
CH	Canopy Height Model	CH_{mean}, CH_{min}, CH_{max}, CH_{q90}, CH_{q75}, CH_{q50}, CH_{q25}, CH_{sd}	8
VI	Vegetation indices visible to near-infrared spectrum	See Table 4	16
GLCM	GLCM texture features parameters for each image band	$GLCM_{contrast}$, $GLCM_{entropy}$, $GLCM_{homogeneity}$ $GLCM_{mean}$ $GLCM_{dissimilarity}$ $GLCM_{second\text{-}moment}$	35

To evaluate the predictive capabilities of the extracted features, we utilized two machine learning techniques: Random Forest (RF) and Partial Least Squares regression (PLS). These non-parametric methods were chosen due to their proven effectiveness in handling the complex nature of our dataset, aligning with methodologies validated in similar studies.

5.2.5.1 Cross-validation

In our research, we applied a nested cross-validation (CV) approach, partitioning the data into three folds for the outer loop and three folds for the inner loop, chosen through a random splitting process and following a similar methodology used by Pranga *et al.*(2021). The inner loop's primary function was to calibrate the hyperparameter values and select the optimal model, while the outer loop was dedicated to assessing the model's predictive capabilities for different dataset folds. We repeated this process five times to mitigate the impact of random variation. The nested CV protocol and parameter tuning were executed in R, employing the 'caret' package.

Model performance was assessed using statistical metrics: Coefficient of Determination (R^2), absolute and relative Root Mean Square Error, RMSE and rRMSE, respectively. ANOVAs, followed by Tukey's post hoc tests, were performed to identify whether a statistically significant difference exists between the R^2, rRMSE, and RMSE of compared models (datasets). We selected a significance level of $\alpha = 0.05$.

5.2.5.2 Hyper-parameter tuning

Hyper-parameter tuning was performed in both machine learning models (RF and PLS) to achieve optimal performance as recommended in previous literature. To this end, we conducted a systematic optimization of the hyper-parameters for employing a grid search approach, a systematic method of working through multiple combinations of hyper-parameter values to find the best solution for our models. This involves creating a 'grid' of all possible value combinations for the hyper-parameters we want to tune and evaluating the model performance for each combination to identify the most effective settings.

For the RF algorithm, we adjusted two key hyper-parameters: 'num.trees', which is the number of trees in the forest, and 'nodesize', the minimum size of the terminal nodes of the trees. The 'mtry' parameter, which determines the number of variables randomly sampled as candidates at each split, was set to its default value, which is the square root of the number of features in the dataset. The grid search combined 'num.trees' parameter values of 50,100, 250, and 500 and nodesize values of 1 to 5, resulting in 20 combinations.

For the PLS method, we tuned the number of components ('ncomp') used in the model, considering values from 1 to the maximum number of possible features. For example, in our model with 59 features (7. CH + VI + GLCM), the 'ncomp' was tuned from 2 up to 59 to determine the most effective number of components to use.

5.2.5.3 Variable importance

A conditional variable importance technique was implemented to interpret which predictor variables were relevant while generating a RF and PLS model. The higher the importance score,

the more influential the predictor variable is.

The relative importance of the predictor variables for each treatment and all data sets using RF and PLS models was calculated based on both algorithms' built-in feature importance measures, which are included in the 'caret' package of R, enabling the most important variables in each model run to be interpreted.

For the RF model, the importance of each predictor was determined based on the increase in mean square error when the values of the variable were permuted across the out-of-bag samples. This metric quantifies the extent to which the model's predictive accuracy decreases when the variable's information is obscured, thus highlighting the variables that the model relies on most.

In the PLS model, feature importance is less straightforward to assess than in tree-based methods like RF. However, we can evaluate the importance of the variables by examining the weights and coefficients assigned to each predictor in the PLS components, which contribute to the model's predictive capabilities. Variables with more significant absolute coefficients in the PLS model are considered more important as they significantly impact the response variable.

The workflow of the model development process, including feature integration, machine learning, and performance evaluation, is illustrated in Figure 5.3.

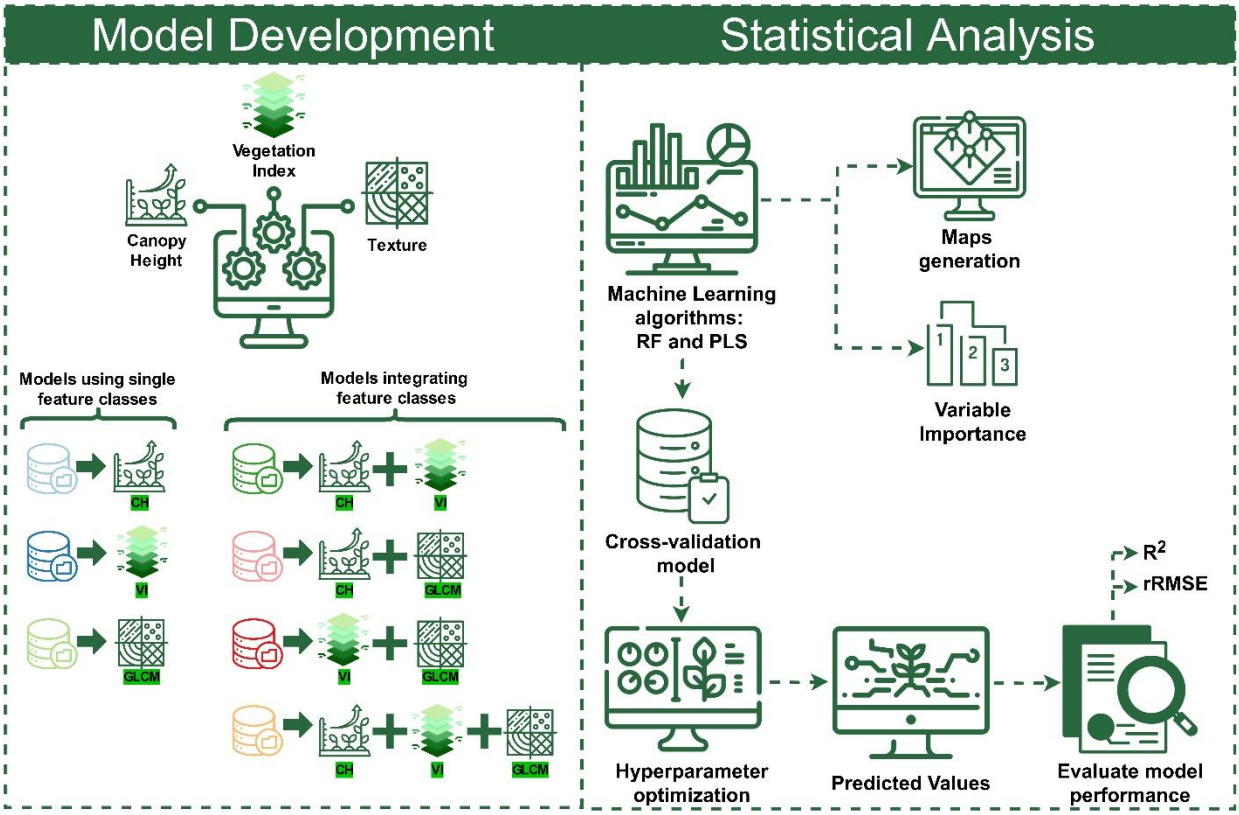

Figure 5.3. Workflow of the model development and statistical analysis process. The diagram illustrates the steps involved, from UAV data processing using individual feature classes (canopy height, vegetation indices, and texture) to the integration of these features. Machine learning

algorithms (Random Forest and Partial Least Squares) were applied, followed by cross-validation, hyperparameter tuning, and evaluation of model performance through R^2 and rRMSE metrics.

5.3 Results

5.3.1 Average species richness by vegetation zone, cutting system and date

In 2022, species richness varied across the different cutting systems and vegetation zones. As shown in Figure 5.4a, the two-cut and four-cut systems generally exhibited higher species richness compared to the three-cut system.

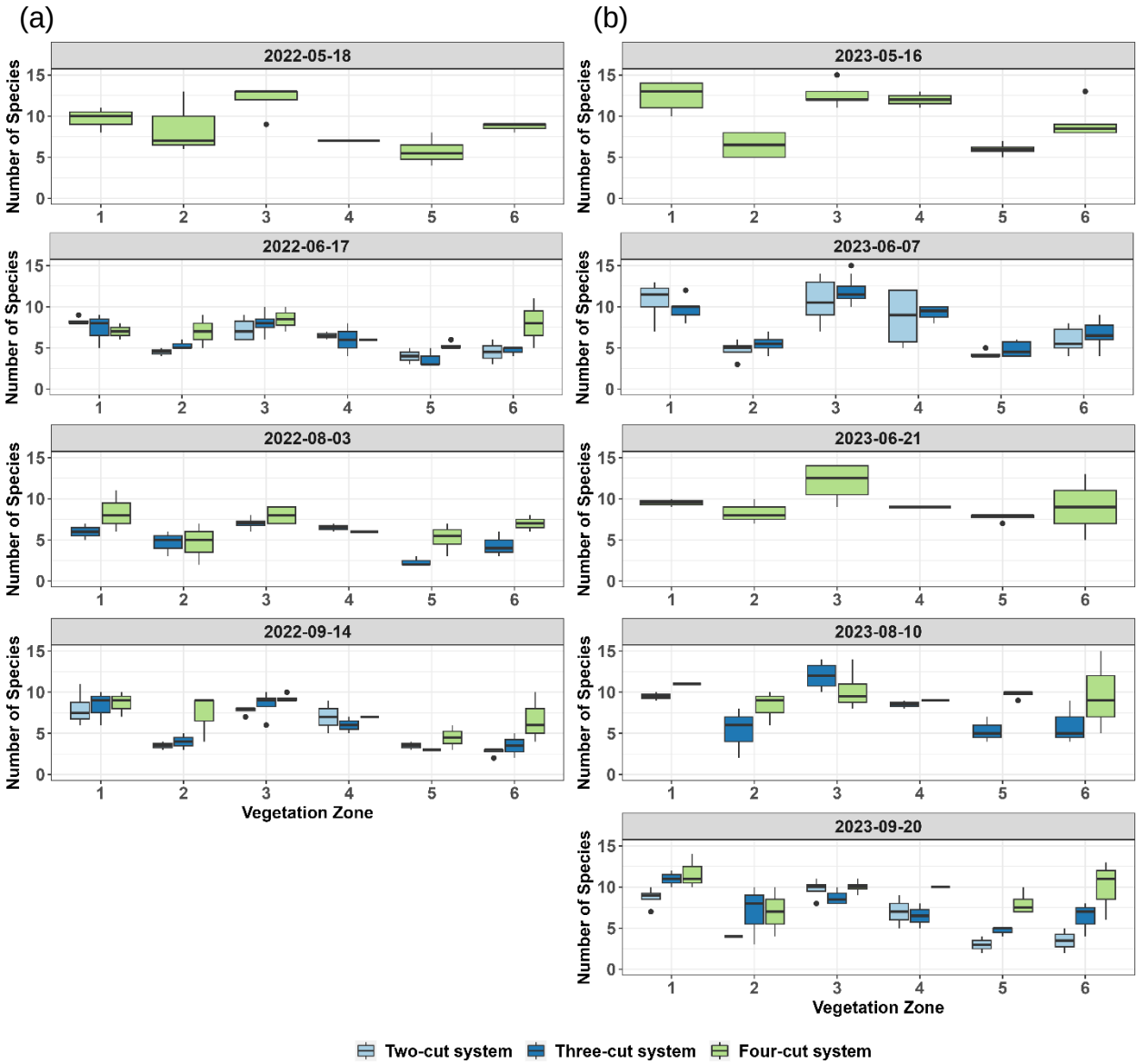

Figure 5.4. Species richness measured in the different cutting systems within six vegetation zones during years a) 2022 and b) 2023.

There were also variations between vegetation zones and dates. For instance, in May 2022, Zones 1 and 3 had higher species richness across all cutting systems, while Zones 5 and 6 consistently showed lower species richness. By June and August, species richness increased slightly in most zones, with peaks typically observed in the early months of the growing season. This trend continued in 2023 (Figure 5.4b), where overall species richness was higher across all cutting systems and zones compared to 2022. The four-cut system showed the highest species richness, particularly in Zones 1 and 6, during the early months of May and June.

The annual mean species richness across the six vegetation zones for each cutting system is summarized in Table 5.4. The four-cut system generally supported higher species richness, particularly in Zones 1 and 6, with averages of 12.8 and 9.6 species, respectively (Table 5.4). The three-cut system also showed improvements, with increases in Zones 1 and 6 compared to the previous year. Zone 5 remained the area with the lowest species richness, although it also experienced an increase compared to 2022.

Table 5.4. Annual mean species richness measured in six vegetation zones and three cutting systems during the study period.

Year	Cutting System	Zone 1	Zone 2	Zone 3	Zone 4	Zone 5	Zone 6
2022	Two-cut	8.1	4.0	7.5	6.8	3.7	3.6
	Three-cut	7.2	4.7	7.8	6.2	3.0	4.3
	Four-cut	8.4	5.1	9.5	6.5	4.8	7.6
2023	Two-cut	9.8	4.8	10.4	8.0	3.8	4.9
	Three-cut	11.8	5.9	10.9	8.2	4.4	6.2
	Four-cut	12.8	6.8	12.0	8.5	8.1	9.6

5.3.2 Comparative evaluation of feature class performance for species richness across different cutting systems

The results were compared across three distinct grass cutting treatments and pooled data to discern the influence of management practices on the predictive capability of the models. Box plots of R^2 and rRMSE (Figures 5.5 and 5.6), and mean values (Table C1, supplementary material) underscored significant differences within and between models and feature classes.

The results suggest that estimation of species richness pivoted towards texture and spectral features. This was even more obvious in the PLS model of the two-cut system, where models based on GLCM and VI established themselves with more robust correlations to species richness (Figs. 5.5a and 5.6a). This suggests that for predicting species richness, even with the prediction accuracy relatively low for all models, textural and spectral aspects of the data can be more informative than

structural height alone.

Model performances showed variable results among different cutting systems. The RF model revealed a subtle trend: as cutting frequency increased, the predictive relevance of CH diminished, highlighting texture and spectral indices as more consistent indicators of species diversity. Within the two-cut system, models based on VI and GLCM or their combination exhibited the highest R^2 values of 0.49 and 0.39, respectively, suggesting these features' better capability in capturing species richness (Fig. 5.5a, Table C1, supplementary material). However, with increasing cutting frequency, combining features from VI and GLCM led to better results. For the three-cut system, the VI features remained the best performer in the RF model, with an R^2 of 0.36 (Fig. 5.5b, Table C1, supplementary material) and an rRMSE of 36.3 % (Fig. 5.6b, Table C1, supplementary material). The CH+VI+GLCM combination, however, showed the lowest rRMSE of 37.50 %, suggesting an enhanced precision. The PLS model presented similar results, with CH+VI+GLCM achieving the highest R^2 of 0.42 and an rRMSE of 37.5 %. A similar pattern was observed in the four-cut system, where the CH+VI+GLCM combination stood out for both RF and PLS models, with R^2 values of 0.32 and 0.34 (Fig. 5.5c, Table C1, supplementary material) and rRMSE values of 33,0 % and 39,6 %, respectively (Fig. 5.6c, Table C1, supplementary material). For the combined data from all treatments, the CH+VI+GLCM set in the RF model displayed high accuracy with an R^2 of 0.30 (Fig. 5.5d, Table C1, supplementary material) and a favorable rRMSE of 36,5 % (Fig. 5.6d, Table C1, supplementary material). The PLS model also produced solid results for the same feature combination, yielding an R^2 of 0.26 and an rRMSE of 38.7 % (Table C1, supplementary material).

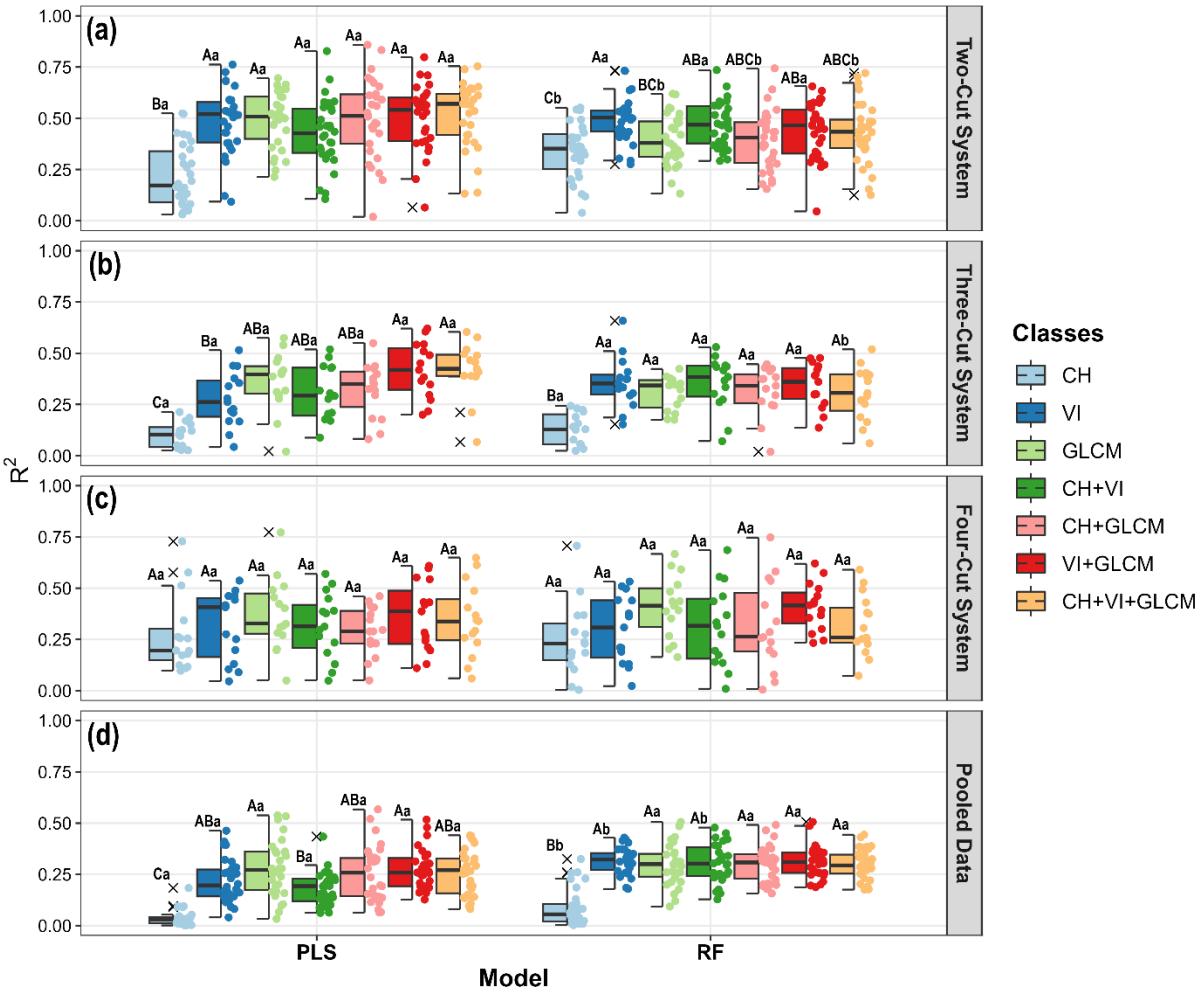

Figure 5.5. Box-dot plots for R^2 values for species richness prediction, using two distinct machine learning algorithms: Partial Least Squares Regression (PLS) and Random Forest (RF). The models incorporate various feature classes, including Canopy Height (CH), Vegetation Indices (VI), and texture features (GLCM), applied across different grassland management treatments: two-cut (a), three-cut (b), and four-cut systems (c), as well as a pooled data analysis combining all treatments (d). Uppercase letters compare feature class performance within the same model: identical letters imply no significant differences while differing letters signify significant differences. Lowercase letters evaluate differences between the models for each feature class: identical letters indicate no significant differences, and varying letters denote significant differences.

In the PLS model, VI alone appeared as the stronger predictor with R^2 of 0.48 and a comparable rRMSE of 35.8 % (Table C1, supplementary material). The aggregation of all three features (CH+VI+GLCM) slightly increased R^2 to 0.52 while maintaining a similar rRMSE, underscoring the integrated approach's effectiveness.

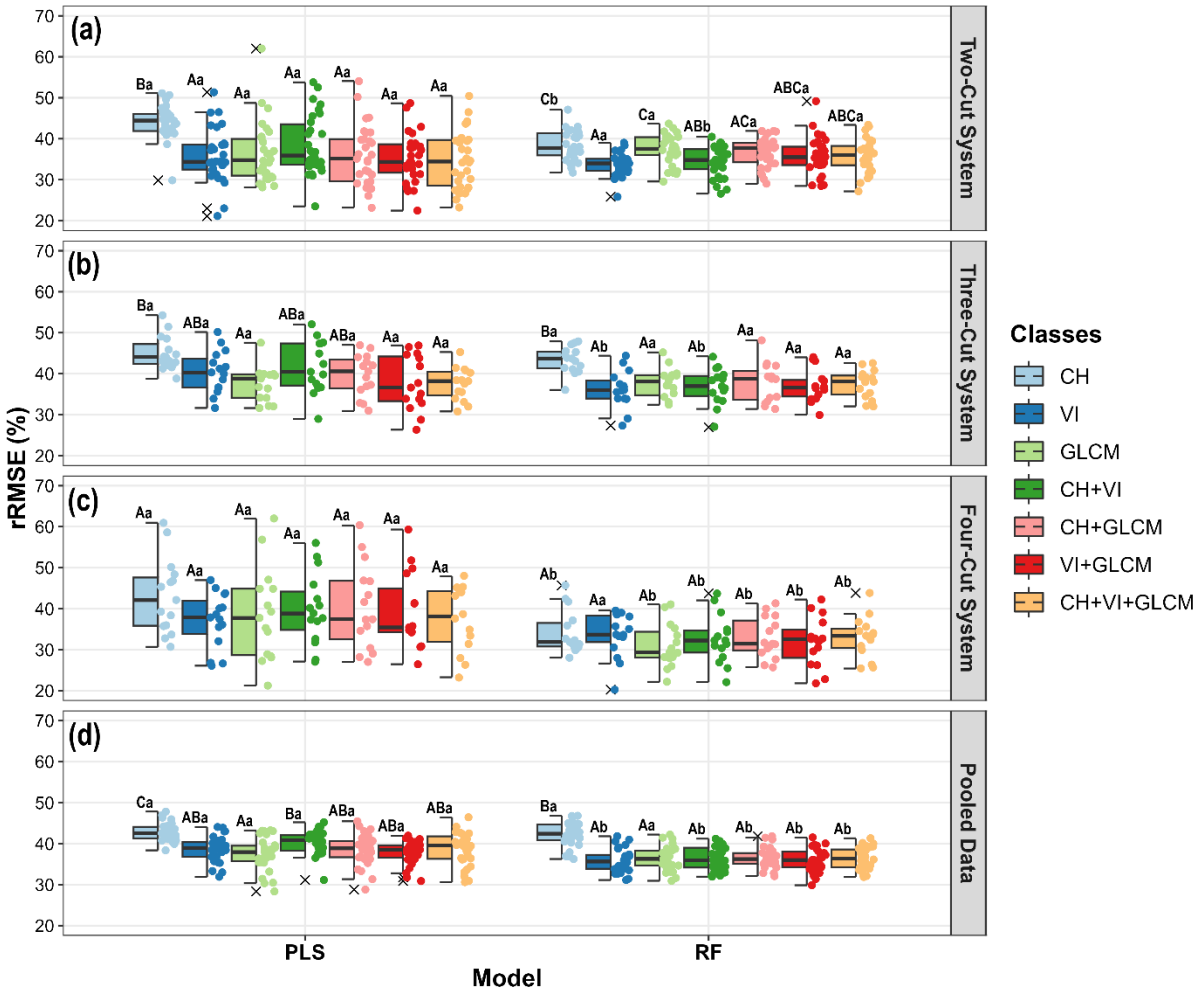

Figure 5.6. Box-dot plots for rRMSE (%) values for species richness prediction, using two distinct machine learning algorithms: Partial Least Squares Regression (PLS) and Random Forest (RF). The models incorporate various feature classes, including Canopy Height (CH), Vegetation Indices (VI), and texture features (GLCM), applied across different grassland management treatments: two-cut (a), three-cut (b), and four-cut systems (c), as well as a pooled data analysis combining all treatments (d). Uppercase letters compare feature class performance within the same model: identical letters imply no significant differences while differing letters signify significant differences. Lowercase letters evaluate differences between the models for each feature class: identical letters indicate no significant differences, and varying letters denote significant differences.

5.3.3 Variable importance for species richness estimation across cutting systems

Overall, the variable importance scores for species richness estimation indicate less reliance on CH features, especially for specific treatments (Fig. 5.7). Instead, the models demonstrate the importance of spectral and textural features, underscoring their critical role in capturing the nuances of species variability in grasslands subject to varying cutting frequencies. In the two-cut system, textural features like '$GLCM_{variance\_NIR}$' and VIs like 'VI_{RDVI}' and 'VI_{MSAVI}' become more

significant, emphasizing their predictive power in scenarios with less frequent cutting. This change is further accentuated by the RF model, which demonstrates the strong significance of NIR textural metrics - '$GLCM_{mean\_NIR}$' and '$GLCM_{variance\_NIR}$' - in the three and four-cut systems as well as in the pooled data. These textural factors have high importance ratings, illustrating how species diversity and NIR texture are closely related in complex management systems.

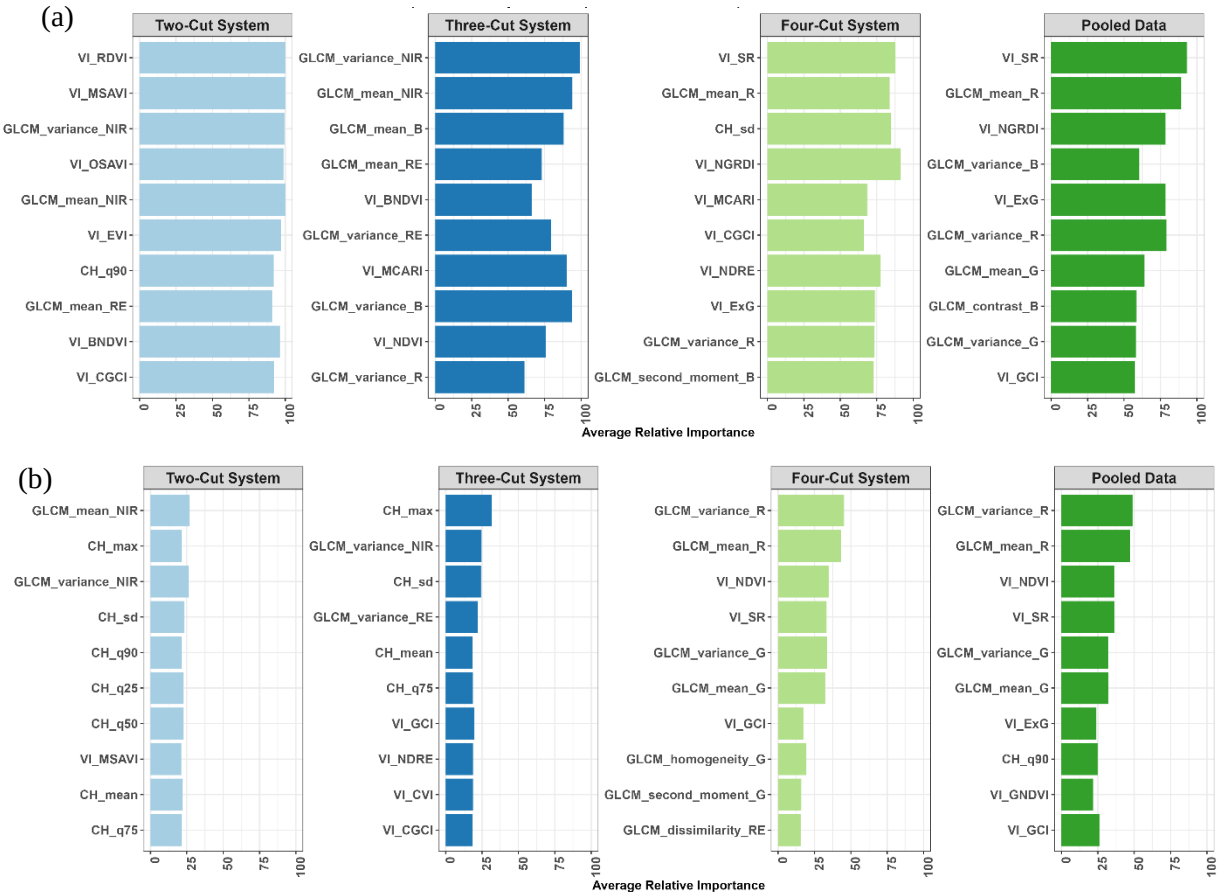

Figure 5.7. The relative importance of the top ten predictor variables as measured by the feature importance metric for Partial Least Square (PLS) (a) and Random Forest (RF) (b) models predicting species richness.

The results of the treatment-specific analysis show that in the two-cut system VIs and NIR texture variables are more significant than CH features. This trend is consistent in higher-frequency cut systems, where indices such as 'VI_{NDRE}' in the four-cut system for PLS and 'VI_{GCI}' in the pooled data for RF are significant, suggesting their enhanced sensitivity to species richness under intensive management.

5.3.4 Mapping species richness using CH, VI, and GLCM features integration for RF and PLS models

Maps were generated for all feature combinations and collection dates; however, due to the large

volume of data, this paper presents maps using the integration of CH, VI, and GLCM features for the five collection dates in 2023 to illustrate the results obtained. The species richness maps for 2023, shown in Figure 8, compare the RF and PLS models.

On May 16, the RF model (Figure 5.8b) shows higher resolution and more detailed variation in species richness compared to the PLS model (Figure 5.8a). The highest species richness is found in zones one and six and lower species number in zones two and five, which aligns with the field data presented in Figure 2.

On June 7, the RF model (Figure 5.8d) shows a finer distinctions in species richness across the zones compared to the PLS model (Figure 5.8c). Zones one, three, and six show higher species richness and zones two and five with lower values, which is consistent with the patterns seen in the field data. Both models (Figures 5.8e and f) show an increase in species richness across most zones by June 21, 2023. Similar with previous dates and field data, zones one, three, and six continue to exhibit the highest species richness.

The species richness starts to decline slightly on August 10, 2023 (Figures 5.8h and g). Consistent with the temporal decline seen in the field data, the overall pattern indicates lower species richness in zones two and five, while zones one and six continue to exhibit higher levels of richness. By September 20, 2023, there is a further decline in species richness towards the end of the growing season. The RF model (Figure 5.8j) captures more nuances variations compared to the PLS model (Figure 5.8i). Zones one and six still show relatively higher species richness, while zones two and five remain lower. These outcomes are consistent with the end-of-season field data.

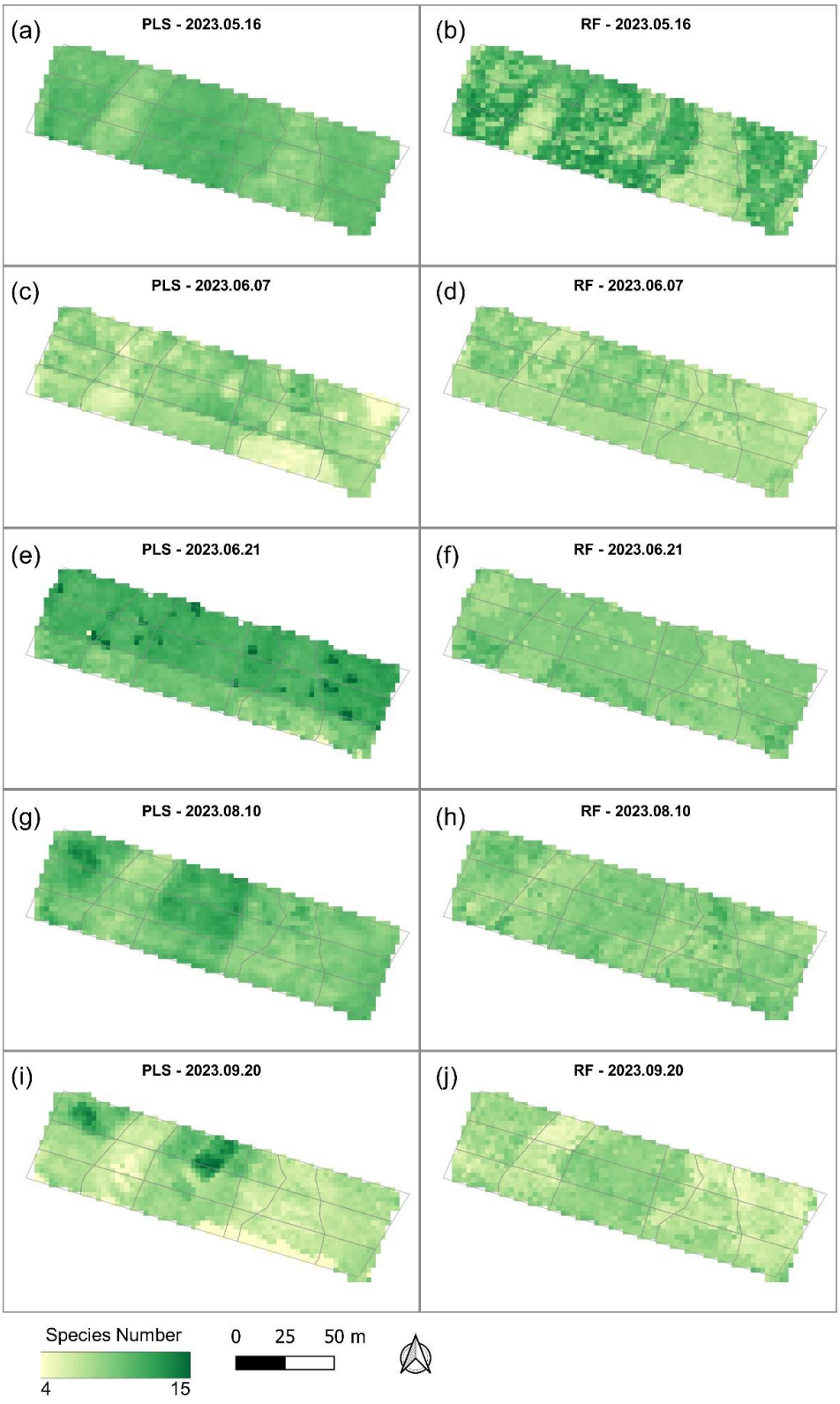

Figure 5.8. Species richness maps for 2023 using the integration of CH, VI, and GLCM features for Random Forest (RF) and Partial Least Squares (PLS) models across five collection dates: (a, b) May 16, (c, d) June 7, (e, f) June 21, (g, h) August 10, and (i, j) September 20.

5.4 Discussion

5.4.1 Integrating UAV-derived data for predicting plant species richness under different cutting systems

The application of remote sensing techniques to detect patterns in plant richness is a growing field of study (Viedma *et al.*, 2012; Chitale, Behera and Roy, 2019; Fauvel *et al.*, 2020; Imran *et al.*, 2021; Muro *et al.*, 2022). Our proposed method to integrate multiple UAV-derived features – spectral, textural, and structural – has proven to be an effective approach for improving the prediction of species richness in grasslands. While spectral data alone, such as vegetation indices (VIs), have traditionally been used to assess plant diversity, the inclusion of texture and structural features provides a more comprehensive view of the ecosystem's complexity. In our study, we observed that combining VIs with texture and structural data generally improved model accuracy (Table C1, supplementary material) although the extent of these improvements varied depending on the management system and the complexity of the grassland ecosystem.

For a better classification of the following discussion, it should be taken into account that the investigated grassland can be characterized as comparatively species-poor. Furthermore, the species numbers are within a relatively small range of 3.0-12.8 (Table 5.4). This context helps frame the application and effectiveness of remote sensing techniques in our study.

The R^2 coefficients achieved in our study (Fig. 5.5) are consistent with previous studies that have applied multispectral and hyperspectral imagery for predicting species richness or other biodiversity indicators, such as Simpson or Shannon indices. For instance, Fauvel *et al.* (2020) reported an R^2 of approximately 0.4 when predicting grassland plant diversity through satellite image time series. Aneece *et al.* (2017) achieved the maximum R^2 value of the correlation between the optical diversity and α-diversity of 0.43 in an artificial ecosystem. Wang *et al.* (2018b) achieved an R^2 up to 0.58 in an artificial grassland study, while Peng *et al.* (2019) observed a highest R^2 of 0.40 in research focused on natural grasslands. Muro *et al.* (2022) reported the highest R^2 of 0.43 using a Deep Neural Network (DNN) approach to predict species richness in temperate grasslands from satellite imagery.

However, direct comparisons with other studies are difficult due to significant differences in ecosystem types, sensor technologies, and methodological approaches. For instance, the majority of research on grasslands have focused on relatively homogeneous or artificially established plant communities, which differ substantially in structure and complexity from natural grassland ecosystems (Imran *et al.*, 2021). Moreover, few studies have investigated grasslands biodiversity estimation under different management regimes (Imran *et al.*, 2021; Rossi *et al.*, 2021; Muro *et al.*, 2022). In terms of methodology, most studies have primarily relied on spectral data, such as individual spectral bands or VIs, with only a few exploring the potential of textural features (Viedma *et al.*, 2012; Cabezas, Galleguillos and Perez-Quezada, 2016; Taddeo, Dronova and Harris, 2021). To our knowledge, no studies have evaluated structural data related to canopy height,

for species richness estimation in grasslands, which we have incorporated in our analysis.

The combination of spectral, textural, and structural features offers distinct advantages in capturing the complexity of grassland ecosystems. Texture features, in particular, have been shown to quantify spatial heterogeneity, which is often linked to habitat complexity and species diversity (Culbert *et al.*, 2009; Cabezas, Galleguillos and Perez-Quezada, 2016). In our study, the inclusion of texture features derived from GLCM consistently improved model performance, especially in more intensively managed systems, and particularly when combined with VIs. For instance, in the three-cut system, adding GLCM to VIs increased the R^2 of the RF model from 0.35 to 0.43, and reduced the rRMSE from 43.16% to 41.30%. Similarly, in the four-cut system, the R^2 of the RF model increased from 0.32 to 0.40, with a corresponding rRMSE decrease from 45.55% to 43.09%. The PLS models exhibited comparable improvements, with the R^2 increasing by approximately 5% and 7% in the three- and four-cut systems, respectively.

The local variance within pixels at a defined neighborhood, induced by different cutting frequency system treatments in our study, could be better distinguished by texture variables when compared to spectral signature variations alone. Additionally, compared to spectral bands and VIs, image texture can also better inhibit saturation and handle high spatial heterogeneity, especially in the late stages of crop growth (Sibanda *et al.*, 2017; Taddeo, Dronova and Harris, 2021). Similar findings were reported by Cabezas *et al.* (2016) who observed that combining texture metrics with spectral indices enhanced the prediction of plant richness in wetland ecosystems. Taddeo *et al.* (2021) also found that integrating texture data into models of managed grasslands improved accuracy, especially in systems where management practices induced variations in vegetation structure.

The incorporation of structural information, such as canopy height, provided mixed results in our study. While canopy height provided valuable information about vertical vegetation structure in some cases, its contribution to model performance varied depending on the management regime. Specifically, canopy height contributed most significantly in systems with lower management intensity (e.g. two-cut systems), where vertical growth is more pronounced and contributes to greater ecological complexity. In contrast, frequent cutting in the three-cut and four-cut systems limited plant development, resulting in lower model performance compared to the two-cut system. In intensively managed systems or those with low biomass variability (e.g. four-cut systems) the addition of canopy height had lower contribution to the models' accuracy. The reduced structural variability in these high-frequency cutting regimes made canopy height a less reliable predictor of species richness. This suggests that in systems where the vertical structure is relatively uniform or where the management regime minimizes height variability, canopy height may not provide significant additional information. In these cases, the models benefited more from the integration of spectral indices and texture features, which became crucial for capturing the finer-scale differences in vegetation that structural data could not distinguish.

Beyond the statistical validation, the robustness of our models can also be qualitatively assessed through the visual interpretation of the generated maps. The predicted spatial distribution

of species richness aligns well with the field data map delineation (Fig 5.8), indicating higher species richness in zones one and six and lower richness in zones two and five. Such spatial insights offer crucial practical value, allowing for more targeted monitoring of species richness across different management regimes.

5.4.1.1 Feature class performance for RF and PLS model

In this section we compare the performance of the both modelling approaches, RF and PLS. In our analysis of individual treatments, it was evident that management intensity significantly affects the performance of both predictive models. Specifically, we observed the highest efficacy in model based estimation of species richness in the two-cut system. The PLS model, employing the CH+VI+GLCM feature class, showed an R^2 of 0.52 and an rRMSE of 34.9 % (Table C1, supplementary material), as compared to the R^2 of 0.48 and rRMSE of 36.5% of RF for the same feature class.

In contrast, the three-cut and four-cut systems management present a more complex scenario, where the increased cutting frequency may lead to a homogenized canopy structure. Especially in the four-cut system, the shorter intervals between cuts do not allow plants to fully recover and reach distinct phenological stages, thus limiting the effectiveness of remote sensing for species differentiation. This is consistent with the findings of Gholizadeh *et al.* (2020), who suggested that removing aboveground plant tissue, such as through frequent cutting or fire, can significantly reduce plant diversity by preventing plants from reaching their developmental peaks.

In both the three-cut and four-cut systems, the Random Forest (RF) model outperformed the PLS model. The superior performance of the RF model is likely due to its capacity to handle the complexity and variability introduced by frequent cutting (Belgiu and Drăguţ, 2016). RF's ability to manage this variability, particularly when texture features were integrated, resulted in more accurate species richness predictions (Cabezas, Galleguillos and Perez-Quezada, 2016).

The analysis of pooled data, which combined all management treatments, revealed a decline in model performance, particularly for models utilizing canopy height (CH) data. This decline is likely due to competing variables holding different levels of relevance across management scenarios, complicating the identification of clear patterns. While the RF model performed robustly in individual treatments, it faced challenges in the pooled data, likely due to the dilution of treatment-specific signals that weakened the model's predictive capacity.

Similarly, PLS models, despite maintaining consistent variable importance profiles with an emphasis on texture and spectral features, also underperformed in pooled data models compared to individual treatments. This indicates that pooling data dilutes the signals specific to each treatment, reducing the impact of distinct spectral and textural characteristics that are essential for predicting species richness within each management regime.

This difference in model effectiveness emphasizes grassland ecosystems' complexity and underscores the necessity for management-specific modeling. Our study also suggests that

ecological responses depend on the intensity of management and characteristics of each regime. Furthermore, our models for species richness show a temporal dependency, indicating that the impact of spectral bands and their texture metrics may differ in response to shifts in plant physiology. This emphasizes the dynamic nature of vegetation responses and the importance of models that can adapt to these temporal variations, especially when incorporating multitemporal data.

5.4.1.2 Variables' importance for RF and PLS models

The importance of predictive variables for species richness changed across different cutting systems. In the two-cut system, structural variables, particularly canopy height (CH) metrics, dominate the importance rankings. Seven out of the ten most important variables in the RF model are CH-related, indicating that the physical structure of the canopy is a strong indicator of species diversity in these less frequently disturbed systems. For the PLS model, while CH metrics remain important, texture and spectral features such as '$GLCM_{mean\_NIR}$' and 'VI_{MSAVI}' also play a significant role, emphasizing the utility of combining different data types.

As cutting frequency increases in the three-cut system, the importance of CH variables decreases. In the RF model, only five CH-related variables remain among the top predictors, with spectral and texture features gaining prominence. This shift is due to the homogenization of the canopy structure caused by more frequent cutting, making variables such as 'VI_{GCI}' and texture metrics from the NIR band more relevant. For the PLS model, spectral indices such as 'NDVI' and texture features like '$GLCM_{dissimilarity\_NIR}$' become more significant.

In the four-cut system, none of the top variables in the RF model are CH-related. Instead, texture and spectral features dominate, with variables such as '$GLCM_{mean\_R}$,' '$GLCM_{variance\_R}$,' and 'VI_{NGRDI}' becoming crucial. These features from the Red and NIR bands capture fine-scale variations in vegetation essential for predicting species richness in highly disturbed systems. The PLS model similarly emphasizes texture and spectral features, with '$GLCM_{variance\_NIR}$' and '$GLCM_{contrast\_R}$' being among the top predictors. These results suggest that as management intensity increases, the use of multidimensional data becomes essential for accurate predictions.

Despite the differences between models and the challenge of generalizing across pooled data, a significant factor remains constant: within the most influential texture and spectral variables for predicting species richness, a substantial proportion is associated with the Red, Red-edge and NIR bands. The Red (630–690 nm), Red-edge (680–740 nm) and NIR (760–900 nm) bands are well-recognized for their ability to capture vegetation structure, consistently featuring in models predicting species diversity (Gould, 2000). The Red-edge portion of the electromagnetic spectrum is particularly useful because of its high sensitivity to changes in chlorophyll content, which are often induced by disturbances such as mowing (Filella and Peñuelas, 1994). These disturbances can cause reductions in leaf area distribution and leaf area index (LAI), leading to variations in the vegetation's spectral signature that are better detected by Red-edge derivatives compared to

traditional broadband vegetation indices (Sibanda *et al.*, 2017). In our study, the Red, Red-edge and NIR band's ability to capture these subtle changes in vegetation could possibly explain its consistent prominence across different management regimes.

This observation is consistent with previous studies that focused on species richness estimation. For instance, Rocchini (2007) underscored the NIR band's significance in differentiating plant species, as demonstrated using the QuickBird satellite. Similarly, findings by Blanco-Sacristán *et al.* (2019) and Imran *et al.* (2021) indicated that the spectral bands in the Red region were particularly effective in estimating biodiversity in grassland ecosystems. The consistent importance of these spectral bands across different management regimes suggests they are reliable indicators for remote sensing-based biodiversity assessments. Therefore, these spectral regions are promising focal points for future research on estimating species diversity through spectral analysis.

5.4.2 Implication for ecological monitoring and study limitations

Grasslands are increasingly vulnerable to global changes, such as altered land use, climate variability, and shifts in disturbance regimes. Understanding how grassland biodiversity responds to various management interventions, such as mowing and grazing, is essential for efficiently monitoring and managing current ecological conditions. By assessing the impact of different management practices, we could better understand the present state of grassland ecosystems and develop more effective strategies for promoting resilience and sustainability in these landscapes. This knowledge will support informed decision-making aimed at preserving the biodiversity and ecological services provided by grasslands.

The species richness maps generated using the integration of CH, VI, and GLCM features not only provided spatially detailed variations in species richness, reflecting the observed patterns in field data across different cutting regimes, but also serve as essential tools for conservation and management efforts. Particularly, the predicted map derived from the first data collection demonstrated the most distinct patterns in species richness variation. This better performance is likely due to the timing of the data acquisition, which occurred before the implementation of the first cut, thus the signal of each species in the matured grassland canopy becomes stronger (Zlinszky *et al.*, 2014).

As previous discussed in this study, the vegetation at this stage is more mature, leading to more distinct structural and spectral differences between species, which facilitates greater accuracy in remote sensing-based species differentiation. Similarly, Lu and He (2017) and Liu *et al.* (2024) reported that remote sensing imagery obtained during the peak growth season, particularly in late spring and summer, produced higher classification accuracies for grasslands, highlighting the importance of collecting data during these optimal growth periods. For example, Lu and He (2017) found that June, the peak period for Canadian grasslands, provided the highest accuracy (86%) in plant classification. Tarantino *et al.* (2019) also emphasized the importance of aligning remote

sensing data acquisition with the growing seasons of specific vegetation communities, concluding that this approach enhances the interpretation and classification of vegetation. Finally, Zlinszky et al. (2014), stressed that data acquisition should coincide with the mature phase of the meadows, but occur before the first mowing, to ensure that the vegetation is fully developed, allowing for more distinct differentiation between plant species.

By aligning data collection with key phenological moments, it becomes possible to capture clearer distinctions in vegetation zones, which are otherwise harder to discern after management interventions. Therefore, precise timing and careful consideration of vegetation development stages are essential to enhance the effectiveness of biodiversity monitoring and management planning in grassland ecosystems.

Despite the demonstrated potential of integrating UAV-derived data with machine learning models for assessing species richness in managed wet grasslands, some limitations must be acknowledged. The complexity of the wet grassland ecosystem, marked by variable hydrological conditions and diverse management practices, posed significant challenges for remote sensing and modeling species richness. The fluctuating hydrological conditions, combined with the dynamic nature of plant communities and their interactions with various ecological factors, added complexity to the task of accurately capturing the ecological dynamics. Moreover, site-specific factors such as varying terrain elevation, molehills, uneven groundwater levels, and lodging in some treatment areas added further complexity in data collection and analysis. Yet, the fact that we found comparable performance metrics to other studies demonstrated the robustness of such data-driven models when exposed to diverse conditions. The accuracy of our estimates was highly dependent on the frequency and precision of data acquisition. The time-sensitive nature of UAV flights campaigns, dictated by weather conditions and logistical constraints, posed challenges for ensuring consistent data collection across extended periods.

Another option to explore is to use hyperspectral sensors that capture a wider range of spectral bands, allowing for the identification of more subtle variations in plant spectral signatures. These variations could be crucial for species classification, especially in complex ecosystems such as wet grasslands, where spectral characteristics of plants may overlap in more general multispectral bands. For structural data, we primarily explored canopy height, which was extracted from RGB images using SfM software. Although this approach provided useful information about vegetation structure, the use of a LiDAR sensor could offer more detailed insights into the three-dimensional structure of the vegetation (Coverdale and Davies, 2023).

While species richness is a common and valuable metric, it may not fully capture the complexity of grassland ecosystems functions. Recent studies conducted by Wang *et al.* (2018) and Rossi *et al.* (2022) suggest that incorporating additional metrics, such as species evenness and functional traits, improve the prediction of biodiversity using remote-sensing techniques. In our study, we provided a framework for identifying the number of species across a managed field, but the quality of species to associate with a particular evenness and functional traits is still a work in progress. Future research should explore the inclusion of various plant diversity indices that

incorporate species abundance and trait diversity to improve the accuracy of remote sensing models for biodiversity estimation.

To enhance the applicability and interpretability of our models in wet grasslands, future research should focus on synchronizing model complexity with advanced techniques from the field of ecological informatics. Techniques such as machine learning algorithms optimized for large, complex ecological datasets and network-based analyses that model species-environment interactions offer promising avenues. These methodologies will be important in improving our understanding of the complex interactions between species, environmental conditions, and management practices. Fully exploiting the diverse features provided by UAV-derived data—such as spectral, textural, and structural information—offers significant benefits for biodiversity monitoring. While integrating these features may improve model accuracy, the growing number of features sensors may impose an operational limit for data acquisition and processing. Identifying the key features for data-driven applications enables the optimization and development of this approach in a parsimonious way while also providing a better monitoring and prediction more of how various management regimes affect species richness. By refining these methods, we can develop more effective strategies for conserving wet grasslands and ensuring their resilience in the face of changing environmental and land-use pressures.

5.5 Conclusion

This study evaluated the potential of integrating UAV-derived canopy height (CH), spectral data (VI), and texture features (GLCM) to predict species richness in managed wet grasslands. The findings emphasize a shift in the importance of data types with varying management intensities. While CH provided foundational structural insights, it was the spectral (VI) and texture features (GLCM) that consistently played a more decisive role in predicting species richness across different cutting regimes.

The research demonstrated that in lower frequency cutting systems, such as the two-cut treatment, models incorporating VI and GLCM offered significantly enhanced predictive accuracy, achieving an increase in R^2 from 0.48 to 0.52 and a reduction in rRMSE from 36.5% to 34.9% compared to models that did not integrate texture and spectral features. In systems with more frequent cuts, the integration of VI and GLCM continued to provide superior model performance, with improvements in R^2 from 0.39 to 0.45 and a reduction in rRMSE from 40.7% to 37.2%, demonstrating the importance of these features in capturing fine-scale variations.

Overall, the integrated models that combined all three types of data generally provided the best outcomes with an average R^2 improvement from 0.41 to 0.48 and a decrease in rRMSE from 39.2% to 36.5% across the cutting systems. The superior performance of integrated models that combine multiple data types suggests that a multidimensional approach is necessary to capture the full complexity of these ecosystems. By integrating structural, spectral, and textural data, researchers and practitioners can develop more comprehensive models that reflect the dynamic nature of wet

grassland. Our study helps to identify the key variables and ML models to develop this methodology in a parsimonious way for accurate assessments of biodiversity and the impacts of different management practices in wet grasslands.

CHAPTER VI

GENERAL DISCUSSION AND CONCLUSIONS

6.1 General discussion

This thesis explored the application of UAV-based sensors, vegetation indices and different advanced statistical image processing methods to enhance the estimation of aboveground biomass and biodiversity in grasslands. The studies presented in this thesis complement each other by addressing different aspects of UAV-based ecological monitoring. The initial review established a baseline for the understanding of UAV methods, while subsequent studies addressed specific challenges such as field disturbances and data integration. The final study on species richness assessment demonstrated the broader applicability of UAV technology and image processing, extending its relevance beyond biomass estimation. Here, we synthesize the key findings, discuss their interactions and implications, and suggest directions for future research.

6.1.1 Challenges in UAV-based biomass estimation in grassland ecosystems

Estimating biomass in grasslands presents unique challenges not commonly encountered in cropping systems on arable land. Crops are typically planted in uniform rows and tend to have a relatively homogeneous structure, making biomass estimation usually less challenging. In contrast, grasslands exhibit high spatial and temporal variability due to the presence of multiple plant species with different growth forms, phenology stage, heights, and densities. This heterogeneity complicates the development of accurate biomass models.

Studies such as Grüner, Wachendorf and Astor (2020) and Michez *et al.* (2020) indicated that species-rich and structurally diverse grasslands yield lower prediction accuracies compared to monocultures due to their complex canopy structures and species variability. Villoslada Peciña *et al.* (2021) also demonstrated that biomass estimation models perform better in homogeneous, short-sward grasslands compared to high-yielding areas with significant structural heterogeneity. These findings highlight the challenge of adapting biomass models to accommodate the variability inherent in natural and managed grasslands.

The concept of "grassland" itself is broad, encompassing a range of ecosystems from managed pastures to natural prairies and meadows. Each type of grassland has distinct characteristics that influence biomass estimation. For example, a homogeneous pasture, which may be dominated by one or two grass species, can be easier to model than a heterogeneous natural grassland with a diverse mix of species and varying environmental conditions. Moreover, cultivated grasslands or managed pastures typically show more uniformity and controlled conditions, facilitating easier biomass estimation. In contrast, natural or permanent grasslands, with their complex interactions and biodiversity, pose significant challenges for accurate biomass modeling. These systems are influenced by numerous factors such as varying topography, soil types, and climatic conditions, all of which must be accounted for in the models.

While UAV technology for biomass estimation aims to reduce the dependency on continuous field sampling, reference field data collection remains an important component for calibrating and

validating UAV-based biomass models. High-quality field reference data guarantees the reliability of UAV-derived biomass estimates. However, collecting this data in grasslands is challenging due to the often inaccessible and uneven terrain, dense vegetation, and the need for temporal consistency to capture changes over time. To overcome these logistical challenges, effective field reference data requires meticulous planning and execution.

Despite these inherent challenges, our review in the Chapter II has identified a general workflow commonly employed in UAV-based biomass estimation for grasslands. This workflow, illustrated in Figure 2.3, involves several key steps: data acquisition using UAVs, pre-processing of the collected data, model development, and subsequent validation against field reference data. This systematic approach helps in standardizing the estimation process, though the specifics may vary based on the type of grassland being studied.

According to the results of or review paper (Chapter II) the primary methods for grassland biomass estimation using UAV data rely on structural and spectral information. Structural data often involve the use of Canopy Height Models (CHM). CHMs are advantageous due to their relatively simple processing requirements and the ability to use RGB sensors, which are more accessible and cost-effective than other sensor types (Possoch *et al.*, 2016). However, the simplicity of CHMs comes with limitations (Bareth *et al.*, 2015). They rely on the assumption that there is a direct relationship between canopy height and biomass, which may not always hold true (Kümmerer, Noack and Bauer, 2023). Factors such as species diversity, vegetation structure, and field disturbances can affect this relationship, leading to potential inaccuracies in biomass estimation (Viljanen *et al.*, 2018; Dos Reis *et al.*, 2020).

To address these challenges, in the third chapter of this thesis, we investigated how common field disturbances, such as lodging and mole hills, can affect the canopy height-biomass relationship. The study found that areas affected by lodging showed discrepancies in canopy height measurements, resulting in potential biases in biomass estimates. These results have important implications for ecological monitoring and grassland management since lodging can happen frequently and irregularly, requiring robust models that can account for such variations (Chauhan *et al.*, 2019; Tan *et al.*, 2021; X. Li *et al.*, 2021).

Previous studies have highlighted the influence of lodging on biomass estimation models. Bendig *et al.* (2014) emphasized that lodging in barley fields reduces the accuracy of CHMs due to the flattened canopy. Kümmerer, Noack and Bauer (2023) also noted that conventional CHM methods often overestimate canopy height in mixed or lodged stands, as only the tallest parts of plants are considered, ignoring gaps and non-apical parts of the canopy. Similarly, Chao *et al.* (2019) identified lodging in late growth stages as a significant limitation, leading to reduced crop height measurements and weakening the relationship between biomass and plant height.

Incorporating disturbance effects into the calibration and validation processes of biomass models is crucial (Zhang et al. 2023; Chauhan et al. 2019). Field reference data collected in disturbed areas can help refine the models to better account for these variations. This ensures that the models are robust and can provide accurate estimates under different field conditions (Li et al.

2021). Additionally, the development of advanced algorithms to detect and adjust for disturbances such as lodging is essential. These algorithms can be integrated into the data processing workflow to automatically identify and correct for irregularities in the canopy structure, enhancing the reliability of CHMs.

Understanding how disturbances affect biomass estimation can also inform grassland management practices. For example, areas prone to molehills might require specific management strategies to mitigate their impact on biomass estimates. In Germany and many other European countries, moles (*Talpa europaea*) are protected by law under nature conservation regulations, making it illegal to kill or trap them without specific authorization (Federal Ministry for the Environment and Nature Conservartion, 2010). Consequently, non-lethal strategies such as soil compaction to reduce mole activity or habitat modification to make areas less favorable for moles are recommended for managing molehills in grasslands. Additionally, UAV-based monitoring can help identify molehill-prone areas, enabling more targeted interventions to minimize their effect on biomass estimations.

In addition to structural data, spectral data is a widely used method and offer distinct advantages for estimating biomass in grasslands. Spectral data is particularly valuable for capturing biochemical characteristics of plants, such as chlorophyll content and water stress, which are key indicators of plant health and quality (Wachendorf, Fricke and Möckel, 2018). For example, in research applications focused on assessing forage quality, hyperspectral sensors provide detailed information that is not achievable with RGB-based data (Barnetson, Phinn and Scarth, 2020; Zhao *et al.*, 2021). Similarly, spectral data is more suitable for monitoring stress factors, such as drought or nutrient deficiencies, in large-scale grassland ecosystems (Barnes *et al.*, 2000). However, this approach presents several significant challenges that were highlighted in the review of literature in Chapter II. Spectral data often require the use of multispectral or hyperspectral sensors, which are still more expensive compared to RGB sensors typically used for capturing structural data. This increased cost can be a barrier for widespread application, particularly in large-scale or resource-limited projects.

Moreover, the processing of multispectral and hyperspectral data is inherently more complex and demands advanced technical expertise. Unlike RGB data, which can be relatively straightforward to process, multispectral and hyperspectral data require more technical knowledge to interpret the spectral signatures of vegetation. This complexity extends to the entire workflow, from data acquisition to final analysis, necessitating a higher level of proficiency in remote sensing and data processing techniques.

Another significant limitation of using spectral data is the necessity for reflectance calibration. Accurate biomass estimation depends on the precise calibration of reflectance values, which requires additional steps during both data capture and processing (Tmušić *et al.*, 2020). In the field, this involves placing calibration panels and capturing images of these panels at the beginning and end of each UAV flight. This extra step increases the workload and operational complexity, as it demands careful planning and execution to ensure the panels are positioned correctly and the

images are captured under consistent conditions.

The post-processing phase also involves an additional calibration step to adjust the reflectance values accurately. This process is labor-intensive and requires meticulous attention to detail to ensure that the data is correctly calibrated. Despite these efforts, spectral data can still be heavily influenced by changes in lighting conditions during image capture. Variability in natural light, such as fluctuations in cloud cover or the angle of the sun, can introduce significant errors into the reflectance data (de Souza, Scharf and Sudduth, 2010; Xue *et al.*, 2023).

In regions such as our study area in Germany, where weather conditions are highly variable, even short UAV flights (around 30 minutes) can experience substantial changes in illumination. These fluctuations can affect the quality and consistency of the spectral data, making it challenging to obtain reliable biomass estimates. The need for consistent lighting conditions adds another layer of complexity to the already demanding process of using spectral data for biomass estimation.

Considering a practical context at the farm level, where larger areas are involved and waiting for perfect weather conditions is not always feasible, and the need for higher technical expertise for image processing, the use of spectral data becomes less viable than using structural data for biomass estimation. However, spectral data offers greater applicability for estimating biomass quality as it can capture more detailed information related to the biochemical characteristics of plants, which are indicative of nutritional content (Oliveira *et al.*, 2020; Franceschini *et al.*, 2022). This capability makes spectral data valuable for assessing aspects of biomass beyond mere quantity, providing insights into plant health and quality.

One alternative, or rather a trend in current studies, for biomass estimation in grasslands is the integration of different types of UAV-derived data to exploit the advantages and mitigate the limitations of each type. According to the results of the review in Chapter II of this thesis, recent studies have increasingly utilized the integration of structural and spectral data. The findings indicate that models employing both data types outperformed those using only one (Viljanen *et al.*, 2018; Lussem *et al.*, 2022). This integration generally leads to better model accuracy, leveraging the detailed structural information from CHMs and the biochemical data from spectral images (Karunaratne *et al.*, 2020; Pranga *et al.*, 2021).

Despite the overall improved accuracy from data integration, this approach involves handling larger and more complex datasets, which has led to an increasing tendency of employing more robust algorithms to manage these models. Consequently, recent work on biomass estimation in grasslands using remote sensing data has increasingly utilized machine learning algorithms. In the review of Chapter II, we identified the main algorithms and types of features, which set the foundation for the fourth chapter of this thesis.

In the fourth chapter, we then investigated the integration of UAV-derived features for biomass estimation in a heterogeneous grasslands field, including texture features. The study concept was resulted from our review in Chapter II, which examined previous studies and identified the potential benefits of combining texture analysis with structural and spectral data. Texture features

describe the variations in intensity or color within an image, capturing the surface structure and spatial arrangement of vegetation. These features provide additional data layers that are correlated with the structural and heterogeneity characteristics of the vegetation, offering important information into the spatial patterns of grasslands.

Few recent studies have explored the use of texture combined with other image-derived features for biomass estimation in grassland. For instance, Grüner, Wachendorf and Astor (2020) demonstrated that integrating spectral and texture features derived from UAV data improved predictions of aboveground biomass in legume-grass mixtures, particularly by capturing variability not accounted for by spectral data alone. In another study, Grüner, Astor and Wachendorf, (2021) showed that texture metrics, when integrated with machine learning algorithms, enhanced the robustness of biomass predictions in heterogeneous grasslands. Similarly, Dos Reis *et al.* (2020) emphasized the utility of texture features from high-resolution satellite imagery for estimating aboveground biomass and canopy height in pastures, showing their potential to enhance predictions under varying environmental conditions.

While these studies highlight the advantage of integrating texture data with other features, most were conducted in controlled field trial settings, where management practices are uniform and environmental variability is minimal. Similar to many works that assessed the combination of structural (CH) and spectral data (Karunaratne *et al.*, 2020; Oliveira *et al.*, 2020; Pranga *et al.*, 2021), these studies typically relied on data from a single growing season, which limits their applicability to more complex grassland systems. In contrast, natural or permanent grassland fields present a higher level of complexity due to their inherent variability, including diverse species compositions, uneven terrain, fluctuating environmental conditions (e.g., soil and groundwater levels), and differing management practices. Our experiment was carried out within a managed wet grassland, which adds another layer of complexity compared to controlled field trials. Specifically, the spatial variability of soil properties, groundwater levels, and the use of different cutting systems introduced additional challenges for biomass estimation, reflecting the complexity of real-world grassland dynamics. These factors make our study more demanding but also more representative of real-world conditions. Due to these specific characteristics, our hypothesis was that integrating various features from UAV data could improve model accuracy in such a complex environment.

The implications of using integrated features were mixed, depending on the specific management practices and cutting regimes analyzed. While our results indicated that models combining structural, spectral, and texture features (CH+VI+GLCM) generally outperformed those relying on a single feature class, the improvements were not always statistically significant. For instance, in the two-cut system, the inclusion of texture features added limited value compared to CH+VI alone, suggesting that in less frequent cutting regimes, the spectral insights from vegetation indices are already sufficient to capture biomass variability. Conversely, in the four-cut system, the integration of all feature types (CH+VI+GLCM) led to meaningful improvements in both R^2 and rRMSE, emphasizing the importance of texture features in capturing subtle structural variations and spatial heterogeneity introduced by frequent cutting.

While the combination of all feature classes showed potential, it is important to critically assess the practical benefits of this approach. For example, CH alone performed comparably well under the three-cut regime, likely due to the balance between structural uniformity and regrowth dynamics. This suggests that in systems with moderately homogeneous canopies, simpler models relying on CH alone may suffice, offering a cost-effective and less labor-intensive alternative for on-farm applications.

6.1.2 Challenges in UAV-based species richness estimation in grassland ecosystems

Estimating biodiversity in grasslands using remote sensing data presents several unique challenges. Grassland ecosystems are inherently complex due to their high spatial heterogeneity, presenting usually a mix of different species with various growth forms and phenological stages, leading to diverse reflectance patterns that are challenging to interpret accurately using remote sensing technologies.

Currently, most studies investigating plant biodiversity estimation in grasslands rely on the Spectral Variation Hypothesis (SVH). Introduced by Palmer *et al.* (2002), the SVH states that the spectral variability of a remote sensing image is linked to the species richness of the captured area. Spectral variability, or spectral diversity, refers to the quantitative differences in the reflectance spectra between the spatial units (pixels) in a remote sensing image. Palmer *et al.* (2002) developed and tested this hypothesis in a tallgrass prairie preserve, a vegetation type known for its high species richness and structural complexity. The study explored spatial extents ranging from small plots (e.g., 10 m × 10 m) to larger areas of several hectares and emphasized the use of high-resolution imagery, typically 1–5 meters per pixel, to effectively capture the fine-scale variability necessary for linking spectral diversity to species richness. The basic assumption of SVH is that increased spectral variability indicates an increased variety of habitats in the surveyed area, which can support more species. Thus, spectral variability, which indirectly reflects the diversity of habitats, can be used as an indicator for species richness.

The SVH has several advantages, including the ability to provide indirect estimates of biodiversity using remote sensing data. This approach can cover large areas relatively quickly and cost-effectively compared to traditional field-based methods. However, there are also notable disadvantages. The spectral-to-species diversity relationship can be influenced by various factors, including vegetation cover, habitat type, and spatial distribution patterns of species, seasonal development of vegetation, and the spatial resolution of the remote sensing data. These factors can introduce variability and potential biases in the estimates.

In the fifth chapter of this thesis, we hypothesized that integrating different UAV-derived features, similar to the methodology proposed for improving biomass estimation accuracy, could enhance the accuracy of species richness estimation in grasslands. We believed that combining structural (CHM), spectral (VI), and texture features would provide a more comprehensive dataset

that captures the complex patterns within the ecosystem, leading to better species richness estimates.

The results from previous studies suggest that seasonal development of vegetation significantly influences species richness estimation using remote sensing data (Wang *et al.*, 2018; 2016; Ludwig, Doktor, and Feilhauer, 2024; Gholizadeh *et al.*, 2018; Taddeo, Dronova, and Harris, 2021; Muro *et al.*, 2022). In our study, this may have been a contributing factor, as species richness was estimated over two years under different cutting treatments, with the best results observed during the peak growing season—defined as the period when vegetation typically reaches its maximum height during the flowering stage. During this time, vegetation structure tends to be more diverse, and spectral signals are more distinct, facilitating species differentiation.

This seasonal effect highlights the importance of selecting the optimal timing for remote sensing-based biodiversity assessments, as the phenological stage of the vegetation can influence the accuracy of species richness estimates. However, frequent cutting regimes may alter the timing of flowering and biomass accumulation, potentially reducing the distinctiveness of the spectral signals during the peak growing season. To address this, the approach may need to be adapted to account for the modified phenological patterns caused by intensive management practices. For instance, assessing species richness shortly before the first cut might yield more reliable results by capturing vegetation at a less homogeneous stage.

Another source of uncertainty that must be considered is the varying phenology of different species within the same sampling unit. While some species may still be actively growing, others might already be in senescence, introducing spectral variability that can influence biodiversity assessments. This temporal dynamic, noted by Gholizadeh *et al.* (2018), highlights the challenges of applying this approach in ecosystems with diverse successional stages or under intensive management practices. Thus, while the peak growing season may provide optimal conditions, incorporating multi-temporal data across various phenological stages, as in our study, can offer a more comprehensive understanding of species richness in heterogeneous grasslands, despite the associated challenges.

Considering the challenges posed by phenological variability and seasonal dynamics, the integration of structural, spectral, and texture features of the grassland proved to be an important approach for improving the accuracy of species richness models. Spectral and texture features were particularly valuable in more frequent cutting treatments, as texture features captured the structural complexity of vegetation, which is critical in diverse grassland ecosystems. This integration allowed us to capture the nuanced differences in vegetation that single data types might miss.

The influence of cutting frequency on feature importance revealed distinct patterns in our models, reflecting the varying dynamics of grassland ecosystems under different management intensities. In high-frequency cutting regimes, such as the three- and four-cut systems, the homogenization of the canopy structure reduced the predictive power of structural variables like canopy height. Instead, the models relied more on spectral features to capture subtle differences in vegetation health and vigor, as well as texture metrics to account for residual variability induced

by management practices (Cabezas, Galleguillos and Perez-Quezada, 2016; Imran *et al.*, 2021; Taddeo, Dronova and Harris, 2021). However, the accuracy of species richness estimation was lower in these regimes, likely because the reduced structural variability limited the additional value that spectral and texture features could provide.

In contrast, the two-cut system provided conditions where structural complexity was more pronounced, allowing canopy height to emerge as a stronger predictor of species richness. The capturing of higher structural variability also translated into improved model performance, with higher R^2 values and lower relative errors compared to the more intensively managed systems. These findings emphasize the importance of aligning feature integration strategies with the physiological and structural effects of different management regimes.

The practical implications of our findings are significant for conservation and management. By accurately assessing species richness, land managers can make informed decisions to promote biodiversity. For example, understanding the effects of different cutting regimes and their interactions with soil conditions on species richness can help in planning site-specific management practices that enhance biodiversity. Additionally, accurate species richness estimates can aid in monitoring the effectiveness of conservation efforts and detecting changes in biodiversity over time.

6.1.3 Practical implications

The integration of UAVs with advanced sensors offers a cost-effective and efficient alternative to traditional ecological monitoring methods. This combination facilitates rapid, non-destructive assessments, particularly valuable for managing dynamic and heterogeneous grassland ecosystems. However, UAVs alone are merely carriers; their effectiveness depends on the selection of appropriate sensors (e.g., multispectral, hyperspectral) and the use of robust image processing techniques to translate raw data into actionable insights. Current sensor technologies and processing methods demonstrate the capability to monitor grassland biomass and species diversity at small to medium scales with promising accuracy (Bazzo *et al.*, 2023; Lyu *et al.*, 2024). Scaling up to larger areas, however, poses challenges, including flight time limitations, data processing demands, and the impact of environmental variability.

To bring UAV-based grassland monitoring closer to practical implementation for farmers, future advancements should focus on developing user-friendly systems with simplified data acquisition and analysis pipelines. Further research should aim to improve the integration of real-time processing capabilities and cloud-based platforms to make these tools accessible for sustainable management and decision-making in grassland ecosystems.

6.1.4 Limitations and suggestions for future research

Several limitations need to be addressed to fully realize the potential of UAV-based ecological

monitoring of grasslands:

Impact of field disturbances

While this thesis highlights the significance of field disturbances, such as molehills and lodging, on biomass estimation, more advanced models are needed to address these variables effectively. For instance, molehills can potentially be excluded from the data using high-resolution UAV imagery and advanced image processing techniques that detect and remove small-scale anomalies. In contrast, lodging poses a greater challenge due to its dynamic nature and irregular occurrence. Developing time-series data from UAV flights during the grass growth period could help model the temporal progression of lodging and allow for better extrapolation to the cutting day. A critical next step would be to develop models capable of not only detecting these disturbances but also incorporating their effects into the estimation process. By integrating disturbance detection and their impacts into the calibration and validation of models, future studies can enhance the reliability and accuracy of biomass and species richness estimations under real-world field conditions.

Generality of findings

The findings of this research are based on data collected from a single grassland field of relatively small size and specific environmental conditions. While these results provide valuable insights, their applicability to other ecosystems or geographical regions remains limited. Future research should aim to generalize these findings by conducting similar studies in diverse grassland types, including natural and cultivated systems, under varying environmental conditions such as contrasting groundwater levels and weather patterns. Expanding the scope of research to include larger and more heterogeneous study areas would also enhance the transferability of UAV-based monitoring approaches to broader ecological and management contexts.

Temporal dynamics

Long-term studies are essential to assess the temporal dynamics of biomass and biodiversity in response to environmental changes with respect to weather conditions. Understanding how grassland growth and development changes over time will provide valuable insights for sustainable management and conservation efforts.

Integration of additional data sources

The integration of structural, spectral, and textural features from UAV data has proven effective, but there is potential to incorporate other data types. For example, hyperspectral imagery, LiDAR data, and environmental sensors can provide additional layers of information, further enhancing the accuracy and comprehensiveness of ecological assessments.

Machine learning and data analytics

Advanced machine learning algorithms have shown great promise in analyzing UAV-derived data (Holloway and Mengersen, 2018; Morais *et al.*, 2021). Future studies should continue to explore and refine these algorithms, potentially incorporating deep learning techniques and automated data processing workflows to handle the increasing volume and complexity of UAV data. Additionally,

the development of large language models, such as ChatGPT, for agricultural applications presents a unique opportunity to enhance data interpretation and decision-making. These models could be adapted to provide contextual insights, assist in anomaly detection, and automate reporting processes, making UAV-based systems more accessible and user-friendly for agricultural stakeholders. Exploring the integration of such tools with machine learning frameworks could open new avenues for efficient and scalable monitoring solutions.

6.2 Conclusions

This thesis demonstrates the potential of UAV-derived data in ecological monitoring, particularly for grassland biomass estimation and biodiversity assessment. By utilizing advancements in remote sensing and machine learning, the research addressed important gaps in current methodologies and provided practical insights into the use of UAVs for studying managed wet grasslands.

The systematic review in Chapter II highlighted the strengths and limitations of UAV-based biomass estimation methods, establishing a robust foundation for subsequent experimental studies. It highlighted the increasing focus on integrating structural, spectral, and textural data as a key strategy for improving model accuracy for estimation of grass biomass. Chapter III evaluated the impact of field disturbances, such as molehills and lodging, on biomass estimation, demonstrating that these disturbances can significantly affect the relationship between canopy height and biomass.

Chapter IV focused on the integration of multiple UAV-derived features for biomass estimation in a heterogeneous grassland field. The study concluded that combining structural, spectral, and texture features of grassland enhances model performance, particularly in capturing the variability and complexity inherent in diverse grassland systems. This integrated approach provided more robust estimates compared to using single data types, offering valuable insights for ecological monitoring under varying management regimes.

Chapter V extended the scope of this research to biodiversity assessment, focusing on species richness estimation. The results showed how phenological variability and management practices affect model performance and demonstrated the benefits of combining different UAV-derived data types in estimation floral diversity. This approach provided valuable insights for monitoring and managing grassland biodiversity under varying ecological conditions and cutting frequencies.

While the potential of UAVs for ecological monitoring is evident, the thesis also identified significant challenges. These include the complexity of processing large datasets, the need for precise calibration of remote sensing models, and logistical constraints associated with UAV-based fieldwork. Future research should focus on simplifying workflows, developing more accessible analytical tools, and scaling these approaches for broader applications

This research provides a strong basis for future work aimed at improving UAV-based methods and integrating them into ecological studies and management practices. By combining technical improvements with ecological knowledge, it is possible to develop more effective tools for

understanding and managing grassland ecosystems. This thesis contributes to these efforts by presenting a comprehensive approach to applying UAV technology in grassland research and supporting its use in both scientific and practical contexts.

References

't Mannetje, L, and R M Jones. 2000. *Field and Laboratory Methods for Grassland and Animal Production Research.* Wallingford: CABI Publishing. https://doi.org/10.1079/9780851993515.0000.

Adar, Shay, Marcelo Sternberg, Tarin Paz-Kagan, Zalmen Henkin, Guy Dovrat, Eli Zaady, and Eli Argaman. 2022. "Estimation of Aboveground Biomass Production Using an Unmanned Aerial Vehicle (UAV) and VENμS Satellite Imagery in Mediterranean and Semiarid Rangelands." *Remote Sensing Applications: Society and Environment* 26 (April): 100753. https://doi.org/10.1016/j.rsase.2022.100753.

Ali, Iftikhar, Fiona Cawkwell, Edward Dwyer, Brian Barrett, and Stuart Green. 2016. "Satellite Remote Sensing of Grasslands: From Observation to Management." *Journal of Plant Ecology* 9 (6): 649–71. https://doi.org/10.1093/jpe/rtw005.

Allen, V G, C Batello, E J Berretta, J Hodgson, M Kothmann, X Li, J. McIvor, et al. 2011. "An International Terminology for Grazing Lands and Grazing Animals." *Grass and Forage Science*. https://doi.org/10.1111/j.1365-2494.2010.00780.x.

Alvarez-Hess, P. S., A. L. Thomson, S. B. Karunaratne, M. L. Douglas, M. M. Wright, J. W. Heard, J. L. Jacobs, E. M. Morse-McNabb, W. J. Wales, and M. J. Auldist. 2021. "Using Multispectral Data from an Unmanned Aerial System to Estimate Pasture Depletion during Grazing." *Animal Feed Science and Technology* 275 (October 2020): 114880. https://doi.org/10.1016/j.anifeedsci.2021.114880.

Alves Oliveira, Raquel, José Marcato Junior, Celso Soares Costa, Roope Näsi, Niko Koivumäki, Oiva Niemeläinen, Jere Kaivosoja, Laura Nyholm, Hemerson Pistori, and Eija Honkavaara. 2022. "Silage Grass Sward Nitrogen Concentration and Dry Matter Yield Estimation Using Deep Regression and RGB Images Captured by UAV." *Agronomy* 12 (6): 1352. https://doi.org/10.3390/agronomy12061352.

Andrade, Bianca O., Christiane Koch, Ilsi I. Boldrini, Eduardo Vélez-Martin, Heinrich Hasenack, Julia Maria Hermann, Johannes Kollmann, Valério D. Pillar, and Gerhard E. Overbeck. 2015. "Grassland Degradation and Restoration: A Conceptual Framework of Stages and Thresholds Illustrated by Southern Brazilian Grasslands." *Natureza & Conservação* 13 (2): 95–104. https://doi.org/10.1016/J.NCON.2015.08.002.

Aneece, Itiya P, Howard Epstein, and Manuel Lerdau. 2017. "Correlating Species and Spectral Diversities Using Hyperspectral Remote Sensing in Early-Successional Fields." *Ecology and Evolution* 7 (10): 3475–88. https://doi.org/10.1002/ece3.2876.

Askari, Mohammad Sadegh, Timothy McCarthy, Aidan Magee, and Darren J. Murphy. 2019. "Evaluation of Grass Quality under Different Soil Management Scenarios Using Remote Sensing Techniques." *Remote Sensing* 11 (15): 1–23. https://doi.org/10.3390/rs11151835.

Atzberger, Clement. 2013. “Advances in Remote Sensing of Agriculture: Context Description, Existing Operational Monitoring Systems and Major Information Needs.” *Remote Sensing* 5 (2): 949–81. https://doi.org/10.3390/rs5020949.

Bar-On, Yinon M, Rob Phillips, and Ron Milo. 2018. “The Biomass Distribution on Earth.” *Proceedings of the National Academy of Sciences of the United States of America* 115 (25): 6506–11. https://doi.org/10.1073/pnas.1711842115.

Bareth, Georg, Andreas Bolten, Jens Hollberg, Helge Aasen, Andreas Burkart, and Jürgen Schellberg. 2015. “Feasibility Study of Using Non-Calibrated UAV-Based RGB Imagery for Grassland Monitoring: Case Study at the Rengen Long-Term Grassland Experiment (RGE), Germany.” *DGPF Tagungsband* 24:55–62. http://www.dgpf.de/src/tagung/jt2015/proceedings/papers/07_DGPF2015_Bareth_et_al.pdf.

Bareth, Georg, and Jürgen Schellberg. 2018. “Replacing Manual Rising Plate Meter Measurements with Low-Cost UAV-Derived Sward Height Data in Grasslands for Spatial Monitoring.” *PFG - Journal of Photogrammetry, Remote Sensing and Geoinformation Science* 86 (3–4): 157–68. https://doi.org/10.1007/s41064-018-0055-2.

Barnes, Edward, T R Clarke, S E Richards, Paul Colaizzi, Julio Haberland, M Kostrzewski, Peter Waller, Christopher Choi, E Riley, and T L Thompson. 2000. “Coincident Detection of Crop Water Stress, Nitrogen Status, and Canopy Density Using Ground Based Multispectral Data.”

Barnetson, Jason, Stuart Phinn, and Peter Scarth. 2020. “Estimating Plant Pasture Biomass and Quality from UAV Imaging across Queensland’s Rangelands.” *AgriEngineering* 2 (4): 523–43. https://doi.org/10.3390/agriengineering2040035.

Barrett, Brian, Ingmar Nitze, Stuart Green, and Fiona Cawkwell. 2014. “Assessment of Multi-Temporal, Multi-Sensor Radar and Ancillary Spatial Data for Grasslands Monitoring in Ireland Using Machine Learning Approaches.” *Remote Sensing of Environment* 152 (529): 109–24. https://doi.org/10.1016/j.rse.2014.05.018.

Batistoti, Juliana, José Marcato, Luís ítavo, Edson Matsubara, Eva Gomes, Bianca Oliveira, Maurício Souza, et al. 2019. “Estimating Pasture Biomass and Canopy Height in Brazilian Savanna Using UAV Photogrammetry.” *Remote Sensing* 11 (20): 1–12. https://doi.org/10.3390/rs11202447.

Bazzo, Clara Oliva Gonçalves, Bahareh Kamali, Christoph Hütt, Georg Bareth, and Thomas Gaiser. 2023. “A Review of Estimation Methods for Aboveground Biomass in Grasslands Using UAV.” *Remote Sensing* 15 (3): 1–50. https://doi.org/10.3390/rs15030639.

Bazzo, Clara Oliva Gonçalves, Bahareh Kamali, Murilo dos Santos Vianna, Dominik Behrend, Hubert Hueging, Inga Schleip, Paul Mosebach, Almut Haub, Axel Behrendt, and Thomas Gaiser. 2024. “Integration of UAV-Sensed Features Using Machine Learning Methods to Assess Species Richness in Wet Grassland Ecosystems.” *Ecological Informatics* 83 (November):102813. https://doi.org/10.1016/J.ECOINF.2024.102813.

Belgiu, Mariana, and Lucian Drăguţ. 2016. “Random Forest in Remote Sensing: A Review of Applications and Future Directions.” *ISPRS Journal of Photogrammetry and Remote Sensing* 114:24–31. https://doi.org/https://doi.org/10.1016/j.isprsjprs.2016.01.011.

Beltman, B, Tom van den Broek, W Martin, M Cate, and S Güsewell. 2003. “Impact of Mowing Regime on Species Richness and Biomass of a Limestone Hay Meadow in Ireland.” *Bulletin of the Geobotanical Institute ETH* 69 (January):17–30.

Bendig, Juliane, Andreas Bolten, Simon Bennertz, Janis Broscheit, Silas Eichfuss, and Georg Bareth. 2014. “Estimating Biomass of Barley Using Crop Surface Models (CSMs) Derived from UAV-Based RGB Imaging.” *Remote Sensing* 6 (11): 10395–412. https://doi.org/10.3390/rs61110395.

Bendig, Juliane, Kang Yu, Helge Aasen, Andreas Bolten, Simon Bennertz, Janis Broscheit, Martin L. Gnyp, and Georg Bareth. 2015. “Combining UAV-Based Plant Height from Crop Surface Models, Visible, and near Infrared Vegetation Indices for Biomass Monitoring in Barley.” *International Journal of Applied Earth Observation and Geoinformation* 39 (July):79–87. https://doi.org/10.1016/J.JAG.2015.02.012.

Bengtsson, J., J. M. Bullock, B. Egoh, C. Everson, T. Everson, T. O’Connor, P. J. O’Farrell, H. G. Smith, and R. Lindborg. 2019. “Grasslands—More Important for Ecosystem Services than You Might Think.” *Ecosphere* 10 (2). https://doi.org/10.1002/ecs2.2582.

Blackburn, Ryan C., Nicholas A. Barber, Anna K. Farrell, Robert Buscaglia, and Holly P. Jones. 2021. “Monitoring Ecological Characteristics of a Tallgrass Prairie Using an Unmanned Aerial Vehicle.” *Restoration Ecology* 29 (S1). https://doi.org/10.1111/rec.13339.

Blanco-Sacristán, Javier, Cinzia Panigada, Giulia Tagliabue, Rodolfo Gentili, Roberto Colombo, Mónica Ladrón de Guevara, Fernando T. Maestre, and Micol Rossini. 2019. “Spectral Diversity Successfully Estimates the α-Diversity of Biocrust-Forming Lichens.” *Remote Sensing* 11 (24): 1–16. https://doi.org/10.3390/rs11242942.

Bonari, Gianmaria, Karel Fajmon, Igor Malenovský, David Zelený, Jaroslav Holuša, Ivana Jongepierová, Petr Kočárek, Ondřej Konvička, Jan Uřičář, and Milan Chytrý. 2017. “Management of Semi-Natural Grasslands Benefiting Both Plant and Insect Diversity: The Importance of Heterogeneity and Tradition.” *Agriculture, Ecosystems & Environment* 246 (August):243–52. https://doi.org/10.1016/J.AGEE.2017.06.010.

Borra-Serrano, Irene, Tom De Swaef, Hilde Muylle, David Nuyttens, Jürgen Vangeyte, Koen Mertens, Wouter Saeys, Ben Somers, Isabel Roldán-Ruiz, and Peter Lootens. 2019. “Canopy Height Measurements and Non-Destructive Biomass Estimation of Lolium Perenne Swards Using UAV Imagery.” *Grass and Forage Science* 74 (3): 356–69. https://doi.org/10.1111/gfs.12439.

Braun-Blanquet, Josias. 1932. “Plant Sociology. The Study of Plant Communities.”

Breiman, Leo. 2001. “Random Forests.” *Machine Learning* 45 (1): 5–32.

https://doi.org/10.1023/A:1010933404324.

Broge, N H, and E Leblanc. 2001. “Comparing Prediction Power and Stability of Broadband and Hyperspectral Vegetation Indices for Estimation of Green Leaf Area Index and Canopy Chlorophyll Density.” *Remote Sensing of Environment* 76 (2): 156–72. https://doi.org/https://doi.org/10.1016/S0034-4257(00)00197-8.

Bueren, S. K. Von, A. Burkart, A. Hueni, U. Rascher, M. P. Tuohy, and I. J. Yule. 2015. “Deploying Four Optical UAV-Based Sensors over Grassland: Challenges and Limitations.” *Biogeosciences* 12 (1): 163–75. https://doi.org/10.5194/bg-12-163-2015.

Bullock, Andy, and Mike Acreman. 2003. “The Role of Wetlands in the Hydrological Cycle.” *Hydrology and Earth System Sciences* 7 (3): 358–89.

Cabezas, Julian, Mauricio Galleguillos, and Jorge F. Perez-Quezada. 2016. “Predicting Vascular Plant Richness in a Heterogeneous Wetland Using Spectral and Textural Features and a Random Forest Algorithm.” *IEEE Geoscience and Remote Sensing Letters* 13 (5): 646–50. https://doi.org/10.1109/LGRS.2016.2532743.

Camargo Neto, Joao. 2004. “A Combined Statistical-Soft Computing Approach for Classification and Mapping Weed Species in Minimum -Tillage Systems.” PhD Dissertation, University of Nebraska, Lincoln, NE.

Capolupo, Alessandra, Lammert Kooistra, Clara Berendonk, Lorenzo Boccia, and Juha Suomalainen. 2015. “Estimating Plant Traits of Grasslands from UAV-Acquired Hyperspectral Images: A Comparison of Statistical Approaches.” *ISPRS International Journal of Geo-Information* 4 (4): 2792–2820. https://doi.org/10.3390/ijgi4042792.

Carlson, Toby N., and David A. Ripley. 1997. “On the Relation between NDVI, Fractional Vegetation Cover, and Leaf Area Index.” *Remote Sensing of Environment* 62 (3): 241–52. https://doi.org/10.1016/S0034-4257(97)00104-1.

Castro, Wellington, José Marcato Junior, Caio Polidoro, Lucas Prado Osco, Wesley Gonçalves, Lucas Rodrigues, Mateus Santos, et al. 2020. “Deep Learning Applied to Phenotyping of Biomass in Forages with Uav-Based Rgb Imagery.” *Sensors (Switzerland)* 20 (17): 1–18. https://doi.org/10.3390/s20174802.

Chang, Geba Jisung. 2023. “Biodiversity Estimation by Environment Drivers Using Machine/Deep Learning for Ecological Management.” *Ecological Informatics* 78 (December):102319. https://doi.org/10.1016/j.ecoinf.2023.102319.

Chao, Zhenhua, Ning Liu, Peidong Zhang, Tianyu Ying, and Kaihui Song. 2019. “Estimation Methods Developing with Remote Sensing Information for Energy Crop Biomass: A Comparative Review.” *Biomass and Bioenergy* 122 (August 2018): 414–25. https://doi.org/10.1016/j.biombioe.2019.02.002.

Chauhan, Sugandh, Roshanak Darvishzadeh, Mirco Boschetti, Monica Pepe, and Andrew Nelson. 2019. “Remote Sensing-Based Crop Lodging Assessment: Current Status and Perspectives.”

ISPRS Journal of Photogrammetry and Remote Sensing 151 (August 2018): 124–40. https://doi.org/10.1016/j.isprsjprs.2019.03.005.

Chen, Jing M. 1996. "Evaluation of Vegetation Indices and a Modified Simple Ratio for Boreal Applications." *Canadian Journal of Remote Sensing* 22 (3): 229–42. https://doi.org/10.1080/07038992.1996.10855178.

Chen, Pengfei, Nicolas Tremblay, Ji-Hua Wang, Wenjiang Huang, and Bao-Guo Li. 2010. "New Index for Crop Canopy Fresh Biomass Estimation." *Guang Pu Xue Yu Guang Pu Fen Xi = Guang Pu* 30:512–17. https://doi.org/10.3964/j.issn.1000-0593(2010)02-0512-06.

Chiarucci, Alessandro. 2007. "To Sample or Not to Sample? That Is the Question... For the Vegetation Scientist." *Folia Geobotanica* 42 (2): 209–16. https://doi.org/10.1007/BF02893887.

Chitale, V. S., M. D. Behera, and P. S. Roy. 2019. "Deciphering Plant Richness Using Satellite Remote Sensing: A Study from Three Biodiversity Hotspots." *Biodiversity and Conservation* 28 (8–9): 2183–96. https://doi.org/10.1007/s10531-019-01761-4.

Clec'h, Solen Le, Robert Finger, Nina Buchmann, Arjan S. Gosal, Lukas Hörtnagl, Olivier Huguenin-Elie, Philippe Jeanneret, Andreas Lüscher, Manuel K. Schneider, and Robert Huber. 2019. "Assessment of Spatial Variability of Multiple Ecosystem Services in Grasslands of Different Intensities." *Journal of Environmental Management* 251 (October 2021). https://doi.org/10.1016/j.jenvman.2019.109372.

Colomina, I., and P. Molina. 2014. "Unmanned Aerial Systems for Photogrammetry and Remote Sensing: A Review." *ISPRS Journal of Photogrammetry and Remote Sensing* 92:79–97. https://doi.org/10.1016/j.isprsjprs.2014.02.013.

Conti, Luisa, Marco Malavasi, Thomas Galland, Jan Komárek, Ondřej Lagner, Carlos P. Carmona, Francesco de Bello, Duccio Rocchini, and Petra Šímová. 2021. "The Relationship between Species and Spectral Diversity in Grassland Communities Is Mediated by Their Vertical Complexity." *Applied Vegetation Science* 24 (3). https://doi.org/10.1111/avsc.12600.

Čop, J, M Vidrih, and J Hacin. 2009. "Influence of Cutting Regime and Fertilizer Application on the Botanical Composition, Yield and Nutritive Value of Herbage of Wet Grasslands in Central Europe." *Grass and Forage Science* 64 (4): 454–65. https://doi.org/https://doi.org/10.1111/j.1365-2494.2009.00713.x.

Costa, Máira Beatriz Teixeira da, Carlos Alberto Silva, Eben North Broadbent, Rodrigo Vieira Leite, Midhun Mohan, Veraldo Liesenberg, Jaz Stoddart, et al. 2021. "Beyond Trees: Mapping Total Aboveground Biomass Density in the Brazilian Savanna Using High-Density UAV-Lidar Data." *Forest Ecology and Management* 491 (January). https://doi.org/10.1016/j.foreco.2021.119155.

Coverdale, Tyler C., and Andrew B. Davies. 2023. "Unravelling the Relationship between Plant Diversity and Vegetation Structural Complexity: A Review and Theoretical Framework."

Journal of Ecology 111 (7): 1378–95. https://doi.org/10.1111/1365-2745.14068.

Crippen, Robert E. 1990. "Calculating the Vegetation Index Faster." *Remote Sensing of Environment* 34 (1): 71–73. https://doi.org/10.1016/0034-4257(90)90085-Z.

Culbert, Patrick D., Anna M. Pidgeon, Véronique St. Louis, Volker C. Radeloff, and Dallas Bash. 2009. "The Impact of Phenological Variation on Texture Measures of Remotely Sensed Imagery." *IEEE Journal of Selected Topics in Applied Earth Observations and Remote Sensing* 2 (4): 299–309. https://doi.org/10.1109/JSTARS.2009.2021959.

Cunliffe, Andrew M., Richard E. Brazier, and Karen Anderson. 2016. "Ultra-Fine Grain Landscape-Scale Quantification of Dryland Vegetation Structure with Drone-Acquired Structure-from-Motion Photogrammetry." *Remote Sensing of Environment* 183:129–43. https://doi.org/10.1016/j.rse.2016.05.019.

D. Schleicher, Tyler, Walter C. Bausch, Jorge A. Delgado, and Paul D. Ayers. 2001. "Evaluation and Refinement of the Nitrogen Reflectance Index (NRI) for Site-Specific Fertilizer Management." *2001 ASAE Annual Meeting*. ASABE Paper No. 011151. St. Joseph, MI: ASAE. https://doi.org/https://doi.org/10.13031/2013.7357.

Dandois, Jonathan P, and Erle C Ellis. 2013. "High Spatial Resolution Three-Dimensional Mapping of Vegetation Spectral Dynamics Using Computer Vision." *Remote Sensing of Environment* 136:259–76. https://doi.org/https://doi.org/10.1016/j.rse.2013.04.005.

Darvishzadeh, Roshanak, Andrew Skidmore, Martin Schlerf, Clement Atzberger, Fabio Corsi, and Moses Cho. 2008. "LAI and Chlorophyll Estimation for a Heterogeneous Grassland Using Hyperspectral Measurements." *ISPRS Journal of Photogrammetry and Remote Sensing* 63 (4): 409–26. https://doi.org/10.1016/J.ISPRSJPRS.2008.01.001.

Dash, J, and P J Curran. 2004. "The MERIS Terrestrial Chlorophyll Index." *International Journal of Remote Sensing* 25 (23): 5403–13. https://doi.org/10.1080/0143116042000274015.

Datt, Bisun. 1998. "Remote Sensing of Chlorophyll a, Chlorophyll b, Chlorophyll A+b, and Total Carotenoid Content in Eucalyptus Leaves." *Remote Sensing of Environment* 66 (2): 111–21. https://doi.org/10.1016/S0034-4257(98)00046-7.

Daughtry, C. S.T., C. L. Walthall, M. S. Kim, E. Brown De Colstoun, and J. E. McMurtrey. 2000. "Estimating Corn Leaf Chlorophyll Concentration from Leaf and Canopy Reflectance." *Remote Sensing of Environment* 74 (2): 229–39. https://doi.org/10.1016/S0034-4257(00)00113-9.

Dengler, Jürgen, Idoia Biurrun, Steffen Boch, Iwona Dembicz, and Péter Török. 2020. "Grasslands of the Palaearctic Biogeographic Realm: Introduction and Synthesis." *Encyclopedia of the World's Biomes* 3:617–37.

DiMaggio, Alexandria M., Humberto L. Perotto-Baldivieso, J. Alfonso Ortega-S., Chase Walther, Karelys N. Labrador-Rodriguez, Michael T. Page, Jose de la Luz Martinez, Sandra Rideout-Hanzak, Brent C. Hedquist, and David B. Wester. 2020. "A Pilot Study to Estimate Forage

Mass from Unmanned Aerial Vehicles in a Semi-Arid Rangeland." *Remote Sensing* 12 (15): 1–13. https://doi.org/10.3390/RS12152431.

Dinnage, Russell, Marc W Cadotte, Nick M Haddad, Gregory M Crutsinger, and David Tilman. 2012. "Diversity of Plant Evolutionary Lineages Promotes Arthropod Diversity." https://doi.org/10.1111/j.1461-0248.2012.01854.x.

Dixon, Adam P., D Faber-Langendoen, C Josse, J Morrison, and C J Loucks. 2014. "Distribution Mapping of World Grassland Types." *Journal of Biogeography* 41 (11): 2003–19. https://doi.org/10.1111/jbi.12381.

Dumont, Bertrand, Nicolas Rossignol, Grégory Loucougaray, Pascal Carrère, Joël Chadoeuf, Géraldine Fleurance, Anne Bonis, et al. 2012. "When Does Grazing Generate Stable Vegetation Patterns in Temperate Pastures?" *Agriculture, Ecosystems and Environment* 153 (June):50–56. https://doi.org/10.1016/j.agee.2012.03.003.

Dusseux, P., L. Hubert-Moy, T. Corpetti, and F. Vertès. 2015. "Evaluation of SPOT Imagery for the Estimation of Grassland Biomass." *International Journal of Applied Earth Observation and Geoinformation* 38:72–77. https://doi.org/10.1016/j.jag.2014.12.003.

Edvan, Ricardo L, Leilson R Bezerra, Carlo A T Marques, Maria Socorro S Carneiro, and Ronaldo L Oliveira. 2015. "Methods for Estimating Forage Mass in Pastures in a Tropical Climate Métodos Para Estimar a Massa de Forragem Em Pastagens Em Clima Tropical" 39 (1): 36–45.

Egoh, Benis N, Janne Bengtsson, Regina Lindborg, James M Bullock, Adam P Dixon, and Mathieu Rouget. 2016. "The Importance of Grasslands in Providing Ecosystem Services." In *Routledge Handbook of Ecosystem Services*, 421–41. New York, NY : Routledge, 2016.: Routledge. https://doi.org/10.4324/9781315775302-37.

Eitel, J U H, D S Long, P E Gessler, and A M S Smith. 2007. "Using In-situ Measurements to Evaluate the New RapidEye™ Satellite Series for Prediction of Wheat Nitrogen Status." *International Journal of Remote Sensing* 28 (18): 4183–90. https://doi.org/10.1080/01431160701422213.

Eskandari, Roghieh, Masoud Mahdianpari, Fariba Mohammadimanesh, Bahram Salehi, Brian Brisco, and Saeid Homayouni. 2020. "Meta-analysis of Unmanned Aerial Vehicle (UAV) Imagery for Agro-environmental Monitoring Using Machine Learning and Statistical Models." *Remote Sensing* 12 (21): 1–32. https://doi.org/10.3390/rs12213511.

Fan, Xinyan, Kensuke Kawamura, Tran Dang Xuan, Norio Yuba, Jihyun Lim, Rena Yoshitoshi, Truong Ngoc Minh, Yuzo Kurokawa, and Taketo Obitsu. 2018. "Low-Cost Visible and near-Infrared Camera on an Unmanned Aerial Vehicle for Assessing the Herbage Biomass and Leaf Area Index in an Italian Ryegrass Field." *Grassland Science* 64 (2): 145–50. https://doi.org/10.1111/grs.12184.

FAOStat. 2016. "Database Collection of the Food and Agriculture Organization of the United

Nations." www.fao.org/faostat.

Fauvel, Mathieu, Mailys Lopes, Titouan Dubo, Justine Rivers-Moore, Pierre Louis Frison, Nicolas Gross, and Annie Ouin. 2020. "Prediction of Plant Diversity in Grasslands Using Sentinel-1 and -2 Satellite Image Time Series." *Remote Sensing of Environment* 237 (February):111536. https://doi.org/10.1016/J.RSE.2019.111536.

Federal Ministry for the Environment and Nature Conservartion. 2010. *Act on Nature Conservation and Landscape Management*. *Encyclopedic Dictionary of Landscape and Urban Planning*. Vol. 2009. https://doi.org/10.1007/978-3-540-76435-9_118.

Fidelis, Alessandra, Maria Fernanda di Santi Lyra, and Vânia Regina Pivello. 2013. "Above-and Below-ground Biomass and Carbon Dynamics in B Razilian C Errado Wet Grasslands." *Journal of Vegetation Science* 24 (2): 356–64.

Filella, I., and J. Peñuelas. 1994. "The Red Edge Position and Shape as Indicators of Plant Chlorophyll Content, Biomass and Hydric Status." *International Journal of Remote Sensing* 15 (7): 1459–70. https://doi.org/10.1080/01431169408954177.

Fleishman, Erica, Reed F. Noss, and Barry R. Noon. 2006. "Utility and Limitations of Species Richness Metrics for Conservation Planning." *Ecological Indicators* 6 (3): 543–53. https://doi.org/10.1016/j.ecolind.2005.07.005.

Forsmoo, Joel, Karen Anderson, Christopher J.A. Macleod, Mark E. Wilkinson, and Richard Brazier. 2018. "Drone-Based Structure-from-Motion Photogrammetry Captures Grassland Sward Height Variability." *Journal of Applied Ecology* 55 (6): 2587–99. https://doi.org/10.1111/1365-2664.13148.

Franceschini, Marston H.D., Rolf Becker, Florian Wichern, and Lammert Kooistra. 2022. "Quantification of Grassland Biomass and Nitrogen Content through UAV Hyperspectral Imagery—Active Sample Selection for Model Transfer." *Drones* 6 (3): 1–22. https://doi.org/10.3390/drones6030073.

Fraser, Benjamin T, and Russell G Congalton. 2018. "Issues in Unmanned Aerial Systems (UAS) Data Collection of Complex Forest Environments." *Remote Sensing* 10 (6). https://doi.org/10.3390/rs10060908.

Fu, Yi, Xiaopeng Tan, Yunlong Yao, Lei Wang, Yuanqi Shan, Yuehua Yang, and Zhongwei Jing. 2024. "Uncovering Optimal Vegetation Indices for Estimating Wetland Plant Species Diversity." *Ecological Indicators* 166 (July). https://doi.org/10.1016/j.ecolind.2024.112367.

Gebremedhin, Alem, Pieter Badenhorst, Junping Wang, Fan Shi, Ed Breen, Khageswor Giri, German C. Spangenberg, and Kevin Smith. 2020. "Development and Validation of a Phenotyping Computational Workflow to Predict the Biomass Yield of a Large Perennial Ryegrass Breeding Field Trial." *Frontiers in Plant Science* 11 (May): 1–16. https://doi.org/10.3389/fpls.2020.00689.

Geipel, J., A. K. Bakken, M. Jørgensen, and A. Korsaeth. 2021. "Forage Yield and Quality

Estimation by Means of UAV and Hyperspectral Imaging." *Precision Agriculture* 22 (5): 1437–63. https://doi.org/10.1007/s11119-021-09790-2.

Geipel, J., and A. Korsaeth. 2017. "Hyperspectral Aerial Imaging for Grassland Yield Estimation." *Advances in Animal Biosciences* 8 (2): 770–75. https://doi.org/10.1017/s2040470017000619.

Ghajar, Shayan, and Benjamin Tracy. 2021. "Proximal Sensing in Grasslands and Pastures." *Agriculture (Switzerland)* 11 (8). https://doi.org/10.3390/agriculture11080740.

Gholizadeh, Hamed, John A. Gamon, Christopher J. Helzer, and Jeannine Cavender-Bares. 2020. "Multi-Temporal Assessment of Grassland α- and β-Diversity Using Hyperspectral Imaging." *Ecological Applications* 30 (7): 1–13. https://doi.org/10.1002/eap.2145.

Gholizadeh, Hamed, John A. Gamon, Philip A. Townsend, Arthur I. Zygielbaum, Christopher J. Helzer, Gabriel Y. Hmimina, Rong Yu, Ryan M. Moore, Anna K. Schweiger, and Jeannine Cavender-Bares. 2019. "Detecting Prairie Biodiversity with Airborne Remote Sensing." *Remote Sensing of Environment* 221 (February):38–49. https://doi.org/10.1016/j.rse.2018.10.037.

Gholizadeh, Hamed, John A. Gamon, Arthur I. Zygielbaum, Ran Wang, Anna K. Schweiger, and Jeannine Cavender-Bares. 2018. "Remote Sensing of Biodiversity: Soil Correction and Data Dimension Reduction Methods Improve Assessment of α-Diversity (Species Richness) in Prairie Ecosystems." *Remote Sensing of Environment* 206 (March):240–53. https://doi.org/10.1016/j.rse.2017.12.014.

Gianelle, D, and L Vescovo. 2007. "Determination of Green Herbage Ratio in Grasslands Using Spectral Reflectance. Methods and Ground Measurements." *International Journal of Remote Sensing* 28 (5): 931–42. https://doi.org/10.1080/01431160500196398.

Gibson, David J., and Jonathan A. Newman. 2019. "Grasslands and Climate Change: An Overview." *Grasslands and Climate Change*, no. September, 3–18. https://doi.org/10.1017/9781108163941.003.

Gitelson, Anatoly A. 2004. "Wide Dynamic Range Vegetation Index for Remote Quantification of Biophysical Characteristics of Vegetation." *Journal of Plant Physiology* 161 (2): 165–73. https://doi.org/10.1078/0176-1617-01176.

Gitelson, Anatoly A., Yuri Gritz, and Mark N. Merzlyak. 2003. "Relationships between Leaf Chlorophyll Content and Spectral Reflectance and Algorithms for Non-Destructive Chlorophyll Assessment in Higher Plant Leaves." *Journal of Plant Physiology* 160 (3): 271–82. https://doi.org/10.1078/0176-1617-00887.

Gitelson, Anatoly A., Yoram J. Kaufman, and Mark N. Merzlyak. 1996. "Use of a Green Channel in Remote Sensing of Global Vegetation from EOS-MODIS." *Remote Sensing of Environment* 58 (3): 289–98. https://doi.org/10.1016/S0034-4257(96)00072-7.

Gitelson, Anatoly A., Yoram J. Kaufman, Robert Stark, and Don Rundquist. 2002. "Novel Algorithms for Remote Estimation of Vegetation Fraction." *Remote Sensing of Environment*

80 (1): 76–87. https://doi.org/10.1016/S0034-4257(01)00289-9.

Gitelson, Anatoly, Mark Merzlyak, and Olga Chivkunova. 2001. “Optical Properties and Nondestructive Estimation of Anthocyanin Content in Plant Leaves.” *Photochemistry and Photobiology* 74:38–45. https://doi.org/10.1562/0031-8655(2001)074<0038:OPANEO>2.0.CO;2.

Gitelson, Anatoly, and Mark N. Merzlyak. 1994. “Spectral Reflectance Changes Associated with Autumn Senescence of Aesculus Hippocastanum L. and Acer Platanoides L. Leaves. Spectral Features and Relation to Chlorophyll Estimation.” *Journal of Plant Physiology* 143 (3): 286–92. https://doi.org/10.1016/S0176-1617(11)81633-0.

Gnyp, Martin L., Yuxin Miao, Fei Yuan, Susan L. Ustin, Kang Yu, Yinkun Yao, Shanyu Huang, and Georg Bareth. 2014. “Hyperspectral Canopy Sensing of Paddy Rice Aboveground Biomass at Different Growth Stages.” *Field Crops Research* 155 (January):42–55. https://doi.org/10.1016/j.fcr.2013.09.023.

Gobron, Nadine, Bernard Pinty, Michel Verstraete, and J.-L Widlowski. 2000. “Advanced Vegetation Indices Optimized for Up-Coming Sensors: Design, Performance, and Applications.” *Geoscience and Remote Sensing, IEEE Transactions On* 38:2489–2505. https://doi.org/10.1109/36.885197.

Goel, Narendra S, and Wenhan Qin. 1994. “Influences of Canopy Architecture on Relationships between Various Vegetation Indices and LAI and Fpar: A Computer Simulation.” *Remote Sensing Reviews* 10 (4): 309–47. https://doi.org/10.1080/02757259409532252.

Gong, Zhe, Kensuke Kawamura, Naoto Ishikawa, Mizuki Inaba, and Dalai Alateng. 2016. “Estimation of Herbage Biomass and Nutritive Status Using Band Depth Features with Partial Least Squares Regression in Inner Mongolia Grassland, China.” *Grassland Science* 62 (1): 45–54. https://doi.org/10.1111/grs.12112.

Gould, W. 2000. “Remote Sensing of Vegetation, Plant Species Richness, and Regional Biodiversity Hotspots.” *Ecological Applications* 10 (6): 1861–70. https://doi.org/10.1890/1051-0761(2000)010[1861:RSOVPS]2.0.CO;2.

Grüner, Esther, Thomas Astor, and Michael Wachendorf. 2019. “Biomass Prediction of Heterogeneous Temperate Grasslands Using an SFM Approach Based on UAV Imaging.” *Agronomy* 9 (2). https://doi.org/10.3390/agronomy9020054.

Grüner, Esther, Thomas Astor, and Michael Wachendorf. 2021. “Prediction of Biomass and N Fixation of Legume–Grass Mixtures Using Sensor Fusion.” *Frontiers in Plant Science* 11. https://doi.org/10.3389/fpls.2020.603921.

Grüner, Esther, Michael Wachendorf, and Thomas Astor. 2020. “The Potential of UAV-Borne Spectral and Textural Information for Predicting Aboveground Biomass and N Fixation in Legume-Grass Mixtures.” *PLoS ONE* 15 (6): 1–21. https://doi.org/10.1371/journal.pone.0234703.

Guo, Yuxi, Elizabeth H Boughton, Stephanie Bohlman, Carl Bernacchi, Patrick J Bohlen, Raoul Boughton, Evan DeLucia, et al. 2023. "Grassland Intensification Effects Cascade to Alter Multifunctionality of Wetlands within Metaecosystems." *Nature Communications* 14 (1): 8267. https://doi.org/10.1038/s41467-023-44104-2.

Guyot, G., and F. Baret. 1988. "Utilisation de La Haute Resolution Spectrale Pour Suivre l'etat Des Couverts Vegetaux." *Journal of Chemical Information and Modeling* 53 (9): 1689–99.

Haboudane, Driss, John R. Miller, Elizabeth Pattey, Pablo J. Zarco-Tejada, and Ian B. Strachan. 2004. "Hyperspectral Vegetation Indices and Novel Algorithms for Predicting Green LAI of Crop Canopies: Modeling and Validation in the Context of Precision Agriculture." *Remote Sensing of Environment* 90 (3): 337–52. https://doi.org/10.1016/J.RSE.2003.12.013.

Hakl, J., Z. Hrevušová, M. Hejcman, and P. Fuksa. 2012. "The Use of a Rising Plate Meter to Evaluate Lucerne (Medicago Sativa L.) Height as an Important Agronomic Trait Enabling Yield Estimation." *Grass and Forage Science* 67 (4): 589–96. https://doi.org/10.1111/j.1365-2494.2012.00886.x.

Hall-Beyer, Mryka. 2017. "Practical Guidelines for Choosing GLCM Textures to Use in Landscape Classification Tasks over a Range of Moderate Spatial Scales." *International Journal of Remote Sensing* 38 (5): 1312–38. https://doi.org/10.1080/01431161.2016.1278314.

Haralick, Robert M, K Shanmugam, and Its'Hak Dinstein. 1973. "Textural Features for Image Classification." *IEEE Transactions on Systems, Man, and Cybernetics* SMC-3 (6): 610–21. https://doi.org/10.1109/TSMC.1973.4309314.

Harmoney, Keith R., Kenneth J. Moore, J. Ronald George, E. Charles Brummer, and James R. Russell. 1997. "Determination of Pasture Biomass Using Four Indirect Methods." *Agronomy Journal* 89 (4): 665–72. https://doi.org/10.2134/agronj1997.00021962008900040020x.

Harrison, Susan P., Elise S. Gornish, and Stella Copeland. 2015. "Climate-Driven Diversity Loss in a Grassland Community." *Proceedings of the National Academy of Sciences of the United States of America* 112 (28): 8672–77. https://doi.org/10.1073/pnas.1502074112.

Hart, Leonie, Olivier Huguenin-Elie, Roy Latsch, Michael Simmler, Sébastien Dubois, and Christina Umstatter. 2020. "Comparison of Spectral Reflectance-Based Smart Farming Tools and a Conventional Approach to Determine Herbage Mass and Grass Quality on Farm." *Remote Sensing* 12 (19): 1–19. https://doi.org/10.3390/rs12193256.

Hautier, Yann, Eric W Seabloom, Elizabeth T Borer, Peter B Adler, W Stanley Harpole, Helmut Hillebrand, Eric M Lind, Andrew S MacDougall, Carly J Stevens, and Jonathan D Bakker. 2014. "Eutrophication Weakens Stabilizing Effects of Diversity in Natural Grasslands." *Nature* 508 (7497): 521–25.

Hernández-Clemente, Rocío, Rafael M. Navarro-Cerrillo, Lola Suárez, Fermín Morales, and Pablo J. Zarco-Tejada. 2011. "Assessing Structural Effects on PRI for Stress Detection in Conifer Forests." *Remote Sensing of Environment* 115 (9): 2360–75.

https://doi.org/10.1016/J.RSE.2011.04.036.

Hill, Michael J. 2013. “Vegetation Index Suites as Indicators of Vegetation State in Grassland and Savanna: An Analysis with Simulated SENTINEL 2 Data for a North American Transect.” *Remote Sensing of Environment* 137 (October):94–111. https://doi.org/10.1016/J.RSE.2013.06.004.

Hollberg, Jens L, and Jürgen Schellberg. 2017. “Distinguishing Intensity Levels of Grassland Fertilization Using Vegetation Indices.” *Remote Sensing* 9 (1). https://doi.org/10.3390/rs9010081.

Holloway, Jacinta, and Kerrie Mengersen. 2018. “Statistical Machine Learning Methods and Remote Sensing for Sustainable Development Goals: A Review.” *Remote Sensing*. https://doi.org/10.3390/rs10091365.

Hopkins, A., and R. J. Wilkins. 2006. “Temperate Grassland: Key Developments in the Last Century and Future Perspectives.” *Journal of Agricultural Science* 144 (6): 503–23. https://doi.org/10.1017/S0021859606006496.

Huber, Robert, Solen Le’Clec’h, Nina Buchmann, and Robert Finger. 2022. “Economic Value of Three Grassland Ecosystem Services When Managed at the Regional and Farm Scale.” *Scientific Reports* 12 (1): 1–13. https://doi.org/10.1038/s41598-022-08198-w.

Huete, A., K. Didan, T. Miura, E. P. Rodriguez, X. Gao, and L. G. Ferreira. 2002. “Overview of the Radiometric and Biophysical Performance of the MODIS Vegetation Indices.” *Remote Sensing of Environment* 83 (1–2): 195–213. https://doi.org/10.1016/S0034-4257(02)00096-2.

Huete, A. R., H. Q. Liu, K. Batchily, and W. Van Leeuwen. 1997. “A Comparison of Vegetation Indices over a Global Set of TM Images for EOS-MODIS.” *Remote Sensing of Environment* 59 (3): 440–51. https://doi.org/10.1016/S0034-4257(96)00112-5.

Hussain, Raja Imran, Ronnie Walcher, Renate Eder, Brigitte Allex, Peter Wallner, Hans Peter Hutter, Nicole Bauer, Arne Arnberger, Johann G Zaller, and Thomas Frank. 2019. “Management of Mountainous Meadows Associated with Biodiversity Attributes, Perceived Health Benefits and Cultural Ecosystem Services.” *Scientific Reports* 9 (1). https://doi.org/10.1038/s41598-019-51571-5.

Imran, Hafiz Ali, Damiano Gianelle, Michele Scotton, Duccio Rocchini, Michele Dalponte, Stefano Macolino, Karolina Sakowska, Cristina Pornaro, and Loris Vescovo. 2021. “Potential and Limitations of Grasslands α-Diversity Prediction Using Fine-Scale Hyperspectral Imagery.” *Remote Sensing* 13 (14): 2649. https://doi.org/10.3390/rs13142649.

Insua, Juan R., Santiago A. Utsumi, and Bruno Basso. 2019. “Estimation of Spatial and Temporal Variability of Pasture Growth and Digestibility in Grazing Rotations Coupling Unmanned Aerial Vehicle (UAV) with Crop Simulation Models.” *PLoS ONE* 14 (3): 1–21. https://doi.org/10.1371/journal.pone.0212773.

Isacsson, Martin. 2018. “Snow Layer Mapping by Remote Sensing from Unmanned Aerial

Vehicles : A Mixed Method Study of Sensor Applications for Research in Arctic and Alpine Environments." Master Thesis, Royal Institute of Technology, Stockholm, Sweden.

Jago, Rosemary A., Mark E.J. Cutler, and Paul J. Curran. 1999. "Estimating Canopy Chlorophyll Concentration from Field and Airborne Spectra." *Remote Sensing of Environment* 68 (3): 217–24. https://doi.org/10.1016/S0034-4257(98)00113-8.

Jenal, Alexander, Ulrike Lussem, Andreas Bolten, Martin Leon Gnyp, Jürgen Schellberg, Jörg Jasper, Jens Bongartz, and Georg Bareth. 2020. "Investigating the Potential of a Newly Developed UAV-Based VNIR/SWIR Imaging System for Forage Mass Monitoring." *PFG - Journal of Photogrammetry, Remote Sensing and Geoinformation Science* 88 (6): 493–507. https://doi.org/10.1007/s41064-020-00128-7.

Jin, Xiao Hui, Min Jian Chen, Yu Miao Fan, Hao Duan, and Long Yan. 2019. "Influences of Groundwater and Climatic Factors on Grassland in Xiliao River Plain, Northern China." *Rangeland Ecology and Management* 72 (3): 425–32. https://doi.org/10.1016/j.rama.2018.12.004.

Jin, Yunxiang, Xiuchun Yang, Jianjun Qiu, Jinya Li, Tian Gao, Qiong Wu, Fen Zhao, Hailong Ma, Haida Yu, and Bin Xu. 2014. "Remote Sensing-Based Biomass Estimation and Its Spatio-Temporal Variations in Temperate Grassland, Northern China." *Remote Sensing* 6 (2): 1496–1513. https://doi.org/10.3390/rs6021496.

Jones, M. B., and Alison Donnelly. 2004. "Carbon Sequestration in Temperate Grassland Ecosystems and the Influence of Management, Climate and Elevated CO2." *New Phytologist* 164 (3): 423–39. https://doi.org/10.1111/j.1469-8137.2004.01201.x.

Jordan, Carl F. 1969. "Derivation of Leaf-Area Index from Quality of Light on the Forest Floor." *Ecology* 50 (4): 663–66. https://doi.org/https://doi.org/10.2307/1936256.

Joyce, Chris B. 2014. "Ecological Consequences and Restoration Potential of Abandoned Wet Grasslands." *Ecological Engineering* 66:91–102. https://doi.org/10.1016/j.ecoleng.2013.05.008.

Joyce, Chris B., Matthew Simpson, and Michelle Casanova. 2016a. "Future Wet Grasslands: Ecological Implications of Climate Change." *Ecosystem Health and Sustainability* 2 (9): 1–15. https://doi.org/10.1002/ehs2.1240.

Joyce, Chris B, Matthew Simpson, and Michelle Casanova. 2016b. "Future Wet Grasslands: Ecological Implications of Climate Change." *Ecosystem Health and Sustainability* 2 (9): e01240. https://doi.org/https://doi.org/10.1002/ehs2.1240.

Joyce, Chris B, and P Max Wade. 1998. *European Wet Grasslands: Biodiversity, Management and Restoration.*

Kamali, Bahareh, Seyed Hamid Ahmadi, Thomas Gaiser, Marion Buddeberg, and Claas Nendel. 2024. "Quest to Find Compromised Spatial and Temporal Resolutions for Integrating Remote Sensing Data with an Agro-Ecosystem Model for Grasslands." *International Journal of*

Applied Earth Observation and Geoinformation 128 (April):103705. https://doi.org/10.1016/J.JAG.2024.103705.

Karila, Kirsi, Raquel Alves Oliveira, Johannes Ek, Jere Kaivosoja, Niko Koivumäki, Panu Korhonen, Oiva Niemeläinen, et al. 2022. "Estimating Grass Sward Quality and Quantity Parameters Using Drone Remote Sensing with Deep Neural Networks." https://doi.org/10.3390/rs14112692.

Karunaratne, Senani, Anna Thomson, Elizabeth Morse-McNabb, Jayan Wijesingha, Dani Stayches, Amy Copland, and Joe Jacobs. 2020. "The Fusion of Spectral and Structural Datasets Derived from an Airborne Multispectral Sensor for Estimation of Pasture Dry Matter Yield at Paddock Scale with Time." *Remote Sensing* 12 (12). https://doi.org/10.3390/rs12122017.

Khaledi, Valeh, Bahareh Kamali, Gunnar Lischeid, Ottfried Dietrich, Mariel F Davies, and Claas Nendel. 2024. "Challenges of Including Wet Grasslands with Variable Groundwater Tables in Large-Area Crop Production Simulations." *Agriculture (Switzerland)* 14 (5). https://doi.org/10.3390/agriculture14050679.

Kitagawa, Etsuji, Hirokazu Muraki, Kyouhei Yoshinaga, Jyunki Yamagishi, and Yakumi Tsumura. 2018. "Research on Shape Characteristic of 3D Modeling Software (SfM/MVS) in UAV Aerial Images." *Journal of Japan Society of Civil Engineers, Ser. F3 (Civil Engineering Informatics)* 74 (2): II_143-II_148.

Klemas, Victor. 2011. "Remote Sensing of Wetlands: Case Studies Comparing Practical Techniques." *Journal of Coastal Research* 27 (3): 418–27. https://doi.org/10.2112/JCOASTRES-D-10-00174.1.

Koppe, Wolfgang, Fei Li, Martin L Gnyp, Yuxin Miao, Liangliang Jia, Xinping Chen, Fusuo Zhang, and Georg Bareth. 2010. "Evaluating Multispectral and Hyperspectral Satellite Remote Sensing Data for Estimating Winter Wheat Growth Parameters at Regional Scale in the North China Plain." *Photogrammetrie - Fernerkundung - Geoinformation* 2010 (3): 167–78. https://doi.org/10.1127/1432-8364/2010/0047.

Kümmerer, Robin, Patrick Ole Noack, and Bernhard Bauer. 2023. "Using High-Resolution UAV Imaging to Measure Canopy Height of Diverse Cover Crops and Predict Biomass." *Remote Sensing* 15 (6). https://doi.org/10.3390/rs15061520.

Lamarque, Pénélope, Ulrike Tappeiner, Catherine Turner, Melanie Steinbacher, Richard D Bardgett, Ute Szukics, Markus Schermer, and Sandra Lavorel. n.d. "Stakeholder Perceptions of Grassland Ecosystem Services in Relation to Knowledge on Soil Fertility and Biodiversity." https://doi.org/10.1007/s10113-011-0214-0.

LaRue, Elizabeth A., Jonathan A Knott, Grant M Domke, Han Yh Chen, Qinfeng Guo, Masumi Hisano, Christopher Oswalt, et al. 2023. "Structural Diversity as a Reliable and Novel Predictor for Ecosystem Productivity." *Frontiers in Ecology and the Environment* 21 (1): 33–39. https://doi.org/10.1002/fee.2586.

Lee, Hyowon, Hyo-Jin Lee, Jong-Sung Jung, and Han-Jong Ko. 2015. “Mapping Herbage Biomass on a Hill Pasture Using a Digital Camera with an Unmanned Aerial Vehicle System.” *Journal of The Korean Society of Grassland and Forage Science* 35 (3): 225–31. https://doi.org/10.5333/kgfs.2015.35.3.225.

Lemaire, Gilles, John Hodgson, and Abad Chabbi. 2011. *Grassland Productivity and Ecosystem Services*. Cabi.

Lengyel, Szabolcs, Andrej Kobler, Lado Kutnar, Erik Framstad, Pierre Yves Henry, Valerija Babij, Bernd Gruber, Dirk Schmeller, and Klaus Henle. 2008. “A Review and a Framework for the Integration of Biodiversity Monitoring at the Habitat Level.” *Biodiversity and Conservation*. https://doi.org/10.1007/s10531-008-9359-7.

Li, Fei, Cristiano Piasecki, Reginald J. Millwood, Benjamin Wolfe, Mitra Mazarei, and C. Neal Stewart. 2020. “High-Throughput Switchgrass Phenotyping and Biomass Modeling by UAV.” *Frontiers in Plant Science* 11 (October): 1–15. https://doi.org/10.3389/fpls.2020.574073.

Li, Kai Yun, Niall G. Burnside, Raul Sampaio de Lima, Miguel Villoslada Peciña, Karli Sepp, Ming Der Yang, Janar Raet, Ants Vain, Are Selge, and Kalev Sepp. 2021. “The Application of an Unmanned Aerial System and Machine Learning Techniques for Red Clover-Grass Mixture Yield Estimation under Variety Performance Trials.” *Remote Sensing* 13 (10). https://doi.org/10.3390/rs13101994.

Li, Xiaohan, Xuezhang Li, Wen Liu, Benhui Wei, and Xianli Xu. 2021. “A UAV-Based Framework for Crop Lodging Assessment.” *European Journal of Agronomy* 123 (November 2020): 126201. https://doi.org/10.1016/j.eja.2020.126201.

Liang, Tiangang, Shuxia Yang, Qisheng Feng, Baokang Liu, Renping Zhang, Xiaodong Huang, and Hongjie Xie. 2016. “Multi-Factor Modeling of above-Ground Biomass in Alpine Grassland: A Case Study in the Three-River Headwaters Region, China.” *Remote Sensing of Environment* 186:164–72. https://doi.org/10.1016/j.rse.2016.08.014.

Librán-Embid, Felipe, Felix Klaus, Teja Tscharntke, and Ingo Grass. 2020. “Unmanned Aerial Vehicles for Biodiversity-Friendly Agricultural Landscapes - A Systematic Review.” *Science of the Total Environment* 732:139204. https://doi.org/10.1016/j.scitotenv.2020.139204.

Lin, Xingchen, Jianjun Chen, Peiqing Lou, Shuhua Yi, Yu Qin, Haotian You, and Xiaowen Han. 2021. “Improving the Estimation of Alpine Grassland Fractional Vegetation Cover Using Optimized Algorithms and Multi-Dimensional Features.” *Plant Methods* 17 (1): 1–18. https://doi.org/10.1186/s13007-021-00796-5.

Liu, Wenhao, Wanqiang Han, Guili Jin, Ke Gong, and Jian Ma. 2024. “Classification of Major Species in the Sericite-Artemisia Desert Grassland Using Hyperspectral Images and Spectral Feature Identification.” *PeerJ* 12 (7). https://doi.org/10.7717/peerj.17663.

Londo, G. 1976. “The Decimal Scale for Releves of Permanent Quadrats.” *Vegetatio* 33 (1): 61–64. https://doi.org/10.1007/BF00055300.

López Díaz, Julio Enrique, A I Roca-Fernández, and Antonio González-Rodríguez. 2011. "Measuring Herbage Mass by Non-Destructive Methods: A Review." *Journal of Agricultural Science and Technology* 1 (July):303–14.

Lu, Bing, and Yuhong He. 2017. "Species Classification Using Unmanned Aerial Vehicle (UAV)-Acquired High Spatial Resolution Imagery in a Heterogeneous Grassland." *ISPRS Journal of Photogrammetry and Remote Sensing* 128 (June):73–85. https://doi.org/10.1016/J.ISPRSJPRS.2017.03.011.

Lu, Hua, John Mack, Yongchao Yang, and Zhen Shen. 2014. "Structural Modification Strategies for the Rational Design of Red/NIR Region BODIPYs." *Chem. Soc. Rev.* 43 (13): 4778–4823. https://doi.org/10.1039/C4CS00030G.

Ludwig, Antonia, Daniel Doktor, and Hannes Feilhauer. 2024. "Is Spectral Pixel-to-Pixel Variation a Reliable Indicator of Biodiversity? A Systematic Assessment of the Spectral Variation Hypothesis Highlights (for Review)." *Remote Sensing of Environment* 302 (January): 113988. https://doi.org/10.1016/j.rse.2023.113988.

Lussem, Ulrike, Andreas Bolten, Ireneusz Kleppert, Jörg Jasper, Martin Leon Gnyp, Jürgen Schellberg, and Georg Bareth. 2022. "Herbage Mass, N Concentration, and N Uptake of Temperate Grasslands Can Adequately Be Estimated from UAV-Based Image Data Using Machine Learning." *Remote Sensing* 14 (13): 3066. https://doi.org/10.3390/rs14133066.

Lussem, Ulrike, Andreas Bolten, Jannis Menne, Martin Leon Gnyp, Jürgen Schellberg, and Georg Bareth. 2019. "Estimating Biomass in Temperate Grassland with High Resolution Canopy Surface Models from UAV-Based RGB Images and Vegetation Indices." *Journal of Applied Remote Sensing* 13 (03): 1. https://doi.org/10.1117/1.jrs.13.034525.

Lussem, Ulrike, Jürgen Schellberg, and Georg Bareth. 2020. "Monitoring Forage Mass with Low-Cost UAV Data: Case Study at the Rengen Grassland Experiment." *PFG - Journal of Photogrammetry, Remote Sensing and Geoinformation Science* 88 (5): 407–22. https://doi.org/10.1007/s41064-020-00117-w.

Luthardt, V., O. Brauner, F. Dreger, S. Friedrich, H. Garbe, A.-K. Hirsch, T. Kabus, et al. 2017. "Methodenkatalog Zum Monitoring-Programm Der Ökosystemaren Umweltbeobachtung (ÖUB) in Den Biosphärenreservaten Brandenburgs," 226. http://lanuweb.hnee.de/oeub/pdf/Methodenkatalog_TeilA_komplett_2017.pdf.

Lyu, Xin, Xiaobing Li, Dongliang Dang, Kai Wang, Chenhao Zhang, Wanyu Cao, and Anru Lou. 2024. "Systematic Review of Remote Sensing Technology for Grassland Biodiversity Monitoring: Current Status and Challenges." *Global Ecology and Conservation* 54 (October):e03196. https://doi.org/10.1016/J.GECCO.2024.E03196.

M. Woebbecke, D, G E. Meyer, K Von Bargen, and D A. Mortensen. 1995. "Color Indices for Weed Identification Under Various Soil, Residue, and Lighting Conditions." *Transactions of the ASAE* 38 (1): 259–69. https://doi.org/https://doi.org/10.13031/2013.27838.

Madec, Simon, Fred Baret, Benoît de Solan, Samuel Thomas, Dan Dutartre, Stéphane Jezequel, Matthieu Hemmerlé, Gallian Colombeau, and Alexis Comar. 2017. "High-Throughput Phenotyping of Plant Height: Comparing Unmanned Aerial Vehicles and Ground LiDAR Estimates." *Frontiers in Plant Science* 8 (November). https://doi.org/10.3389/fpls.2017.02002.

Magurran, Anne E. 2021. "Measuring Biological Diversity." *Current Biology* 31 (19): R1174–77.

Mairota, Paola, Barbara Cafarelli, Raphael K. Didham, Francesco P. Lovergine, Richard M. Lucas, Harini Nagendra, Duccio Rocchini, and Cristina Tarantino. 2015. "Challenges and Opportunities in Harnessing Satellite Remote-Sensing for Biodiversity Monitoring." *Ecological Informatics* 30:207–14. https://doi.org/10.1016/j.ecoinf.2015.08.006.

Manfreda, Salvatore, Matthew F. McCabe, Pauline E. Miller, Richard Lucas, Victor Pajuelo Madrigal, Giorgos Mallinis, Eyal Ben Dor, et al. 2018. "On the Use of Unmanned Aerial Systems for Environmental Monitoring." *Remote Sensing* 10 (4). https://doi.org/10.3390/rs10040641.

Marriott, Carol Ann, Michael Fothergill, Bernard Jeangros, Michele Scotton, and Frédérique Louault. 2004. "Long-Term Impacts of Extensification of Grassland Management on Biodiversity and Productivity in Upland Areas. A Review." *Agronomie* 24 (8): 447–62. https://doi.org/10.1051/agro:2004041.

Matese, Alessandro, Piero Toscano, Salvatore Filippo Di Gennaro, Lorenzo Genesio, Francesco Primo Vaccari, Jacopo Primicerio, Claudio Belli, Alessandro Zaldei, Roberto Bianconi, and Beniamino Gioli. 2015. "Intercomparison of UAV, Aircraft and Satellite Remote Sensing Platforms for Precision Viticulture." *Remote Sensing* 7 (3): 2971–90. https://doi.org/10.3390/rs70302971.

Merwe, Deon Van Der, Carol E. Baldwin, and Will Boyer. 2020. "An Efficient Method for Estimating Dormant Season Grass Biomass in Tallgrass Prairie from Ultra-High Spatial Resolution Aerial Imaging Produced with Small Unmanned Aircraft Systems." *International Journal of Wildland Fire* 29 (8): 696–701. https://doi.org/10.1071/WF19026.

Metternicht, G. 2003. "Vegetation Indices Derived from High-Resolution Airborne Videography for Precision Crop Management." *International Journal of Remote Sensing* 24 (14): 2855–77. https://doi.org/10.1080/01431160210163074.

Meyer, George E, Timothy W Hindman, and Koppolu Laksmi. 1999. "Machine Vision Detection Parameters for Plant Species Identification." In *Precision Agriculture and Biological Quality*, edited by George E Meyer and James A DeShazer, 3543:327–35. SPIE. https://doi.org/10.1117/12.336896.

Michez, Adrien, Philippe Lejeune, Sébastien Bauwens, Andriamandroso Andriamasinoro Lalaina Herinaina, Yannick Blaise, Eloy Castro Muñoz, Frédéric Lebeau, and Jérôme Bindelle. 2019. "Mapping and Monitoring of Biomass and Grazing in Pasture with an Unmanned Aerial System." *Remote Sensing* 11 (5): 1–14. https://doi.org/10.3390/rs11050473.

Michez, Adrien, Lejeune Philippe, Knoden David, Cremer Sébastien, Decamps Christian, and Jérôme Bindelle. 2020. “Can Low-Cost Unmanned Aerial Systems Describe the Forage Quality Heterogeneity? Insight from a Timothy Pasture Case Study in Southern Belgium.” *Remote Sensing* 12 (10). https://doi.org/10.3390/rs12101650.

Moeckel, Thomas, Hanieh Safari, Björn Reddersen, Thomas Fricke, and Michael Wachendorf. 2017. “Fusion of Ultrasonic and Spectral Sensor Data for Improving the Estimation of Biomass in Grasslands with Heterogeneous Sward Structure.” *Remote Sensing* 9 (1). https://doi.org/10.3390/rs9010098.

Moher, David, Alessandro Liberati, Jennifer Tetzlaff, and Douglas G Altman. 2009. “Academia and Clinic Annals of Internal Medicine Preferred Reporting Items for Systematic Reviews and Meta-Analyses :” *Annals of Internal Medicine* 151 (4): 264–69.

Morais, Tiago G., Ricardo F.M. Teixeira, Mario Figueiredo, and Tiago Domingos. 2021. “The Use of Machine Learning Methods to Estimate Aboveground Biomass of Grasslands: A Review.” *Ecological Indicators* 130 (October 2020): 108081. https://doi.org/10.1016/j.ecolind.2021.108081.

Mulla, David J. 2013. “Twenty Five Years of Remote Sensing in Precision Agriculture: Key Advances and Remaining Knowledge Gaps.” *Biosystems Engineering* 114 (4): 358–71. https://doi.org/10.1016/J.BIOSYSTEMSENG.2012.08.009.

Muro, Javier, Anja Linstädter, Paul Magdon, Stephan Wöllauer, Florian A. Männer, Lisa Maricia Schwarz, Gohar Ghazaryan, Johannes Schultz, Zbyněk Malenovský, and Olena Dubovyk. 2022. “Predicting Plant Biomass and Species Richness in Temperate Grasslands across Regions, Time, and Land Management with Remote Sensing and Deep Learning.” *Remote Sensing of Environment* 282 (March). https://doi.org/10.1016/j.rse.2022.113262.

Näsi, Roope, Niko Viljanen, Jere Kaivosoja, Katja Alhonoja, Teemu Hakala, Lauri Markelin, and Eija Honkavaara. 2018. “Estimating Biomass and Nitrogen Amount of Barley and Grass Using UAV and Aircraft Based Spectral and Photogrammetric 3D Features.” *Remote Sensing* 10 (7): 1–32. https://doi.org/10.3390/rs10071082.

Nordberg, Maj Liz, and Joakim Evertson. 2003. “Monitoring Change in Mountainous Dry-Heath Vegetation at a Regional Scale Using Multitemporal Landsat TM Data.” *Ambio* 32 (8): 502–9. https://doi.org/10.1579/0044-7447-32.8.502.

O’Donovan, Mike, Pat Dillon, M Rath, and G Stakelum. 2002. “A Comparison of Four Methods of Herbage Mass Estimation.” *Irish Journal of Agricultural and Food Research* 41:17–27.

O’Sullivan, M, W F O’Keeffe, and M J Flynn. 1987. “The Value of Pasture Height in the Measurement of Dry Matter Yield.” *Irish Journal of Agricultural Research* 26 (1): 63–68. http://www.jstor.org/stable/25556178.

Oijen, Marcel van, Gianni Bellocchi, and Mats H glind. 2018. “Effects of Climate Change on Grassland Biodiversity and Productivity: The Need for a Diversity of Models.” *Agronomy*.

MDPI AG. https://doi.org/10.3390/agronomy8020014.

Oldeland, Jens, Dirk Wesuls, Duccio Rocchini, Michael Schmidt, and Norbert Jürgens. 2010. "Does Using Species Abundance Data Improve Estimates of Species Diversity from Remotely Sensed Spectral Heterogeneity?" *Ecological Indicators* 10 (2): 390–96. https://doi.org/10.1016/J.ECOLIND.2009.07.012.

Oliveira, Raquel Alves, Roope Näsi, Oiva Niemeläinen, Laura Nyholm, Katja Alhonoja, Jere Kaivosoja, Lauri Jauhiainen, et al. 2020. "Machine Learning Estimators for the Quantity and Quality of Grass Swards Used for Silage Production Using Drone-Based Imaging Spectrometry and Photogrammetry." *Remote Sensing of Environment* 246 (May): 111830. https://doi.org/10.1016/j.rse.2020.111830.

Palmer, Michael W, Peter G Earls, Bruce W Hoagland, Peter S White, and Thomas Wohlgemuth. 2002. "Quantitative Tools for Perfecting Species Lists." *Environmetrics* 13:121–37. https://doi.org/10.1002/env.516.

Pearson, R.~L., and L.~D. Miller. 1972. "Remote Mapping of Standing Crop Biomass for Estimation of the Productivity of the Shortgrass Prairie." In *Remote Sensing of Environment, VIII*, 1355.

Peng, Yu, Min Fan, Lan Bai, Weiguo Sang, Jinchao Feng, Zhixin Zhao, and Ziye Tao. 2019. "Identification of the Best Hyperspectral Indices in Estimating Plant Species Richness in Sandy Grasslands." *Remote Sensing* 11 (5). https://doi.org/10.3390/rs11050588.

Pereira, F. R.da S., J. P. de Lima, R. G. Freitas, A. A. Dos Reis, L. R.do Amaral, G. K.D.A. Figueiredo, R. A.C. Lamparelli, and P. S.G. Magalhães. 2022. "Nitrogen Variability Assessment of Pasture Fields under an Integrated Crop-Livestock System Using UAV, PlanetScope, and Sentinel-2 Data." *Computers and Electronics in Agriculture* 193 (April 2021). https://doi.org/10.1016/j.compag.2021.106645.

Perry, Charles R., and Lyle F. Lautenschlager. 1984. "Functional Equivalence of Spectral Vegetation Indices." *Remote Sensing of Environment* 14 (1–3): 169–82. https://doi.org/10.1016/0034-4257(84)90013-0.

Petermann, Jana S., and Oksana Y. Buzhdygan. 2021. "Grassland Biodiversity." *Current Biology* 31 (19): R1195–1201. https://doi.org/10.1016/J.CUB.2021.06.060.

Piggot, G. J. 1989. "A Comparison of Four Methods for Estimating Herbage Yield of Temperate Dairy Pastures." *New Zealand Journal of Agricultural Research* 32 (1): 121–23. https://doi.org/10.1080/00288233.1989.10423486.

Pilgrim, Emma S., Christopher J.A. Macleod, Martin S.A. Blackwell, Roland Bol, David V. Hogan, David R. Chadwick, Laura Cardenas, et al. 2010. "Interactions Among Agricultural Production and Other Ecosystem Services Delivered from European Temperate Grassland Systems." *Advances in Agronomy* 109 (C): 117–54. https://doi.org/10.1016/B978-0-12-385040-9.00004-9.

Plaza, Javier, Marco Criado, Nilda Sánchez, Rodrigo Pérez-Sánchez, Carlos Palacios, and Francisco Charfolé. 2021. "Uav Multispectral Imaging Potential to Monitor and Predict Agronomic Characteristics of Different Forage Associations." *Agronomy* 11 (9): 1–22. https://doi.org/10.3390/agronomy11091697.

Pohl, M., M. Hoffmann, U. Hagemann, M. Giebels, E. Albiac Borraz, M. Sommer, and J. Augustin. 2015. "Dynamic C and N Stocks - Key Factors Controlling the C Gas Exchange of Maize in Heterogenous Peatland." *Biogeosciences* 12 (9): 2737–52. https://doi.org/10.5194/bg-12-2737-2015.

Pol, A Van Den, Talea Becker, Adrian Botana Fernandez, Thia Hennessy, and Giovanni Peratoner. 2018. "Social and Economic Impacts of Grass Based Ruminant Production." In *Sustainable Meat and Milk Production from Grasslands*, 23:697–708.

Poley, Lucy G., and Gregory J. McDermid. 2020. "A Systematic Review of the Factors Influencing the Estimation of Vegetation Aboveground Biomass Using Unmanned Aerial Systems." *Remote Sensing* 12 (7). https://doi.org/10.3390/rs12071052.

Possoch, M., S. Bieker, D. Hoffmeister, A. A. Bolten, J. Schellberg, and G. Bareth. 2016. "Multi-Temporal Crop Surface Models Combined with the Rgb Vegetation Index from UAV-Based Images for Forage Monitoring in Grassland." *International Archives of the Photogrammetry, Remote Sensing and Spatial Information Sciences - ISPRS Archives* 2016-Janua (June): 991–98. https://doi.org/10.5194/isprsarchives-XLI-B1-991-2016.

Pranga, Joanna, Irene Borra-Serrano, Jonas Aper, Tom De Swaef, An Ghesquiere, Paul Quataert, Isabel Roldán-Ruiz, Ivan A. Janssens, Greet Ruysschaert, and Peter Lootens. 2021. "Improving Accuracy of Herbage Yield Predictions in Perennial Ryegrass with UAV-Based Structural and Spectral Data Fusion and Machine Learning." *Remote Sensing* 13 (17): 3459. https://doi.org/10.3390/rs13173459.

Psomas, A., M. Kneubühler, S. Huber, K. Itten, and N. E. Zimmermann. 2011. "Hyperspectral Remote Sensing for Estimating Aboveground Biomass and for Exploring Species Richness Patterns of Grassland Habitats." *International Journal of Remote Sensing* 32 (24): 9007–31. https://doi.org/10.1080/01431161.2010.532172.

Qi, J., A. Chehbouni, A. R. Huete, Y. H. Kerr, and S. Sorooshian. 1994. "A Modified Soil Adjusted Vegetation Index." *Remote Sensing of Environment* 48 (2): 119–26. https://doi.org/10.1016/0034-4257(94)90134-1.

Qin, Yu, Shuhua Yi, Yongjian Ding, Yan Qin, Wei Zhang, Yi Sun, Xiumin Hou, et al. 2021. "Effects of Plateau Pikas' Foraging and Burrowing Activities on Vegetation Biomass and Soil Organic Carbon of Alpine Grasslands." *Plant and Soil* 458 (1–2): 201–16. https://doi.org/10.1007/s11104-020-04489-1.

R Core Team. 2022. "R: A Language and Environment for Statistical Computing." Vienna, Austria: R Foundation for Statistical Computing. https://www.r-project.org/.

Ramoelo, A., A. K. Skidmore, M. A. Cho, M. Schlerf, R. Mathieu, and I. M.A. Heitkönig. 2012. "Regional Estimation of Savanna Grass Nitrogen Using the Red-Edge Band of the Spaceborne Rapideye Sensor." *International Journal of Applied Earth Observation and Geoinformation* 19 (1): 151–62. https://doi.org/10.1016/j.jag.2012.05.009.

Rapinel, Sébastien, Cendrine Mony, Lucie Lecoq, Bernard Clément, Alban Thomas, and Laurence Hubert-Moy. 2019. "Evaluation of Sentinel-2 Time-Series for Mapping Floodplain Grassland Plant Communities." *Remote Sensing of Environment* 223 (March):115–29. https://doi.org/10.1016/j.rse.2019.01.018.

Reis, Aliny A. Dos, João P.S. Werner, Bruna C Silva, Gleyce K.D.A. Figueiredo, João F.G. Antunes, Júlio C.D.M. Esquerdo, Alexandre C Coutinho, Rubens A.C. Lamparelli, Jansle V Rocha, and Paulo S.G. Magalhães. 2020. "Monitoring Pasture Aboveground Biomass and Canopy Height in an Integrated Crop-Livestock System Using Textural Information from Planetscope Imagery." *Remote Sensing* 12 (16). https://doi.org/10.3390/RS12162534.

Richardson, A. J., and C. L. Wiegand. 1977. "Distinguishing Vegetation from Soil Background Information." *Photogrammetric Engineering and Remote Sensing* 43 (12): 1541–52.

Rocchini, Duccio. 2007. "Effects of Spatial and Spectral Resolution in Estimating Ecosystem α-Diversity by Satellite Imagery." *Remote Sensing of Environment* 111 (4): 423–34. https://doi.org/10.1016/j.rse.2007.03.018.

Rocchini, Duccio, Nicole Salvatori, Carl Beierkuhnlein, Alessandro Chiarucci, Florian de Boissieu, Michael Förster, Carol X. Garzon-Lopez, et al. 2021. "From Local Spectral Species to Global Spectral Communities: A Benchmark for Ecosystem Diversity Estimate by Remote Sensing." *Ecological Informatics* 61 (November 2020). https://doi.org/10.1016/j.ecoinf.2020.101195.

Rondeaux, Geneviève, Michael Steven, and Frédéric Baret. 1996. "Optimization of Soil-Adjusted Vegetation Indices." *Remote Sensing of Environment* 55 (2): 95–107. https://doi.org/10.1016/0034-4257(95)00186-7.

Rosa, Daniele De, Bruno Basso, Matteo Fasiolo, Johannes Friedl, Bill Fulkerson, Peter R. Grace, and David W. Rowlings. 2021. "Predicting Pasture Biomass Using a Statistical Model and Machine Learning Algorithm Implemented with Remotely Sensed Imagery." *Computers and Electronics in Agriculture* 180 (October 2020): 105880. https://doi.org/10.1016/j.compag.2020.105880.

Rosenthal, Gert. 2006. "Restoration of Wet Grasslands - Effects of Seed Dispersal, Persistence and Abundance on Plant Species Recruitment." *Basic and Applied Ecology* 7 (5): 409–21. https://doi.org/10.1016/j.baae.2006.05.006.

Rosenthal, Gert. 2010. "Secondary Succession in a Fallow Central European Wet Grassland." *Flora: Morphology, Distribution, Functional Ecology of Plants* 205 (3): 153–60. https://doi.org/10.1016/j.flora.2009.02.003.

Rossi, Christian, Mathias Kneubühler, Martin Schütz, Michael E. Schaepman, Rudolf M. Haller, and Anita C. Risch. 2021. “Remote Sensing of Spectral Diversity: A New Methodological Approach to Account for Spatio-Temporal Dissimilarities between Plant Communities.” *Ecological Indicators* 130 (November):108106. https://doi.org/10.1016/j.ecolind.2021.108106.

Rossi, Christian, Mathias Kneubühler, Martin Schütz, Michael E Schaepman, Rudolf M Haller, and Anita C Risch. 2022. “Spatial Resolution, Spectral Metrics and Biomass Are Key Aspects in Estimating Plant Species Richness from Spectral Diversity in Species-Rich Grasslands.” *Remote Sensing in Ecology and Conservation* 8 (3): 297–314. https://doi.org/10.1002/rse2.244.

Roth, Lukas, and Bernhard Streit. 2018. “Predicting Cover Crop Biomass by Lightweight UAS-Based RGB and NIR Photography: An Applied Photogrammetric Approach.” *Precision Agriculture* 19 (1): 93–114. https://doi.org/10.1007/s11119-017-9501-1.

Roujean, Jean Louis, and François Marie Breon. 1995. “Estimating PAR Absorbed by Vegetation from Bidirectional Reflectance Measurements.” *Remote Sensing of Environment* 51 (3): 375–84. https://doi.org/10.1016/0034-4257(94)00114-3.

Rouse, John Wilson, Robert H Haas, John A Schell, and D W Deering. 1973. “Monitoring Vegetation Systems in the Great Plains with ERTS.” In .

Rueda-Ayala, Victor P., José M. Peña, Mats Höglind, José M. Bengochea-Guevara, and Dionisio Andújar. 2019. “Comparing UAV-Based Technologies and RGB-D Reconstruction Methods for Plant Height and Biomass Monitoring on Grass Ley.” *Sensors (Switzerland)* 19 (3). https://doi.org/10.3390/s19030535.

Sala, Osvaldo E., and José M. Paruelo. 1997. “Ecosystem Services in Grasslands.” *Nature’s Services: Societal Dependence on Natural Ecosystems*, 237–52.

Sanderson, Matt A, C Alan Rotz, Stanley W Fultz, and Edward B Rayburn. 2001. “Estimating Forage Mass with a Commercial Capacitance Meter, Rising Plate Meter, and Pasture Ruler.” *Agronomy Journal* 93 (6): 1281–86. https://doi.org/https://doi.org/10.2134/agronj2001.1281.

Santillan, R. A., W. R. Ocumpaugh, and G. O. Mott. 1979. “ Estimating Forage Yield with a Disk Meter 1 .” *Agronomy Journal* 71 (1): 71–74. https://doi.org/10.2134/agronj1979.00021962007100010017x.

Schellberg, Jürgen, Michael J. Hill, Roland Gerhards, Matthias Rothmund, and Matthias Braun. 2008. “Precision Agriculture on Grassland: Applications, Perspectives and Constraints.” *European Journal of Agronomy* 29 (2–3): 59–71. https://doi.org/10.1016/j.eja.2008.05.005.

Schils, René L.M., Conny Bufe, Caroline M. Rhymer, Richard M. Francksen, Valentin H. Klaus, Mohamed Abdalla, Filippo Milazzo, et al. 2022. “Permanent Grasslands in Europe: Land Use Change and Intensification Decrease Their Multifunctionality.” *Agriculture, Ecosystems and Environment* 330 (January). https://doi.org/10.1016/j.agee.2022.107891.

Schmidt, K. S., and A. K. Skidmore. 2003. “Spectral Discrimination of Vegetation Types in a Coastal Wetland.” *Remote Sensing of Environment* 85 (1): 92–108. https://doi.org/10.1016/S0034-4257(02)00196-7.

Schucknecht, Anne, Alexander Krämer, Sarah Asam, Abraham Mejia-Aguilar, Noelia Garcia-Franco, Max A. Schuchardt, Anke Jentsch, and Ralf Kiese. 2020. “Vegetation Traits of Pre-Alpine Grasslands in Southern Germany.” *Scientific Data* 7 (1): 1–11. https://doi.org/10.1038/s41597-020-00651-7.

Schucknecht, Anne, Bumsuk Seo, Alexander Krämer, Sarah Asam, Clement Atzberger, and Ralf Kiese. 2022. “Estimating Dry Biomass and Plant Nitrogen Concentration in Pre-Alpine Grasslands with Low-Cost UAS-Borne Multispectral Data-a Comparison of Sensors, Algorithms, and Predictor Sets.” *Biogeosciences* 19 (10): 2699–2727. https://doi.org/10.5194/bg-19-2699-2022.

Schulze-Brüninghoff, Damian, Michael Wachendorf, and Thomas Astor. 2021. “Remote Sensing Data Fusion as a Tool for Biomass Prediction in Extensive Grasslands Invaded by L. Polyphyllus.” *Remote Sensing in Ecology and Conservation* 7 (2): 198–213. https://doi.org/10.1002/rse2.182.

Schweiger, Anna K, Anita C Risch, Alexander Damm, Mathias Kneubühler, Rudolf Haller, Michael E Schaepman, and Martin Schütz. 2015. “Using Imaging Spectroscopy to Predict Above-Ground Plant Biomass in Alpine Grasslands Grazed by Large Ungulates.” *Journal of Vegetation Science* 26 (1): 175–90. https://doi.org/10.1111/jvs.12214.

Sha, Zongyao, Yuwei Wang, Yongfei Bai, Yujin Zhao, Hua Jin, Ya Na, and Xiaoliang Meng. 2018. “Comparison of Leaf Area Index Inversion for Grassland Vegetation through Remotely Sensed Spectra by Unmanned Aerial Vehicle and Field-Based Spectroradiometer.” *Journal of Plant Ecology* 12 (3): 395–408. https://doi.org/10.1093/jpe/rty036.

Shahbazi, Mozhdeh, Jérôme Théau, and Patrick Ménard. 2014. “GIScience & Remote Sensing Recent Applications of Unmanned Aerial Imagery in Natural Resource Management Recent Applications of Unmanned Aerial Imagery in Natural Resource Management.” https://doi.org/10.1080/15481603.2014.926650.

Shi, Yan, Jay Gao, Xilai Li, Jiexia Li, and Gary Brierley. 2022. “Effects of Disturbances on Aboveground Biomass of Alpine Meadow in the Yellow River Source Zone, Western China.” *Ecology and Evolution* 12 (3): 1–14. https://doi.org/10.1002/ece3.8640.

Shi, Yan, Jay Gao, Xilai Li, Jiexia Li, Daniel Marc G. Dela Torre, and Gary John Brierley. 2021. “Improved Estimation of Aboveground Biomass of Disturbed Grassland through Including Bare Ground and Grazing Intensity.” *Remote Sensing* 13 (11). https://doi.org/10.3390/rs13112105.

Shorten, P. R., and M. R. Trolove. 2022. “UAV-Based Prediction of Ryegrass Dry Matter Yield.” *International Journal of Remote Sensing* 43 (7): 2393–2409. https://doi.org/10.1080/01431161.2022.2058890.

Sibanda, Mbulisi, Onisimo Mutanga, Mathieu Rouget, and Lalit Kumar. 2017. “Estimating Biomass of Native Grass Grown under Complex Management Treatments Using Worldview-3 Spectral Derivatives.” *Remote Sensing* 9 (1). https://doi.org/10.3390/rs9010055.

Sims, Daniel A., and John A. Gamon. 2002. “Relationships between Leaf Pigment Content and Spectral Reflectance across a Wide Range of Species, Leaf Structures and Developmental Stages.” *Remote Sensing of Environment* 81 (2–3): 337–54. https://doi.org/10.1016/S0034-4257(02)00010-X.

Sinde-González, Izar, Mariluz Gil-Docampo, Marcos Arza-García, José Grefa-Sánchez, Diana Yánez-Simba, Patricio Pérez-Guerrero, and Víctor Abril-Porras. 2021. “Biomass Estimation of Pasture Plots with Multitemporal UAV-Based Photogrammetric Surveys.” *International Journal of Applied Earth Observation and Geoinformation* 101 (April). https://doi.org/10.1016/j.jag.2021.102355.

Smith, M W, J L Carrivick, and D J Quincey. 2015. “Structure from Motion Photogrammetry in Physical Geography.” *Progress in Physical Geography: Earth and Environment* 40 (2): 247–75. https://doi.org/10.1177/0309133315615805.

Smith, R C G, J Adams, D J Stephens, and P T Hick. 1995. “Forecasting Wheat Yield in a Mediterranean-Type Environment from the NOAA Satellite.” *Australian Journal of Agricultural Research* 46 (1): 113–25. https://doi.org/10.1071/AR9950113.

Sousa, Celio, Carolina Souza, Lisiane Zanella, and Luis Carvalho. 2012. “Analysis of Rapideye’s Red Edge Band for Image Segmentation and Classification.” *Proceedings of the 4th GEOBIA, Rio de Janeiro, Brazil* 79 (518): 7–9.

Souza, Eduardo G. de, Peter C. Scharf, and Kenneth A. Sudduth. 2010. “Sun Position and Cloud Effects on Reflectance and Vegetation Indices of Corn.” *Agronomy Journal* 102 (2): 734–44. https://doi.org/10.2134/agronj2009.0206.

Sripada, Ravi. 2005. “Determining In-Season Nitrogen Requirements for Corn Using Aerial Color-Infrared Photography.” Raleigh, NC: North Carolina State University.

Sripada, Ravi P, Ronnie W Heiniger, Jeffrey G White, and Alan D Meijer. 2006. “Aerial Color Infrared Photography for Determining Early In-Season Nitrogen Requirements in Corn.” *Agronomy Journal* 98 (4): 968–77. https://doi.org/https://doi.org/10.2134/agronj2005.0200.

Sun, Weiwei, Daosheng Chen, Zhouyuan Li, Saiqiang Li, Siying Cheng, Xiaomeng Niu, Yimeng Cai, et al. 2024. “Monitoring Wetland Plant Diversity from Space: Progress and Perspective.” *International Journal of Applied Earth Observation and Geoinformation*. Elsevier. https://doi.org/10.1016/j.jag.2024.103943.

Tackenberg, Oliver. 2007. “A New Method for Non-Destructive Measurement of Biomass, Growth Rates, Vertical Biomass Distribution and Dry Matter Content Based on Digital Image Analysis.” *Annals of Botany* 99 (4): 777–83. https://doi.org/10.1093/aob/mcm009.

Taddeo, Sophie, Iryna Dronova, and Nicholas Depsky. 2019. “Spectral Vegetation Indices of

Wetland Greenness: Responses to Vegetation Structure, Composition, and Spatial Distribution." *Remote Sensing of Environment* 234 (December):111467. https://doi.org/10.1016/j.rse.2019.111467.

Taddeo, Sophie, Iryna Dronova, and Kendall Harris. 2021. "Greenness, Texture, and Spatial Relationships Predict Floristic Diversity across Wetlands of the Conterminous United States." *ISPRS Journal of Photogrammetry and Remote Sensing* 175 (May):236–46. https://doi.org/10.1016/J.ISPRSJPRS.2021.03.012.

Tallowin, J R B. 1996. "Effects of Inorganic Fertilizers on Flower-Rich Hay Meadows: A Review Using a Case Study on the Somerset Levels, UK." In *Grassland and Forage Abstracts*, 66:147–52. CABI International, Wallingford, Oxon (CABI).

Tamburlin, Daniel, Michele Torresani, Enrico Tomelleri, Giustino Tonon, and Duccio Rocchini. 2021. "Testing the Height Variation Hypothesis with the R Rasterdiv Package for Tree Species Diversity Estimation." https://doi.org/10.3390/rs13183569.

Tan, Suiyan, Anders Krogh Mortensen, Xu Ma, Birte Boelt, and René Gislum. 2021. "Assessment of Grass Lodging Using Texture and Canopy Height Distribution Features Derived from UAV Visual-Band Images." *Agricultural and Forest Meteorology* 308–309 (August). https://doi.org/10.1016/j.agrformet.2021.108541.

Tang, Ze, Yangjian Zhang, Nan Cong, Li Wang, Yixuan Zhu, Zhaolei Li, and Guang Zhao. 2021. "Remotely Piloted Aircraft Systems Remote Sensing Can Effectively Retrieve Ecosystem Traits of Alpine Grasslands on the Tibetan Plateau at a Landscape Scale." *Remote Sensing in Ecology and Conservation* 7 (3): 382–96. https://doi.org/10.1002/rse2.196.

Tarantino, Cristina, Francesca Casella, Maria Adamo, Richard Lucas, Carl Beierkuhnlein, and Palma Blonda. 2019. "Ailanthus Altissima Mapping from Multi-Temporal Very High Resolution Satellite Images." *ISPRS Journal of Photogrammetry and Remote Sensing* 147 (January):90–103. https://doi.org/10.1016/J.ISPRSJPRS.2018.11.013.

Tasset, E., T. Boulanger, S. Diquélou, P. Laîné, and S. Lemauviel-Lavenant. 2019. "Plant Trait to Fodder Quality Relationships at Both Species and Community Levels in Wet Grasslands." *Ecological Indicators* 97 (October 2018): 389–97. https://doi.org/10.1016/j.ecolind.2018.10.035.

Taylor, Shawn D., and Dawn M. Browning. 2021. "Multi-Scale Assessment of a Grassland Productivity Model." *Biogeosciences* 18 (6): 2213–20. https://doi.org/10.5194/bg-18-2213-2021.

Théau, Jérôme, Étienne Lauzier-Hudon, Lydiane Aubé, and Nicolas Devillers. 2021. "Estimation of Forage Biomass and Vegetation Cover in Grasslands Using UAV Imagery." *PLoS ONE* 16 (1 January): 1–18. https://doi.org/10.1371/journal.pone.0245784.

Thornley, Rachael H, France F Gerard, Kevin White, and Anne Verhoef. 2023. "Prediction of Grassland Biodiversity Using Measures of Spectral Variance: A Meta-Analytical Review."

Remote Sensing. https://doi.org/10.3390/rs15030668.

Tian, Yuan, and Gang Fu. 2022. "Quantifying Plant Species α-Diversity Using Normalized Difference Vegetation Index and Climate Data in Alpine Grasslands." *Remote Sensing* 14 (19). https://doi.org/10.3390/rs14195007.

Tilman, David, David Wedin, and Johannes Knops. 1996. "Productivity and Sustainability Influenced by Biodiversity in Grassland Ecosystems." *Nature* 379 (6567): 718–20.

Tmušić, Goran, Salvatore Manfreda, Helge Aasen, Mike R. James, Gil Gonçalves, Eyal Ben-Dor, Anna Brook, et al. 2020. "Current Practices in UAS-Based Environmental Monitoring." *Remote Sensing* 12 (6). https://doi.org/10.3390/rs12061001.

Togeiro de Alckmin, Gustavo, Lammert Kooistra, Richard Rawnsley, and Arko Lucieer. 2021. "Comparing Methods to Estimate Perennial Ryegrass Biomass: Canopy Height and Spectral Vegetation Indices." *Precision Agriculture* 22 (1): 205–25. https://doi.org/10.1007/s11119-020-09737-z.

Torresani, Michele, Duccio Rocchini, Ruth Sonnenschein, Marc Zebisch, Heidi C. Hauffe, Michael Heym, Hans Pretzsch, and Giustino Tonon. 2020. "Height Variation Hypothesis: A New Approach for Estimating Forest Species Diversity with CHM LiDAR Data." *Ecological Indicators* 117 (October):106520. https://doi.org/10.1016/J.ECOLIND.2020.106520.

Tucker, Compton J. 1979. "Red and Photographic Infrared Linear Combinations for Monitoring Vegetation." *Remote Sensing of Environment* 8 (2): 127–50. https://doi.org/10.1016/0034-4257(79)90013-0.

Viedma, Olga, Iván Torres, Beatriz Pérez, and José M. Moreno. 2012. "Modeling Plant Species Richness Using Reflectance and Texture Data Derived from QuickBird in a Recently Burned Area of Central Spain." *Remote Sensing of Environment* 119 (April): 208–21. https://doi.org/10.1016/j.rse.2011.12.024.

Viljanen, Niko, Eija Honkavaara, Roope Näsi, Teemu Hakala, Oiva Niemeläinen, and Jere Kaivosoja. 2018. "A Novel Machine Learning Method for Estimating Biomass of Grass Swards Using a Photogrammetric Canopy Height Model, Images and Vegetation Indices Captured by a Drone." *Agriculture (Switzerland)* 8 (5). https://doi.org/10.3390/agriculture8050070.

Villoslada, M., T. F. Bergamo, R. D. Ward, N. G. Burnside, C. B. Joyce, R. G.H. Bunce, and K. Sepp. 2020. "Fine Scale Plant Community Assessment in Coastal Meadows Using UAV Based Multispectral Data." *Ecological Indicators* 111 (November 2019): 105979. https://doi.org/10.1016/j.ecolind.2019.105979.

Villoslada Peciña, M., T. F. Bergamo, R. D. Ward, C. B. Joyce, and K. Sepp. 2021. "A Novel UAV-Based Approach for Biomass Prediction and Grassland Structure Assessment in Coastal Meadows." *Ecological Indicators* 122. https://doi.org/10.1016/j.ecolind.2020.107227.

Viña, Andrés, Anatoly A Gitelson, Donald C Rundquist, Galina Keydan, Bryan Leavitt, and James

Schepers. 2004. “Monitoring Maize (Zea Mays L.) Phenology with Remote Sensing.” *Agronomy Journal* 96 (4): 1139–47. https://doi.org/https://doi.org/10.2134/agronj2004.1139.

Vincini, M, E Frazzi, and P D’Alessio. 2008. “A Broad-Band Leaf Chlorophyll Vegetation Index at the Canopy Scale.” *Precision Agriculture* 9 (5): 303–19. https://doi.org/10.1007/s11119-008-9075-z.

Vogel, Sebastian, Robin Gebbers, Marcel Oertel, and Eckart Kramer. 2019. “Evaluating Soil-Borne Causes of Biomass Variability in Grassland by Remote and Proximal Sensing.” *Sensors (Switzerland)* 19 (20): 1–16. https://doi.org/10.3390/s19204593.

Vooren, Laura Van, Bert Reubens, Steven Broekx, Dirk Reheul, and Kris Verheyen. 2018. “Assessing the Impact of Grassland Management Extensification in Temperate Areas on Multiple Ecosystem Services and Biodiversity.” *Agriculture, Ecosystems & Environment* 267 (November):201–12. https://doi.org/10.1016/J.AGEE.2018.08.016.

Wachendorf, M., T. Fricke, and T. Möckel. 2018. “Remote Sensing as a Tool to Assess Botanical Composition, Structure, Quantity and Quality of Temperate Grasslands.” *Grass and Forage Science* 73 (1): 1–14. https://doi.org/10.1111/gfs.12312.

Wang, Chuyuan, Kevin P. Price, Deon Van Der Merwe, Nan An, and Huan Wang. 2014. “Modeling Above-Ground Biomass in Tallgrass Prairie Using Ultra-High Spatial Resolution SUAS Imagery.” *Photogrammetric Engineering and Remote Sensing* 80 (12): 1151–59. https://doi.org/10.14358/PERS.80.12.1151.

Wang, Dongliang, Xiaoping Xin, Quanqin Shao, Matthew Brolly, Zhiliang Zhu, and Jin Chen. 2017. “Modeling Aboveground Biomass in Hulunber Grassland Ecosystem by Using Unmanned Aerial Vehicle Discrete Lidar.” *Sensors (Switzerland)* 17 (1): 1–19. https://doi.org/10.3390/s17010180.

Wang, Jiyan, Ainong Li, and Jinhu Bian. 2016. “Simulation of the Grazing Effects on Grassland Aboveground Net Primary Production Using DNDC Model Combined with Time-Series Remote Sensing Data-a Case Study in Zoige Plateau, China.” *Remote Sensing* 8 (3). https://doi.org/10.3390/rs8030168.

Wang, Ran, and John A. Gamon. 2019. “Remote Sensing of Terrestrial Plant Biodiversity.” *Remote Sensing of Environment* 231 (September):111218. https://doi.org/10.1016/j.rse.2019.111218.

Wang, Ran, John A. Gamon, Anna K. Schweiger, Jeannine Cavender-Bares, Philip A. Townsend, Arthur I. Zygielbaum, and Shan Kothari. 2018. “Influence of Species Richness, Evenness, and Composition on Optical Diversity: A Simulation Study.” *Remote Sensing of Environment* 211 (September 2017): 218–28. https://doi.org/10.1016/j.rse.2018.04.010.

Wang, Ran, John A Gamon, Rebecca A Montgomery, Philip A Townsend, Arthur I Zygielbaum, Keren Bitan, David Tilman, and Jeannine Cavender-Bares. 2016. “Seasonal Variation in the NDVI-Species Richness Relationship in a Prairie Grassland Experiment (Cedar Creek).” *Remote Sensing* 8 (2). https://doi.org/10.3390/rs8020128.

Wang, Tianhai, Yadong Liu, Minghui Wang, Qing Fan, Hongkun Tian, Xi Qiao, and Yanzhou Li. 2021. “Applications of UAS in Crop Biomass Monitoring: A Review.” *Frontiers in Plant Science* 12 (April): 1–16. https://doi.org/10.3389/fpls.2021.616689.

Wang, Zhihui, Philip A. Townsend, Anna K. Schweiger, John J. Couture, Aditya Singh, Sarah E. Hobbie, and Jeannine Cavender-Bares. 2019. “Mapping Foliar Functional Traits and Their Uncertainties across Three Years in a Grassland Experiment.” *Remote Sensing of Environment* 221 (December 2018): 405–16. https://doi.org/10.1016/j.rse.2018.11.016.

Weiss, M, D Troufleau, F Baret, H Chauki, L Prévot, A Olioso, N Bruguier, and N Brisson. 2001. “Coupling Canopy Functioning and Radiative Transfer Models for Remote Sensing Data Assimilation.” *Agricultural and Forest Meteorology* 108:113–28.

Wengert, Matthias, Jayan Wijesingha, Damian Schulze-Brüninghoff, Michael Wachendorf, and Thomas Astor. 2022. “Multisite and Multitemporal Grassland Yield Estimation Using UAV-Borne Hyperspectral Data.” *Remote Sensing* 14 (9). https://doi.org/10.3390/rs14092068.

Whitcraft, Alyssa K., Eric F. Vermote, Inbal Becker-Reshef, and Christopher O. Justice. 2015. “Cloud Cover throughout the Agricultural Growing Season: Impacts on Passive Optical Earth Observations.” *Remote Sensing of Environment* 156:438–47. https://doi.org/10.1016/j.rse.2014.10.009.

White, R, S Murray, and M Rohweder. 2000. “Grassland Ecosystems. Pilot Analysis of Global Ecosystems.” *World Resources Institute, Washington DC*.

Wijesingha, Jayan, Thomas Moeckel, Frank Hensgen, and Michael Wachendorf. 2019. “Evaluation of 3D Point Cloud-Based Models for the Prediction of Grassland Biomass.” *International Journal of Applied Earth Observation and Geoinformation* 78 (October): 352–59. https://doi.org/10.1016/j.jag.2018.10.006.

Wilke, Norman, Bastian Siegmann, Lasse Klingbeil, Andreas Burkart, Thorsten Kraska, Onno Muller, Anna van Doorn, Sascha Heinemann, and Uwe Rascher. 2019. “Quantifying Lodging Percentage and Lodging Severity Using a UAV-Based Canopy Height Model Combined with an Objective Threshold Approach.” *Remote Sensing* 11 (5). https://doi.org/10.3390/rs11050515.

Willkomm, M., A. Bolten, and G. Bareth. 2016. “Non-Destructive Monitoring of Rice by Hyperspectral in-Field Spectrometry and UAV-Based Remote Sensing: Case Study of Field-Grown Rice in North Rhine-Westphalia, Germany.” *International Archives of the Photogrammetry, Remote Sensing and Spatial Information Sciences - ISPRS Archives* 2016-Janua (July): 1071–77. https://doi.org/10.5194/isprsarchives-XLI-B1-1071-2016.

Wilmanns, O. 1989. “Ökologische Pflanzensoziologie. Uni-Taschenbücher, 269. 4. Aufl., 378 S., 45 Abb., 17 Tab., 31 Tabell. Übersichten. Quelle Und Meyer Verlag, Heidelberg, Wiesbaden, 1989. ISBN 3-494-02168-6.” *Feddes Repertorium* 103 (1–2): 142. https://doi.org/https://doi.org/10.1002/fedr.19921030123.

Wood, Eric M., Anna M. Pidgeon, Volker C. Radeloff, and Nicholas S. Keuler. 2012. “Image Texture as a Remotely Sensed Measure of Vegetation Structure.” *Remote Sensing of Environment* 121:516–26. https://doi.org/10.1016/j.rse.2012.01.003.

Wu, Liji, Huasong Chen, Dima Chen, Shaopeng Wang, Ying Wu, Bing Wang, Shengen Liu, Linyan Yue, Jie Yu, and Yongfei Bai. 2023. “Soil Biota Diversity and Plant Diversity Both Contributed to Ecosystem Stability in Grasslands.” *Ecology Letters* 26 (6): 858–68. https://doi.org/10.1111/ele.14202.

Xu, Kexin, Yanjun Su, Jin Liu, Tianyu Hu, Shichao Jin, Qin Ma, Qiuping Zhai, et al. 2020. “Estimation of Degraded Grassland Aboveground Biomass Using Machine Learning Methods from Terrestrial Laser Scanning Data.” *Ecological Indicators* 108 (January):105747. https://doi.org/10.1016/j.ecolind.2019.105747.

Xue, Beibei, Bo Ming, Jiangfeng Xin, Hongye Yang, Shang Gao, Huirong Guo, Dayun Feng, Chenwei Nie, Keru Wang, and Shaokun Li. 2023. “Radiometric Correction of Multispectral Field Images Captured under Changing Ambient Light Conditions and Applications in Crop Monitoring” 7:223. https://doi.org/10.3390/drones7040223.

Xue, Jinru, and Baofeng Su. 2017. “Significant Remote Sensing Vegetation Indices: A Review of Developments and Applications.” *Journal of Sensors*. https://doi.org/10.1155/2017/1353691.

Yang, Chenghai, James H. Everitt, Joe M. Bradford, and Dale Murden. 2004. “Airborne Hyperspectral Imagery and Yield Monitor Data for Mapping Cotton Yield Variability.” *Precision Agriculture* 5 (5): 445–61. https://doi.org/10.1007/s11119-004-5319-8.

Yang, Xiaohui. 2013. *Assessing Responses of Grasslands to Grazing Management Using Remote Sensing Approaches.* Library and Archives Canada = Bibliothèque et Archives Canada.

Yang, Xiuchun, Bin Xu, Yunxiang Jin, Jinya Li, and Xiaohua Zhu. 2012. “On Grass Yield Remote Sensing Estimation Models of China’s Northern Farming-Pastoral Ecotone.” *Advances in Intelligent and Soft Computing* 141 (January):281–91. https://doi.org/10.1007/978-3-642-27957-7_35.

Yang, Zhengwei, Patrick Willis, and Rick Mueller. 2008. “Impact of Band-Ratio Enhanced AWIFS Image on Crop Classification Accuracy.” *Proceedings of the 17th William Pecora Memorial Remote Sensing Symposium*.

Younes, Nicolas, Karen E. Joyce, and Stefan W. Maier. 2021. “All Models of Satellite-Derived Phenology Are Wrong, but Some Are Useful: A Case Study from Northern Australia.” *International Journal of Applied Earth Observation and Geoinformation* 97 (May):102285. https://doi.org/10.1016/J.JAG.2020.102285.

Yue, Jibo, Guijun Yang, Qingjiu Tian, Haikuan Feng, Kaijian Xu, and Chengquan Zhou. 2019. “Estimate of Winter-Wheat above-Ground Biomass Based on UAV Ultrahigh-Ground-Resolution Image Textures and Vegetation Indices.” *ISPRS Journal of Photogrammetry and Remote Sensing* 150 (April):226–44. https://doi.org/10.1016/J.ISPRSJPRS.2019.02.022.

Zeng, Na, Xiaoli Ren, Honglin He, Li Zhang, Pan Li, and Zhongen Niu. 2021. “Estimating the Grassland Aboveground Biomass in the Three-River Headwater Region of China Using Machine Learning and Bayesian Model Averaging.” *Environmental Research Letters* 16 (11). https://doi.org/10.1088/1748-9326/ac2e85.

Zeng, Na, Xiaoli Ren, Honglin He, Li Zhang, Dan Zhao, Rong Ge, Pan Li, and Zhongen Niu. 2019. “Estimating Grassland Aboveground Biomass on the Tibetan Plateau Using a Random Forest Algorithm.” *Ecological Indicators* 102 (July):479–87. https://doi.org/10.1016/J.ECOLIND.2019.02.023.

Zhang, Ce, Peter M. Atkinson, Charles George, Zhaofei Wen, Mauricio Diazgranados, and France Gerard. 2020. “Identifying and Mapping Individual Plants in a Highly Diverse High-Elevation Ecosystem Using UAV Imagery and Deep Learning.” *ISPRS Journal of Photogrammetry and Remote Sensing* 169 (November):280–91. https://doi.org/10.1016/j.isprsjprs.2020.09.025.

Zhang, Gan, Haifeng Yan, Dongyan Zhang, Huihui Zhang, Tao Cheng, Gensheng Hu, Shuhao Shen, and Haifeng Xu. 2023. “Enhancing Model Performance in Detecting Lodging Areas in Wheat Fields Using UAV RGB Imagery: Considering Spatial and Temporal Variations.” *Computers and Electronics in Agriculture* 214 (October): 108297. https://doi.org/10.1016/j.compag.2023.108297.

Zhang, Huifang, Yi Sun, Li Chang, Yu Qin, Jianjun Chen, Yan Qin, Jiaxing Du, Shuhua Yi, and Yingli Wang. 2018. “Estimation of Grassland Canopy Height and Aboveground Biomass at the Quadrat Scale Using Unmanned Aerial Vehicle.” *Remote Sensing* 10 (6). https://doi.org/10.3390/rs10060851.

Zhang, Huifang, Zhonggang Tang, Binyao Wang, Baoping Meng, Yu Qin, Yi Sun, Yanyan lv, Jianguo Zhang, and Shuhua Yi. 2022. “A Non-Destructive Method for Rapid Acquisition of Grassland Aboveground Biomass for Satellite Ground Verification Using UAV RGB Images.” *Global Ecology and Conservation* 33 (June 2021): e01999. https://doi.org/10.1016/j.gecco.2022.e01999.

Zhang, Xiang, Yuhai Bao, Dongliang Wang, Xiaoping Xin, Lei Ding, Dawei Xu, Lulu Hou, and Jie Shen. 2021. “Using Uav Lidar to Extract Vegetation Parameters of Inner Mongolian Grassland.” *Remote Sensing* 13 (4): 1–18. https://doi.org/10.3390/rs13040656.

Zhao, Fen, Bin Xu, Xiuchun Yang, Yunxiang Jin, Jinya Li, Lang Xia, Shi Chen, and Hailong Ma. 2014. “Remote Sensing Estimates of Grassland Aboveground Biomass Based on MODIS Net Primary Productivity (NPP): A Case Study in the Xilingol Grassland of Northern China.” *Remote Sensing* 6 (6): 5368–86. https://doi.org/10.3390/rs6065368.

Zhao, Xiaoxia, Yanjun Su, Tianyu Hu, Mengqi Cao, Xiaoqiang Liu, Qiuli Yang, Hongcan Guan, Lingli Liu, and Qinghua Guo. 2022. “Analysis of UAV Lidar Information Loss and Its Influence on the Estimation Accuracy of Structural and Functional Traits in a Meadow Steppe.” *Ecological Indicators* 135:108515. https://doi.org/10.1016/j.ecolind.2021.108515.

Zhao, Yonggan, Huancheng Pang, Jing Wang, Long Huo, and Yuyi Li. 2014. “Effects of Straw

Mulch and Buried Straw on Soil Moisture and Salinity in Relation to Sunflower Growth and Yield." *Field Crops Research* 161 (May): 16–25. https://doi.org/10.1016/j.fcr.2014.02.006.

Zhao, Yuanyuan, Zhifeng Liu, and Jianguo Wu. 2020. "Grassland Ecosystem Services: A Systematic Review of Research Advances and Future Directions." *Landscape Ecology* 35 (4): 793–814. https://doi.org/10.1007/s10980-020-00980-3.

Zhao, Yujin, Yihan Sun, Xiaoming Lu, Xuezhen Zhao, Long Yang, Zhongyu Sun, and Yongfei Bai. 2021. "Hyperspectral Retrieval of Leaf Physiological Traits and Their Links to Ecosystem Productivity in Grassland Monocultures." *Ecological Indicators* 122:107267. https://doi.org/10.1016/j.ecolind.2020.107267.

Zlinszky, András, Anke Schroiff, Adam Kania, Balázs Deák, Werner Mücke, Ágnes Vári, Balázs Székely, and Norbert Pfeifer. 2014. "Categorizing Grassland Vegetation with Full-Waveform Airborne Laser Scanning: A Feasibility Study for Detecting Natura 2000 Habitat Types." *Remote Sensing* 6 (9): 8056–87. https://doi.org/10.3390/rs6098056.

Appendix A. Supplementary material from article "A Review of Estimation Methods for Aboveground Biomass in Grasslands Using UAV"

Table A1. Studies using UAV data to estimate grassland above ground biomass (AGB).

No.	Title	Ref	Year	Journal	Main Objective
1	Modeling above-ground biomass in tallgrass prairie using ultra-high spatial resolution sUAS imagery	(Wang *et al.*, 2014)	2014	*Photogrammetric Engineering & Remote Sensing*	To examine relationship between herbaceous AGB for the tallgrass prairie and its biophysical parameters derived from ultra-high-spatial-resolution imagery.
2	Estimating plant traits of grasslands from UAV-acquired hyperspectral images: a comparison of statistical approaches.	(Capolupo *et al.*, 2015)	2015	*International Journal of Geo-Information*	To investigate the utility of hyperspectral images acquired from UAV for predicting vegetation traits in grasslands considering the plant phenology and fertilization on spectral data.
3	Mapping Herbage Biomass on a Hill Pasture using a Digital Camera with an Unmanned Aerial Vehicle System	(Lee *et al.*, 2015)	2015	*Journal of The Korean Society of Grassland and Forage Science*	To develop a simple and cost-effective low-altitude aerial platform system with a commercial digital camera on an UAV system to collect images and estimate the herbage biomass using statistical analyses.
4	Ultra-fine grain landscape-scale quantification of dryland vegetation structure with drone-acquired structure-from-motion photogrammetry	(Cunliffe, Brazier and Anderson, 2016)	2016	*Remote Sensing of Environment*	To develop a new technique to quantify biomass and associated carbon stocks in heterogeneous and dynamic short sward semi-arid rangelands.
5	Hyperspectral aerial imaging for grassland yield estimation	(Geipel and Korsaeth, 2017)	2017	*Advances in Animal Biosciences*	To investigate the potential of UAV imaging spectroscopy for in-season grassland yield estimation.
6	Modeling Aboveground Biomass in Hulunber Grassland Ecosystem by Using Unmanned Aerial Vehicle Discrete Lidar	(Wang *et al.*, 2017)	2017	*Sensors*	To investigate if the canopy height, fraction cover, and aboveground biomass can be derived using models established from UAV-based discrete LIDAR data with desirable accuracy at quadrat and subplot scales.
7	Low-cost visible and near-infrared camera on an unmanned aerial vehicle for assessing the herbage biomass and leaf area index in an Italian ryegrass field	(Fan *et al.*, 2018)	2018	*Grassland Sciences*	To demonstrate the use of a UAV system equipped with a low-cost visible and near-infrared (V-NIR) camera to assess the spatial variability in herbage biomass and LAI in an Italian ryegrass field.
8	Estimating biomass and nitrogen amount of barley and grass	(Näsi *et al.*, 2018)	2018	*Remote Sensing*	To develop and assess a methodology for crop biomass and nitrogen estimation, integrating spectral and 3D features that can

	using UAV and aircraft based spectral and photogrammetric				be extracted using airborne miniaturized multispectral, hyperspectral, and color (RGB) cameras.
9	A novel machine learning method for estimating biomass of grass swards using a photogrammetric canopy height model, images and vegetation indices captured by a drone.	(Viljanen *et al.*, 2018)	2018	*Agriculture*	To develop and assess a novel machine learning technique for the estimation of canopy height and biomass of grass swards utilizing multispectral photogrammetric camera data.
10	Estimation of Grassland Canopy Height and Aboveground Biomass at the Quadrat Scale Using Unmanned Aerial Vehicle	(Zhang *et al.*, 2018)	2018	*Remote Sensing*	To develop a novel method for estimating the quadrat-scale aboveground biomass of low-statute vegetation.
11	Evaluation of grass quality under different soil management scenarios using remote sensing techniques.	(Askari *et al.*, 2019)	2019	*Remote Sensing*	To evaluate the efficiency of hyperspectral and multispectral (UAV and satellite) remote sensing techniques for predicting and mapping grass biomass and crude protein under conventional grassland management in a temperate maritime climate.
12	Estimating pasture biomass and canopy height in Brazilian savanna using UAV photogrammetry.	(Batistoti *et al.*, 2019)	2019	*Remote Sensing*	To estimate the canopy height using UAV photogrammetry and to propose an equation for the estimation of biomass of Brazilian savanna (Cerrado) pastures based on UAV canopy height.
13	Canopy height measurements and non-destructive biomass estimation of *Lolium perenne* swards using UAV imagery.	(Borra-Serrano *et al.*, 2019)	2019	*Grass and Forage Science*	To develop a methodology for monitoring the spatial and temporal dynamics of biomass accumulation of perennial ryegrass plots throughout the growing season in an affordable, easy-to-use, reliable, and non-destructive way using an RGB camera mounted on a UAV.
14	Biomass Prediction of Heterogeneous Temperate Grasslands Using an SfM Approach Based on UAV Imaging	(Grüner, Astor and Wachendorf, 2019)	2019	*Agronomy*	To develop of prediction models for dry matter yield in temperate grassland based on canopy height data generated by UAV RGB imaging over a whole growing season including four cuts.
15	Estimation of spatial and temporal variability of pasture growth and digestibility in grazing rotations coupling unmanned aerial vehicle (UAV) with crop simulation models	(Insua, Utsumi and Basso, 2019)	2019	*PLOS One*	To monitor, assess and manage changes in pasture growth, morphology, and digestibility by integrating information from an UAV and two process-based models.
16	Estimating biomass in temperate grassland with high resolution canopy surface models from	(Lussem *et*	2019	*Journal of Applied Remote Sensing*	To evaluate the potential of low-cost UAV-based canopy surface models to monitor sward height as an indicator of grassland

	UAV-based RGB images and vegetation indices	*al.*, 2019)			biomass and compare with established methods for biomass monitoring.
17	Mapping and monitoring of biomass and grazing in pasture with an unmanned aerial system	(Michez *et al.*, 2019)	2019	*Remote Sensing*	To evaluate the potential of UAV as a tool for the characterization of pasture 3D structure (sward height) and aboveground biomass at a very fine spatial scale.
18	Comparing UAV-Based Technologies and RGB-D Reconstruction Methods for Plant Height and Biomass Monitoring on Grass Ley	(Rueda-Ayala *et al.*, 2019)	2019	*Sensors*	To evaluate aerial and on-ground methods to characterize grass ley fields, composed of different species mixtures and estimate plant height, biomass and volume, using digital grass models, and avoiding the unnecessary destruction of the swards.
19	Evaluating soil-borne causes of biomass variability in grassland by remote and proximal sensing		2019	*Sensors*	To investigate the relationship between soil characteristics and biomass production to identify high- and low-yielding regions within the field and their possible soil-borne causes.
20	Evaluation of 3D point cloud-based models for the prediction of grassland biomass	(Wijesingha *et al.*, 2019)	2019	*International Journal of Applied Earth Observation and Geoinformation*	To evaluate 3D point clouds derived from a terrestrial laser scanner (TLS) and an UAV-borne SfM approach for grassland biomass estimation over three grasslands with different composition and management practice in northern Hesse, Germany.
21	Estimating Plant Pasture Biomass and Quality from UAV Imaging across Queensland's Rangelands	(Barnetson, Phinn and Scarth, 2020)	2020	*AgriEngineering*	To demonstrate the use of UAV hyperspectral remote sensing to detect both crude protein and acid detergent fiber in a range of native pastures across the rangelands of Queensland, Australia.
22	Deep learning applied to phenotyping of biomass in forages with UAV-based RGB imagery	(Castro *et al.*, 2020)	2020	*Sensors*	To propose a deep learning approach to estimate biomass in forage breeding programs and pasture fields using only UAV-RGB imagery and AlexNet and ResNet deep learning architectures.
23	A Pilot Study to Estimate Forage Mass from Unmanned Aerial Vehicles in a Semi-Arid Rangeland	(DiMaggio *et al.*, 2020)	2020	*Remote Sensing*	To develop a method to estimate forage mass in rangelands using high-resolution imagery derived from the UAV using a South Texas pasture as a pilot site.
24	Development and validation of a phenotyping computational workflow to predict the biomass yield of a large perennial ryegrass breeding field trial	(Gebremedhin *et al.*, 2020)	2020	*Frontiers in Plant Science*	To validate a computational phenotyping workflow for image acquisition, processing, and analysis of spaced-planted perennial ryegrass to estimate the biomass yield of 48,000 individual plants through NDVI and plant height data extraction.
25	The potential of UAV-borne spectral and textural information for predicting aboveground biomass and N fixation in legume-grass mixtures	(Grüner, Wachendorf and	2020	*PLOS One*	To develop harvestable biomass and aboveground nitrogen fixation estimation models from UAV multispectral imaging of legume–grass mixtures with varying legume proportions (0–100%).

		Astor, 2020)			
26	Comparison of Spectral Reflectance-Based Smart Farming Tools and a Conventional Approach to Determine Herbage Mass and Grass Quality on Farm	(Hart *et al.*, 2020)	2020	*Remote Sensing*	To evaluate two spectral reflectance-based smart farming tools for determining herbage mass and quality of multi-species grasslands—a portable NIRS and a model to analyze multispectral imagery.
27	Investigating the potential of a newly developed UAV-based VNIR/SWIR imaging system for forage mass monitoring	(Jenal *et al.*, 2020)	2020	*Journal of Photogrammetry, Remote Sensing and Geoinformation Science*	To investigate the potential of a multi-camera system with a novel approach to extend spectral sensitivity from visible-to-near-infrared (VNIR) to short-wave infrared (SWIR) (400–1700 nm) for estimating forage mass from an aerial carrier platform.
28	The fusion of spectral and structural datasets derived from an airborne multispectral sensor for estimation of pasture dry matter yield at paddock scale with time	(Karunaratne *et al.*, 2020)	2020	*Remote Sensing*	To develop empirical pasture dry matter (DM) yield prediction models using an UAV-borne sensor at four flying altitudes.
29	High-throughput switchgrass phenotyping and biomass modeling by UAV	(Li *et al.*, 2020)	2020	*Frontiers in Plant Science*	To exploit UAV-based imagery (LiDAR and multispectral approaches) to measure plant height, perimeter, and biomass yield in field-grown switchgrass in order to make predictions of bioenergy traits.
30	Monitoring Forage Mass with Low-Cost UAV Data: Case Study at the Rengen Grassland Experiment	(Lussem, Schellberg and Bareth, 2020)	2020	*Journal of Photogrammetry, Remote Sensing and Geoinformation Science*	To investigate the potential of sward height metrics derived from low-cost UAV image data to predict forage yield.
31	Can Low-Cost Unmanned Aerial Systems Describe the Forage Quality Heterogeneity? Insight from a Timothy Pasture Case Study in Southern Belgium	(Michez *et al.*, 2020)	2020	*Remote Sensing*	To investigate the potential of off-the-shelf UAS systems in modeling essential parameters of pasture productivity in a precision livestock context: sward height, biomass, and forage quality.
32	Machine learning estimators for the quantity and quality of grass swards used for silage production using drone-based imaging spectrometry and photogrammetry	(Oliveira *et al.*, 2020)	2020	*Remote Sensing of Environment*	To develop and assess a machine learning technique for the estimation of the quantity and quality of grass swards based on drone spectral imaging and photogrammetry.
33	An efficient method for estimating dormant season grass biomass in tallgrass prairie from ultra-high spatial resolution aerial imaging produced with	(Van Der Merwe, Baldwin	2020	*International Journal of Wildland Fire*	To investigate the viability UAV image data to estimate dormant season grassland biomass, based on the assumption that grassland canopy height correlates with grassland biomass.

	small unmanned aircraft systems.	and Boyer, 2020)			
34	Fine scale plant community assessment in coastal meadows using UAV based multispectral data	(Villoslada *et al.*, 2020)	2020	*Ecological Indicators*	To assess the potential of UAVs and multispectral cameras for classifying and fine-scale mapping of plant communities in coastal meadows.
35	Using multispectral data from an unmanned aerial system to estimate pasture depletion during grazing	(Alvarez-Hess *et al.*, 2021)	2021	*Animal Feed Science and Technology*	To develop and validate empirical models to estimate pasture depletion in paddocks while cattle are grazing using an UAV-borne multispectral sensor with rising plate meter measurements as the reference data.
36	Monitoring ecological characteristics of a tallgrass prairie using an unmanned aerial vehicle	(Blackburn *et al.*, 2021)	2021	*Restoration Ecology*	To evaluate the potential applications of UAV derived data within restored tallgrass prairies using an affordable sensor and UAV.
37	Predicting pasture biomass using a statistical model and machine learning algorithm implemented with remotely sensed imagery	(De Rosa *et al.*, 2021)	2021	*Computers and Electronics in Agriculture*	To test the performance of an integrated method combining remote sensing imagery acquired with a multispectral camera mounted on an UAV, statistical models, and machine learning algorithms implemented with publicly available data to predict future pasture biomass loads.
38	Forage yield and quality estimation by means of UAV and hyperspectral imaging	(Geipel *et al.*, 2021)	2021	*Precision Agriculture*	To investigate the potential of in-season airborne hyperspectral imaging for the calibration of robust forage yield and quality estimation models.
39	Prediction of Biomass and N Fixation of Legume–Grass Mixtures Using Sensor Fusion	(Grüner, Astor and Wachendorf, 2021)	2021	*Frontiers in Plant Science*	To develop a multi-temporal estimation model for aboveground biomass and nitrogen fixation of two legume–grass mixtures.
40	The Application of an Unmanned Aerial System and Machine Learning Techniques for Red Clover-Grass Mixture Yield Estimation Under Variety Performance Trials	(K. Y. Li *et al.*, 2021)	2021	*Remote Sensing*	To present a rapid, non-destructive, low-cost framework for field-based red-clover DM yield modeling.
41	A novel UAV-based approach for biomass prediction and grassland structure assessment in coastal meadows	(Villoslada Peciña *et al.*, 2021)	2021	*Ecological Indicators*	To compare two temporal pre-harvest dry matter prediction capabilities under one- and two-year clover–grass cultivation fields with three different treatments and compare the performance of three machine learning algorithms and their corresponding variable importance rankings in estimating clover–grass mixture dry matter.

42	UAV Multispectral Imaging Potential to Monitor and Predict Agronomic Characteristics of Different Forage Associations	(Plaza *et al.*, 2021)	2021	*Agronomy*	To show a first screening of the potential of airborne multispectral images captured with UAVs for the monitoring and prediction of several in situ agronomic parameters of different forage associations by exploring the relationships between a few spectral indices UAV-based and simultaneous field measurements over several fields of forage associations.
43	Improving Accuracy of Herbage Yield Predictions in Perennial Ryegrass with UAV-Based Structural and Spectral Data Fusion and Machine Learning	(Pranga *et al.*, 2021)	2021	*Remote Sensing*	To examine the potential of UAV-based structural and spectral features and their combination in herbage yield predictions across diploid and tetraploid varieties and breeding populations of perennial ryegrass.
44	Effects of plateau pikas' foraging and burrowing activities on vegetation biomass and soil organic carbon of alpine grasslands	(Qin *et al.*, 2021)	2021	*Plant and Soil*	To quantitatively assess the foraging and burrowing effects of plateau pikas on vegetation biomass and soil organic carbon at plot scale.
45	Estimating dry biomass and plant nitrogen concentration in pre-Alpine grasslands with low-cost UAS-borne multispectral data–a comparison of sensors, algorithms, and predictor sets.	(Schucknecht *et al.*, 2022)	2021	*Biogeosciences Discussions*	To investigate the potential of low-cost UAS-based multispectral sensors for estimating aboveground biomass (dry matter) and plant community nitrogen concentration of managed pre-alpine grasslands.
46	Remote sensing data fusion as a tool for biomass prediction in extensive grasslands invaded by *L. polyphyllus*	(Schulze-Brüninghoff, Wachendorf and Astor, 2021)	2021	*Remote Sensing in Ecology and Conservation*	To develop prediction models from sensor data fusion for fresh and dry matter yield in extensively managed grasslands with variable degrees of invasion by *Lupinus polyphyllus*.
47	Improved Estimation of Aboveground Biomass of Disturbed Grassland through Including Bare Ground and Grazing Intensity	(Shi *et al.*, 2021)	2021	*Remote Sensing*	To estimate alpine meadow AGB from multi-temporal drone images at a micro-scale and improve estimation accuracy in relation to two types of external disturbances (mowing-simulated grazing and rodents).
48	Biomass estimation of pasture plots with multitemporal UAV-based photogrammetric surveys	(Sinde-González *et al.*, 2021)	2021	*International Journal of Applied Earth Observation and Geoinformation*	To investigate the use of multitemporal UAV-based imagery and SfM photogrammetry to estimate the AGB of pastures at a fine spatial scale.
49	Remotely piloted aircraft systems remote sensing can effectively retrieve ecosystem	(Tang *et al.*, 2021)	2021	*Remote Sensing in Ecology and Conservation*	To propose a framework for monitoring ecosystem traits by UAV visible remote sensing, verify the feasibility in monitoring

	traits of alpine grasslands on the Tibetan Plateau at a landscape scale				ecosystem traits, quantify the contribution of each band in prediction, validate the prediction model, and generate high-spatial-resolution maps of ecosystem traits.
50	Estimation of forage biomass and vegetation cover in grasslands using UAV imagery	(Théau *et al.*, 2021)	2021	*PLOS One*	To test and compare three approaches based on multispectral imagery acquired by UAV to estimate forage biomass or vegetation cover in grasslands.
51	Using UAV LiDAR to Extract Vegetation Parameters of Inner Mongolian Grassland	(Zhang *et al.*, 2021)	2021	*Remote Sensing*	To investigate the ability of Riegl VUX-1 to model the AGB at a 0.1 m pixel resolution in the Hulun Buir grazing platform under different grazing intensities.
52	Hyperspectral retrieval of leaf physiological traits and their links to ecosystem productivity in grassland monocultures.	(Zhao *et al.*, 2021)	2021	*Ecological Indicators*	To evaluate the remotely sensed retrieval of plant physiological traits and test the links between the intra- and inter-species trait variations and ecosystem productivity based on a grassland monoculture experiment.
53	A non-destructive method for rapid acquisition of grassland aboveground biomass for satellite ground verification using UAV RGB images	(Zhang *et al.*, 2022)	2022	*Global Ecology and Conservation*	To develop and assess the vertical and horizontal indices from UAV RGB images as predictors of grassland AGB at quadrat scale using the RF machine learning technique and verify whether the indices and methods are suitable for different grassland ecosystems over a large region.
54	Analysis of UAV LIDAR information loss and its influence on the estimation accuracy of structural and functional traits in a meadow steppe	(Zhao *et al.*, 2022)	2022	*Ecological Indicators*	To investigate how UAV LIDAR information loss may occur and how it may influence the estimation accuracy of grassland structural and functional traits by comparing it with terrestrial laser scanning (TLS) and field measurements in a meadow steppe of northern China.
55	Estimation of aboveground biomass production using an unmanned aerial vehicle (UAV) and VENμS satellite imagery in Mediterranean and semiarid rangelands	(Adar *et al.*, 2022)	2022	*Remote Sensing Applications: Society and Environment*	To develop a synergistic UAV and satellite imagery method to estimate AGB by integrating high-resolution UAV data with moderate resolution satellite data, and to assess AGB under different grazing pressures.
56	Beyond trees: Mapping total aboveground biomass density in the Brazilian savanna using high-density UAV-LiDAR data	(da Costa *et al.*, 2021)	2022	*Forest Ecology and Management*	To assess the ability of high-density UAV-LiDAR to estimate and map AGB across the structurally complex vegetation formations of the Cerrado in Brazil.
57	Quantification of Grassland Biomass and Nitrogen Content through UAV Hyperspectral Imagery—Active Sample Selection for Model Transfer	(Franceschini *et al.*, 2022)	2022	*Drones*	To evaluate the use of UAV hyperspectral imagery for the quantification of forage yield and nitrogen nutrition status and implement and validate a supervised approach for model transfer.
58	Estimating Grass Sward Quality and Quantity Parameters Using Drone Remote Sensing with Deep Neural Network	(Karila *et al.*, 2022)	2022	*Remote Sensing*	To investigate the potential of novel neural network architectures for measuring the quality and quantity parameters of silage grass swards, using drone RGB and

					hyperspectral images, and compare the results with the random forest (RF) method and handcrafted features.
59	Herbage Mass, N Concentration, and N Uptake of Temperate Grasslands Can Adequately Be Estimated from UAV-Based Image Data Using Machine Learning	(Lussem *et al.*, 2022)	2022	*Remote Sensing*	To estimate aboveground dry matter yield (DMY), nitrogen concentration (N%), and uptake (Nup) of temperate grasslands from UAV-based image data using machine learning (ML) algorithms.
60	Silage Grass Sward Nitrogen Concentration and Dry Matter Yield Estimation Using Deep Regression and RGB Images Captured by UAV	(Alves Oliveira *et al.*, 2022)	2022	*Agronomy*	To assess the suitability of CNN-based approaches by comparing different deep regression network architectures and optimizers to estimate grass sward nitrogen concentration (N) and dry matter yield (DMY) using RGB images collected from a drone.
61	Nitrogen variability assessment of pasture fields under an integrated crop-livestock system using UAV, PlanetScope, and Sentinel-2 data	(Pereira *et al.*, 2022)	2022	*Computers and Electronics in Agriculture*	To evaluate the spatial distribution of N in pasture fields cultivated under an integrated crop–livestock system (ICLS) using unmanned aerial vehicle (UAV) and satellite data.
62	Effects of disturbances on aboveground biomass of alpine meadow in the Yellow River Source Zone, Western China	(Shi *et al.*, 2022)	2022	*Ecology and Evolution*	To quantify the singular and combined effects of artificial grazing and pika disturbance severities on AGB and its changes in an alpine grassland on the Qinghai–Tibet Plateau, assessing the relative importance of both disturbances.
63	UAV-based prediction of ryegrass dry matter yield	(Shorten and Trolove, 2022)	2022	*International Journal of Remote Sensing*	To determine the accuracy of UAV-based prediction of percentage cover, vegetation volume, and DM yield in autumn from ryegrass sub-plots and compared to the current manual practice of harvesting, drying, and weighing.
64	Multisite and Multitemporal Grassland Yield Estimation Using UAV-Borne Hyperspectral Data	(Wengert *et al.*, 2022)	2022	*Remote Sensing*	To develop and evaluate UAV-based models with the goal of forage yield estimation of eight grassland habitats along a gradient of management intensities.

Table A2. A summary of data field collection from papers assessed in the review.

Reference	Local	Type of Field	Type of Grassland	Number of Sites	UAV Platform	Sensors	Flight Altitude (m)	Overlap, Side Overlap (%)	GCP	GSD (cm/Pixel)	Frequency of Data Collection	Biomass Ground Truth Data	Total Number of Biomass Samples	Biomass Sample Size (m^2)	Canopy Height Measurement
(Alvarez-Hess et al., 2021)	Australia	Grassland Farm	Mono	2	Quadcopter	MS	50	80/80	10	n/a	2 collections in one year	RPM calibration	529	n/a	RPM
(Adar et al., 2022)	Israel	Natural Grassland	Mixed	2	Quadcopter	RGB	n/a	80/80	15 to 20	n/a	5 collections between April 2018 and April 2020	Not specified	600	0.25	n/a
(Askari et al., 2019)	Ireland	Experimental Site	Mixed	1	Rotary	MS	30 and 120	75/75	n/a	2.86 and 11.29	6 collections in 2017, 2 collections in 2018	Mechanical	126	n/a	n/a
(Barnetson, Phinn and Scarth, 2020)	Australia	Natural Grassland	Mixed	19	Hexacopter	RGB and HS	50	85/85	n/a	1	5 collections 2019 and 1 collection in 2020	Mechanical	n/a	0.25	Electronic RPM
(Batistoti et al., 2019)	Brazil	Experimental Site	Mono	1	Quadcopter	RGB	50	80/60	5	1.55	7 collections in 2017 and 8 collections in 2018	Not specified	66	n/a	Ruler
(Blackburn et al., 2021)	USA	Natural Grassland	Mixed	19	Fixed-wing	MS	122	80/75	n/a	n/a	1 collection in 2017	Manual	190	0.01	n/a
(Borra-Serrano et al., 2019)	Belgium	Experimental Site	Mono	1	Dodeca-copter	RGB	30	80/80	35	0.6	22 collections in one year	n/a	154	1.05	RPM
(Capolupo et al., 2015)	Germany	Experimental Site	Mono	1	Octocopter	HS	70	n/a	n/a	2	2 collections in one year	Mechanical	120	12	RPM
(Castro et al., 2020)	Brazil	Experimental Site	Mono	1	Quadcopter	RGB	18	81/61	n/a	0.5	1 collection in 2019	Mechanical	330	4.5	n/a
(Cunliffe, Brazier and Anderson, 2016)	USA	Natural Grassland	Mixed	7	Hexacopter	RGB	15–20	70/65	10 to 18	0.4 to 0.7	1 collection in 2014	Not specified	n/a	1	n/a
(da Costa et al., 2021)	Brazil	Natural Grassland	Mixed	1	Hexacopter	LiDAR	100	n/a	n/a	n/a	1 collection in 2019	Manual	20	1	n/a
(De Rosa et al., 2021)	Australia	Grassland Farm	n/a	2	Quadcopter	MS	80	n/a	n/a	5	n/a	RPM calibration	504	n/a	n/a
(DiMaggio et al., 2020)	USA	Natural Grassland	Mixed	1	Quadcopter	RGB	30, 40, and 50	80/80	6	2.5	1 collection in 2018	Manual	20	0.25	n/a

(Fan et al., 2018)	Japan	Experimental Site	Mono	1	Quadcopter	MS	100	50/50	13	2	1 collection in 2016	Not specified	36	0.25	Not specified
(Franceschini et al., 2022)	Germany	Experimental Site	Mono	1	Octocopter	RGB and HS	30	n/	4 to 8	RGB = 0.8 and 1.5; Hyper = 7.8 and 15.6	2 collections in 2014 and 3 in 2017	Not specified	245	n/a	n/a
(Gebremedhin et al., 2020)	Australia	Experimental Site	Mono	1	Quadcopter	MS	20	75/75	9	2	3 collections in 2018	Manual and mechanical	480 individual plants for calibration and 500 plots for validation	n/a	Ground-based platform (PhenoRover)
(Geipel and Korsaeth, 2017)	Norway	Experimental Site	Mono and Mixed	1	Octocopter	HS	50	n/a	n/a	n/a	3 collections in 2016	Manual and mechanical	120	n/a	n/a
(Geipel et al., 2021)	Norway	Experimental Site	Mixed	2	Octocopter	HS	50	80/60	n/a	n/a	3 collections in 2016 and 3 collections in 2017	Mechanical	707	~ 9	n/a
(Grüner, Astor and Wachendorf, 2019)	Germany	Experimental Site	Mixed	1	Quadcopter	RGB	20	80/80	7	0.07 to 0.08	4 collections in 2017	Manual	192	0.25	Ruler
(Grüner, Wachendorf and Astor, 2020)	Germany	Experimental Site	Mixed	1	Quadcopter	MS and RGB	20 and 50	100/100	8	2 and 4	3 collections in 2018	Manual	144	0.25	n/a
(Grüner, Astor and Wachendorf, 2021)	Germany	Experimental Site	Mixed	1	Quadcopter	MS and RGB	n/a	n/a	7	n/a	3 collections in 2018 and § collections in 2019	Not specified	140	0.25	n/a
(Hart et al., 2020)	Switzerland	Grassland Farm	Mixed	6	Quadcopter	MS	50	80/80	8	5	4 collections in 2018	Mechanical	162	6.5 and 1	n/a
(Insua, Utsumi and Basso, 2019)	USA	Grassland Farm	Mixed	2	Quadcopter	MS and LiDAR	100	75/75	n/a	6	2 collections in 2015 and 2 collections in 2016	Mechanical	n/a	0.25	Rapid Pasture Meter (machine) and ruler

(Jenal et al., 2020)	Germany	Experimental Site	n/a	1	Octocopter	RGB	30	n/a	16	4	1 collection in one year	Mechanical	156	0.54 × 5.46 m^2	n/a
(Karila et al., 2022)	Finland	Experimental Site	Mixed	1	Quadcopter	RGB and HS	30 and 50	n/a	n/a	RGB = 0.8, Hyper = 4 cm	4 collections in 2017	Mechanical	220	3.9 (n = 96), ~19.5 (n = 16), 4.5 (n = 108)	n/a
(Karunaratne et al., 2020)	Australia	Grassland Farm	Mono	1	Quadcopter	MS	25, 50, 75, and 100	80/80	10	1.74, 3.47, 5.21, 6,94	4 collections in 2019	Mechanical	101	0.25	n/a
(Lee et al., 2015)	Korea	Grassland Farm	Mixed	1	Fixed-wing	MS and RGB	50	n/a	n/a	30	2 collections in 2014	Not specified	56	0.03	n/a
(Li et al., 2020)	USA	Experimental Site	Mixed	1	Hexacopter	MS and LiDAR	20	85/75	7	3	1 collection in 2019	Manual	1320	Individual Plant	Ruler
(Li et al., 2021)	Estonia	Experimental Site	Mixed	2	Fixed-wing	MS	120	80/75	n/a	10	2 collections in 2019	Not specified	144	n/a	n/a
(Lussem et al., 2019)	Germany	Experimental Site	Mixed	1	Quadcopter	RGB	25	85/85	12	n/a	9 collections in 2017	Mechanical	n/a	4.5	RPM
(Lussem, Schellberg and Bareth, 2020)	Germany	Experimental Site	Mixed	1	Quadcopter	RGB	20	90	15	2	2 collections in 2014, 2 collections in 2015, and collections in 2016	Mechanical	140	15	RPM
(Lussem et al., 2022)	Germany	Experimental Site	Mixed	1	Octocopter	RGB and MS	95	RGB = 80/80; MS = 75/70	15	RGB = 0.7, MS = 2.3	3 collections in 2018 and § collections in 2019	Mechanical	832	3	n/a
(Michez et al., 2019)	Belgium	Experimental Site	Mixed	1	Octocopter	RGB and HS	50	80/80	8	RGB = 2 and MS = 5	1 collection in 2017	Not specified	40	0.09	LiDAR laser scans
(Michez et al., 2020)	Belgium	Experimental Site	Mono	1	Quadcopter	MS and RGB	30	n/a	12	RGB = 1 and MS = 2.5	1 collection in 2019	Mechanical	29	10.5	Ruler
(Näsi et al., 2018)	Finland	Experimental Site	Mixed	2	Hexacopter	RGB and HS	50 and 140	73 and 93/65 and 82	32	RGB = 1 and 5 HS = 5 and 14	1 collection in 2016	Mechanical	32	15	Ruler
(Oliveira et al., 2020)	Finland	Experimental Site	Mixed	4	Quadcopter	RGB and HS	30 and 50	84–87/65–81	n/a	HS = 6 and 3, RGB = 0.64 and 0.39	3 collections in 2017	Mechanical	108	Different sizes	n/a
(Alves Oliveira et al., 2022)	Finland	Experimental Site	Mixed	1	Quadcopter	RGB	50	n/a	n/a	1	4 collections in 2017	Mechanical	96	~ 4	n/a

(Pereira et al., 2022)	Brazil	Grassland Farm	Mixed	1	Quadcopter	MS	115	75/75	n/a	8	3 collections in 2019	Manual	116	1	n/a
(Plaza et al., 2021)	Spain	Grassland Farm	Mixed	1	Quadcopter	MS	43	n/a	4	3	7 collections in 2020	Not specified	112	0.125	n/a
(Pranga et al., 2021)	Belgium	Experimental Site	Mono	1	Hexacopter	MS and RGB	RGB = 40, MS = 30	80/70	9	RGB = 0.4, MS = 1.8	3 collections in 2020	Mechanical	1403	7.83	n/a
(Qin et al., 2021)	China	Natural Grassland	Mixed	82	Quadcopter	RGB	20	n/a	n/a	1	1 collection in 2017 and 1 collection in 2018	Manual	300	0.25	n/a
(Rueda-Ayala et al., 2019)	Norway	Experimental Site	Mixed	2	Quadcopter	RGB	30	90/60	n/a	n/a	1 collection in 2017	Not specified	20	1	RPM and Ruler
(Schucknecht et al., 2021)	Germany	Grassland Farm	Mixed	3	Quadcopter and Fixed-wing	MS	Quadcopter = 70, Fixed-wing = 80	Quadcopter = 80/80, Fixed-wing = 75/75	10	8.7–12.9 cm;	1 collection in 2018	Not specified	n/a	0.25	RPM
(Schulze-Brüninghoff, Wachendorf and Astor, 2021)	Germany	Natural Grassland	Mixed	4	Quadcopter	HS	20	80/60	6	~20 for spectral images and ~1 for panchromatic band	3 collections in 2018	Not specified	223	1	n/a
(Shi et al., 2021)	China	Natural Grassland	Mixed	1	Quadcopter	RGB	40	n/a	n/a	1	1 collection in 2018 and 1 collection in 2019	Manual	432	1	n/a
(Shi et al., 2022)	China	Natural Grassland	Mixed	1	Quadcopter	RGB	40	n/a	n/a	n/a	1 collection in 2018, 1 collection in 2019, and 1 collection in 2020	Manual	648	1	n/a
(Shorten and Trolove, 2022)	New Zealand	Experimental Site	Mono	1	Quadcopter	RGB	20	n/a	n/a	n/a	2 collections in one 2018	Not specified	370	1.5 (n = 300), 2.4 (n = 70)	n/a
(Sinde-González et al., 2021)	Ecuador	Grassland Farm	Mono	1	Quadcopter	RGB	70	80/70	8	3	1 collection in 2018	Manual	54	0.25	n/a
(Tang et al., 2021)	China	Natural Grassland	Mixed	4	Quadcopter	RGB	10	80/65	3	2.5	1 collection in one year	Manual	623	n/a	Not specified
(Théau et al., 2021)	Canada	Experimental Site	Mixed	1	Quadcopter	MS and RGB	65	75/75	60	RGB = 1.7, MS = 6.4	2 collections in 2017	Mechanical	99	0.25	n/a

(Van Der Merwe, Baldwin and Boyer, 2020)	USA	Natural Grassland	Mixed	11	Quadcopter	RGB	40	90/85	n/a	1	1 collection in 2017 and one collection in 2018	Manual	n/a	1	n/a
(Viljanen et al., 2018)	Finland	Experimental Site	Mixed	1	Quadcopter	RGB and HS	30 and 50	RGB = 84/65, MS = 87/81	5	RGB = 0.39 and 0.64; MS = 3 and 5	4 collections in 2017	Mechanical	96	~ 4	RPM and ruler
(Villoslada et al., 2020)	Estonia	Natural Grassland	Mixed	3	Fixed-wing	MS	120	n/a	11	10	1 collection in 2018	Manual	140	0.09	n/a
(Villoslada et al., 2021)	Estonia	Natural Grassland	Mixed	9	Fixed-wing	MS and RGB	120	n/a	n/a	RGB = 3.5, MS = 10	1 collection in 2019	Manual	520	0.09	n/a
(Vogel et al., 2019)	Germany	Grassland Farm	Mixed	1	Hexacopter	RGB	100	70/70	n/a	n/a	1 collection in 2016	Not specified	20	1	n/a
(Y. Zhao et al., 2014)	USA	Natural Grassland	Mixed	n/a	Hexacopter	MS	5, 20, and 50	n/a	n/a	5 m = 0.09; 20 m = 0.36, 50 m = 0.89	1 collection in 2013	Manual	13	0.1	n/a
(Wang et al., 2017)	China	Experimental Site	Mixed	1	Octocopter	LiDAR	10–120 at intervals of 10 m and 120	n/a	n/a	n/a	1 collection in 2015	Manual	90	1	Ruler
(Wengert et al., 2022)	Germany	Grassland Farm And Natural Grassland	Mixed	4	Octocopter	HS	20	n/a	6	20	3 collections in 2018	Manual	320	1	n/a
(Wijesingha et al., 2019)	Germany	Grassland Farm	Mixed	3	Quadcopter	RGB	25	80/80	n/a	n/a	8 collections in 2017	Not specified	194	1	n/a
(Zhang et al., 2021)	China	Experimental Site	Mixed	1	Quadcopter	LiDAR	40–110 (at intervals of 10 m)	n/a	n/a	n/a	1 collection in 2018	Manual	96	0.25	Ruler
(Zhang et al., 2022)	China	Natural Grassland	Mixed	3	Quadcopter	RGB	2	n/a	n/a	n/a	1 collection in 2018	Manual	208	0.25	n/a
(Zhang et al., 2018)	China	Natural Grassland	Mixed	3	Quadcopter	RGB	2 and 20	70/70	n/a	1	1 collection in 2017	Not specified	75	0.25	n/a
(Zhao et al., 2021)	China	Experimental Site	Mono	1	Hexacopter	HS	30	n/a	n/a	3	1 collection in 2018	Manual	n/a	0.09	n/a
(Zhao et al., 2022)	China	Natural Grassland	Mixed	24	Fixed-wing	LiDAR	100~120	80/80	n/a	1	1 collection in one year	Manual	96	1	Ruler

Table A3. Data analysis methods and essential results of the papers considered in this review.

Reference	Data Analysis Parameters				Data Analysis Methods and r^2 from Dry Mass (DM) [1]
	Spectral Data	Structural Data	Other Data	Terrain Model Source	
(Alvarez-Hess et al., 2021)	5 reflectance bands and 15 spectral indices	n/a	AM plot data only (AP), AM plot plus extreme data (APEX), small polygon data only (SP), and small polygon plus extreme data (SPEX)	n/a	SVR = 0.45
(Adar et al., 2022)	12 reflectance bands	n/a	Mixed pixels from UAV and satellite, vegetation cover	n/a	SVR = 0.76
(Askari et al., 2019)	21 spectral indices	n/a	n/a	n/a	PLSR = 0.77, MLR = 0.76
(Barnetson, Phinn and Scarth, 2020)	n/a	Canopy height	n/a	DTMs derived from ground point classification	LR and Automated Machine Learning
(Batistoti et al., 2019)	n/a	Canopy height	n/a	DTM derived from ground point classification	LR = 0.74
(Blackburn et al., 2021)	4 spectral bands and 26 spectral indices	n/a	n/a	n/a	Ridge Estimated Linear models
(Borra-Serrano et al., 2019)	10 spectral indices	7 canopy height metrics	GDD, ΔGDD between cuts	DTMs from interpolation of ground points and from leaf-off flights	LR = 0.67, MLR = 0.81, PLSR = 0.58, RF = 0.70
(Capolupo et al., 2015)	4 spectral indices	n/a	n/a	n/a	PLSR = 0.83
(Castro et al., 2020)	n/a	n/a	n/a	n/a	CNNs = 0.88
(Cunliffe, Brazier and Anderson, 2016)	n/a	Canopy height and Canopy volume	Surface cover	DTM derived from ground point classification	LR = 0.95
(da Costa et al., 2021)	n/a	16 canopy height metrics	Vegetation cover percentage	LiDAR point cloud classification	LR = 0.78
(De Rosa et al., 2021)	NDVI	n/a	n/a	n/a	GAM = 0.60, RF = 0.68
(DiMaggio et al., 2020)	n/a	Mean canopy height and vegetation volume	n/a	DTM by selecting the bare soil lowest point	LR = 0.65
(Fan et al., 2018)	DN of each band	n/a	n/a	n/a	MLR = 0.84
(Franceschini et al., 2022)	DN of each band	n/a	Variable importance in the projection (VIP)	n/a	PLSR = 0.92
(Gebremedhin et al., 2020)	NDVI	Mean plot height	n/a	n/a	LR = 0.81
(Geipel and Korsaeth, 2017)	NDVI, REIP, and GrassI	Mean plot height	n/a	GPS measurements taken on the ground	PPLSR, MLS and SLR = 0.77
(Geipel et al., 2021)	NDVI and REIP	Mean plot height	n/a	DTM from interpolation of ground points	PPLSR = 0.91; SLR = 0.67

(Grüner, Astor and Wachendorf, 2019)	n/a	Mean plot height	n/a	DTM from interpolation of ground points	LR = 0.72
(Grüner, Wachendorf and Astor, 2020)	4 spectral bands and 13 spectral indices	n/a	8 GLCM texture features	n/a	PLSR = 0.76, RF = 0.87
(Grüner, Astor and Wachendorf, 2021)	13 spectral indices	15 crop surface height	8 texture features of each spectral band (4 bands) and 8 texture features of mean CSH, FM, and DM	DTM from TLS data	RF = 0.90
(Hart et al., 2020)	MSI reflectance maps	n/a	Near-infrared reflectance spectroscopy	n/a	LR = 0.29
(Insua, Utsumi and Basso, 2019)	NDVI	Plant height and average ruler sward height	Growth rate	n/a	LR = 0.80
(Jenal et al., 2020)	12 spectral indices and spectral ground truth	n/a	n/a	n/a	LR = 0.94
(Karila et al., 2022)	RGB and HIS features (spectral bands, several handcrafted vegetation, and spectral indexes)	Canopy height 3D features	n/a	DTM from point cloud classification	Deep pre-trained neural network architectures and CNNs = 0.90
(Karunaratne et al., 2020)	5 spectral bands and 15 spectral indices	10 plant height metrics	4 flight altitudes	DTM from point cloud classification	RF = 0.91
(Lee et al., 2015)	NDVI	n/a	n/a	n/a	LR = 0.77
(Li et al., 2020)	4 spectral indices	Plant canopy perimeter and canopy height	n/a	DTM from LiDAR data	LR = 0.93
(Li et al., 2021)	6 spectral indices	n/a	n/a	n/a	RF = 0.9, SVR = 0.89, ANN = 0.99
(Lussem et al., 2019)	6 spectral indices	Mean sward height and 90th percentile of the sward height	n/a	DTM from leaf-off flight	Bivariate and MLR = 0.73
(Lussem, Schellberg and Bareth, 2020)	n/a	5 sward height metrics	n/a	DTM from leaf-off flight	LR = 0.86
(Lussem et al., 2022)	5 spectral bands and 19 spectral indices	8 sward height metrics	n/a	DTM from leaf-off flight	LR, PLSR, RF and SVM = 0.9
(Michez et al., 2019)	4 spectral bands and 4 spectral indices	Sward height model	n/a	DTM from LiDAR data	Multivariate models = 0.49
(Michez et al., 2020)	14 spectral indices	Sward height model	n/a	DTM from LiDAR data	MLR = 0.74
(Näsi et al., 2018)	39 spectral bands and 13 spectral indices	8 canopy height metrics	2 flight altitudes	DTM from point cloud classification	RF and LR = 0.78

(Oliveira et al., 2020)	38 spectral bands and 23 spectral indices	8 canopy height metrics	2 flight altitudes	DTM from point cloud classification	RF and MLR = 0.97
(Alves Oliveira et al., 2022)	n/a	n/a	n/a	n/a	CNNs = 0.79
(Pereira et al., 2022)	5 spectral bands and 25 spectral indices	n/a	PlanetScope and Sentinel-2A	n/a	RF = 0.7
(Plaza et al., 2021)	6 spectral indices	n/a	n/a	n/a	PLSR = 0.782
(Pranga et al., 2021)	21 spectral indices	3 canopy height metrics	n/a	DTMs from ground-based GPS interpolation	PLSR, RF and SVM
(Qin et al., 2021)	Excess Green Index	Fractional vegetation cover	Pika tunnel length and diameter, pika pile diameter	n/a	LR = 0.446
(Rueda-Ayala et al., 2019)	n/a	Mean plot volume	n/a	n/a	LR = 0.54
(Schucknecht et al., 2021)	9 spectral bands and 26 spectral indices	In situ bulk canopy height	n/a	n/a	GBM = 0.59, RF = 0.67
(Schulze-Brüninghoff, Wachendorf and Astor, 2021)	n/a	Canopy surface height	Terrestrial laser scanning data	n/a	RF = 0.81
(Shi et al., 2021)	RGBVI	n/a	Bare ground	n/a	LR = 0.88
(Shi et al., 2022)	RGBVI	n/a	Bare ground and mowing ration	n/a	LR
(Shorten and Trolove, 2022)	Mean spectral bands for vegetative and soil material	Percent vegetation cover and forage volume	n/a	DTM from interpolation of ground points	LR = 0.66
(Sinde-González et al., 2021)	n/a	Density factor and volume	n/a	DTM from bare ground	Descriptive statistic = 0.78
(Tang et al., 2021)	Band mean and band standard deviation of DN values	n/a	n/a	n/a	PLSR = 0.48
(Théau et al., 2021)	9 spectral indices	Mean plot volume	Vegetation cover classification	DTMs from ground-based GPS interpolation	LR = 0.94
(Van Der Merwe, Baldwin and Boyer, 2020)	n/a	Canopy height model	n/a	DTM from interpolation of dense point clouds	LR = 0.91
(Viljanen et al., 2018)	8 vegetation indices	8 canopy height metrics	n/a	DTM from bare ground and DTM from automatic point classification	MLR = 0.98, RF = 0.97
(Villoslada et al., 2020)	13 vegetation indices	n/a	n/a	n/a	RF = 0.67
(Villoslada Peciña et al., 2021)	13 vegetation indices	n/a	n/a	DTM from interpolating the points classified as ground by the Cloth	RF = 0.981

				Simulation Filtering algorithm	
(Vogel et al., 2019)	Reflectance of red, green, and blue; hue: saturation, value, NDVI, and VARI	n/a	n/a	n/a	LR = 0.8119
(Y. Zhao et al., 2014)	NDVI	n/a	n/a	n/a	OLSR = 0.4
(Wang et al., 2017)	n/a	Mean and maximum canopy height and fractional canopy cover	Different flight heights	DTM from LiDAR data	LR = 0.34
(Wengert et al., 2022)	118 spectral bands	n/a	n/a	n/a	PLSR = 0.45; RF = 0.73, SVR = 0.74, CBR = 0.75
Wijesingha et al., 2019)	n/a	10 canopy height metrics	n/a	DTM from TLS data	LR = 0.62
(Zhang et al., 2021)	n/a	3 canopy height metrics and Fractional vegetation cover	n/a	DTM from LiDAR data	MLR = 0.54
(Zhang et al., 2022)	6 color space indices and 3 vegetation indices	Canopy height model from point clouds	n/a	n/a	RF = 0.78
(Zhang et al., 2018)	n/a	5 canopy height metrics	n/a	DTM from point cloud ground point classification	LR = 0.76–0.78
(Zhao et al., 2021)	NDVI	n/a	n/a	n/a	PLSR = 0.85
(Zhao et al., 2022)	n/a	5 canopy height metrics, canopy cover and canopy volume	n/a	n/a	SMR = 0.25

[1] SVR = support vector regression; PLSR = partial least squares regression; MLR = multiple linear regression; LR = linear regression; RF = random forest; CNNs = convolutional neural networks; GAM = generalized additive model; PPLSR = powered partial least squares; ANN = artificial neural network; SVM = support vector machines; GBM = gradient boosting machines; OLSR = ordinary least squares regression; CBR = cubist regression.

Table A4. Biomass indices used in the papers assessed in this review.

Vegetation Index	Equation	Papers
Anthocyanin Reflectance Index 1 (Gitelson, Merzlyak and Chivkunova, 2001)	$ARI1 = \left(\frac{1}{G}\right) - \left(\frac{1}{Redge}\right)$	(Karunaratne *et al.*, 2020; Alvarez-Hess *et al.*, 2021)
Blue Normalized Difference Vegetation Index (Yang *et al.*, 2004)	$BNDVI = \frac{(NIR - B)}{(NIR + B)}$	(Lussem *et al.*, 2022)
Canopy Chlorophyll Concentration Index (Jago, Cutler and Curran, 1999)	$CGCI = \frac{\left(\frac{(NIR - Redge)}{(NIR + Redge)}\right)}{NDVI}$	(Karunaratne *et al.*, 2020; Alvarez-Hess *et al.*, 2021; Lussem *et al.*, 2022)
Chlorophyll Vegetation Index (Vincini, Frazzi and D'Alessio, 2008)	$CVI = \frac{NIR}{Green} \times \frac{Red}{Green}$	(Michez *et al.*, 2019, 2020; Villoslada *et al.*, 2020; Villoslada Peciña *et al.*, 2021; Pereira *et al.*, 2022)
Colouration Index (Pearson and Miller, 1972)	$CI = \frac{(R - B)}{R}$	(Pranga *et al.*, 2021)
Datt1 (Datt, 1998)	$Datt1 = \frac{(NIR - RE)}{(NIR - R)}$	(Théau *et al.*, 2021)
Datt4 (Datt, 1998)	$Datt4 = \frac{R}{G} * Redge$	(Villoslada *et al.*, 2020; Villoslada Peciña *et al.*, 2021)
Difference Vegetation Index (Tucker, 1979)	$DVI = NIR - Red$	(Villoslada *et al.*, 2020; Villoslada Peciña *et al.*, 2021)
Enhanced Vegetation Index (Huete *et al.*, 1997)	$EVI = 2.5 \times \frac{NIR - Red}{NIR + 6Red - 7.5B + 1}$	(Li *et al.*, 2020; Pranga *et al.*, 2021; Pereira *et al.*, 2022)
Enhanced Vegetation Index 2 (Huete *et al.*, 2002)	$EVI2 = \frac{2.5 \times (NIR - R)}{\left(NIR + (2.4 \times R)\right)}$	(Karunaratne *et al.*, 2020; Alvarez-Hess *et al.*, 2021; Lussem *et al.*, 2022)
Excess Green (M. Woebbecke *et al.*, 1995)	$ExG = 2\,G - R - B$	(Näsi *et al.*, 2018; Viljanen *et al.*, 2018; Borra-Serrano *et al.*, 2019; Oliveira *et al.*, 2020; Pranga *et al.*, 2021; Qin *et al.*, 2021; Zhang *et al.*, 2022)
Excess Green Combined with Canopy Height Model (Näsi *et al.*, 2018)	$ExG + CHM$	(Viljanen *et al.*, 2018; Lussem *et al.*, 2019; Oliveira *et al.*, 2020)
Excess Green-Red (Camargo Neto, 2004)	$ExGR = ExG - ExR$	(Viljanen *et al.*, 2018; Borra-Serrano *et al.*, 2019; Oliveira *et al.*, 2020; Pranga *et al.*, 2021)

Excess Red (Meyer et al., 1998) (Meyer, Hindman and Laksmi, 1999)	$ExR = 1.4\,R - G$	(Viljanen *et al.*, 2018; Oliveira *et al.*, 2020; Pranga *et al.*, 2021)
GnyLi Vegetation Index (Bendig *et al.*, 2015)	$GnyLi = \frac{R_{910} \times R_{1100} - R_{980} \times R_{1200}}{R_{910} \times R_{1100} + R_{980} \times R_{1200}}$	(Jenal *et al.*, 2020)
Grassland Index (Bareth *et al.*, 2015)	$GrassI = RGBVI + CHM$	(Näsi *et al.*, 2018; Lussem *et al.*, 2019; Oliveira *et al.*, 2020)
Green Atmospherically Resistant Vegetation Index (Gitelson, Kaufman and Merzlyak, 1996)	$GARI = \frac{NIR - \left(G - (B - Red)\right)}{NIR + \left(G - (B - Red)\right)}$	(Pranga *et al.*, 2021)
Green Chlorophyll Index (Gitelson, Gritz and Merzlyak, 2003)	$GCI = \left(\frac{NIR}{G}\right) - 1$	(Näsi *et al.*, 2018; Askari *et al.*, 2019; Grüner, Wachendorf and Astor, 2020; Jenal *et al.*, 2020; Karunaratne *et al.*, 2020; Oliveira *et al.*, 2020; Alvarez-Hess *et al.*, 2021; Grüner, Astor and Wachendorf, 2021; Pranga *et al.*, 2021; Pereira *et al.*, 2022)
Green Difference Index (Sripada, 2005)	$GDI = NIR - G$	(Karunaratne *et al.*, 2020)
Green Difference Index (Gianelle and Vescovo, 2007)	$GDI = NIR - R + G$	(Villoslada Peciña *et al.*, 2021)
Green Difference Vegetation Index (Sripada *et al.*, 2006)	$GDVI = NIR - G$	(Karunaratne *et al.*, 2020; Villoslada *et al.*, 2020; Alvarez-Hess *et al.*, 2021; Villoslada Peciña *et al.*, 2021)
Green Index (H = hue, S = saturation, V = brightness) (Carlson and Ripley, 1997)	$GI = 9 \times \left(\frac{H \times 3.14159}{180}\right) + 3 \times S + V$	(Zhang *et al.*, 2022)
Green Infrared Percentage Vegetation Index (Crippen, 1990)	$GIPVI = \frac{NIR}{(NIR + G)}$	(Villoslada *et al.*, 2020)
Green Leaf Index (Gobron *et al.*, 2000)	$GLI = \frac{(2 \times G - R - B)}{(2 \times G + R + B)}$	(Pranga *et al.*, 2021; Pereira *et al.*, 2022)
Green Normalized Difference Vegetation Index (Gitelson, Kaufman and Merzlyak, 1996)	$GNDVI = \frac{NIR - G}{NIR + G}$	[29,45–48,61,63,67,83,97,99–101,120]
Green Ratio Vegetation Index (Daughtry *et al.*, 2000)(Sripada *et al.*, 2006)	$GDVI = \frac{NIR}{G}$	(Askari *et al.*, 2019; Karunaratne *et al.*, 2020; Alvarez-Hess *et al.*, 2021)
Green Red Difference Index (Tucker, 1979)	$GRVI = \frac{G - R}{G + R}$	(Näsi *et al.*, 2018; Viljanen *et al.*, 2018; Michez *et al.*, 2019,

		2020; Oliveira *et al.*, 2020; Villoslada *et al.*, 2020; Plaza *et al.*, 2021)
Green Red Edge Vegetation Index	$GRVI_{edge} = \frac{G - Red}{G + Red}$	(Plaza *et al.*, 2021)
Greenness Red Edge	$Gr_{redge} = \frac{G}{Red + G + B}$	(Plaza *et al.*, 2021)
Leaf Chlorophyll Index (Hollberg and Schellberg, 2017)	$LCI = \frac{(NIR - Redge)}{(NIR - R)}$	(Askari *et al.*, 2019)
Log Ratio (Théau *et al.*, 2021)	$LogR^h = log\frac{(NIR)}{(R)}$	(Théau *et al.*, 2021)
Medium-Resolution Imaging Spectrometer (MERIS) Terrestrial Chlorophyll Index (Dash and Curran, 2004)	$MTCI = \frac{(NIR - Redge)}{(Redge - R)}$	(Capolupo *et al.*, 2015; Näsi *et al.*, 2018; Askari *et al.*, 2019; Jenal *et al.*, 2020; Karunaratne *et al.*, 2020; Oliveira *et al.*, 2020; Alvarez-Hess *et al.*, 2021; Pereira *et al.*, 2022)
Modified Chlorophyll Absorption in Reflectance Index (Daughtry *et al.*, 2000)	$MCARI = \left[\left((Redge - R) - 0.2\right) \times (Redge - G)\right] \times \left(\frac{Redge}{Red}\right)$	(Capolupo *et al.*, 2015; Näsi *et al.*, 2018; Askari *et al.*, 2019; Grüner, Wachendorf and Astor, 2020; Oliveira *et al.*, 2020; Grüner, Astor and Wachendorf, 2021; Pranga *et al.*, 2021; Lussem *et al.*, 2022; Pereira *et al.*, 2022)
Modified Chlorophyll Absorption in Reflectance Index 2 (Haboudane *et al.*, 2004)	$MCARI2 = \frac{\left[1.5[2.5(R_{nir} - R_{red}) - 1.3(R_{nir} - R_{green})]\right]}{\sqrt{[(2R_{nir} + 1)^2 - (6R_{nir} - 5\sqrt{R_{red}}) - 5]}}$	(Pereira *et al.*, 2022)
Combined Index with MCARI (Eitel *et al.*, 2007)	$MCARI\_MTVI2 = \frac{(MCARI)}{(MTVI2)}$	(Pereira *et al.*, 2022)
Modified Green Red Vegetation Index (Bendig *et al.*, 2014)	$MGRVI = \frac{(R_G)^2 - (R_R)^2}{(R_G)^2 + (R_R)^2}$	(Viljanen *et al.*, 2018; Michez *et al.*, 2020; Oliveira *et al.*, 2020)
Modified Non-Linear Index (Yang, Willis and Mueller, 2008)	$MNLI = \frac{(NIR^2 - R) \times (1 + L)}{NIR^2 + R + L}$	(Askari *et al.*, 2019)
Modified Simple Ratio (Chen, 1996)	$MSR = \frac{\frac{NIR}{R} - 1}{\sqrt{\frac{NIR}{R} + 1}}$	(Grüner, Wachendorf and Astor, 2020; Villoslada *et al.*, 2020; Grüner, Astor and Wachendorf, 2021; K. Y. Li *et al.*, 2021; Lussem *et al.*, 2022)

Modified Soil-Adjusted Vegetation Index (Qi *et al.*, 1994)	$MSAVI = \frac{2\,NRI + 1 - \sqrt{(2\,NIR + 1)^2 - 8 \times (NIR - Red)}}{2}$	(Näsi *et al.*, 2018; Jenal *et al.*, 2020; Oliveira *et al.*, 2020; Villoslada *et al.*, 2020; Pranga *et al.*, 2021; Théau *et al.*, 2021; Villoslada Peciña *et al.*, 2021; Lussem *et al.*, 2022; Pereira *et al.*, 2022)
Modified Triangular Vegetation Index (Haboudane *et al.*, 2004)	$MTVI = 1.2[1.2(NIR - G) - 2.5(R - G)]$	(Näsi *et al.*, 2018; Askari *et al.*, 2019; Oliveira *et al.*, 2020; Lussem *et al.*, 2022)
Second Modified Triangular Vegetation Index (Haboudane *et al.*, 2004)	$MTVI2 = \frac{\left[1.5[2.5(R_{nir} - R_{red}) - 2.5\left(R_{nir} - R_{green}\right)]\right]}{\sqrt{[(2.\,R_{nir} + 1)^2 - 6R_{nir} - 5\sqrt{(R_{red}}) - 0.5]}}$	(Pereira *et al.*, 2022)
Nitrogen Reflectance Index (D. Schleicher *et al.*, 2001)	$NRI = \frac{(G - R)}{(G + R)}$	(Askari *et al.*, 2019)
Near-Infrared to Red Edge Ratio (Ramoelo *et al.*, 2012)	$NIR.RE = \frac{NIR}{RE}$	(Lussem *et al.*, 2022)
Non-Linear Index (Goel and Qin, 1994)	$NLI = \frac{(NIR^2 - R)}{NIR^2 + R}$	(Askari *et al.*, 2019)
Normalized Difference Red Edge (Barnes *et al.*, 2000)	$NDRE = \frac{(NIR - RE)}{(NIR + RE)}$	[29,45–48,58,63,67,69,83,97,100,101,104,112,120]
Normalized Difference Vegetation Index (Rouse *et al.*, 1973)	$NDVI = \frac{NIR - R}{NIR + R}$	[18,29,42,45–48,56,61,63,66–69,73,84,85,97,99–101,103–106,112,116]
Normalized Green Intensity (M. Woebbecke *et al.*, 1995)	$NGI = \frac{G}{R + G + B}$	(Plaza *et al.*, 2021; Pranga *et al.*, 2021)
Normalized Green Red Difference Index (Tucker, 1979)	$NGRDI = \frac{(G - R)}{(G + R)}$	(Lussem *et al.*, 2019, 2022; Michez *et al.*, 2020; Villoslada *et al.*, 2020; K. Y. Li *et al.*, 2021; Pranga *et al.*, 2021; Pereira *et al.*, 2022)
Normalized Pigment Chlorophyll Ratio Index (Pereira *et al.*, 2022)	$NPCI = \frac{(R - B)}{(R + B)}$	(Pereira *et al.*, 2022)
Normalized Ratio Index (Koppe *et al.*, 2010)	$NRI = \frac{R_{910} - R_{1200}}{R_{910} + R_{1200}}$	(Jenal *et al.*, 2020)
Optimization Soil-Adjusted Vegetation Index (Rondeaux, Steven and Baret, 1996)	$OSAVI = \frac{NIR - R}{NIR + R + 0.16}$	(Capolupo *et al.*, 2015; Näsi *et al.*, 2018; Viljanen *et al.*, 2018; Jenal *et al.*, 2020; Oliveira *et al.*, 2020; Théau *et al.*, 2021; Lussem *et al.*, 2022; Pereira *et al.*, 2022)

Perpendicular Vegetation Index (Richardson and Wiegand, 1977)	$PVI = \sin(a)\, NIR - \cos(a)\, R$	(Pranga *et al.*, 2021)
Photochemical Reflectance Index (512.531) (Hernández-Clemente *et al.*, 2011)	$PRI = \frac{R_{512} - R_{531}}{R_{512} + R_{531}}$	(Näsi *et al.*, 2018; Jenal *et al.*, 2020; Oliveira *et al.*, 2020; Pranga *et al.*, 2021)
Plant Pigment Ratio Index Red (Metternicht, 2003)	$PPRI = \frac{(G - B)}{(G + B)}$	(Lussem *et al.*, 2022)
Plant Senescence Reflectance Index (Hill, 2013)	$PSRI = \frac{R - G}{NIR}$	(Askari *et al.*, 2019)
Ratio Vegetation Index (Pearson and Miller, 1972)	$RVI = \frac{NIR}{R}$	(Viljanen *et al.*, 2018; Jenal *et al.*, 2020; Li *et al.*, 2020; Michez *et al.*, 2020; Oliveira *et al.*, 2020)
Red Difference Index (Tucker, 1979)	$RDI = NIR - R$	(Karunaratne *et al.*, 2020; Alvarez-Hess *et al.*, 2021)
Red Edge Triangular Difference Vegetation Index (core only) (Chen *et al.*, 2010)	$RTVIcore = 100(NIR - Redge) - 10(NIR - G)$	(Karunaratne *et al.*, 2020; Villoslada *et al.*, 2020; Alvarez-Hess *et al.*, 2021; Villoslada Peciña *et al.*, 2021)
Red Green Blue Vegetation Index Excess (Bendig *et al.*, 2015)	$RGBVI = \frac{(R_G)^2 - (R_B - R_R)}{(R_G)^2 + (R_B - R_R)}$	(Näsi *et al.*, 2018; Lussem *et al.*, 2019, 2022; Michez *et al.*, 2020; Oliveira *et al.*, 2020; Shi *et al.*, 2021, 2022)
Red Edge Chlorophyll Index (Gitelson, Gritz and Merzlyak, 2003)	$ReCI = \left(\frac{NIR}{Redge}\right) - 1$	(Capolupo *et al.*, 2015; Näsi *et al.*, 2018; Askari *et al.*, 2019; Karunaratne *et al.*, 2020; Oliveira *et al.*, 2020; Alvarez-Hess *et al.*, 2021; Pereira *et al.*, 2022)
Red Edge Inflection Point (Guyot and Baret, 1988)	$REIP = 700 + 40 \times \frac{\frac{R_{670} + R_{780}}{2} - R_{700}}{R_{740} + R_{700}}$	(Näsi *et al.*, 2018; Jenal *et al.*, 2020; Oliveira *et al.*, 2020; Geipel *et al.*, 2021)
Red Edge Simple Ratio 2 (Gitelson and Merzlyak, 1994)	$SR2 = \frac{NIR}{Redge}$	(Askari *et al.*, 2019; Grüner, Wachendorf and Astor, 2020; Karunaratne *et al.*, 2020; Alvarez-Hess *et al.*, 2021; Grüner, Astor and Wachendorf, 2021; Pranga *et al.*, 2021;

		Villoslada Peciña *et al.*, 2021)
Red Edge to Red Ratio (Ramoelo *et al.*, 2012)	$RE.R = \frac{Redge}{R}$	(Lussem *et al.*, 2022)
Renormalized Difference Vegetation Index (Roujean and Breon, 1995)	$RDVI = \frac{NIR - Red}{\sqrt{NIR + Red}}$	(Näsi *et al.*, 2018; Lussem *et al.*, 2019, 2022; Grüner, Wachendorf and Astor, 2020; Jenal *et al.*, 2020; Oliveira *et al.*, 2020; Grüner, Astor and Wachendorf, 2021)
Simple Ratio (Jordan, 1969)	$SR = \frac{NIR}{R}$	(Askari *et al.*, 2019; Karunaratne *et al.*, 2020; Lussem *et al.*, 2022; Pereira *et al.*, 2022)
Soil Adjusted Vegetation Index (Rondeaux, Steven and Baret, 1996)	$SAVI = \frac{(1 + L) \times (NIR - R)}{(NIR + R) + L}$	(Askari *et al.*, 2019; Grüner, Wachendorf and Astor, 2020; Karunaratne *et al.*, 2020; Villoslada *et al.*, 2020; Alvarez-Hess *et al.*, 2021; Grüner, Astor and Wachendorf, 2021; Pranga *et al.*, 2021; Théau *et al.*, 2021; Pereira *et al.*, 2022)
Spectral Ratio 3 (Sims and Gamon, 2002)	$SR3 = \frac{R}{G}$	(Askari *et al.*, 2019)
Spectral Ratio 4 (Smith *et al.*, 1995)	$SR4 = \frac{G}{R}$	(Askari *et al.*, 2019)
Spectral Ratio 6 (Lu *et al.*, 2014)	$SR6 = \frac{R}{NIR}$	(Askari *et al.*, 2019)
Spectral Ratio 7 (Sousa *et al.*, 2012)	$SR7 = \frac{Redge}{NIR}$	(Askari *et al.*, 2019)
Transformed Vegetation Index 1 (Perry and Lautenschlager, 1984)	$TVI1 = \frac{NDVI + 0.5}{ABS\ (NDVI + 0.5)} \times \sqrt{ABS\ (NDVI + 0.5)}$	(Théau *et al.*, 2021)
Triangular Vegetation Index (Broge and Leblanc, 2001)	$TVI = 0.5[120(NIR - G) - 200(R - G)]$	(Pereira *et al.*, 2022)
Triangular Greenness Index (Pereira *et al.*, 2022)	$TGI = -0.5\ [(\lambda_{red} - \lambda_{blue})(R_{red} - R_{green}) - (\lambda_{red} - \lambda_{green})(R_{red} - R_{blue})]$	(Pereira *et al.*, 2022)
Transformed Chlorophyll Absorption Reflectance Index (Haboudane *et al.*, 2004)	$TCARI = 3\left[\left((Redge - R) - 0.2\right) \times (Redge - G)\right] \times \left(\frac{Redge}{Red}\right)$	(Pereira *et al.*, 2022)
TCARI Combined Index With OSAVI (Haboudane *et al.*, 2004)	$\text{TCARI\_OSAVI} = \frac{TCARI}{OSAVI}$	(Pereira *et al.*, 2022)
Visible Atmospherically Resistant Index (Gitelson *et al.*, 2002)	$VARI = \frac{G - R}{G + R - B}$	(Lussem *et al.*, 2019, 2022; Vogel *et al.*,

		2019; Michez *et al.*, 2020; Pranga *et al.*, 2021; Pereira *et al.*, 2022)
Visible Atmospherically Resistant Index Red Edge (Viña *et al.*, 2004)	$VARIrededge = \frac{(Redge - 1.7R + 0.7B)}{(Redge + 2.3R + 1.3B)}$	(Pereira *et al.*, 2022)
Wide Dynamic Range Vegetation Index (Gitelson, 2004)	$WDRVI = \frac{\propto NIR - R}{\propto NIR + R}$	(Pranga *et al.*, 2021)

Appendix B. Supplementary material from article "Grassland Ecosystem Assessments: Integrating UAV-Derived Features for Aboveground Biomass Estimation"

Table B1. Above Ground Biomass (AGB) estimates with learning algorithms, Random Forest (RF) and Partial Least Squares Regression (PLS) based on: canopy height model (CH), Vegetation Indices (VI), texture feature (GLCM) and combination of features: canopy height models plus VI (CH+VI), canopy height models plus texture feature (CH+GLCM), VI plus texture feature (VI+GLCM), canopy height models plus VI plus texture feature (CH+VI+GLCM). Models were tested for all the treatments separated (two-cut, three-cut and four-cut system) and all treatment combined (pooled data).

Treatment	Features Classes	RF			PLS		
		RMSE (g m^{-2})	rRMSE (%)	R^2	RMSE (g m^{-2})	rRMSE (%)	R^2
Two-cut	CH	192.47	29.43	0.71	228.18	34.93	0.60
	VI	190.15	29.19	0.73	213.86	32.77	0.66
	GLCM	257.35	39.40	0.49	256.51	39.35	0.53
	CH+VI	165.02	25.26	0.78	200.10	30.78	0.73
	CH+GLCM	175.76	26.84	0.76	204.53	31.29	0.70
	VI+GLCM	204.78	31.37	0.71	206.81	31.69	0.69
	CH+VI+GLCM	174.03	26.58	0.77	189.92	29.10	0.73
Three-Cut	CH	151.87	37.64	0.82	158.01	39.19	0.81
	VI	196.12	48.71	0.71	246.35	61.12	0.54
	GLCM	205.68	51.13	0.68	187.46	46.57	0.73
	CH+VI	142.16	35.28	0.84	153.61	38.08	0.82
	CH+GLCM	132.92	32.86	0.86	140.20	34.65	0.85
	VI+GLCM	207.72	51.50	0.68	175.77	43.56	0.78
	CH+VI+GLCM	131.79	32.56	0.87	141.13	34.94	0.85
Four-cut	CH	86.11	36.39	0.63	84.46	35.74	0.65
	VI	94.02	39.63	0.58	96.07	40.61	0.58
	GLCM	83.27	35.16	0.66	82.72	34.98	0.69
	CH+VI	76.49	32.31	0.71	80.68	34.07	0.70
	CH+GLCM	69.84	29.47	0.77	72.23	30.56	0.76
	VI+GLCM	80.97	34.18	0.69	81.99	34.68	0.69
	CH+VI+GLCM	69.66	29.44	0.76	73.45	31.02	0.75
Pooled Data	CH	157.18	36.49	0.78	174.25	40.24	0.74
	VI	193.25	45.02	0.67	225.60	53.32	0.54
	GLCM	213.67	49.55	0.60	215.32	49.79	0.60
	CH+VI	140.14	32.49	0.83	157.05	36.46	0.79
	CH+GLCM	135.46	31.38	0.84	165.10	38.21	0.77
	VI+GLCM	190.58	44.38	0.69	186.90	43.39	0.70
	CH+VI+GLCM	134.90	31.25	0.84	156.39	36.25	0.79

Appendix C. Supplementary material from article "Integration of UAV-sensed features using machine learning methods to assess species richness in wet grassland ecosystems"

Table C1. Number of species estimated with learning algorithms, Random Forest (RF) and Partial Least Squares Regression (PLS) based on: canopy height model (CH), Vegetation Indices (VI), texture feature (GLCM) and combination of features: canopy height models plus Vegetation Indices (CH+VI), canopy height models plus texture feature (CH+GLCM), Vegetation Indices plus texture feature (VI+GLCM), canopy height models plus Vegetation Indices plus texture feature (CH+VI+GLCM). Models were tested for all the treatments separated (two-cut system, three-cut system and four-cut system) and all treatment combined (pooled data).

Treatment	Features Classes	RF			PLS		
		RMSE (n)	rRMSE (%)	R^2	RMSE (n)	rRMSE (%)	R^2
Two-cut	CH	2.64	38.30	0.34	3.03	44.09	0.22
	VI	2.32	33.75	0.49	2.46	35.76	0.48
	GLCM	2.58	37.43	0.39	2.49	36.33	0.49
	CH+VI	2.37	34.41	0.47	2.63	38.35	0.43
	CH+GLCM	2.54	36.80	0.39	2.43	35.27	0.50
	VI+GLCM	2.46	35.80	0.44	2.44	35.36	0.50
	CH+VI+GLCM	2.47	35.85	0.43	2.39	34.92	0.52
Three-Cut	CH	3.06	43.32	0.13	3.18	45.00	0.10
	VI	2.56	36.26	0.36	2.86	40.46	0.28
	GLCM	2.67	37.70	0.31	2.66	37.50	0.36
	CH+VI	2.61	36.87	0.35	2.95	41.67	0.30
	CH+GLCM	2.68	37.86	0.31	2.80	39.64	0.32
	VI+GLCM	2.62	37.07	0.34	2.66	37.69	0.42
	CH+VI+GLCM	2.65	37.50	0.30	2.66	37.49	0.42
Four-cut	CH	2.93	34.14	0.25	3.74	43.02	0.27
	VI	2.90	33.60	0.30	3.21	37.13	0.32
	GLCM	2.68	30.98	0.41	3.31	38.47	0.37
	CH+VI	2.81	32.48	0.31	3.43	39.94	0.32
	CH+GLCM	2.84	32.85	0.31	3.49	40.43	0.29
	VI+GLCM	2.75	31.90	0.41	3.39	39.26	0.36
	CH+VI+GLCM	2.84	32.95	0.32	3.43	39.59	0.34
Pooled Data	CH	3.23	42.31	0.09	3.27	42.86	0.04
	VI	2.73	35.86	0.32	2.95	38.63	0.22
	GLCM	2.78	36.47	0.30	2.86	37.52	0.28
	CH+VI	2.76	36.22	0.30	3.07	40.27	0.18
	CH+GLCM	2.78	36.50	0.30	2.95	38.65	0.26
	VI+GLCM	2.74	35.98	0.31	2.89	37.85	0.27
	CH+VI+GLCM	2.78	36.50	0.30	2.95	38.65	0.26